

# **Protection against oxidative DNA damage by antioxidants, hormone-receptor blockers and HMG-CoA-reductase inhibitors**

Dissertation zur Erlangung des  
naturwissenschaftlichen Doktorgrades  
der Bayerischen Julius-Maximilians-Universität zu Würzburg

vorgelegt von  
Ursula Schmid  
aus Rottweil

Würzburg 2008



Eingereicht am: .....

Mitglieder der Promotionskommission:

Vorsitzender:.....

Gutachter: .....

Gutachter: .....

Tag des Promotionskolloquiums: .....

Doktorurkunde ausgehändigt am: .....

# Index

<b>1. INTRODUCTION</b>	<b>3</b>
1.1. OXIDATIVE STRESS AND GENOMIC DAMAGE	3
1.2. RENIN-ANGIOTENSIN-ALDOSTERONE SYSTEM (RAAS)	9
1.3. MODULATION OF THE RENIN-ANGIOTENSIN-ALDOSTERONE SYSTEM	12
1.4. OXIDATIVE DNA DAMAGE CAUSED BY LIPID DISORDER	15
1.5. IDENTIFICATION AND QUANTIFICATION OF OXIDATIVE DNA DAMAGE	16
1.5.1. Comet Assay	16
1.5.2. Micronucleus frequency test	17
1.5.3. Quantification of reactive oxygen species	19
<b>2. OBJECTIVES</b>	<b>20</b>
<b>3. ABBREVIATIONS</b>	<b>22</b>
<b>4. ANTIOXIDANTS</b>	<b>25</b>
4.1. BENFOTIAMINE EXHIBITS DIRECT ANTIOXIDATIVE CAPACITY AND PREVENTS INDUCTION OF DNA DAMAGE IN VITRO	25
4.1.1. Background	25
4.1.2. Experimental	29
4.1.2.1. Material	29
4.1.2.2. Cell culture	29
4.1.2.3. Comet Assay	29
4.1.2.4. Micronucleus frequency test	30
4.1.2.5. Flow cytometric analysis of oxidative stress	30
4.1.2.6. RNA isolation and semi quantitative reverse transcriptase PCR	31
4.1.2.7. Ferric reducing ability of plasma assay (FRAP)	31
4.1.2.8. Transketolase activity assay	32
4.1.2.9. Statistics	32
4.1.3. Results	33
4.1.3.1. Oxidative stress - Benfotiamine	33
4.1.3.2. Genomic damage - Benfotiamine	36
4.1.3.3. Apoptosis and Proliferation - Benfotiamine	38
4.1.3.4. Transketolase expression and activity - Benfotiamine	38
4.1.3.5. Oxidative Stress – $\alpha$ -Tocopherol	40
4.1.3.6. Genomic damage – $\alpha$ -Tocopherol	41
4.1.3.7. Apoptosis and proliferation – $\alpha$ -Tocopherol	42
4.1.4. Discussion	44
<b>5. RECEPTOR BLOCKADE – ANGIOTENSIN II TYPE 1 RECEPTOR (AT<sub>1</sub>R)</b>	<b>46</b>
5.1. ANGIOTENSIN II-INDUCED GENOMIC DAMAGE IN RENAL CELLS CAN BE PREVENTED BY ANGIOTENSIN II TYPE 1 RECEPTOR BLOCKADE OR RADICAL SCAVENGING	46
5.1.1. Background	46
5.1.2. Experimental	48
5.1.2.1. Material	48
5.1.2.2. Cell culture	48
5.1.2.3. Comet assay	48
5.1.2.4. Micronucleus frequency test	49
5.1.2.5. Quantification of apoptotic cells	49
5.1.2.6. Proliferation index	49
5.1.2.7. RT-PCR experiments	49
5.1.2.8. Flow cytometric analysis of oxidative stress	50
5.1.2.9. Statistical analysis	51
5.1.3. Results	52
5.1.4. Discussion	61
5.2. ANGIOTENSIN II INDUCES DNA DAMAGE IN THE ISOLATED PERFUSED KIDNEY	63
5.2.1. Background	63
5.2.2. Experimental	65
5.2.2.1. Material	65
5.2.2.2. Cell culture	65
5.2.2.3. Isolated perfused mouse kidneys	65
5.2.2.4. Comet Assay	67
5.2.2.5. RNA isolation and semi quantitative reverse transcriptase PCR	68
5.2.2.6. Determination of formamidopyrimidine DNA glycosylase (FPG) sensitive sites	68
5.2.2.7. Detection of phosphorylated $\gamma$ -H2AX sites	69
5.2.2.8. Detection of abasic sites	70

# Index

5.2.2.9. Micronucleus frequency test	70
5.2.2.10. Statistics	70
5.2.3. <i>Results</i>	72
5.2.3.1. Isolated perfused mouse kidney	72
5.2.3.2. Cell culture experiments	75
5.2.4. <i>Discussion</i>	81
<b>6. RECEPTOR BLOCKADE – MINERALOCORTICOID RECEPTOR</b>	<b>84</b>
6.1. ALDOSTERONE CAUSES DNA STRAND BREAKS AND MICRONUCLEI IN RENAL CELLS	84
6.1.1. <i>Background</i>	84
6.1.2. <i>Experimental</i>	86
6.1.2.1. Material	86
6.1.2.2. Cell culture	86
6.1.2.3. Comet assay	87
6.1.2.4. Micronucleus frequency test	87
6.1.2.5. Quantification of apoptotic cells	87
6.1.2.6. Proliferation index	87
6.1.2.7. Vitality assay	87
6.1.2.8. RT-PCR experiments	88
6.1.2.9. Flow cytometric analysis of oxidative stress	88
6.1.2.10. Statistical analysis	88
6.1.3. <i>Results</i>	89
6.1.4. <i>Discussion</i>	98
6.2. ALDOSTERONE INDUCES OXIDATIVE STRESS AND GENOMIC DAMAGE IN VIVO	100
6.2.1. <i>Background</i>	100
6.2.2. <i>Experimental</i>	102
6.2.2.1. Material	102
6.2.2.2. Treatment of DOCA rats	102
6.2.2.3. Extraction of primary kidney cells	103
6.2.2.4. Comet Assay	103
6.2.2.5. Micronucleus frequency test	104
6.2.2.6. Flow cytometric analysis of oxidative stress	104
6.2.2.7. Statistics	104
6.2.3. <i>Results</i>	105
6.2.3.1. Oxidative stress	105
6.2.3.2. DNA damage	106
6.2.3.3. Micronuclei, Mitoses and Apoptoses	107
6.2.4. <i>Discussion</i>	111
<b>7. ACTIVATION OF DEFENSE MECHANISMS</b>	<b>113</b>
7.1. ROSUVASTATIN PROTECTS AGAINST OXIDATIVE STRESS AND DNA DAMAGE IN VITRO VIA UP-REGULATION OF GLUTATHIONE SYNTHESIS	113
7.1.1. <i>Background</i>	113
7.1.2. <i>Experimental</i>	115
7.1.2.1. Material	115
7.1.2.2. Cell culture	115
7.1.2.3. Single cell gel electrophoresis	115
7.1.2.4. Total glutathione determination	116
7.1.2.5. Flow cytometric analysis of oxidative stress	116
7.1.2.6. Determination of superoxide dismutase (SOD) activity	116
7.1.2.7. Assay of cellular catalase (CAT)	117
7.1.2.8. Determination of glutathione peroxidase (GPX) activity	117
7.1.2.9. Determination of $\gamma$ -glutamylcysteine synthetase activity ( $\gamma$ -GCS)	117
7.1.2.10. RNA isolation and semiquantitative PCR	118
7.1.2.11. Statistics	120
7.1.3. <i>Results</i>	121
7.1.4. <i>Discussion</i>	133
<b>8. DISCUSSION</b>	<b>136</b>
<b>9. SUMMARY</b>	<b>142</b>
<b>10. ZUSAMMENFASSUNG</b>	<b>146</b>
<b>11. REFERENCES</b>	<b>151</b>
<b>12. ACKNOWLEDGEMENTS</b>	<b>171</b>

## 1. Introduction

### 1.1. Oxidative Stress and genomic damage

Reactive oxygen species (ROS) are formed continuously in living cells as a consequence of metabolic and other biochemical reactions and as a response to external factors.

The ROS family consists of several molecules that have manifold effects on physiological cellular processes. Examples are regulation of cell growth and differentiation, modulation of extracellular matrix production and breakdown, inactivation of nitric oxide (NO), stimulation of many kinases and proinflammatory genes, DNA, protein, carbohydrate and lipid damage [1, 2] as well as function as second messengers in signal transduction [3]. Interestingly, many of these actions are associated with pathological changes observed in various disease patterns in whose development ROS play a major role. These pathological conditions include cardiovascular disease, neurodegenerative disorders, hypertension, atherosclerosis, diabetes mellitus, cardiac hypertrophy, heart failure, ischemia-reperfusion injury, stroke and cancer, all arising mainly from surplus production of oxidants, decreased nitric oxide (NO) bioavailability and decreased antioxidant capacity in the vasculature and kidneys [4].

ROS are reactive chemical compounds comprising two major groups:

1. free radicals e. g. superoxide ( $\text{O}_2^-$ ), hydroxyl ( $\text{OH}^\cdot$ ) and nitric oxide ( $\text{NO}^\cdot$ ) which are highly reactive and unstable because of an unpaired electron and
2. non-radical derivatives of  $\text{O}_2$ , e. g. hydrogen peroxide ( $\text{H}_2\text{O}_2$ ) or peroxynitrite ( $\text{ONOO}^-$ ), which are less reactive [5].

An enzyme complex responsible for the generation of ROS is the NAD(P)H oxidase (Figure 1). This enzyme complex catalyzes the NAD(P)H-dependent reduction of  $\text{O}_2$  into the superoxide anion. Upon stimulation, the membrane-bound component flavocytochrome  $b_{558}$ , the catalytic core of the respiratory burst oxidase consisting of gp91phox and p22phox, assembles with the water-soluble proteins of cytosolic origin, namely p67phox, phosphorylated p47phox, p40phox as well as RAC, and generates superoxide.

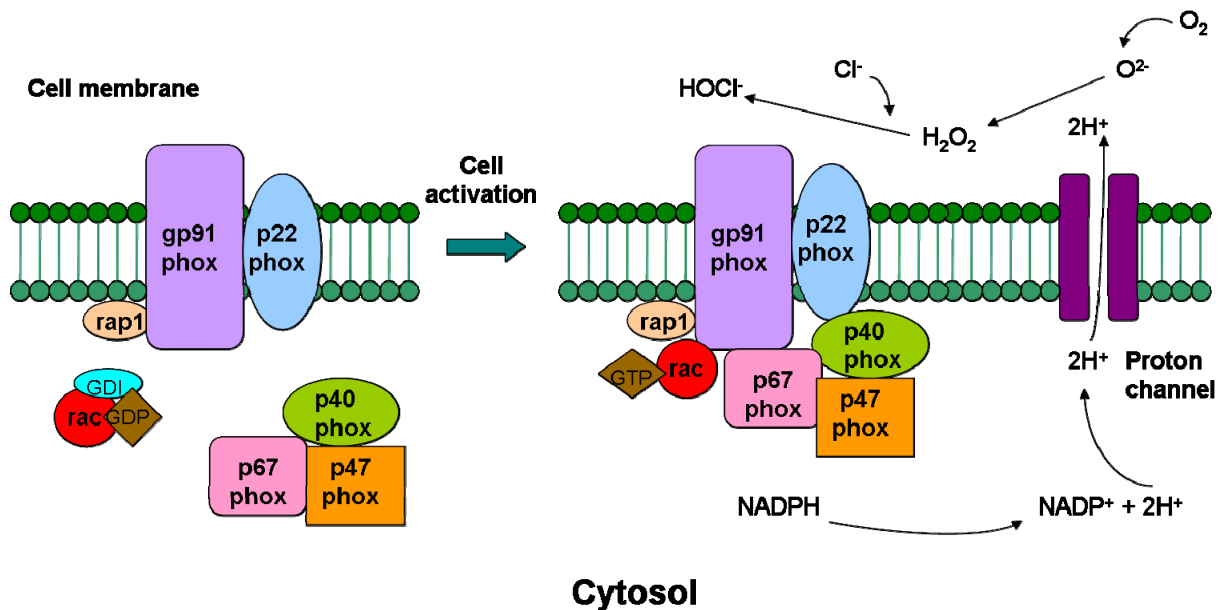


**Figure 1:** Schematic representation of the NAD(P)H oxidase enzyme. The integral membrane of the phagocyte consists of the two subunits p22phox and gp91phox which respectively produce the smaller and larger chain of the cytochrome  $b_{558}$ . Upon cell activation the two cytosolic subunits p67phox and p47phox, the p40phox accessory protein and the Rac-GTP binding protein then translocate to the cell membrane to form the NAD(P)H oxidase complex which generates a respiratory burst. Superoxide can react to form hydrogen peroxide and hypochlorous acid, which together participate in bacterial killing. © Modified after [www.medimmunol.com/content/5/1/4/figure/F1](http://www.medimmunol.com/content/5/1/4/figure/F1)

Genetic defects concerning any of the subunits of the NAD(P)H oxidase result in chronic granulomatous disease which is characterized by severe and recurrent infections, thus emphasizing the role of superoxide and its derivatives hydrogen peroxide and hypochlorous acid (HOCl) in host defense against invading microorganisms [6].

The term “oxidative stress” describes cellular conditions involving a deflection of the physiological equilibrium in favor of the oxidative processes [7], a condition, which has been found to be present in various cancer cells and thus may be related to oncogenic stimulation [8]. Reactive oxygen species, also known as “oxygen-derived species”, “oxidants” or commonly as “free radicals”, are produced as intermediates in redox reactions e. g. in the course of the respiratory chain, leading from  $O_2$  to  $H_2O$ . Inhaled smoke, polluted air and ingested food can also contain ROS or compounds which in turn generate ROS [9]. Furthermore, a variety of carcinogens like aflatoxin and benzo[a]pyrene may exert their effect partly through generation of ROS during their metabolism [10]. In addition, processes like the reperfusion of ischemic tissues, arachidonic acid metabolism and the respiratory burst from leukocytes include the release of ROS [11, 12].

Knowledge about the pathogenesis of cancer is a prerequisite for both, prevention and treatment of cancer. ROS are able to damage DNA and division of cells with unrepaired or misrepaired damage leads to mutations. If critical genes like oncogenes or tumor suppressor genes are affected, tumor initiation and/or progression may result. ROS can interfere either directly with cell signalling and growth [13] or induce mitosis by inflicting cellular damage, thereby increasing the risk that damaged DNA leads to mutations and increasing the exposure of DNA to mutagens including ROS [14].

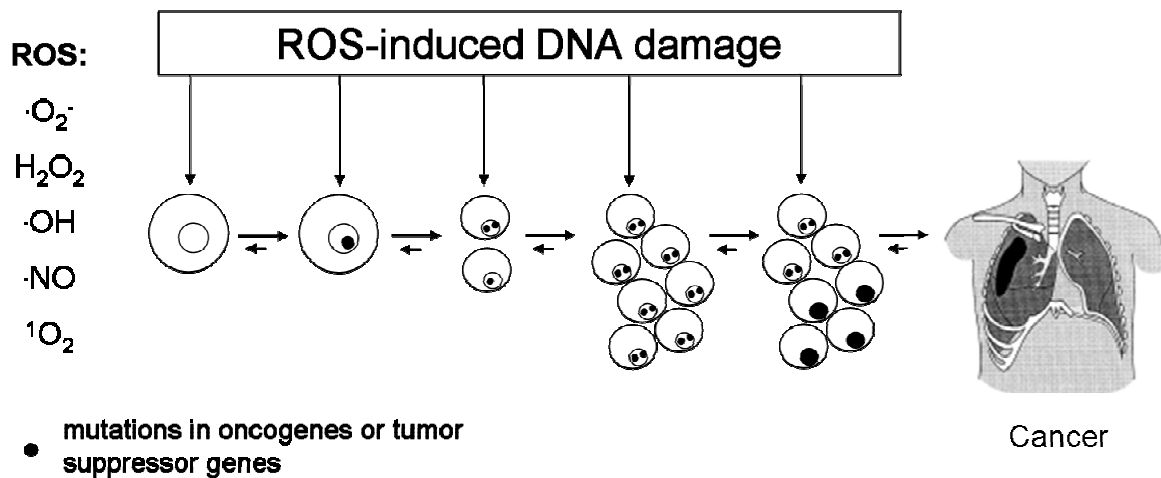


**Figure 2:** Possible roles of ROS in multistage carcinogenesis. © Modified after: Loft, Poulsen; "Cancer risk and oxidative DNA damage in man"; J Mol Med. 1996 Jun;74(6):297-312.

In biological systems, ROS are rapidly detoxified by enzymatic mechanisms. The antioxidant enzymes superoxide dismutase (SOD), catalase (CAT) and glutathione peroxidase (GPX) are the backbone of the cellular antioxidant defense system [15]. SOD is responsible for the dismutation of  $\cdot\text{O}_2\cdot$  to hydrogen peroxide which in turn is detoxified by CAT via redox reaction yielding  $\text{H}_2\text{O}$  and  $\text{O}_2$ . GPX reduces both  $\text{H}_2\text{O}_2$  and organic hydroperoxides using reduced glutathione (GSH) as electron donor [16]. In the absence of oxidative stress, ROS are kept at basal levels by balanced action of these three enzymes [17]. Yet, the decrease in antioxidant enzyme activity and altered expression of one of these enzymes increase the susceptibility of mammalian cells to ROS [18].

In addition to the enzymatic antioxidant defense mechanisms, endogenous non-enzymatic and exogenous antioxidant molecules have to be alluded. Intracellularly, there are several non-enzymatic antioxidants providing the primary defense against extra- and intracellular ROS, including a variety of lipophilic substances, e. g.

bilirubin, or hydrophilic molecules like GSH and uric acid or protein components, for example sulfhydryl groups on cysteine that act as free radical scavengers [15].

Exogenous antioxidant molecules such as  $\alpha$ -tocopherol, one of several isomers which together are commonly known as vitamin E,  $\beta$ -carotene, a metabolic precursor of vitamin A and ascorbic acid (vitamin C) have called scientific as well as public attention. The lipophilic molecule  $\alpha$ -tocopherol is able to protect biological membranes from lipid peroxidation [15], thus discontinuing the free radical chain reaction. Although high  $\alpha$ -tocopherol levels exerted beneficial effects *in vitro* and were correlatable with decreased cancer rates in humans [19], supplementation with neither  $\alpha$ -tocopherol nor  $\beta$ -carotene could reduce lung cancer in smokers [20], the incidence of non-melanoma skin cancer [21] or colorectal carcinoma [22].

Vitamin C is yet another compound which proved to be successful in animal models but could in clinical trials not keep up with the promising results gained in animal models. It has been shown that vitamin C deficiency is associated with increased oxidative damage in humans [23]. However, even in deficient subjects, supplementation had no effect on cancer incidence, neither beneficial nor harmful [24].

These controverse results may be due to the fact that there are major differences between human and animal antioxidant defense systems. Ascorbic acid for example is an exogenous antioxidant for humans, but is produced endogenously in many mammalian species. In contrast, uric acid, which exhibits very high plasma levels in humans, plays a minor role in animals and therefore could serve then as substitution for endogenous ascorbic acid [25].

Although ROS can cause DNA damage leading to base changes, strand breaks and increased expression of proto-oncogenes, and oxidative stress has been shown to induce malignant transformations in cells in culture [26, 27], the development of diseases, especially cancer, depends on many other factors. Examples are the extent of DNA damage, as excessive DNA damage can cause cell suicide, levels of antioxidant defenses, DNA repair systems and the cytotoxic effect of ROS in large amounts as opposed to their growth-promoting effects in small amounts [28-30].

The endogenous reactions that are likely to contribute to ongoing DNA damage *in vivo* are oxidation, methylation, depurination and deamination [31]. Conversion of guanine to 8-hydroxydeoxyguanosine (8-oxodG) has been found to alter the enzymatic methylation of adjacent cytosines [32]. This occurs upon exposure of DNA

to several ROS. Especially the hydroxyl radical is able to react with all components of the DNA molecule, namely the desoxyribose backbone, the purine bases and the pyrimidine bases [33]. 8-oxodG seems to be the most common base lesion and the one most often measured as an index of oxidative DNA damage [34], occurring in approximately 1 in  $10^5$  guanidine residues in a normal human cell [35]. Methylation of cytosines in DNA is important for the regulation of gene expression, and normal methylation patterns can be altered during carcinogenesis.

In addition to these base lesions, the phosphodiester backbone of the DNA can readily be attacked by free radicals. The resulting damages can displace bases, oxidize desoxyribose, and fragment the sugar. The subsequently occurring strand breaks are hallmarks of oxidative damaging agents like x-rays and hydrogen peroxide and all of these damages cause a complete loss of genetic information in the affected strand. Radical attack at C 1 or C 4 leaves the DNA chain intact but generates an abasic site which is labile in alkali and therefore allows the release of the abasic sites from oxidized DNA [36].

Organisms have evolved to efficiently respond to DNA insults that result from either endogenous sources like for example ROS, alkylation and mismatch of DNA bases or exogenous sources, e. g. ionizing radiation or various chemical agents. At the cellular level, DNA that is not properly repaired can lead to genomic instability, apoptosis or senescence which can greatly affect the organism's development and ageing process. More importantly, loss of genomic integrity predisposes the organism to immunodeficiency, neurological disorders and cancer. Therefore, it is essential for cells to efficiently respond to DNA damage through coordinated and integrated DNA-damage repair pathways [37-39].

To inhibit the formation of heritable mutations, there are several endogenous repair mechanisms whose importance is illustrated in various human syndromes where DNA repair defects impair the removal of ROS-induced DNA lesions [40, 41]. In these patients, free radical attack results not only in multiple skin cancers from ultraviolet radiation, but also in an increased risk to develop various types of internal cancers [42].

Different DNA-repair pathways exist which perform major roles at cellular as well as at organ levels, namely the direct reversal pathway, the mismatch repair pathway, the nucleotide excision repair pathway, the base excision repair pathway and the homologous recombination pathway (Figure 3).



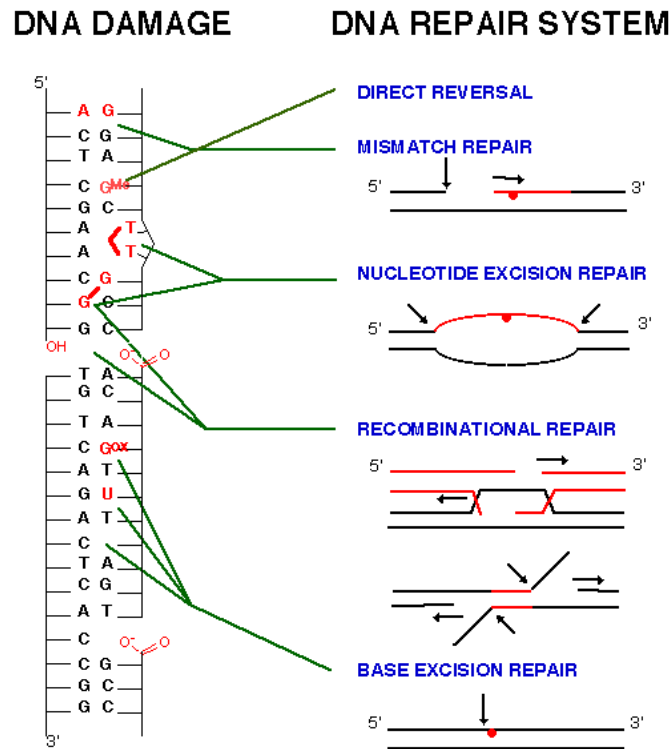


**Figure 3:** DNA repair mechanisms. © bbrp.llnl.gov/repair/html/overview.html

Direct reversal of DNA damage does not involve multiple proteins and does not require the excision of the damaged bases. An example for a DNA lesion that is repaired by direct reversal is the alkylated guanine. Here, the O<sup>6</sup>-methylguanine-DNA methyltransferase removes the methyl group and transfers it from the oxygen in the DNA to a cysteine residue in its active site. This action leads to the reversal of the base damage and to the inactivation of the enzyme.

The mismatch repair pathway plays an important role in prokaryotes as well as eukaryotes in repairing mismatches, which are small insertions and deletions that take place during DNA replication [43]. Involved in the mismatch repair pathway is a multitude of enzymes, of which MLH1, MSH2 and PMS2 are the most commonly known [44].

The nucleotide excision pathway is a multistep process which consists of two sub-pathways. The global genome nucleotide excision pathway detects and removes lesions throughout the genome, the transcription-coupled nucleotide excision pathway repairs actively transcribed genes. DNA lesions are recognized, followed by incisions at sites flanking the DNA lesion. The process culminates in the removal of the oligonucleotide containing the DNA lesion. Ligation of a newly synthesized oligonucleotide, complementary to the pre-existing strand, serves to fill the gap, thus ending the nucleotide excision repair process [39].

The base excision pathway deals with base damage, the most common insult to cellular DNA. Again, two sub-pathways have been identified, namely the short-patch and the long-patch base excision repair pathway, which replace a single nucleotide or 2 to 13 nucleotides respectively. Both pathways involve the removal of the damaged base by glycosylases followed by strand incision on the left and right side of the apurinic or apyrimidinic site by endonucleases. The newly generated gap is filled by incorporation of nucleotides mediated by DNA polymerases [45].

Furthermore, double strand break repair can be mediated by homologous recombination or non-homologous end joining repair pathway. Homologous recombination prevails in bacteria and yeast, whereas more than 90 % of double strand breaks in mammalian cells are repaired by the non-homologous end joining pathway. Homologous recombination is a multistep pathway requiring several proteins and operating at the S or G2 phase of the cell cycle, non-homologous end joining is active especially at G1 and is prone to errors [46].

Although there exist numerous proteins which are involved in several DNA damage repair pathways, loss or inactivation of only one of these proteins can have disastrous consequences with regard to increased cancer predisposition, immunodeficiency and neurological defects for the affected organism [41].

## ***1.2. Renin-Angiotensin-Aldosterone System (RAAS)***

Recent research indicated that activation of the renin-angiotensin-aldosterone system (RAAS) is involved in the formation of oxidative stress [47, 48]. Approximately one fourth of the world's population suffers from hypertension [49] and associated diseases like end stage renal disease (ESRD) and diabetes mellitus which often come along with elevated angiotensin II- or aldosterone levels. As epidemiological studies found a higher cancer mortality and an increased risk to develop renal cancer [50, 51] in hypertensive patients, these two hormones and drugs interfering with their signalling pathways attract scientific attention.

The RAAS (Figure 4) is through its modulation of salt and water homeostasis a major regulator of blood pressure. The physiological role of this complex system of neuroendocrine interactions is to protect heart, endothelium, brain and kidney from sustained exposure to elevated blood pressure and to regulate the vascular response to inflammation and injury [52].

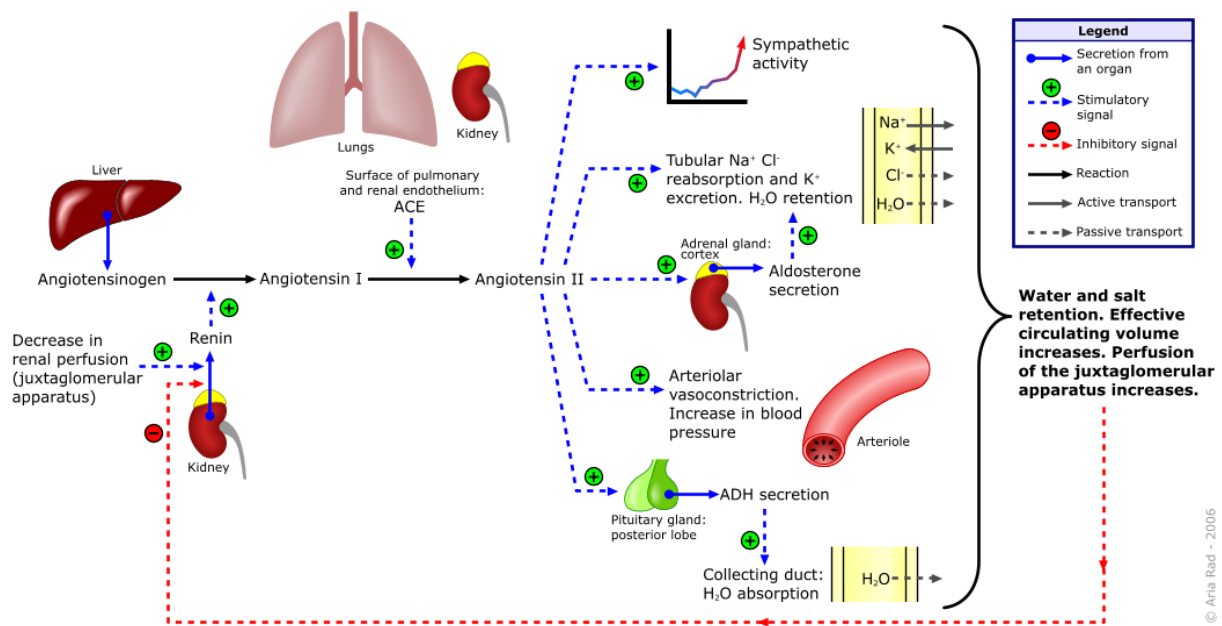


**Figure 4:** The renin-angiotensin-aldosterone system (RAAS).

[http://commons.wikimedia.org/wiki/Image:Renin-angiotensin-aldosterone\\_system.png](http://commons.wikimedia.org/wiki/Image:Renin-angiotensin-aldosterone_system.png)

Besides the systemic RAAS which is responsible for plasma angiotensin II levels, several local RAAS have been identified, for example in kidney, heart and brain [53]. Constant activation of the RAAS leads to hypertension and perpetuates a cascade of proinflammatory, prothrombotic and atherogenic effects associated with end-organ damage [54]. There are two main effectors of the RAAS, namely angiotensin II and aldosterone.

Angiotensin II is a long known peptide hormone. Upon triggers like hypotension, decreased sodium levels and sympathetic activation, renin is released and cleaves the precursor hormone angiotensinogen, an  $\alpha$ -2-globulin produced constitutively in the liver, to the inactive decapeptide angiotensin I. This in turn is cleaved by the angiotensinogen converting enzyme (ACE) to the active octapeptide angiotensin II (Figure 5).

### Asp-Arg-Val-Tyr-Ile-His-Pro-Phe

**Figure 5:** Amino-acid structure of angiotensin II.

Its actions are mediated via angiotensin II receptor type 1 (AT<sub>1</sub>R), which is existent in many tissues, and angiotensin II receptor type 2 (AT<sub>2</sub>R) which is predominantly expressed in fetal tissues. Functions like vasoconstriction, sympathetic activation, cellular growth, fibrosis, thrombosis and release of aldosterone by the adrenal glands are regulated via AT<sub>1</sub>R; vasodilatation, inflammation, inhibition of cellular growth, fetal tissue development and apoptosis are regulated via AT<sub>2</sub>R [55]. Many of the

pathologic effects of angiotensin II-like induction of oxidative stress and activation of transforming growth factor  $\beta$  are thought to be mediated through interaction with  $AT_1R$  [52].

Aldosterone (Figure 6) classically regulates sodium excretion through mineralocorticoid receptor-dependent genomic effects in the distal nephron of the kidney. It is produced in the adrenal zona glomerulosa upon stimulation by angiotensin II, potassium or the adrenocorticotropic hormone (ACTH). Circulating aldosterone then binds to the inactive cytosolic mineralocorticoid receptor of target cells, resulting in a dissociation of the ligand-activated receptor from a multiprotein complex and a translocation into the nucleus. [56]. The ligands cortisol and aldosterone can be bound with equal affinity but as cortisol can be converted by dehydrogenases into its inactive 11-ketometabolite, mineralocorticoid receptors are primarily occupied by aldosterone [57]. The mineralocorticoid receptor is not only expressed in the principal cells of the collecting duct and in monocytes, but also in the vasculature, the heart, the hippocampus and in the kidney [58]. In addition to its effects on gene expression, aldosterone is able to exert non-genomic effects which occur within minutes and can not be blocked by inhibitors of transcription [59].

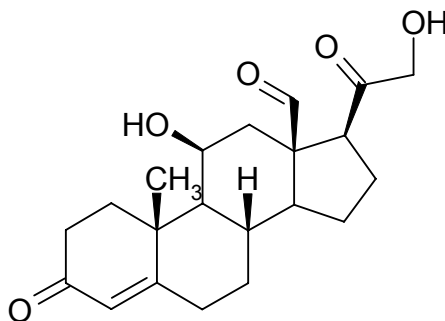


**Figure 6:** Chemical structure of aldosterone.

The relationship between the RAAS, blood pressure and end-organ damage can be explained by the dual roles of the RAAS in salt and water homeostasis and the vascular response to injury. The increased mechanical strain on the vasculature at a higher blood pressure can cause injury to the endothelial wall. Activation of the RAAS increases blood pressure and stimulates a local inflammatory response to repair the injury. Long-term or repeated response to injury leads to endothelial dysfunction and microvascular damage. Eventually, progressive pathophysiologic changes result in the clinical manifestation of end-organ damage, including for example kidney disease. Many of these changes can be attributed to mechanical injury from elevated blood pressure and oxidative stress [60].

### 1.3. Modulation of the Renin-Angiotensin-Aldosterone System

By the aid of pharmacologic intervention, the renin-angiotensin-aldosterone-system (RAAS) can be modulated (Figure 7).

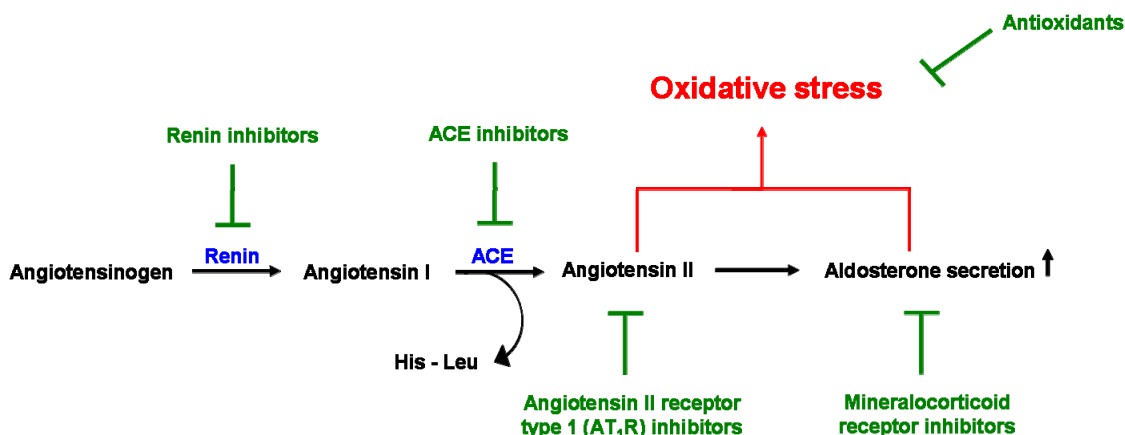


**Figure 7:** Pharmacologic intervention in the renin-angiotensin-aldosterone system.

Pharmacologic inhibition of the RAAS as part of an effective blood pressure lowering regime is a successful strategy for preventing or delaying end-organ damage [61]. The first possibility is to prevent angiotensinogen to be cleaved by renin to angiotensin I. This can be achieved by renin-inhibitors like for example aliskiren. Two drug classes directly target angiotensin II through complementary mechanisms. ACE inhibitors like enalapril (Figure 8) block the conversion of angiotensin I to the active peptide angiotensin II and thus decrease the peripheral resistance of the vessels. In addition, reduced levels of angiotensin II result in a reduced release of aldosterone and thus in a slight diuretic effect. ACE inhibitors are predominantly prodrugs whose active form is generated by hydrolysis of the ester-group. All substances are excreted via the kidney [62].

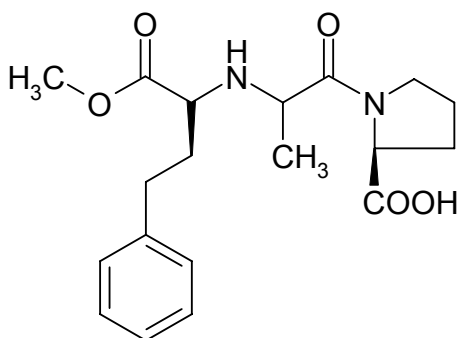


**Figure 8:** Chemical structure of enalapril.

Angiotensin receptor blockers, e. g. candesartan (Figure 9), selectively antagonize angiotensin II at AT<sub>1</sub>R. Beneficial side effects of the angiotensin receptor blockers may also include increased activation of the AT<sub>2</sub>R and modulation of the effects of angiotensin II breakdown products [62, 63].

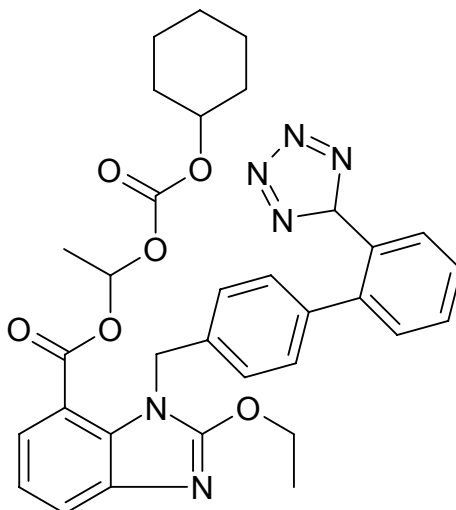


**Figure 9:** Chemical structure of candesartan cilexetil.

Both drug classes are well established and have been attested to reduce loss of renal function and a decrease of morbidity as well as mortality [64, 65]. Most patients require two or more drugs to control their blood pressure. A standard regime, designed especially for diabetic and hypertensive patients with nephropathies is the application of an ACE inhibitor in combination with an angiotensin receptor blocker as long term ACE inhibitor-treatment increases plasma angiotensin II levels, a phenomenon also known as angiotensin II escape. This phenomenon in turn is often associated with elevated aldosterone levels [66].

With the mineralocorticoid receptor antagonists, for example the steroidal substance eplerenone, another class of drugs has recently been rediscovered and found to be effective in the therapy of resistant hypertension and the prevention of end-organ damage [67, 68]. With eplerenone (Figure 10), there is one substance, which blocks selectively the mineralocorticoid receptor but does not have the adverse endocrine side effects of its predecessor spironolactone anymore. Yet, eplerenone is also not tolerated very well [69]. Therefore, there are currently many attempts to design highly specific and non-steroidal mineralocorticoid receptor antagonists.

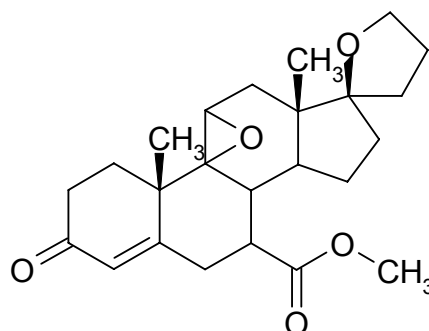


**Figure 10:** Chemical structure of eplerenone.

In addition to highly specific mechanisms like the inhibition of enzymes (ACE) and receptors ( $AT_1R$  and the mineralocorticoid receptor), which have all shown to decrease oxidative stress [47, 70], unspecific antioxidants could possibly exert beneficial effects with regard to end-organ damage, as elevated levels of angiotensin II and aldosterone have shown to induce oxidative stress [47, 71]. In this class, there are long known substances like for example  $\alpha$ -tocopherol or recently identified ones like e. g. benfotiamine [72]. While  $\alpha$ -tocopherol (Figure 11) is a radical scavenger and thus interrupts the radical chain reaction, a number of working mechanisms is discussed for the lipophilic thiamine- (Figure 12 B) prodrug benfotiamine (Figure 12 A) additionally to its direct antioxidative capacity [73].

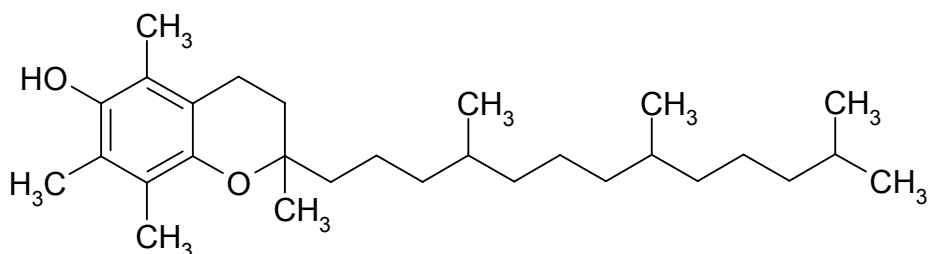


**Figure 11:** Chemical structure of  $\alpha$ -tocopherol.

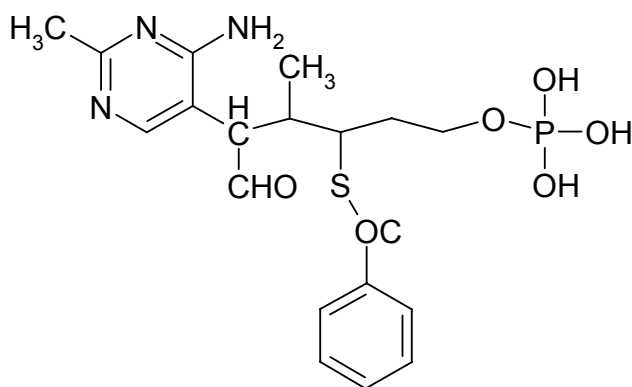


**Figure 12 A:** Chemical structure of benfotiamine.

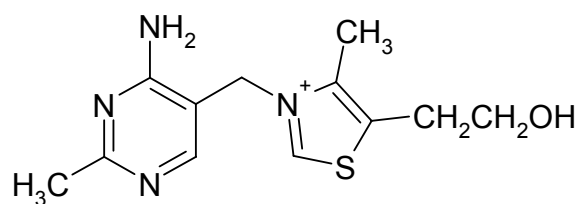


**Figure 12 B:** Chemical structure of thiamine.

#### ***1.4. Oxidative DNA damage caused by lipid disorder***

It is widely accepted that oxidative stress contributes to atherosclerosis and also to kidney end-organ damage [74]. In chronically hemodialyzed patients, antioxidant mechanisms are inefficient, resulting in increased formation of ROS and consequently in oxidative stress. These patients suffer most often not only from end stage renal disease (ESRD) but also from associated diseases like diabetes mellitus, hypertension as well as lipid disorders [75].

With regard to the fact that ESRD-patients have these lipid disorders, the use of 3-hydroxy-3-methylglutaryl-coenzyme A (HMG-CoA) reductase inhibitors, which inhibit the synthesis of mevalonic acid, an essential precursor of isoprenoid compounds including cholesterol [76], has become common in recent years. Furthermore, clinical trials have shown that statins substantially decrease cardiovascular morbidity and mortality in patients with and without coronary disease [77-79]. The effects of statins have been mainly ascribed to the hypolipemic activity, but not all therapeutic benefits can be explained solely by this capacity [80, 81]. Pleiotropic non-lipid-dependent effects include improvement of endothelial dysfunction, reduced inflammatory response, stabilization of atherosclerotic plaques and reduced thrombogenic response [82].

One of the pleiotropic mechanisms receiving high attention is a possible modulation of the endogenous antioxidant system, whose deficiency is recognized as key in increased morbidity and mortality [83]. Mechanisms for this can be either the inhibition of oxidant production by affecting the NAD(P)H oxidase, blockade of the effects of ROS by up-regulation of antioxidant enzymes or the increase in nitric oxide bioavailability which neutralizes radicals [84].

There is growing evidence that DNA is one of the most important targets of oxidative attack. If repair mechanisms fail to eliminate oxidative DNA damage, deleterious consequences for the cells may occur, including age-related dysfunctions and later



development to malignancies [85-87]. Recently, elevated levels of oxidative DNA damage have been found in all cell types of human atherosclerotic plaques of the carotid artery [88].

With regard to the potential role of DNA damage as a culprit both in cancer development and cardiovascular disease, investigations of the modulatory action of HMG-COA reductase inhibitors like for example rosuvastatin (Figure 13) are of special interest.

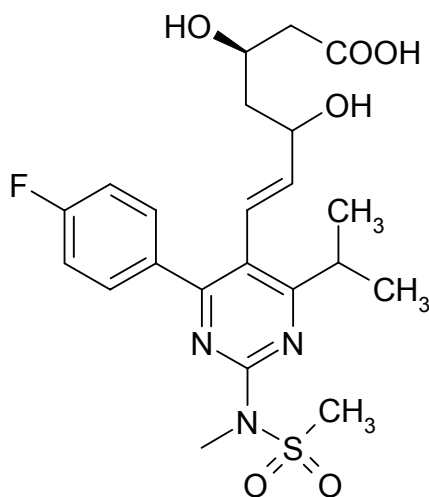


**Figure 13:** Chemical structure of rosuvastatin.

## **1.5. Identification and quantification of oxidative DNA damage**

Two standard methods are widely used in toxicology to assess genomic damage with applications in genotoxicity testing, human biomonitoring and molecular epidemiology as well as ecogenotoxicology, namely the comet assay [89] and the cytokinesis block micronucleus assay [90].

### **1.5.1. Comet Assay**

The comet assay, also known as single cell gel electrophoresis, is a method for the quantification of DNA single and double strand breaks as well as alkali labile sites. It was originally developed in the 1970s by Cook and colleagues [91]. A few years later, Östling and Johanson first demonstrated the comet-like structure (Figure 14) [92].

The comet assay is a simple, sensitive, versatile, speedy and economic method to investigate nuclear structure based on the lysis of cells. This treatment removes membrane, cytoplasm and almost all histones, leaving behind the nucleoid, consisting of RNA and proteins as well as supercoiled DNA [89]. After lysis with

detergent and high salt concentration, the nuclei are embedded in agarose to immobilize DNA for subsequent electrophoresis. The method is suitable for nearly all kinds of animal or human cells, either in culture or isolated from whole blood or from disaggregated tissues, as well as for plant cells after removal of the cellulose [93]. Singh et al. [94] optimized the comet assay by conducting electrophoresis at a high pH, which results in more pronounced comet tails and extends the useful range of damage that can be detected, however thereby not improving sensitivity [95].

Increased sensitivity can be achieved by integration of lesion-specific enzymes in the standard protocol. This can be for example the formamidopyrimidine DNA glycosylase (FPG) which is able to detect the major purine oxidation product 8-hydroxydeoxyguanosine (8-oxodG) as well as other altered purines [96].

DNA is visualized for quantification with fluorescent DNA-binding dyes and measured with the aid of computer based programmes, tail length, relative fluorescence intensity of head and tail or tail moment being the evaluation parameters [89].

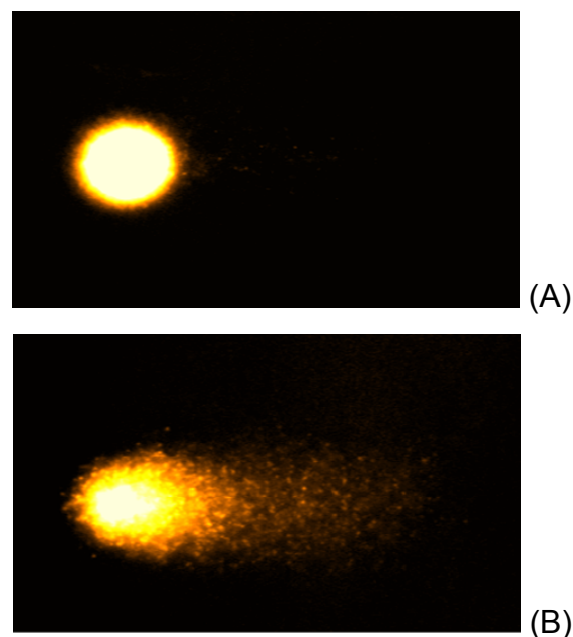


**Figure 14:** Exemplary depiction of LLC-PK1 cells treated either with solvent (A) or the methylating agent methylmethane sulfonate (MMS) [12.5 µg/ml] (B).

### 1.5.2. Micronucleus frequency test

Evidence suggests that chromosome abnormalities are a direct consequence and manifestation of damage at the DNA level. Chromosome breaks for example may result from unrepaired double strand breaks in DNA and chromosome rearrangements may result from misrepair of strand breaks in DNA. It is also

recognized that chromosome loss and malsegregation of chromosomes are an important event in cancer and ageing and that they are probably caused by defects in the spindle, centromere or as a consequence of undercondensation of chromosome structure before metaphase [97, 98]. Classically, chromosomes are studied by counting aberrations in metaphase, a very time consuming and error-prone method because of many confounding effects.

In contrast, scoring of micronuclei is a simple method to detect chromosome breakage as well as chromosome loss in eukaryotic dividing cells. It allows rapid assessment of cells, thus making it an economical procedure to implement in a large scale.

Micronuclei, also known as Howell-Jolly bodies, are expressed in dividing cells, containing either chromosome breaks lacking centromeres or whole chromosomes which cannot travel to the spindle poles during mitosis. During telophase, a nuclear membrane forms around the chromosomes or fragments, which, after uncoiling, assume the morphology of a nucleus during interphase (Figure 15 A), except that they are smaller than the main nucleus (Figure 15 B).

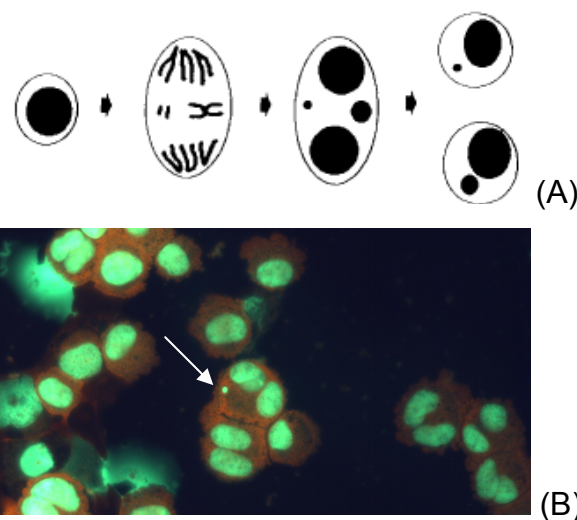


**Figure 15:** Micronucleus expression in a dividing nucleated cell from either lagging chromosomes or chromosome fragments at anaphase. © M. Fenech, “The cytokinesis-block micronucleus technique: A detailed description of the method and its application to genotoxicity studies in human populations” (A) and micronucleus (white arrow) in NRK cells treated with methylmethane sulfonate (MMS) [12.5 µg/ml] (B).

As micronuclei are not expressed until the cell divides, they are scored ideally after the first cell division. Because it is mostly unknown, what happens to micronuclei after the first cell division, and to be sure that the evaluated cells did in fact divide once, there was a need to develop a method which is able to distinguish between

dividing and not-dividing cells. This can be achieved using the cytokinesis block micronucleus technique, where cells are blocked from performing cytokinesis but not from nuclear division by application of the cytokinesis inhibitor cytochalasin B after the completion of one nuclear division [99]. Thus, all dividing cells can be accumulated at the binucleate stage. Micronuclei are then counted only in binucleate cells, thereby enabling reliable comparison of chromosome damage between cell populations that may differ in their cell division kinetics [100].

### 1.5.3. Quantification of reactive oxygen species

A method to assess levels of ROS, which are thought to be the reason underlying the formation of oxidative DNA damage, is the flow cytometric quantification of oxidative stress. 2',7'-Dichlorodihydrofluorescein diacetate (H<sub>2</sub>DCF-DA) is commonly used to detect the generation of reactive oxygen intermediates. During incubation the non-polar, non-ionic H<sub>2</sub>DCF-DA crosses cell membranes and is enzymatically hydrolyzed by intracellular esterases to non fluorescent polar DCFH. In the presence of reactive oxygen species, released for example by NAD(P)H oxidase, DCFH is rapidly oxidized to highly fluorescent 2',7'-dichlorofluorescein (DCF). Thus, the intensity of the fluorescence depends on the amount of oxidized fluorescence dye and thereby on the amount of ROS in the cell [101]. An increase of fluorescence is visualized by a shift to the right on the x-axis (Figure 16).

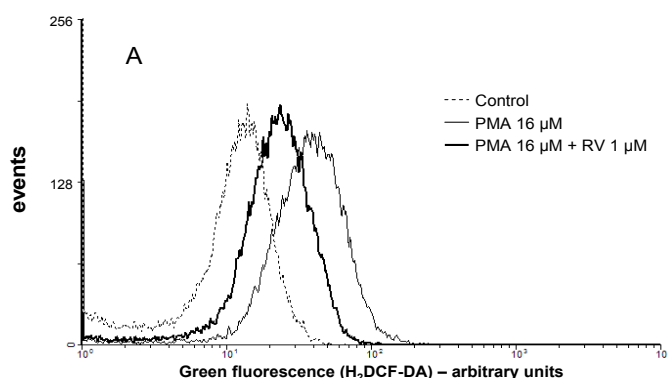


**Figure 16:** Frequency histogram of the green fluorescence of H<sub>2</sub>DCF-positive cells in arbitrary units. Exemplarily depicted are HL-60 control cells (broken line), cells treated with 16 μM PMA (grey solid line) for 4 hours and cells treated simultaneously with 16 μM PMA and 16 μM PMA together with 1 μM rosuvastatin (black solid line) for 4 hours. Quantification can be executed with the aid of the freeware WinMDI 2.9.

## 2. Objectives

There is increasing evidence that excess reactive oxygen species (ROS) are directly associated with the formation of DNA single and double strand breaks and DNA crosslinks which may in turn be involved in cancer development. These surplus ROS occur in many diseases, like hypertension and other pathological conditions associated with the metabolic syndrome, which become more and more endemic especially in the developed countries. Therefore this work was dedicated to the characterization of genomic damage caused by endogenous substances like angiotensin II or aldosterone or by model substances like hydrogen peroxide, 4-nitroquinoline-1-oxide (NQO) or phorbol 12-myristate 13-acetate (PMA). First, the induction of oxidative stress was confirmed and measured semiquantitatively by flow cytometry. The amount of the possible subsequent genomic damage was quantified by two standard genotoxicity assays, namely the comet assay and the cytokinesis block micronucleus test in *in vitro* systems.

First, evidence had to be provided that the hormones angiotensin II and aldosterone, which are elevated in patients suffering from hypertension and other associated diseases due to an activation of the renin-angiotensin-aldosterone system, and the model substances cause oxidative stress and genomic damage. The second aim of this work was to elucidate in more detail the mechanisms underlying the processes leading from the activation of NAD(P)H oxidase and the subsequent release of ROS to DNA single and double strand breaks, chromosomal aberrations, DNA adducts, and to identify modulators of these effects. This was achieved by application of several vitamins or drugs with various mechanisms of action:

- unspecific compounds like the antioxidants benfotiamine and  $\alpha$ -tocopherol
- highly specific receptor antagonists like candesartan (angiotensin II receptor type 1 inhibitor) and spironolactone and eplerenone (steroidal mineralocorticoid receptor inhibitors) and BR-4628 (non-steroidal mineralocorticoid receptor inhibitor)
- an HMG-CoA reductase inhibitor, namely rosuvastatin, which activates endogenous defense mechanisms like the glutathione system

After the flow cytometric confirmation that the chosen compounds were able to inhibit the release of ROS and prevent genomic damage, additional parameters like up- or down-regulation of genes or enzyme activities associated with the respective

mechanism were measured to elucidate the processes by which this inhibition of genomic damage was achieved.

As experimental settings in cell cultures soon proved to be very confined, further experiments were conducted in the isolated mouse kidney and in the DOCA/salt model where rats suffer from hypertension due to hyperaldosteronism, to simulate more accurately the conditions *in vivo*. Here, the processes in intact whole end-organ cells in reaction to exposure of elevated levels of angiotensin II and aldosterone were observed with regard to the release of ROS and the development of genomic damage as measured by comet assay and micronucleus frequency test. Moreover, the possible involvement of ROS in the development of several diseases is discussed.

### 3. Abbreviations

ACTH	adrenocorticotrophic hormone
ADP	adenosine diphosphate
AGEs	advanced glycation endproducts
Aldo	aldosterone
$\alpha$ -TOC	$\alpha$ -tocopherol
$\alpha$ -TTP	$\alpha$ -tocopherol transfer protein
Ang II	angiotensin II
AT <sub>1</sub> R	angiotensin II type 1 receptor
AT <sub>2</sub> R	angiotensin II type 2 receptor
B	benfotiamine
BN	binucleated
bp	base pairs
BSA	bovine serum albumin
BSO	L-buthionine-sulfoximine
Cand	candesartan
CAT	catalase
CBPI	cytokinesis block proliferation index
CHF	congestive heart failure
cm	centimetre
CO <sub>2</sub>	carbon dioxide
DMEM	Dulbecco/Vogt modified Eagle's minimal essential medium
DMSO	dimethyl sulfoxide
DNA	desoxyribonucleic acid
EB	ethidium bromide
EDTA	ethylenediamine-tetraacetic acid disodium salt
ESRD	end stage renal disease
FACS	fluorescence activated cell sorting
FCS	fetal calf serum
FDA	fluorescein diacetate
FPG	formamidopyrimidine DNA glycosylase
FPP	farnesyl pyrophosphate
FRAP	ferric reducing ability of plasma
$\gamma$ -GCS	$\gamma$ -glutamylcysteine synthetase
$\gamma$ -H2AX	phosphorylated histone 2AX
GGPP	geranylgeranyl pyrophosphate
GPX	glutathione peroxidase
GR	glutathione reductase
GSH	glutathione, oxidized form
GSS	glutathione synthetase
GSSG	glutathione, reduced form
h	hour
H2AX	histone 2AX
H <sub>2</sub> DCF-DA	2',7'-dichlorofluorescein diacetate
H <sub>2</sub> O <sub>2</sub>	hydrogen peroxide
HEK	human embryonic kidney cell line
HEPES	4-(2-hydroxyethyl)-1-piperazineethanesulfonic acid
HL-60	human leukemia cell line
HMG-CoA	3-hydroxy-3-methylglutaryl-coenzyme A

---

HOCl	hypochlorous acid
IS	indoxyl sulfate
L	liter
LDH	lactate dehydrogenase
LLC-PK1	porcine kidney cell line
M	mol per liter
Mev	mevalonate
$\mu\text{M}$	micromole per liter
min	minute
mmHg	one millimeter of mercury (= 1 Torr)
mM	millimole per liter
MMS	methylmethane sulfonate
MN	micronuclei / micronucleated
M-Per	mammalian protein extraction reagent
mRNA	messenger RNA
NAC	N-acetyl-cysteine
$\text{NAD}^+$	nicotinamide adenine dinucleotide, oxidized form
NADH	nicotinamide adenine dinucleotide, reduced form
NADPH	nicotinamide adenine dinucleotide phosphate, reduced form
NF- $\kappa$ B	nuclear factor kappa B
nm	nanometer
nM	nanomole per liter
$\cdot\text{NO}$	nitric oxide radical
NOS	nitric oxide synthase
NQO	4-nitroquinoline-1-oxide
NRK	normal rat kidney cell line
$\text{O}_2$	oxygen
$\cdot\text{OH}$	hydroxyl radical
OH-1	heme oxygenase
$\text{ONOO}^-$	peroxynitrite
$\cdot\text{O}_2^-$	superoxide radical
8-oxodG	8-hydroxydeoxyguanosine
PBS	phosphate buffered saline
PBST	PBS / 0.2 % Tween
PCR	polymerase chain reaction
PD 123319	PD 123319 di(trifluoroacetate) salt hydrate
PI	propidium iodide
PKC	protein kinase C
PLC	phospholipase C
pM	picomol per liter
PMA	phorbol 12-myristate 13-acetate
Rac	member of a family of hydrolases that bind and hydrolyze GTP
Ras	member of a family of hydrolases that bind and hydrolyze GTP
RAAS	renin-angiotensin-aldosterone system
Rho	member of a family of hydrolases that bind and hydrolyze GTP
RNA	ribonucleic acid
ROS	reactive oxygen species
RPMI 1640	Roswell Park Memorial Institute medium
RSV	rosuvastatin
RT-PCR	reverse transcription polymerase chain reaction
SOD	superoxide dismutase



---

T	thiamine
Tris	trishydroxymethylaminomethane
U 46619	9,11-Dideoxy-11 $\alpha$ ,9 $\alpha$ -epoxymethanoprostaglandin F <sub>2<math>\alpha</math></sub>

## 4. Antioxidants

### ***4.1. Benfotiamine exhibits direct antioxidative capacity and prevents induction of DNA damage in vitro***

#### **4.1.1. Background**

Diabetic patients are exposed to oxidative stress, which plays a key role in the pathogenesis of both micro- and macrovascular complications [102]. Its existence is based on decreased antioxidant capacity, chronic exposure to increased levels of reactive oxygen species (ROS), as well as increased peroxidation and glycoxidation [103-105]. The mitochondrial electron transport chain is one of the first targets of high glucose, resulting in enhanced oxygen radical formation, which is followed by stimulation of three pathways of hyperglycaemic damage: the activation of protein kinase C isoforms, increased formation of glucose-derived advanced glycation end products (AGEs) and the increased glucose flux through the aldose reductase pathway [106]. Reduced activity of the enzyme transketolase which converts glyceraldehyde-3-phosphate and fructose-6-phosphate to intermediates of the pentose phosphate pathway [107] seems to play an important role in all these cellular changes. Cofactor activity for transketolase is provided by diphosphorylated thiamine (vitamin B1), which has been shown to be deficient in many diabetic patients due to malabsorption and enhanced urinary excretion [108-110]. In experimental diabetes, benfotiamine, the lipophilic prodrug of thiamine, showed a prevention of early renal and retinal changes [111, 112]. This is in line with clinical studies in diabetes, demonstrating a significant relief in neuropathic pain and a marked improvement in vibration perception thresholds in diabetic patients [108].

Benfotiamine (Figure 17 A) is absorbed via passive diffusion through the intestinal mucosa and is rapidly converted to its biologically active form thiamine diphosphate (Figure 17 B) by closure of the open thiazole ring after absorption.

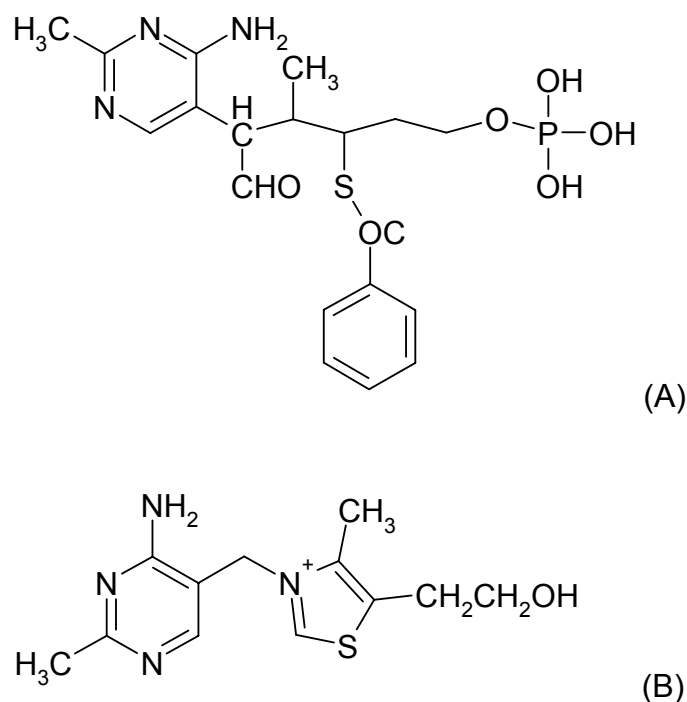


**Figure 17:** Chemical structures of benfotiamine (A) and thiamine (B).

Peak concentrations achieved by application of a lipophilic thiamine derivative turned out to be up to five times higher than those after application of a hydrophilic derivative [113].

Benfotiamine is thought to act by at least three different mechanisms. First, activation of the hexosamine pathway with subsequent decrease of the accumulation of deleterious glucose metabolites seems to be involved. Second, normalization of protein kinase C (PKC) activity along with prevention of nuclear factor kappa B (NF- $\kappa$ B) activation has been found in retinas, and third, correction of imbalances in the polyol pathway by decreasing aldose reductase activity, sorbitol concentrations and intracellular glucose levels seems to play a role [112]. Here, we investigate for the first time a fourth possibility, i.e. whether benfotiamine possesses direct antioxidant properties. Additionally, potential DNA protective effects of benfotiamine were analyzed.

Induction of oxidative stress in our *in vitro* experiments was achieved by addition of three different substances. First, the known mutagen 4-nitroquinoline-1-oxide (NQO), shown to form 8-hydroxydeoxyguanosine (8-oxodG) through ROS [114] was used. Next, indoxyl sulfate, an uremic toxin which is known to induce oxidative stress [115], was applied, and finally, the peptide hormone angiotensin II, which is elevated in diabetes due to stimulation of the renin-angiotensin-aldosterone system (RAAS) [116]. As previously shown, angiotensin II is able to induce oxidative stress by

activating NAD(P)H oxidase probably mediated via angiotensin II receptor type 1 (AT<sub>1</sub>R) [47]. Benfotiamine was examined here with regard to its ability to prevent the induction of oxidative stress by these compounds.

To investigate the associated biological consequences, the influence of benfotiamine on the genomic damage induced by angiotensin II was analyzed using two endpoints for genotoxicity. The first, the comet assay [89], detects single strand breaks, double strand breaks and alkali labile sites. Secondly, the cytokinesis block micronucleus frequency test [117] was conducted. Micronuclei are chromatin-containing structures surrounded by a membrane and resulting from chromosomal fragments or whole chromosomes not correctly distributed to the daughter cells after mitosis [118].

Our findings reveal a direct antioxidant capacity of benfotiamine demonstrated with three compounds and prevention of the induction of genomic damage by angiotensin II.

In addition to the newly identified antioxidant benfotiamine, the well known model-antioxidant  $\alpha$ -tocopherol was tested using the methods described above.  $\alpha$ -Tocopherol naturally does not occur as isolated substance but together with a whole family of tocopherol- und tocotrienol-isomers which are commonly known under the generic and trivial name "vitamin E". Among these substances,  $\alpha$ -tocopherol is the most active form [119]. Discovered in 1922, it soon became obvious that the lipid-soluble vitamin is essential, as  $\alpha$ -tocopherol-deficiency causes infertility and delayed-onset ataxia in animals as well as neurological dysfunctions in humans [120]. Reasons for a deficiency may be fat malabsorption, genetic defects in lipoprotein transport or in the hepatic  $\alpha$ -tocopherol transfer protein ( $\alpha$ -TTP) [121]. In the diet,  $\alpha$ -tocopherol can be found mainly in vegetable oils, cereal grains, green plants, egg yolk, milk fat, liver, nuts, and vegetables [119].

Further research concerning the physiological functions of  $\alpha$ -tocopherol revealed that it is involved in the maintenance of the integrity of cell membranes and plays a major role in antioxidant protection [122]. The best-understood physiological role of vitamin E is as an antioxidant that protects polyunsaturated fats and other lipids and lipid-soluble substances from oxidation by interrupting the radical chain reaction which underlies lipid peroxidation [123]. Thereby formed  $\alpha$ -tocopherol-radicals can be reduced again by vitamin C or glutathione, two other endogenous antioxidants, and thus re-enter the cycle [124].

---

It could be shown that oxidative stress is one of the underlying mechanisms in many pathological processes such as diabetes mellitus - with its late complications like cardiovascular disease, neuropathies, nephropathies and especially endothelial dysfunctions - atherosclerosis and end stage renal disease (ESRD) [125]. It is conceivable that a potent antioxidant like  $\alpha$ -tocopherol could possibly be able to mitigate these disease patterns. Associations between oxidative stress and hypertension, which in turn is associated with high angiotensin II levels, could already be shown [126, 127]. Therefore, angiotensin II was chosen again to provoke the release of reactive oxygen species by activation of the NAD(P)H oxidase via AT<sub>1</sub>R [47] during the following experiments and thus simulate the conditions in hypertensive diabetic patients. The conducted experiments show that  $\alpha$ -tocopherol, whose antioxidant capacity could be confirmed in our study, was also able to prevent oxidative stress and the subsequent genomic damage caused by angiotensin II.

## **4.1.2. Experimental**

### **4.1.2.1. Material**

If not mentioned otherwise, all chemicals were purchased from Sigma-Aldrich (Taufkirchen, Germany). Benfotiamine was donated by Wörwag Pharma GmbH (Böblingen, Germany).

### **4.1.2.2. Cell culture**

HEK 293, a human embryonic kidney cell line with proximal tubular properties, was obtained from ATCC (Rockville, USA). Cells were grown in DMEM medium (4.5 g/l glucose) supplemented with 10 % fetal calf serum, 1 % glutamine and antibiotics.

NRK-52E, an epithelial rat kidney cell line with proximal tubular properties, was obtained from ECACC (Salisbury, UK) and grown in DMEM medium (4.5 g/l glucose) supplemented with 10 % fetal calf serum, 1 % glutamine, 1 % non-essential amino acids and antibiotics.

LLC-PK1, an epithelial porcine kidney cell line with proximal tubular properties, was obtained from ATCC (Rockville, USA) and grown in DMEM medium (1.0 g/l glucose) supplemented with 10 % fetal calf serum, 1 % glutamine, 25 mM HEPES buffer and antibiotics.

All cells were split routinely twice (LLC-PK1) or three times (HEK 293, NRK) a week to ensure exponential growth and were, except for LLC-PK1 (10 passages), cultured for no more than 40 passages after thawing them from stock.

### **4.1.2.3. Comet Assay**

$3.5 \cdot 10^5$  cells were treated for 2 h (NRK) or 4 h (LLC-PK1 and HEK 293) with test substances in 5 ml medium. The comet assay was carried out as described by Singh et al. [94] with slight modifications according to Schupp et al. [128] using a fluorescence microscope at a 200-fold magnification and computer aided image analysis (Komet 5, Kinetic Imaging Ltd., UK). After DNA staining with propidium iodide (20  $\mu\text{g/ml}$ ), 25 cells from each of two slides were measured, % tail DNA being the evaluation parameter. The comet assay detects single strand breaks, double strand breaks and alkali labile sites. The DNA fragments move during electrophoresis

due to their negative charge out of the nucleus in direction of the anode. Smaller fragments can move faster through the agarose in which the nuclei are embedded, resulting in characteristic comet-like structures.

#### **4.1.2.4. Micronucleus frequency test**

$3.5 \times 10^5$  cells were incubated with test substances in 5 ml medium. After 2 h (NRK) or 4 h (LLC-PK1 and HEK 293) cytochalasin B (3  $\mu\text{g/ml}$ ) was added. This inhibitor of actin polymerisation blocks the separation of daughter cells but not of daughter nuclei, yielding binucleated cells. By limiting analysis to such binucleated cells, it can be ensured that these cells have actively divided since the treatment. After 24 hours, cells were harvested, applied onto glass slides by cytopsin centrifugation and fixed in methanol ( $-20\text{ }^\circ\text{C}$ ) for at least two hours. Before counting, cells were stained for 5 minutes with acridine orange (62.5  $\mu\text{l/ml}$  in Sørensen buffer, pH 6.8), washed twice with Sørensen buffer and mounted for microscopy. From each of two slides, 1000 binucleated cells were evaluated with regard to micronucleus frequency. Evaluation criteria were according to Fenech [118]. In addition, the cytokinesis block proliferation index (CBPI) was determined from 1000 cells of each sample.

$$\text{CBPI} = \frac{(\text{mononucleated cells} * 1) + (\text{binucleated cells} * 2) + (\text{polynucleated cells} * 3)}{\text{total cell number}}$$

#### **4.1.2.5. Flow cytometric analysis of oxidative stress**

$10^6$  cells were treated with test substances in 5 ml culture medium after 10 minutes pre-treatment with 10  $\mu\text{M}$  2',7'-dichlorodihydrofluorescein diacetate ( $\text{H}_2\text{DCF-DA}$ ) and harvested after 2 h (NRK) and 4 h (LLC-PK1 and HEK 293). Cells were washed once with PBS/1 % BSA, counterstained with propidium iodide (1  $\mu\text{g/ml}$ ) to exclude dead cells and  $3 \times 10^5$  cells per sample were analyzed by using a FACS LSR I (Becton-Dickinson, Mountain View, CA). Medians of the histograms were assessed using the free software WinMDI 2.8 (Scripps Research Institute Cytometry Software, <http://facs.scripps.edu/software.html>)

#### **4.1.2.6. RNA isolation and semi quantitative reverse transcriptase PCR**

RNA isolation from cells treated with test substances for 2 h (NRK) and 4 h (LLC-PK1 and HEK 293) and PCR was performed as described previously [129]. Primers were designed using the primer design service of MWG Biotech AG, Germany. Sequences, annealing temperatures and PCR conditions were:

Transketolase NRK (EDL88992.1, 54 °C, 35 cycles, 413 bp):

For: 5'-ACCAACAGCCATCATTGCC-3'; Rev: 5'-TGCTCACCATGTTCTGCTC-3';)

Transketolase LLC-PK1 (XM\_001492163.1, 54 °C, 35 cycles, 553 bp):

For: 5'-CTATTGCTTGCTGGGAGACG-3'; Rev: 5'-GGAGTGGCCAGGATCCTCTT-3'

Transketolase HEK 293 (NM\_001101, 54 °C, 35 cycles, 500 bp):

For: 5'-CCCCACATCAACTCTTTTA-C-3'; Rev: 5'-TACCAAACATCTTCGCAGCTC-3'

β-actin NRK (EF156276.1, 54 °C, 35 cycles, 411 bp):

For: 5'-AGCCATGTACGTAGCCATCC-3'; Rev: 5'-AGGAAGGAAGGCTGGAAGAG-3';

β-actin LLC-PK1, HEK 293 (DQ407611, 54 °C, 35 cycles, 610 bp):

For: 5'-TCCCTGGAGAAGAGCTACGA-3'; Rev: 5'-GTCACCTTCACCGTTCCAGT-3'

Electrophoresis was conducted using a 1.5 % agarose gel stained with ethidium bromide. Density of the DNA band was measured using the Gel Doc (BioRad, Hercules, CA, USA). Results are shown compared to the housekeeping gene β-actin.

#### **4.1.2.7. Ferric reducing ability of plasma assay (FRAP)**

This method determines the reduction of a ferric-tripyridyltriazine complex to its ferrous, coloured form in the presence of plasma antioxidants or other antioxidative substances [130, 131]. The FRAP assay was performed photometrically as described by Benzie and Strain [132] using dilutions of benfotiamine and thiamine instead of plasma. 300 µl freshly prepared FRAP reagent (25 ml acetate buffer (300 mM acetate buffer, pH 3.6 and 16 ml C<sub>2</sub>H<sub>4</sub>O<sub>2</sub> per liter of buffer solution), 2.5 ml 2,4,6-tripyridyl-s-triazine (TPTZ) solution (10 mM TPTZ in 40 mM HCl) and 2.5 ml FeCl<sub>3</sub>\*6 H<sub>2</sub>O (20 mM FeCl<sub>3</sub>\*6 H<sub>2</sub>O) solution) was warmed to 37 °C and a reagent blank reading was taken at 593 nm. 10 µl of sample was then added, along with 30 µl H<sub>2</sub>O. Absorbance (A) readings were taken after 9 s and every 10 s thereafter during the



monitoring period. The change in absorbance ( $\Delta A_{593\text{nm}}$ ) between the final reading selected and the reading at timepoint 0 was calculated for each sample and related to  $\Delta A_{593\text{nm}}$  of a  $\text{Fe(II)SO}_4$  standard solution tested in parallel.

#### **4.1.2.8. Transketolase activity assay**

Transketolase activity was measured using a reaction mix containing 14.8 mM ribose-phosphate, 0.25 mM NADH, 92.5 U triosephosphate isomerase (Roche), 37.5 U glycerol-3-phosphate isomerase and 0.002 % thiamine pyrophosphate. The reaction was started by the addition of 100  $\mu\text{l}$  cell lysate. Absorbance at 340 nm was measured for 30 minutes and the rate of decrease in absorbance between 5 to 20 minutes was used to assess the rate of oxidation of NADH.

#### **4.1.2.9. Statistics**

If not mentioned otherwise, data from at least 3 independent experiments  $\pm$  standard deviation are depicted. Statistical significance among multiple groups was tested with Kruskal-Wallis test over all groups and Mann-Whitney test was used to determine significance between two groups. Results were considered significant if the p value was  $\leq 0.05$ .

### 4.1.3. Results

#### 4.1.3.1. Oxidative stress - Benfotiamine

To assess the potential antioxidant effect of benfotiamine, oxidative stress was induced in three kidney cell lines of human, rat and porcine origin by three compounds. The elevated oxidative stress induced by application of 10.5  $\mu\text{M}$  4-nitroquinoline-1-oxide (NQO) was reduced by simultaneous, but not by previous incubation with 300  $\mu\text{M}$  benfotiamine (Figure 18 A). This concentration of benfotiamine proved to have best antioxidative effects and least cytotoxicity in preliminary studies and was used for all further experiments.

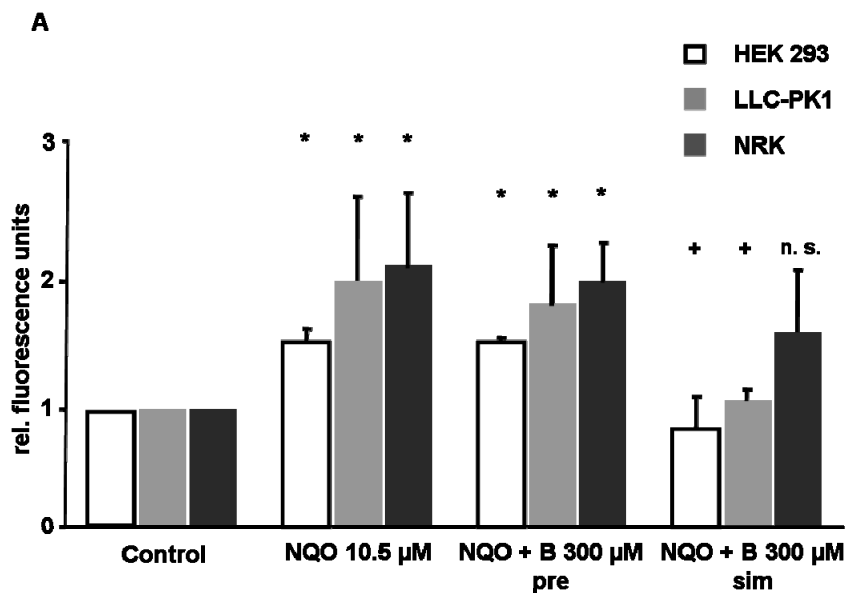


**Figure 18 A:** Oxidative stress induced by 4-nitroquinoline-1-oxide (NQO) alone, with simultaneous incubation with benfotiamine (B) or with pre-incubation with benfotiamine in kidney cell lines. Shown are means  $\pm$  standard deviation of three independent experiments, each normalized to its control. Significance ( $p \leq 0.05$ ) compared to the control is shown by “\*”, significant reduction ( $p \leq 0.05$ ) of the induced effect by “+” and not significant reduction by “n. s.”.

The uremic toxin indoxyl sulfate (IS, 250-1000  $\mu\text{M}$ ) also induced oxidative stress in LLC-PK1 pig kidney cells which was again reduced by addition of 300  $\mu\text{M}$  benfotiamine (Figure 18 B).

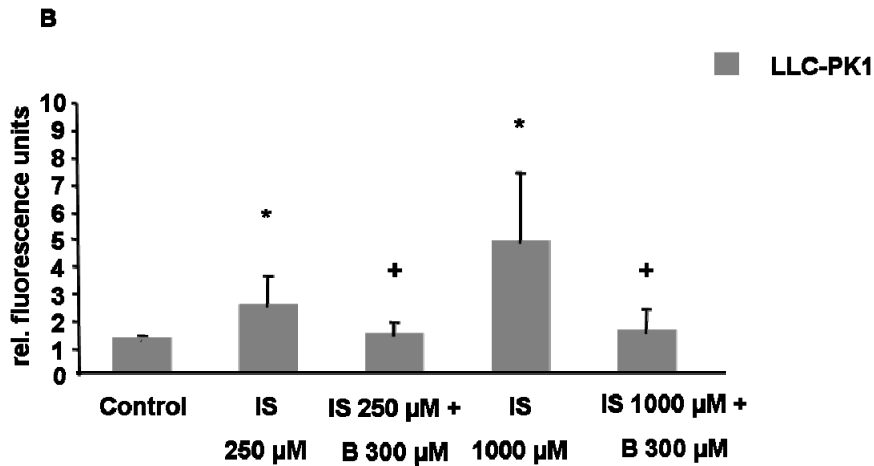


**Figure 18 B:** Oxidative stress induced by indoxyl sulfate (IS) alone and in combination with benfotiamine (B) in LLC-PK1 cells. Shown are means  $\pm$  standard deviation of three independent experiments. Significance ( $p \leq 0.05$ ) compared to the control is shown by “\*”, significant reduction ( $p \leq 0.05$ ) of the induced effect by “+”.

Generation of oxidative stress by 200 nM angiotensin II was completely prevented by addition of 300  $\mu$ M benfotiamine (Figure 19 A) but not by thiamine (Figure 19 B).

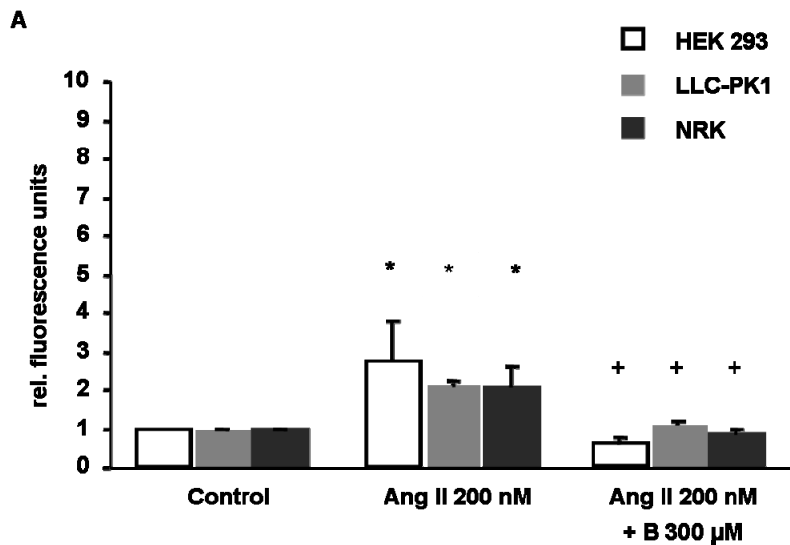


**Figure 19 A:** Oxidative stress induced by angiotensin II (Ang II) alone and in combination with benfotiamine (B) in kidney cell lines. Shown are means  $\pm$  standard deviation of three independent experiments, each normalized to its control. Significance ( $p \leq 0.05$ ) compared to the control is shown by “\*”, significant reduction ( $p \leq 0.05$ ) of the induced effect by “+” and not significant induction or reduction by “n. s.”.

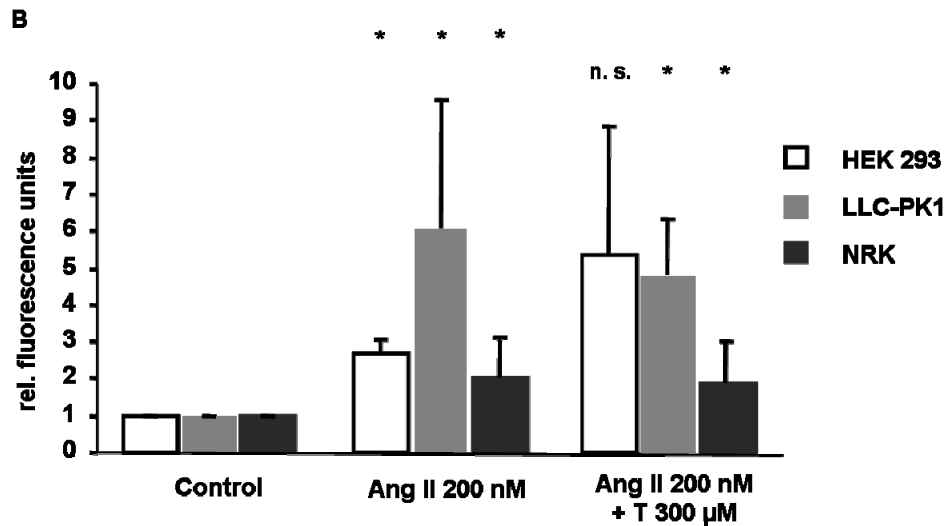


**Figure 19 B:** Oxidative stress induced by angiotensin II (Ang II) alone and in combination thiamine (T) in kidney cell lines. Shown are means  $\pm$  standard deviation of three independent experiments, each normalized to its control. Significance ( $p \leq 0.05$ ) compared to the control is shown by “\*”, significant reduction ( $p \leq 0.05$ ) of the induced effect by “+” and not significant induction or reduction by “n. s.”.

These findings imply a direct antioxidant action of benfotiamine which was confirmed in the photometric FRAP assay, which shows that under acid conditions benfotiamine, but not thiamine is able to reduce the ferric-tripyridyltriazine complex to its ferrous, coloured form (Figure 20).

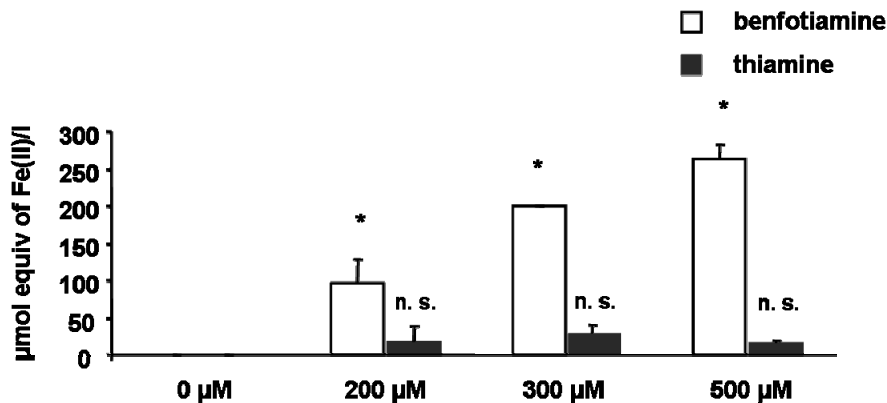


**Figure 20:** Ferric reducing ability of cell-free solutions of benfotiamine or thiamine in various concentrations assessed by utilisation of the photometric FRAP-assay. Shown are means  $\pm$  standard deviation of three independent experiments, significant increase in antioxidative capacity ( $p \leq 0.05$ ) compared to the control is shown by “\*”, not significant increase by “n. s.”.

#### 4.1.3.2. Genomic damage - Benfotiamine

For investigation of biological consequences of the antioxidant effect of benfotiamine, comet assay experiments were performed. 200 nM angiotensin II significantly induced DNA-damage in all three cell lines, which was completely prevented by co-treatment with 300  $\mu$ M benfotiamine but not by co-treatment with thiamine except in NRK cells (Figures 21 A and B).

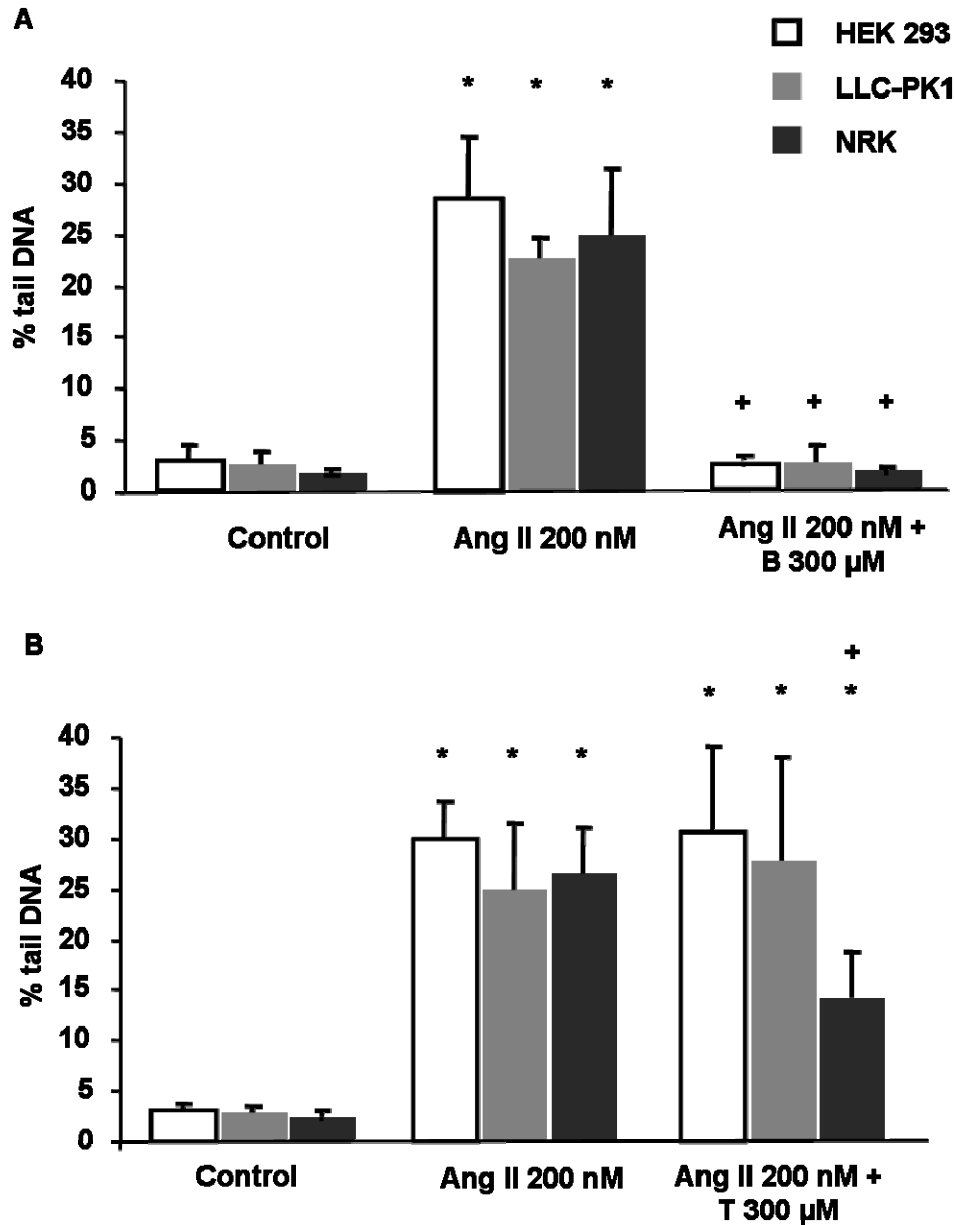


**Figure 21:** Comet assay analysis of angiotensin II (Ang II)-induced DNA-damage with and without addition of (A) benfotiamine (B) or (B) thiamine (T) in three kidney cell lines. Shown are means  $\pm$  standard deviation of three independent experiments. Significance ( $p \leq 0.05$ ) compared to the control is shown by “\*”, significant reduction ( $p \leq 0.05$ ) of the induced effect by “+”.

To include a second endpoint for genotoxicity the micronucleus test was performed. After 200 nM angiotensin II, again a significant increase of micronucleated cells was found in all three cell lines and this effect was prevented by addition of 300  $\mu$ M benfotiamine, but not by co-treatment with thiamine (Figures 22 A and B).

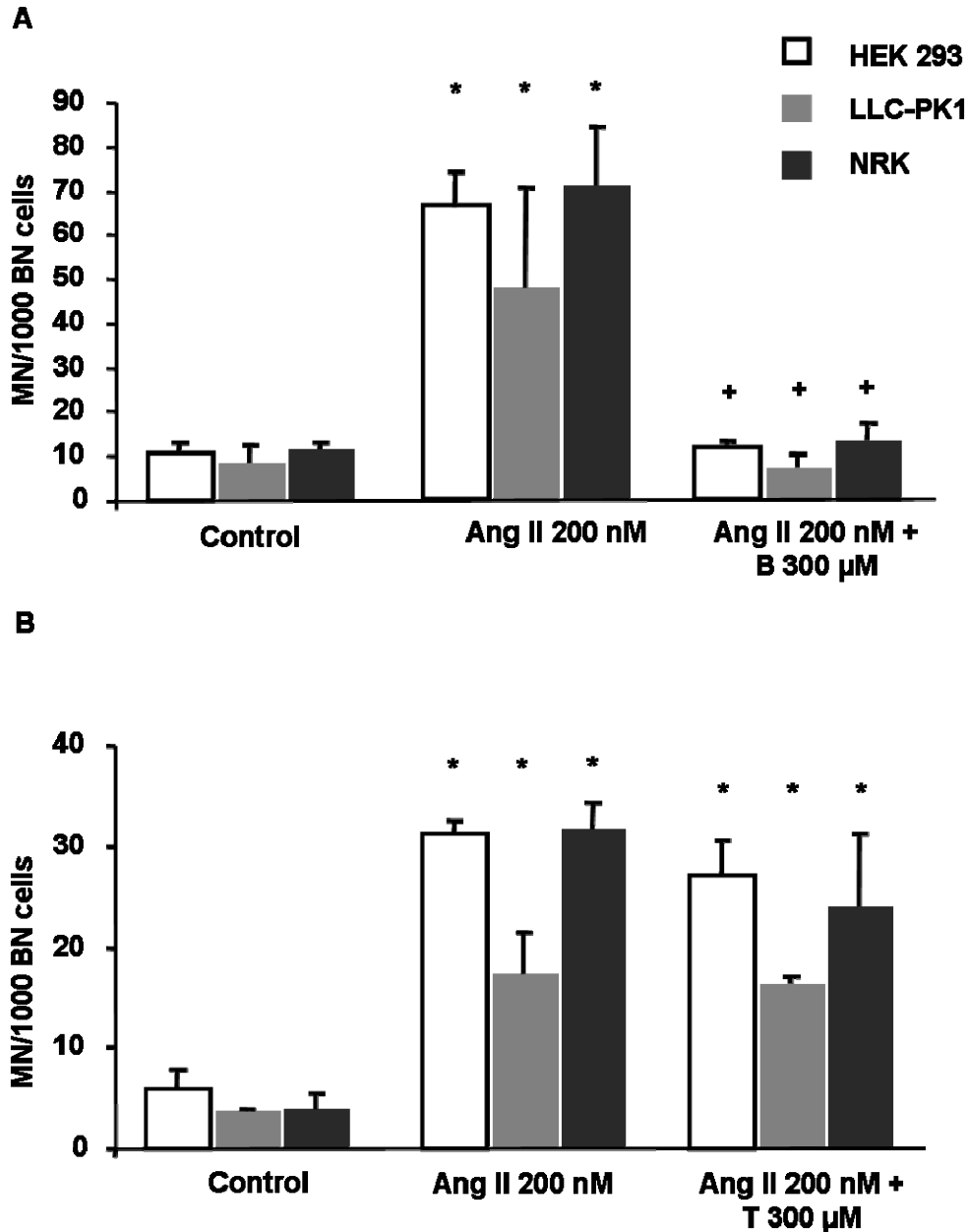


**Figure 22:** Micronucleus induction by angiotensin II (Ang II) with and without addition of (A) benfotiamine (B) or (B) thiamine (T) in three kidney cell lines. Shown are means  $\pm$  standard deviation of three independent experiments. Significance ( $p \leq 0.05$ ) compared to the control is shown by “\*”, significant reduction ( $p \leq 0.05$ ) of the induced effect by “+”.

#### 4.1.3.3. Apoptosis and Proliferation - Benfotiamine

On the same slides that had been analyzed for micronuclei, the presence of apoptotic cells as detected by morphological appearance was quantified for all treatments. 200 nM angiotensin II induced an increase in apoptosis in HEK cells and in LLC-PK1 cells, which was not significant due to inter-experimental variation (Table 1). In HEK cells, this increase was reduced by addition of benfotiamine. Furthermore, the cytokinesis block proliferation index (CBPI) was calculated after assessment of numbers of cells with one, two, three and more nuclei on the same slides and was found not to be altered by any of the treatments in all three cell lines (Table 1).

**Table 1:** Frequency of apoptosis and cytochalasin B proliferation index (CBPI) in the micronucleus experiments with three different renal cell lines. Shown are means  $\pm$  standard deviation of three independent experiments. Ang II = angiotensin II; B = benfotiamine.

Cell line	Treatment (concentration)	Apoptotic cells (%)	CBPI
HEK	Control	4.2 $\pm$ 2.0	2.0 $\pm$ 0.02
	Ang II 200nM	28.3 $\pm$ 33.9	2.2 $\pm$ 0.06
	Ang II 200nM + B 300 $\mu$ M	12.5 $\pm$ 8.8	2.1 $\pm$ 0.04
LLC-PK1	Control	7.5 $\pm$ 1.8	2.0 $\pm$ 0.01
	Ang II 200nM	15.3 $\pm$ 11.5	2.0 $\pm$ 0.02
	Ang II 200nM + B 300 $\mu$ M	12.3 $\pm$ 5.9	2.0 $\pm$ 0.004
NRK	Control	3.3 $\pm$ 3.3	2.0 $\pm$ 0.04
	Ang II 200nM	4.7 $\pm$ 3.0	2.1 $\pm$ 0.02
	Ang II 200nM + B 300 $\mu$ M	3.7 $\pm$ 2.5	2.0 $\pm$ 0.02

#### 4.1.3.4. Transketolase expression and activity - Benfotiamine

Since benfotiamine is thought to activate transketolase and thereby reduce concentrations of advanced glycation end products (AGEs) in experimental diabetes, we investigated the expression of transketolase using semi-quantitative reverse transcriptase PCR. Density measurement of the DNA bands showed an increase of transketolase gene expression in cells treated with 300  $\mu$ M benfotiamine and 200 nM

angiotensin II plus 300  $\mu$ M benfotiamine compared to the untreated control and angiotensin II treatment alone (Figure 23 A).

Measurements of transketolase activity showed a significant increase in all three cell lines when treated with 300  $\mu$ M benfotiamine and in LLC-PK1 and NRK cells when treated with 300  $\mu$ M thiamine. Furthermore, a significant increase could be observed in LLC-PK1 cells treated with 200 nM angiotensin II and 300  $\mu$ M benfotiamine simultaneously (Figure 23 B).

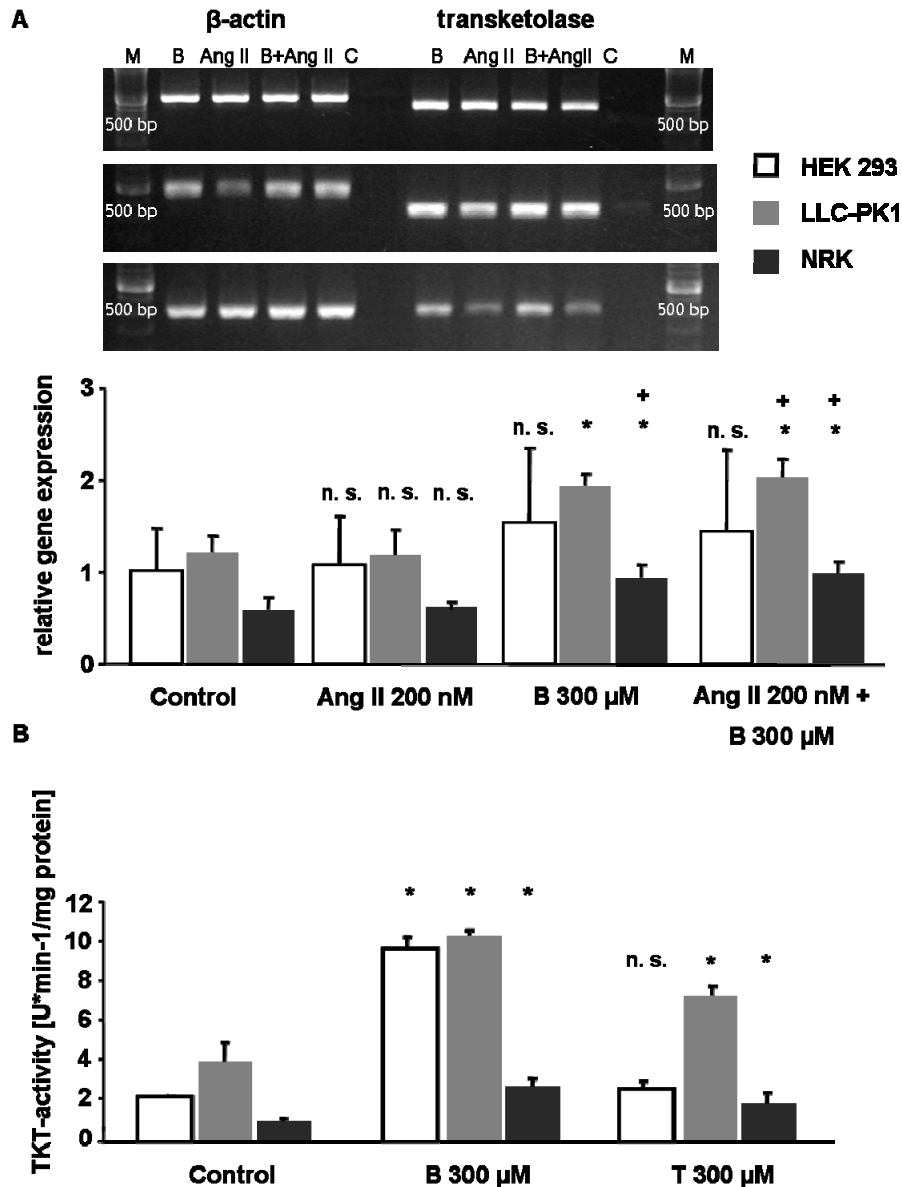


**Figure 23:** Transketolase expression in three kidney cell lines after treatment with angiotensin II (Ang II) or benfotiamine (B) alone and angiotensin II in combination with benfotiamine. Quantification of band densities derived from three independent experiments (with standard deviations, normalized to the housekeeping enzyme  $\beta$ -actin) are shown in (A). Transketolase activity corresponding to protein concentration in kidney cell lines after treatment with benfotiamine (B) or thiamine (T) is shown in (B). Shown are means  $\pm$  standard deviation of three independent experiments. Significance ( $p \leq 0.05$ ) compared to the control is shown by “\*”, significance compared to angiotensin II ( $p \leq 0.05$ ) by “+” and not significant induction compared to the control by “n. s.”. M = Marker; C = Control.



#### 4.1.3.5. Oxidative Stress – $\alpha$ -Tocopherol

The measurement of oxidative stress in the three different kidney cell lines revealed, as shown before that 200 nM angiotensin II was able to significantly induce the release of reactive oxygen species compared to the untreated control. Furthermore, the simultaneous incubation with angiotensin II and  $\alpha$ -tocopherol in a concentration of 750  $\mu$ M yielded a significant decrease of oxidative stress compared to the angiotensin II-treatment,  $\alpha$ -tocopherol alone induced no effect compared to the untreated control (Figure 24).

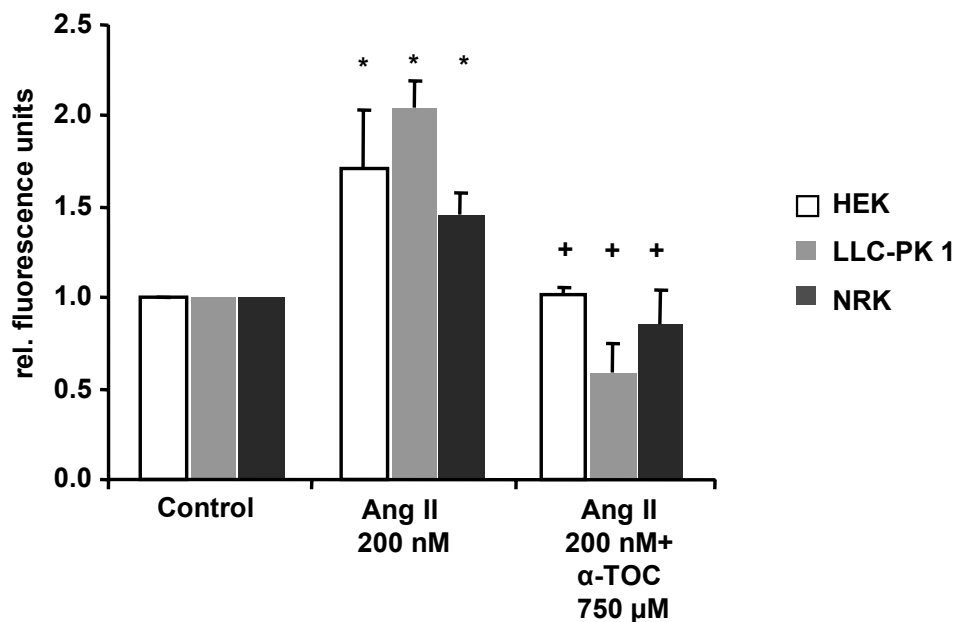


**Figure 24:** Oxidative stress induced by angiotensin II (Ang II) alone and in combination with  $\alpha$ -tocopherol ( $\alpha$ -TOC) in HEK, NRK and LLC-PK1 cells. Shown are means  $\pm$  standard deviation of three independent experiments, each normalized to its control. Significance ( $p \leq 0.05$ ) compared to the control is shown by “\*”, significant reduction ( $p \leq 0.05$ ) of the induced effect by “+”.

As literature research indicated a direct antioxidant capacity of  $\alpha$ -tocopherol, the cell-free FRAP-Assay was performed additionally. This experiment showed that compared to a solution containing no  $\alpha$ -tocopherol, the antioxidative capacity increased significantly from concentrations of 200  $\mu$ M on (Figure 25).

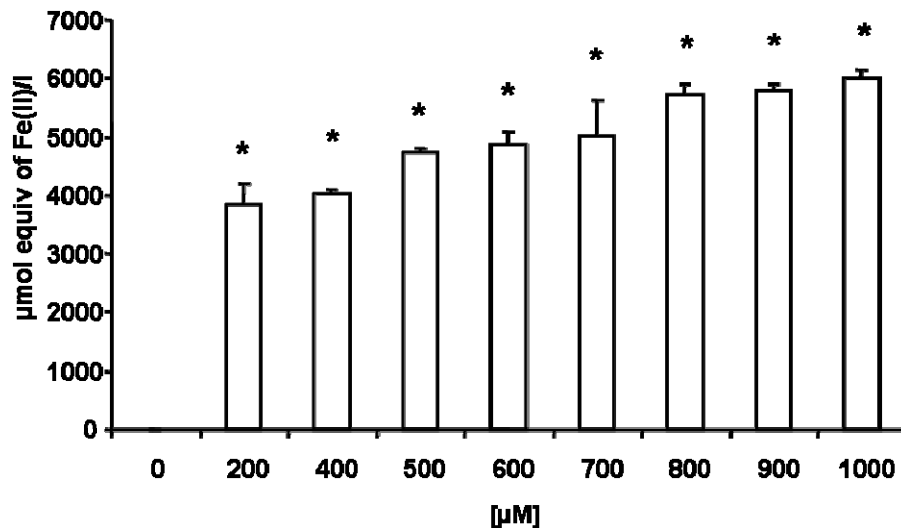


**Figure 25:** Ferric reducing ability of cell-free solutions of  $\alpha$ -tocopherol in various concentrations assessed by utilisation of the photometric FRAP-assay. Shown are means  $\pm$  standard deviation of three independent experiments, significant increase in antioxidative capacity ( $p \leq 0.05$ ) compared to the control is shown by “\*”.

#### 4.1.3.6. Genomic damage – $\alpha$ -Tocopherol

To assess the ability of  $\alpha$ -tocopherol to prevent genomic damage, DNA strand breaks were induced by 200 nM angiotensin II. Comet Assay analysis revealed that the significant increase in strand breaks caused by angiotensin II-treatment could be completely prevented by co-incubation with 750  $\mu$ M  $\alpha$ -tocopherol, which induced no damage when incubated alone, in all three cell lines, (Figure 26).

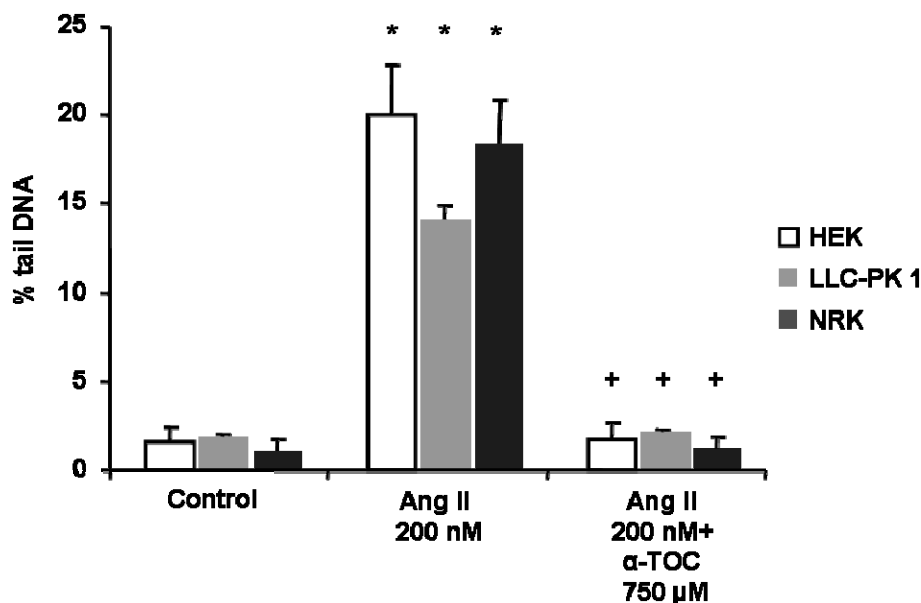


**Figure 26:** Comet assay analysis of angiotensin II (Ang II)-induced DNA-damage with and without addition of  $\alpha$ -tocopherol ( $\alpha$ -TOC) in three kidney cell lines. Shown are means  $\pm$  standard deviation of three independent experiments. Significance ( $p \leq 0.05$ ) compared to the control is shown by “\*”, significant reduction ( $p \leq 0.05$ ) of the induced effect by “+”.

In the micronucleus frequency test, the second endpoint for genotoxic effects, a significant increase in chromosomal aberrations manifesting themselves as micronuclei, could be observed after treatment with 200 nM angiotensin II and an also significant decrease after co-incubation with angiotensin II and 750  $\mu$ M  $\alpha$ -tocopherol, which again had no effect when incubated alone (Figure 27).

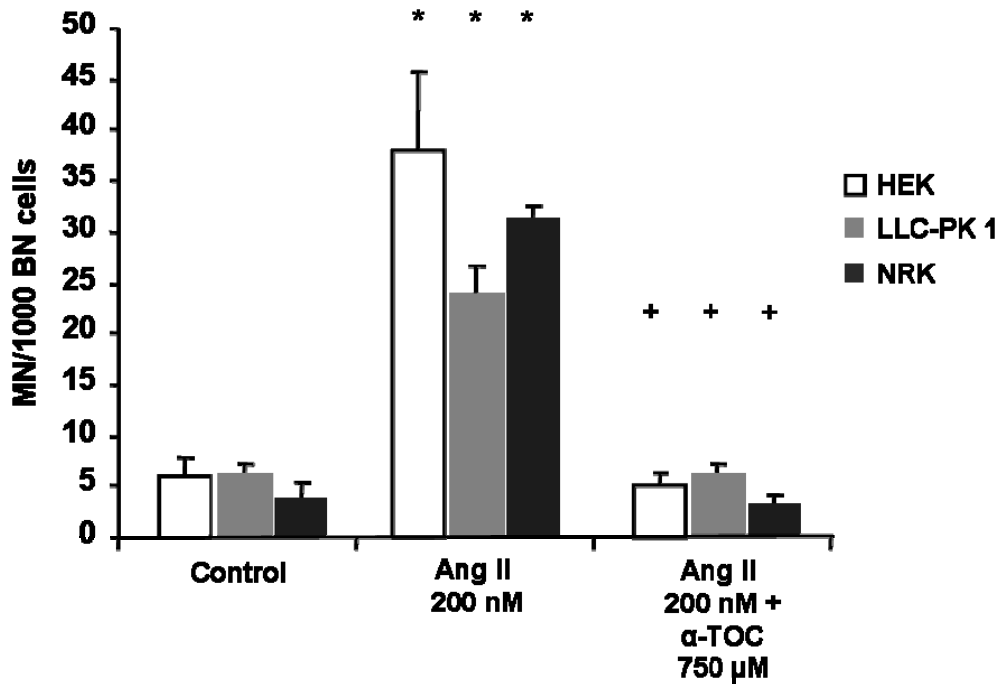


**Figure 27:** Micronucleus induction by angiotensin II (Ang II) with and without addition of  $\alpha$ -tocopherol ( $\alpha$ -TOC) in three kidney cell lines. Shown are means  $\pm$  standard deviation of three independent experiments. Significance ( $p \leq 0.05$ ) compared to the control is shown by “\*”, significant reduction ( $p \leq 0.05$ ) of the induced effect by “+”.

#### 4.1.3.7. Apoptosis and proliferation – $\alpha$ -Tocopherol

The evaluation of apoptosis and proliferation indicated that angiotensin II in a concentration of 200 nM induced an increase in apoptosis in HEK and NRK cells, which was again not significant due to variations from experiment to experiment and this time could not be reduced by simultaneous treatment with  $\alpha$ -tocopherol. The proliferation index was not affected by treatment with the test substances (Table 2).

**Table 2:** Frequency of apoptosis and cytochalasin B proliferation index (CBPI) in the micronucleus experiments with three different renal cell lines. Shown are means  $\pm$  standard deviation of three independent experiments. Ang II = angiotensin II;  $\alpha$ -TOC =  $\alpha$ -tocopherol.

Cell line	Treatment (concentration)	Apoptotic cells (%)	CBPI
<b>HEK</b>	Control	6.8 $\pm$ 1.3	2.0 $\pm$ 0.05
	Ang II 200nM	9.3 $\pm$ 5.8	2.1 $\pm$ 0.06
	Ang II 200nM + $\alpha$ -TOC 750 $\mu$ M	9.3 $\pm$ 5.3	2.0 $\pm$ 0.02
<b>LLC-PK1</b>	Control	9.5 $\pm$ 2.8	2.0 $\pm$ 0.01
	Ang II 200nM	7.5 $\pm$ 2.3	2.0 $\pm$ 0.02
	Ang II 200nM + $\alpha$ -TOC 750 $\mu$ M	4.0 $\pm$ 1.9	2.0 $\pm$ 0.004
<b>NRK</b>	Control	5.5 $\pm$ 1.0	1.92 $\pm$ 0.03
	Ang II 200nM	12.0 $\pm$ 1.9	1.93 $\pm$ 0.07
	Ang II 200nM + $\alpha$ -TOC 750 $\mu$ M	13.0 $\pm$ 4.1	1.92 $\pm$ 0.03

#### 4.1.4. Discussion

Potential antioxidative effects of benfotiamine were explored by inducing oxidative stress and DNA damage in human, rat and porcine renal cells, with and without addition of benfotiamine. Oxidative stress was induced by three different agents, the mutagenic model compound NQO [114], the uremic toxin indoxyl sulfate [115] and the peptide hormone angiotensin II, which is enhanced in diabetes due to RAAS stimulation [116]. Genomic damage, evaluated by comet- and micronucleus-formation, was also investigated after treatment of cells with angiotensin II. Benfotiamine was able to reduce oxidative stress and genomic damage exerted by these agents. Since the vitamin B1-prodrug was only active upon simultaneous treatment with NQO and not if limited to a pre-treatment, a direct antioxidant activity could be inferred. This was confirmed in the FRAP assay, which is a cell-free assay. The feasible oxidation of thiamine to thiochromes by iron (III) is of little importance in this case because all *in vitro* experiments were conducted under neutral conditions and the cell free FRAP assay under acid conditions, meaning that the thiochromes are not likely to form. To our knowledge, no comparable data concerning a direct antioxidant capacity of benfotiamine has been published to date.

In comparison to the antioxidant vitamin C, benfotiamine shows a ten-fold lower antioxidative capacity in the FRAP assay ( $2391 \pm 67$  vs.  $200 \pm 1$   $\mu\text{mol}$  equiv of Fe(II)/l). So it is assumable that its antioxidative capacity, because low, is not the only means by which benfotiamine exerts direct antioxidant effects. Angiotensin II induces oxidative stress and genomic damage via the AT<sub>1</sub>R [47], subsequently activating phospholipase C (PLC), protein kinase C (PKC) and NAD(P)H oxidase. In an *in vivo* study with male Sprague-Dawley rats with streptozotocin-induced diabetes mellitus, activation of protein kinase C and its suppression by high dose benfotiamine treatment was observed [133]. This ability of benfotiamine to suppress increased PKC activation may contribute to our findings of the direct antioxidative effect.

Furthermore, an increased transketolase activity could be observed in samples incubated with benfotiamine or thiamine. This is in line with previously published findings [134]. In addition, the elevated transketolase expression after co-incubation with angiotensin II and benfotiamine corresponds to the published effects in experimental diabetes [135].

Thiamine in contrast to benfotiamine showed neither antioxidant potential in the cellular assays nor in the cell-free assay, while it did increase transketolase expression and activity. These observations also show that the up-regulation of transketolase, while surely important in the organism in antagonizing AGEs, is not responsible for the protective effects of benfotiamine against oxidative stress, because thiamine is ineffective in this regard.

It is conceivable that benfotiamine supplementation of diabetic patients reduces the clinical complications, including peripheral neuropathy [108, 136], at least in part due to its antioxidant effect. Possibly, a reduction of genomic damage could also be achieved *in vivo*, offering a form of cancer-prevention to diabetes patients.

Glycation and oxidative stress are two important processes known to play a key role in complications of many pathological processes. Collective evidence from the literature reveals that  $\alpha$ -tocopherol among others mitigates the process of protein glycation. Therefore, in an additional series of experiments, the antioxidative effects of  $\alpha$ -tocopherol were analyzed by induction of oxidative stress and DNA damage in the previously introduced human, rat and porcine kidney cells. The widely known antioxidative effect of  $\alpha$ -tocopherol was confirmed in the cell free FRAP assay, where it showed a 3-fold higher antioxidative capacity as vitamin C ( $2391 \pm 67$  vs.  $200 \pm 1$   $\mu\text{mol}$  equiv of  $\text{Fe(II)/I}$ ). Furthermore oxidative stress in human, rat and porcine renal cells induced by the peptide hormone angiotensin II, which is often elevated in hypertensive patients, could be prevented [127]. Genomic damage, evaluated by comet assay and micronucleus frequency test, was also investigated after treatment of cells with angiotensin II alone and together with  $\alpha$ -tocopherol.  $\alpha$ -Tocopherol was able to reduce the genomic damage occurring subsequently to oxidative stress exerted by the peptide hormone angiotensin II. This is in contrast to recent findings in large human studies, where  $\alpha$ -tocopherol was effective only in subgroups of patients suffering for example from a genetic polymorphism [137] or in individuals with poor or suboptimal nutritional status [138] or where its effects were limited to the amelioration of symptoms and could not prevent late complications [139]. Our findings indicate that  $\alpha$ -tocopherol - at least *in vitro* - is able to prevent the formation of DNA strand breaks and micronuclei, succeeding the release of reactive oxygen species, which may be associated with the development of cancer [140].

## **5. Receptor Blockade – Angiotensin II Type 1 Receptor (AT<sub>1</sub>R)**

### ***5.1. Angiotensin II-induced genomic damage in renal cells can be prevented by angiotensin II type 1 receptor blockade or radical scavenging***

#### **5.1.1. Background**

Epidemiological studies exploring the connection between hypertension and cancer incidence found a higher cancer mortality in hypertensive patients [141] and an increased risk to develop kidney cancer [50, 51]. In most patients with hypertension, the activity of renin is either inappropriately normal (in relation to sodium balance) or even elevated [142]. Elevated levels are a typical feature of patients with renoparenchymal, especially renal vascular, hypertension. In particular the renoprotection by blockade of the renin-angiotensin-aldosterone system (RAAS) in hypertension supports the role of a stimulated RAAS [143]. Angiotensin II is one of the oldest known peptide hormones. It is generated from the precursor protein angiotensinogen, predominantly by the actions of renin and angiotensin converting enzyme (ACE). Angiotensin II, the main effector of the RAAS, is a major regulator of blood pressure and cardiovascular homeostasis, and can cause hypertension and kidney diseases. Beside the systemic RAAS, which produces the plasma angiotensin II, a functional local RAAS, and accordingly a local angiotensin II production, has been found in various organs, for example in the kidney, heart, and brain [53, 144].

The actions of angiotensin II are mediated by two receptor molecules, the angiotensin II type 1 receptor (AT<sub>1</sub>R) and the angiotensin II type 2 receptor (AT<sub>2</sub>R). AT<sub>1</sub>R are expressed in many tissues, while AT<sub>2</sub>R are highest in fetal tissues [55]. All classic physiological effects of angiotensin II, such as vasoconstriction, aldosterone and vasopressin release, sodium and water retention, are mediated by the AT<sub>1</sub>R. Via this receptor, angiotensin II is also involved in cell proliferation, nephrosclerosis, endothelial dysfunction, and processes leading to athero-thrombosis. The AT<sub>2</sub>R often functions as a counter-regulatory receptor and is involved in, for example, cell differentiation, and apoptosis [145, 146].

In proximal tubule cells, activation of the AT<sub>1</sub>R by angiotensin II led to the induction of NAD(P)H oxidase, a multi-enzyme complex which enhances intracellular synthesis of reactive oxygen species (ROS) [147]. Increased formation of ROS, of various aetiology, is associated with the induction of genomic damage [148].

The following study was undertaken to characterize the genotoxic effects of angiotensin II *in vitro* in the epithelial porcine kidney cell line LLC-PK1. We hypothesize these effects to be mediated by the AT<sub>1</sub>R, which upon activation causes oxidative stress. To prove this, we modulated the genotoxicity of angiotensin II with an AT<sub>1</sub>R antagonist and with antioxidants. Two standard genotoxicity assays were employed: the micronucleus frequency test, which detects a subset of chromosomal aberrations, inherited to the first generation of daughter cells after mitosis and the comet assay, which detects structural DNA damage, which may partially or completely be transient, then leading to repair before mitosis or to cell death.



## **5.1.2. Experimental**

### **5.1.2.1. Material**

If not mentioned otherwise, all chemicals were purchased from Sigma-Aldrich, Taufkirchen, Germany. Candesartan was provided by AstraZeneca, Wedel, Germany.

### **5.1.2.2. Cell culture**

LLC-PK1 cells, an epithelial porcine kidney cell line with proximal tubule properties, were obtained from ATCC and grown as described by [128]. For experiments, 10<sup>6</sup> cells were treated with test compounds in 5 ml culture medium. The cells were harvested after 24 h incubation with tested compounds for the comet assay and after 48 h for the micronucleus frequency test.

HL-60 cells (human promyelocytic cells) were kindly donated by Prof. R. Schinzel, Vasopharm, Würzburg, Germany. They were grown in RPMI medium, supplemented with 10 % fetal calf serum, 1 % glutamine and antibiotics. NRK cells, an epithelial rat kidney cell line with proximal tubule properties were obtained from ECACC and grown in DMEM medium (4.5 g glucose/l), supplemented with 10 % fetal calf serum, 1 % glutamine, 1 % non-essential amino acids and antibiotics.

All cells were routinely split twice a week to keep the exponential growth conditions and except for HL-60 (forty passages) were cultured for no more than twenty passages after thawing them from stock.

### **5.1.2.3. Comet assay**

The comet assay was carried out according to Singh et al. [94], with slight modifications, as described earlier [128]. A fluorescence microscope at 200-fold magnification and a computer-aided image analysis system (Komet 5, Kinetic Imaging LTD, Liverpool, UK) were used for analysis. 50 cells in total (25 per slide) were analyzed and results were expressed as percentage of DNA in the tail region.

#### **5.1.2.4. Micronucleus frequency test**

Cells were incubated for 48 h with the tested compounds, after 24 h 5 µg/ml cytochalasin B was added to obtain binucleated cells (BN). For the analysis of the effect of α-tocopherol on angiotensin II-induced micronuclei the cells were incubated for 24 hours simultaneously with test compounds and cytochalasin B. After this incubation, the cells were brought onto glass slides by cytopspin centrifugation and fixed with methanol (-20 °C, 1 h). For staining, the slides were incubated with acridine orange (62.5 µg/ml in Sørensen buffer, pH 6.8) for 5 min, washed twice with Sørensen buffer for 5 min, and mounted for microscopy. The frequency of micronuclei was obtained after scoring 1000 BN cells on each of two slides. The averages of three independent experiments are shown.

#### **5.1.2.5. Quantification of apoptotic cells**

During the analysis of the slides prepared for the micronucleus frequency test, also cells with nuclei which show characteristics of apoptotic nuclei (highly condensed chromatin) were counted and their number was referred to 1000 BN cells.

#### **5.1.2.6. Proliferation index**

Furthermore, the slides prepared for the micronucleus frequency test were used to calculate the proliferation index of the cells treated with angiotensin II, using the following formula:

$$\text{CBPI} = \frac{(\text{mononucleated cells} * 1) + (\text{binucleated cells} * 2) + (\text{polynucleated cells} * 3)}{\text{total cell number}}$$

The result is the proliferation index (CBPI).

#### **5.1.2.7. RT-PCR experiments**

The expression of mRNA was detected using the reverse transcription polymerase reaction (RT-PCR). Total RNA was isolated from LLC-PK1 cells with the RNeasy mini kit (Qiagen, Hilden, Germany) and 2.5 µg of RNA was used for cDNA synthesis using

RevertAid™ First Strand cDNA Synthesis Kit (Fermentas GmbH, St. Leon-Rot, Germany).

Sequences, annealing temperatures and PCR conditions were:

AT<sub>1</sub> receptor (D11340, 54 °C, 35 cycles, 664 bp)

For: 5'-ATACCAGAGCCTCCAGCTCA-3'; Rev: 5'-CCAGCGGTATTCCATAGCAG-3';

AT<sub>2</sub> receptor (AF195509, 50 °C, 40 cycles, 420 bp):

For: 5'-ATCCCTGGCAAGCCTCTTAT-3'; Rev: 5'-GCTGACCATTGGGCATATTT-3'

All primers were designed with the program Primer 3 [149].

PCR products were resolved on a 1.5 % agarose gel, stained with ethidium bromide. For quantification of the mRNA the density of the bands was measured using the Gel Doc 2000 (Bio-Rad, Hercules, CA, USA).

PCR products destined for sequencing were cut out of the gel, eluted with the MinElute Gel Extraction Kit (Qiagen, Hilden, Germany) and ligated into the pGEM-T-easy vector (Promega, Madison, WI, USA) and transformed into DH5 $\alpha$  cells (Invitrogen, Carlsbad, CA, USA). After overnight culture, the plasmids were isolated using the HighSpeed Plasmid Midi Kit (Qiagen, Hilden, Germany) and were sent to MWG-Biotech (Ebersberg, Germany) for sequencing.

#### **5.1.2.8. Flow cytometric analysis of oxidative stress**

2',7'-Dichlorodihydrofluorescein diacetate (H<sub>2</sub>DCF-DA) was used to detect ROS production in cells. LLC-PK1 cells were pre-incubated with 10  $\mu$ M H<sub>2</sub>DCF-DA for 5 min at 37 °C and then angiotensin II alone, or together with N-acetylcysteine (NAC) or candesartan, was added for additional 4 h. As a positive control 0.5 M hydrogen peroxide was used after an incubation time of 30 min. For the analysis of the potential antioxidative capacity of candesartan, after the pre-incubation with H<sub>2</sub>DCF-DA, 1.25  $\mu$ M hydrogen peroxide, which yields a similar amount of ROS as 170 nM angiotensin II, alone, or together with NAC,  $\alpha$ -tocopherol or candesartan, was added for additional 30 min. Cells were harvested, washed three times with PBS/1 % BSA, and analyzed ( $3 \times 10^5$  cells/sample) by flow cytometry using a FACS LSR I (Becton-

Dickinson, Mountain View, CA, USA) after incubation for 10 min on ice with 1 µg/ml propidium iodide.

#### **5.1.2.9. Statistical analysis**

If not mentioned otherwise, data from 3 independent experiments are shown ± standard error. Statistical significance among multiple groups was tested with the nonparametric Kruskal-Wallis test. Individual groups were then tested using the Mann-Whitney test. A *P* value of ≤ 0.05 was considered significant. For calculations SPSS 13.0 was used. Analysis of flow cytometry histograms was done with the free software WinMDI 2.8 (Scripps Research Institute Cytometry Software page at <http://facs.scripps.edu/software.html>).

### 5.1.3. Results

The presence of the expression of the AT<sub>1</sub>R and the AT<sub>2</sub>R in LLC-PK1 cells was verified by RT-PCR. The obtained sequences were compared to the database GenBank, yielding 99 % identity of the LLC-PK1 AT<sub>1</sub>R to the database sequence of *Sus sp.* mRNA for AT<sub>1</sub>R and 100 % identity of the LLC-PK1 AT<sub>2</sub>R to the database sequence of *Sus sp.* mRNA for AT<sub>2</sub>R.

Angiotensin II, in our experiments with LLC-PK1, did not change cell proliferation (Table 3). Also, angiotensin II did not induce apoptosis, since the number of apoptotic cells observed under the microscope did not rise when increasing doses of angiotensin II were applied (Table 3). Of the two other cell lines HL-60 (human promyelocytic cells) and NRK (rat proximal tubule cells) also tested for apoptosis and proliferation after incubation with angiotensin II, only the NRK cells showed an induction of both apoptosis and proliferation (Table 3).

**Table 3:** Effect of 170 nM angiotensin II (Ang II) on the apoptosis and proliferation rate in human promyelocytic cells (HL-60), porcine kidney cells (LLC-PK1) and rat kidney cells (NRK). Also shown is the number of micronuclei (MN) per 1000 binucleated cells (BN) in untreated cells and in cells treated with 170 nM, as well as the magnitude of micronuclei-induction. The respective cell line was treated in the optimal way to form micronuclei with Ang II: 24 hour incubation for HL-60, 48 hour incubation for LLC-PK1 and 2 hour incubation for NRK. The values are the means of three independent experiments. n. s.: not statistically significant. (Micronuclei-experiments with HL-60 cells were performed by Nilesh Kanase, MSc).

Cell line	-fold induction of apoptoses 170 nM Ang II	-fold increase in proliferation 170 nM Ang II	MN/1000 BN Control	MN/1000 BN 170 nM Ang II	-fold induction of MN
HL-60	0.99 n.s.	1.72 n.s.	2.84 ± 0.92	11.73 ± 0.77	4.16 p ≤ 0.01
LLC-PK1	0.95 n.s.	1.57 n.s.	6.04 ± 0.59	27.00 ± 8.57	4.47 p ≤ 0.05
NRK	1.08 p ≤ 0.05	2.97 p ≤ 0.05	12.83 ± 1.48	59.00 ± 1.00	4.60 p ≤ 0.01

Angiotensin II-induced DNA damage was first measured in LLC-PK1 cells with the comet assay (Figure 28). Upon treatment with angiotensin II, a dose-dependent increase in genomic damage was demonstrated (Figure 28 B). A statistically significant genomic damage appeared at 85 nM angiotensin II and increased with higher doses.

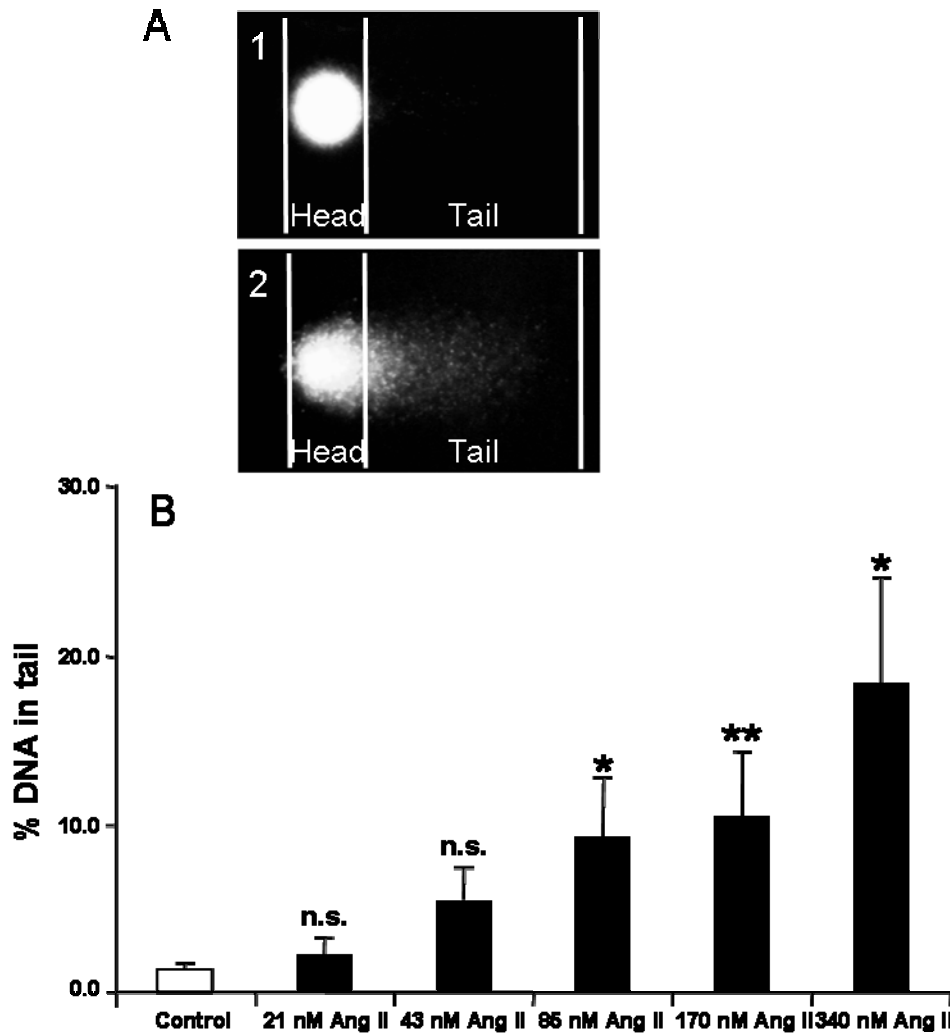


**Figure 28 A:** Representative images of a healthy (1) and a highly damaged (2) cell in the comet assay, stained with propidium iodide. A computer-aided analysis system determines the extent of migrated DNA. **B:** DNA damage in LLC-PK1 cells as measured by the comet assay, after a 24 h treatment with various concentrations of angiotensin II (Ang II). Control: no treatment. The positive control methylmethane sulfonate yielded a DNA damage of  $50.69 \pm 5.30$  % DNA in tail. \*  $p \leq 0.05$  vs. control, \*\*  $p \leq 0.01$  vs. control. (This experiment was performed by Ursula Lakner, MSc.)

To analyze the role of the AT<sub>1</sub>R in angiotensin II-induced comet formation, the AT<sub>1</sub>R antagonist candesartan (Cand) was added simultaneously with angiotensin II to the cells (Figure 29). Candesartan prevented the angiotensin II-induced genomic damage completely.

Angiotensin II is known to induce oxidative stress via its AT<sub>1</sub>R, which can lead to genomic damage. To demonstrate the participation of oxidative stress in angiotensin II-induced comet formation, the cells were co-incubated with angiotensin II and the antioxidant N-acetylcysteine (NAC). NAC, like candesartan, prevented the angiotensin II-induced genomic damage (Figure 29). Incubation with NAC or

candesartan alone did not lead to the formation of comets (data included in the figure legends).

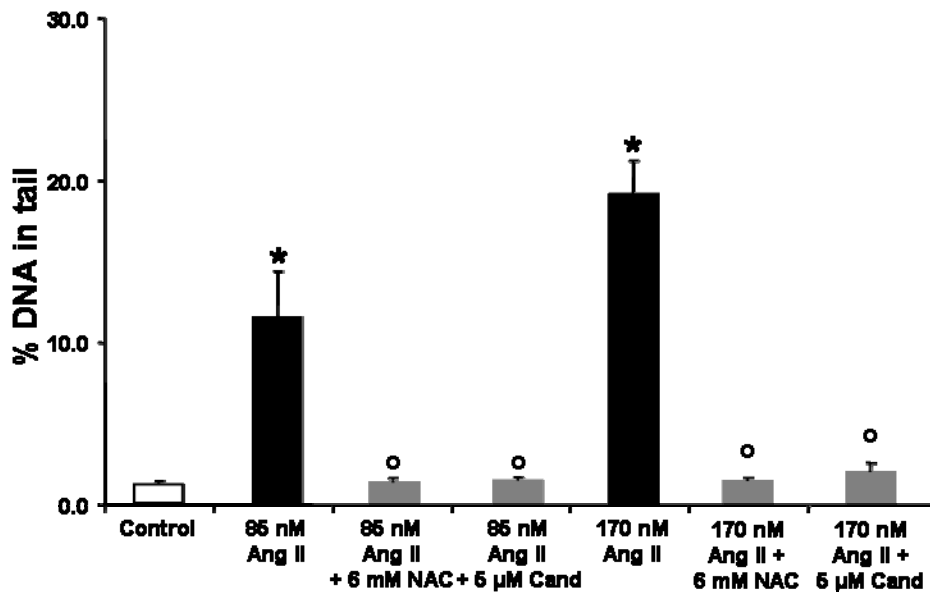


**Figure 29:** DNA damage in LLC-PK1 cells as measured by the comet assay, after 24 h treatment with two concentrations of angiotensin II (Ang II) with and without co-incubation with either 6 mM N-acetylcysteine (NAC) or 5 μM candesartan (Cand). Control: no treatment. 6 mM NAC or 5 μM candesartan alone had no effect on the DNA ( $1.04 \pm 0.07$  and  $1.11 \pm 0.35$  % DNA in tail respectively). The positive control methylmethane sulfonate yielded a DNA damage of  $62.30 \pm 2.00$  % DNA in tail. \*  $p \leq 0.05$  vs. control, °  $p \leq 0.05$  vs. Ang II treatment.

As a second method to measure DNA damage, the micronucleus frequency test was chosen. Angiotensin II caused the induction of micronuclei in LLC-PK1 cells (Figure 30), which could also be reduced by NAC and candesartan. The number of micronuclei in cells treated with 170 nM angiotensin II combined with NAC and candesartan and in cells treated with 340 nM angiotensin II combined with candesartan did not differ from the control cells. NAC was not able to prevent the induction of micronuclei caused by 340 nM angiotensin II completely, however, it did reduce them significantly.

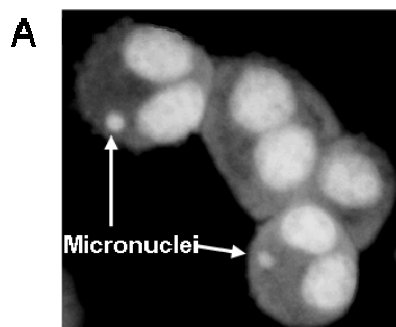


**Figure 30 A:** Representative micronuclei-containing binucleated cells, stained with acridine orange.

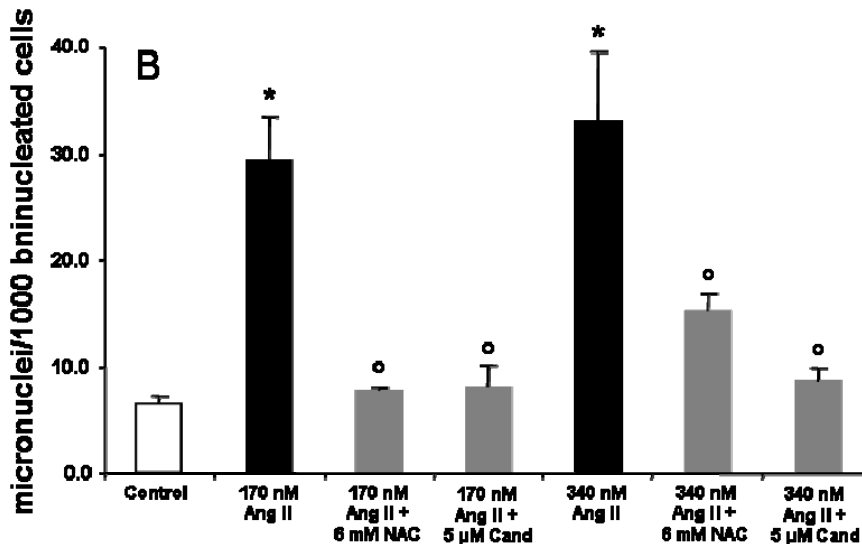


**Figure 30 B:** Micronuclei frequencies in binucleate LLC-PK1 cells after treatment for 48 hours with two angiotensin II (Ang II) concentrations with and without co-incubation with either 6 mM N-acetylcysteine (NAC) or 5 μM candesartan (Cand). After 24 h 2 μg/ml cytochalasin B was added to all samples in order to yield binucleated cells by inhibiting cytokinesis. Control: treatment only with cytochalasin B. The positive control methylmethane sulfonate yielded  $34.13 \pm 4.49$  micronuclei per 1000 binucleated cells (not shown). \*  $p \leq 0.05$  vs. control, °  $p \leq 0.05$  vs. Ang II treatment.

Since it was reported that NAC inhibits the binding of angiotensin II to AT<sub>1</sub>R due to its ability to reduce disulfide bonds [150], the effect of a second antioxidant, which contains no free sulfhydryl groups, α-tocopherol, on angiotensin II-induced DNA damage was examined. As can be seen in Figure 31 A comet formation due to angiotensin II incubation was prevented completely. Also the formation of micronuclei by 170 nM angiotensin II was inhibited (Figure 31 B).

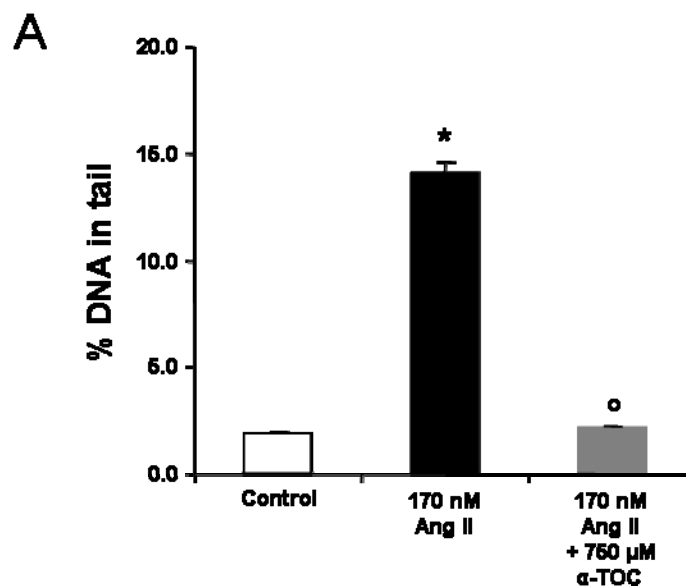


**Figure 31 A:** DNA damage in LLC-PK1 cells as measured by the comet assay, after 4 h treatment with 170 nM angiotensin II (Ang II) with and without co-incubation with 750 μM α-tocopherol (α-TOC). Control: no treatment. 750 μM (α-TOC) alone had no effect on the DNA ( $2.20 \pm 0.07$  % DNA in tail). \*  $p \leq 0.05$  vs. control, °  $p \leq 0.05$  vs. Ang II treatment.



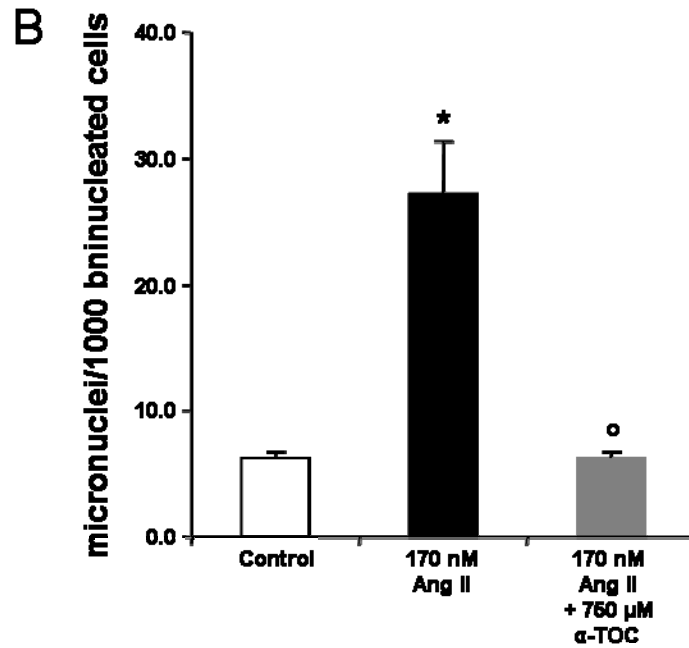


**Figure 31 B:** Micronuclei frequencies in binucleate LLC-PK1 cells after treatment for 24 hours with 170 nM angiotensin II (Ang II) with and without 750 µM α-tocopherol (α-TOC). Control: no treatment. \*  $p \leq 0.05$  vs. control, °  $p \leq 0.05$  vs. Ang II treatment.

The application of the AT<sub>2</sub>R antagonist PD 123319 to angiotensin II-treated LLC-PK1 cells showed that this substance had no effect on the angiotensin II-induced comet formation (Figure 32 A).

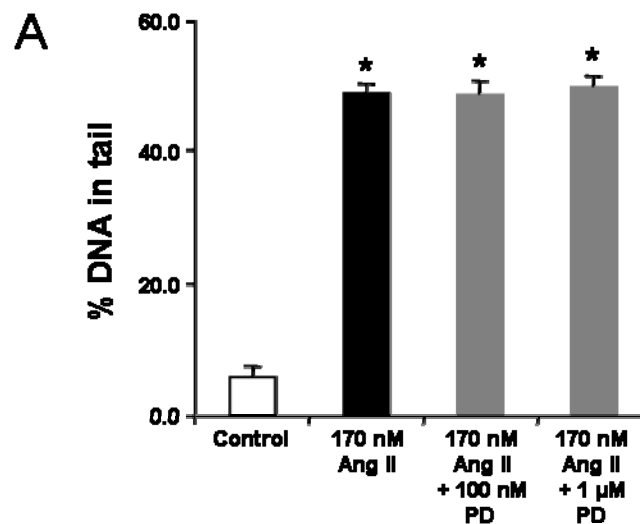


**Figure 32 A:** DNA damage in LLC-PK1 cells as measured by the comet assay, after 24 h treatment of angiotensin II (Ang II) with and without co-incubation with either 100 nM or 1 µM PD 123319 (PD). Control: no treatment. 1 µM PD 123319 alone had no effect on the DNA ( $6.24 \pm 1.37$  % DNA in tail). The positive control methylmethane sulfonate yielded a  $51.21 \pm 2.79$  fold induction of DNA damage. \*  $p \leq 0.05$  vs. control

PD 123319 lessened the angiotensin II-caused micronuclei number slightly, but was not able to reduce them significantly (Figure 32 B).

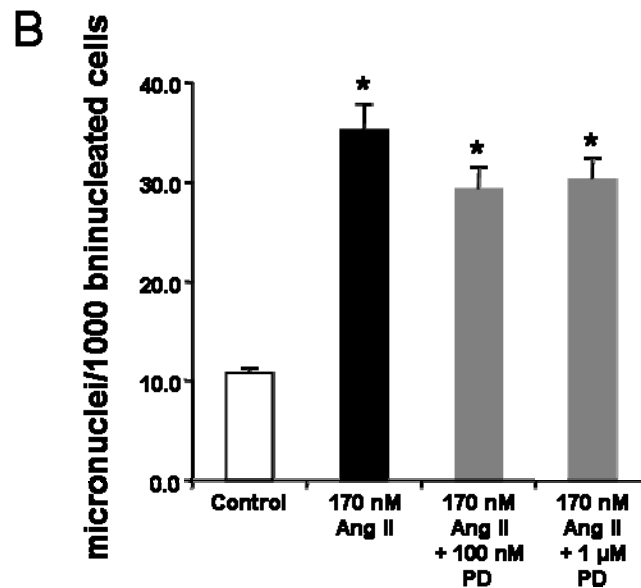


**Figure 32 B:** Micronuclei frequencies in binucleate LLC-PK1 cells after treatment for 48 hours with Ang II with and without co-incubation with either 100 nM or 1 μM PD 123319 (PD). Control: no treatment. The positive control methylmethane sulfonate (MMS) yielded  $54.33 \pm 4.21$  micronuclei.

\*  $p \leq 0.05$  vs. control. (Comet Assay- and Micronuclei-experiments with PD 123319 were performed by Nilesh Kanase, MSc.)

The induction of micronuclei by angiotensin II was confirmed in two other cell lines, HL-60 and NRK, which also showed an increase in micronuclei-containing cells (Table 3). All cell lines (HL-60, LLC-PK1 and NRK) had a similar factor of micronuclei induction around 4 (Table 3).

Since we assume that the angiotensin II-induced genomic damage is caused by the formation of reactive oxygen species (ROS) upon AT<sub>1</sub>R-mediated activation of the NAD(P)H oxidase, the generation of ROS was measured by flow cytometry. As shown in Figure 33, angiotensin II led to a significant formation of ROS, which could be prevented either by candesartan, NAC or α-tocopherol.

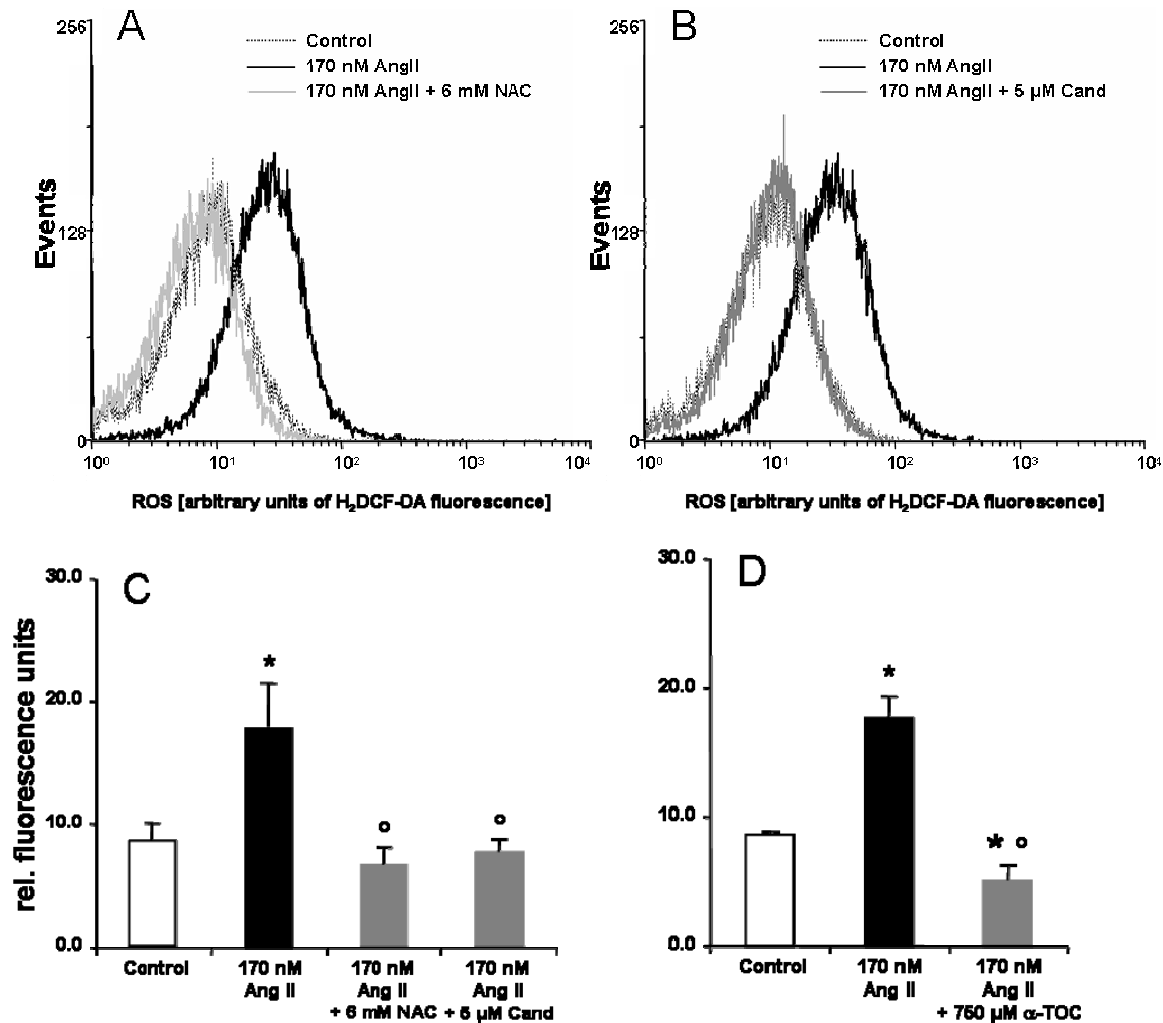


**Figure 33:** Flow cytometric analysis of angiotensin II (Ang II)-induced reactive oxygen species (ROS) production in LLC-PK1 cells. **A:** Shown is a representative frequency histogram of the green fluorescence of H<sub>2</sub>DCF-positive cells of control cells (broken line), and cells after 4 hours incubation with 170 nM Ang II without (fat solid line) and with co-incubation with 6 mM N-acetylcysteine (NAC, light grey solid line). **B:** Shown is a representative frequency histogram of the green fluorescence of H<sub>2</sub>DCF-positive cells of untreated cells (broken line), and cells after 4 hours incubation with 170 nM Ang II without (fat solid line) and with co-incubation with 5 μM candesartan (Cand, dark grey solid line). **C:** Quantification of the flow cytometry measurements by WinMDI 2.8. Shown are the relative fluorescence units. Control: treatment with only H<sub>2</sub>DCF-DA. **D:** Quantification of the flow cytometry measurements of cells incubated 4 hours with 170 nM Ang II with and without 750 μM α-tocopherol (α-TOC). Control: no treatment. \*  $p \leq 0.05$  vs. control, °  $p \leq 0.05$  vs. Ang II treatment.

To exclude the possibility of candesartan being a radical scavenger itself, a co-incubation of LLC-PK1 cells with hydrogen peroxide (H<sub>2</sub>O<sub>2</sub>) and candesartan was performed (Figures 34 A to D).

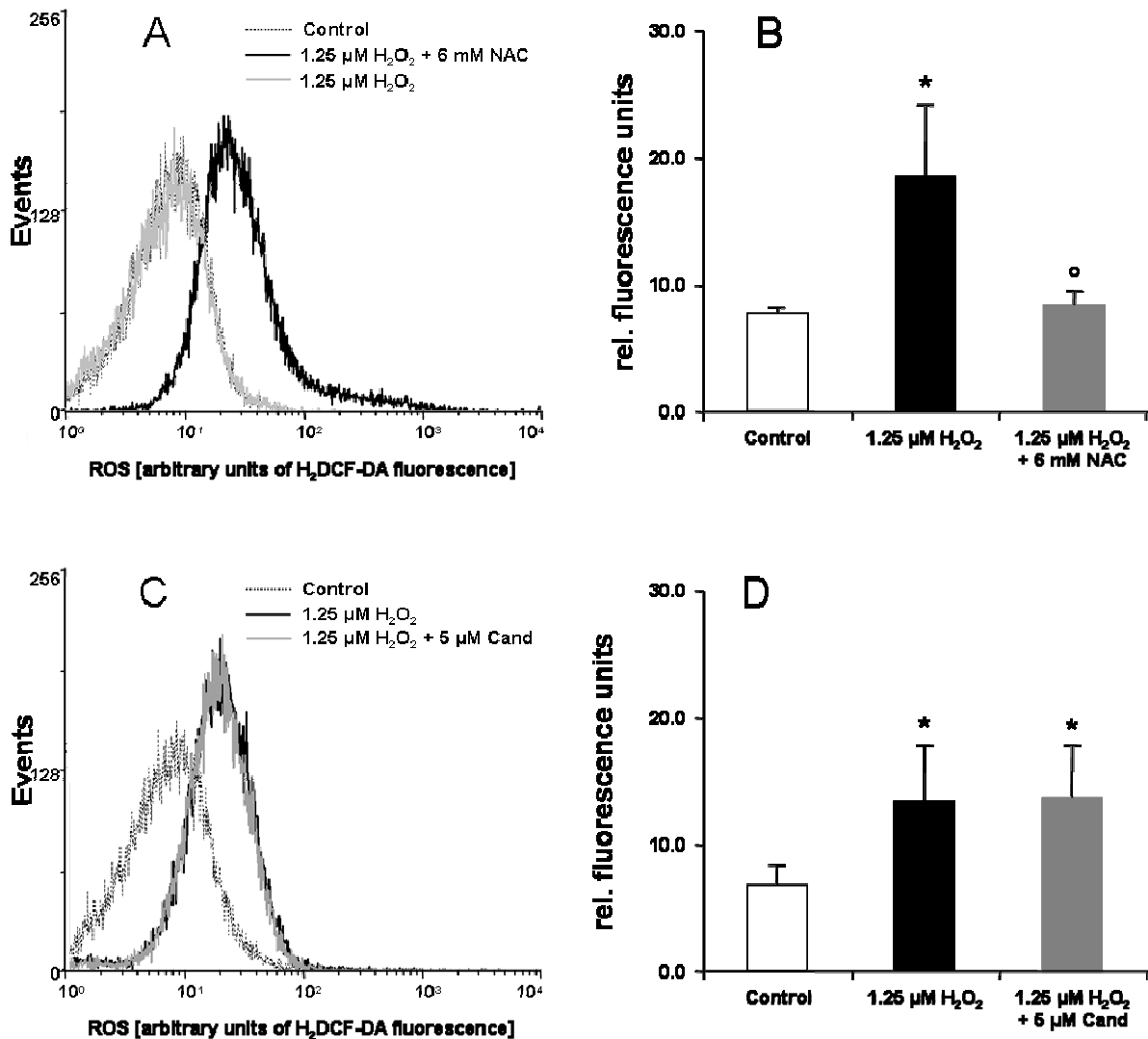


**Figure 34:** Flow cytometric analysis of a potential antioxidative effect of candesartan. **A:** Shown is a representative frequency histogram of the green fluorescence of H<sub>2</sub>DCF-positive cells of control cells (broken line), and cells after 30 min incubation with 1.25 μM hydrogen peroxide (H<sub>2</sub>O<sub>2</sub>) without (fat solid line) and with co-incubation with 6 mM N-acetylcysteine (NAC, light grey solid line). **B:** Quantification of the flow cytometry measurements by WinMDI 2.8. Shown are the relative fluorescence units. **C:** Shown is a representative frequency histogram of the green fluorescence of H<sub>2</sub>DCF-positive cells of control cells (broken line), and cells after 30 min incubation with 1.25 μM H<sub>2</sub>O<sub>2</sub> without (fat solid line) and with 5 μM candesartan (dark grey solid line). **D:** Quantification of the flow cytometry measurements by WinMDI 2.8. Shown are the relative fluorescence units. Control: treatment with only H<sub>2</sub>DCF-DA. \*  $p \leq 0.05$  vs. control, <sup>o</sup>  $p \leq 0.05$  vs. hydrogen peroxide treatment.

An H<sub>2</sub>O<sub>2</sub> concentration was chosen, which led to a shift to the right of the curve, comparable to the shift caused by 170 nM angiotensin II (see Figure 33) and which also caused DNA damage in the comet assay (Figure 34 E). The flow cytometric analysis of this experiment showed that candesartan could not reduce the H<sub>2</sub>O<sub>2</sub>-induced oxidative stress in the cells, in contrast to NAC, which could.

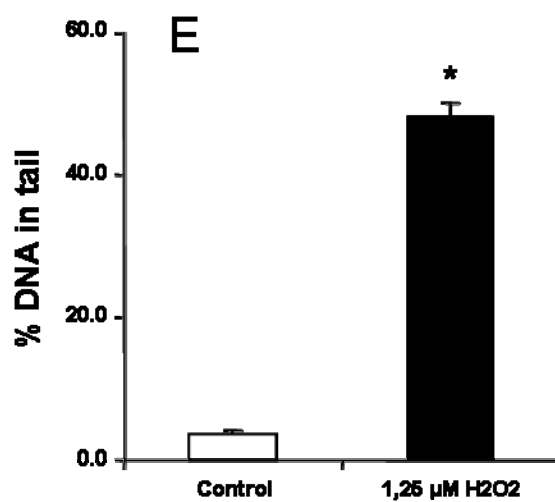


**Figure 34 E:** DNA damage in LLC-PK1 cells as measured by the comet assay, after 30 min treatment with 1.25 µM H<sub>2</sub>O<sub>2</sub>. Control: no treatment. \* p ≤ 0.05 vs. control

#### 5.1.4. Discussion

In LLC-PK1 pig kidney cells we detected with the aid of the comet assay a direct DNA damaging potential of angiotensin II. Thus, our data confirm and extend similar observations in cells of the ascending limb of the loop of Henle [151] and in microvessel endothelial cells [152]. For the first time, chromosomal mutations caused by angiotensin II as revealed by micronucleus-formation were observed. Micronuclei were induced in three different cell lines, in LLC-PK1, in rat kidney cells (NRK) and in human promyelocytic cells (HL-60).

Depending on the cell type, the stimulation of the AT<sub>1</sub>R leads to cellular contraction, hypertrophy, proliferation and/or apoptosis [153]. In LLC-PK1 angiotensin II had no impact on the proliferation or the apoptosis rate in contrast to observations by Hannken et al. [147], who detected a cell cycle arrest in LLC-PK1. This difference might be due to the presence of serum in our experiments, while Hannken et al. incubated in media containing no serum. Of the other two cell lines we analyzed for micronuclei induction with angiotensin II, only the rat kidney cells showed enhanced proliferation and apoptosis.

Co-incubation with the AT<sub>1</sub>R antagonist candesartan prevented the appearance of genomic damage detected with the comet assay and the micronucleus frequency test, while the application of the AT<sub>2</sub>R antagonist PD 123319 had no effect.

It is well known that angiotensin II binding to the AT<sub>1</sub>R induces NAD(P)H oxidases, resulting in the generation of superoxide anions [154]. This was also already demonstrated for LLC-PK1 cells [147]. Here, it is shown for the first time that the genotoxic action of angiotensin II, detected in the comet assay, and its micronuclei-inducing effect could be prevented by the antioxidants N-acetylcysteine and  $\alpha$ -tocopherol, linking the formation of ROS to the genotoxic effects.

DNA damage caused by ROS involves single- or double-stranded DNA breaks, purine, pyrimidine or desoxyribose modifications, and DNA crosslinks [8]. DNA repair, which starts after the oxidative attack on the chromosomes, often transforms the above mentioned modifications to additional strand breaks. The comet assay detects such structural DNA damage [155], which, as we have shown, was also induced by incubation with angiotensin II. Micronuclei are formed for example after double strand breaks which lead to chromosome fragments lagging behind at the anaphase during nuclear division [90]. Hydrogen peroxide induces DNA double strand breaks in a

time- and dose-dependent manner, as revealed by an antibody specifically detecting double strand breaks [156]. Superoxide anions, released after angiotensin II-mediated stimulation of NAD(P)H oxidase, are rapidly converted to hydrogen peroxide [157], which can lead to the angiotensin II-induced micronuclei.

Our evidence for angiotensin II-induced genomic damage in renal tubular cells could be of significance with regard to the increased occurrence of kidney carcinomas under an activated RAAS [50, 51]. In animal models it was shown that the concentration of angiotensin II in the kidney is 25 to 1000 times higher than in plasma [158, 159]. Under pathological conditions the angiotensin II concentration in the renal interstitial fluid of dogs can reach 800 nM [159] implying a physiological relevance of a genotoxic effect of 85 nM angiotensin II.

In the presence of hypertension the incidence of renal cancer is enhanced [160]. The potential involvement of a stimulated RAAS in the kidney is underlined by the observation that long-term treatment with diuretics is associated with an increased risk of renal cancer [141]. On the contrary, ACE inhibitors have been discussed as anticancer drugs [161], and AT<sub>1</sub>R receptor blockers have been tested in a pilot study with patients who suffer from advanced hormone-refractory prostate cancer [162, 163].

In conclusion our *in vitro* results show that angiotensin II induces genomic damage in mammalian cells, most likely via oxidative mechanisms. This injury can be prevented by AT<sub>1</sub>R blockade and by antioxidants.

## ***5.2. Angiotensin II induces DNA damage in the isolated perfused kidney***

### **5.2.1. Background**

The renin-angiotensin-aldosterone system (RAAS) plays an integral role in the homeostasis of arterial pressure, tissue perfusion, and extracellular volume. Increased levels of angiotensin II can cause hypertension and kidney diseases [47]. It is widely accepted that elevated levels of angiotensin II may contribute to the increased mortality [141] and cancer incidence [50, 51] detected in patients suffering from hypertension. We observed previously the formation of DNA damage *in vitro* following treatment with angiotensin II [47]. This damaging effect has been ascribed to the activation of the angiotensin II type 1 receptor (AT<sub>1</sub>R) with subsequent release of reactive oxygen species (ROS). ROS on their part are able to evoke oxidative DNA damage [157]. To corroborate these cell culture results in a more physiological context of an intact kidney, we examined the effect of angiotensin II in the isolated perfused mouse kidney model. The intact isolated perfused kidney is widely used for studies of renal physiology and pathophysiology in the absence of interindividual influences of systemic confounding factors [164, 165]. While the application of angiotensin II *in vivo* is accompanied by marked hemodynamic effects that might indirectly induce genotoxicity, the isolated kidney allows the observation of effects under controlled conditions, for example under a constant perfusion pressure.

The alkaline comet assay was performed for the first time with cells extracted from the isolated perfused kidney. The comet assay is a rapid, visual and quantitative method to measure DNA damage in any tissue, provided that a single cell suspension can be obtained [166, 167]. Its greatest advantage is its applicability on terminally differentiated non-dividing cells, such as cells out of the isolated perfused kidney.

As further indicators for the involvement of oxidative stress, changes of the expression of heme oxygenase or glutathione peroxidase in the isolated perfused kidneys were assessed. These two proteins are widely accepted oxidative stress markers on the protein level [168-170].

Cell culture experiments served to characterize the DNA damage caused by angiotensin II. As an alternative marker for DNA damage the activation



---

phosphorylation of histone H2AX ( $\gamma$ -H2AX) was used, which is thought to be a platform for the recruitment and/or retention of DNA repair and signalling molecules at sites of DNA damage [171]. Cleavage at oxidatively altered bases by the enzyme formamidopyrimidine DNA glycosylase (FPG) [89] is another sign for the participation of ROS in the development of the DNA damage. To show the base modifications after angiotensin II treatment, the comet assay with FPG-preincubation was carried out. Also the reparability of the angiotensin II-induced genomic lesions was investigated using the comet assay and the detection of  $\gamma$ -H2AX.

## **5.2.2. Experimental**

### **5.2.2.1. Material**

If not mentioned otherwise, all chemicals were purchased from Sigma Aldrich, Taufkirchen, Germany. Anti-phospho-Histone H2AX (flow cytometry) was purchased from Upstate/Millipore, Schwalbach/Ts., Germany, Rabbit polyclonal to gamma H2A.X (immunofluorescence) from Abcam, Cambridge, UK. Alexa-Fluor 488 goat anti-mouse IgG (flow cytometry), FITC-goat anti-rabbit IgG (immunofluorescence) and Alexa Fluor 488 C<sub>5</sub>-aminooxyacetamide, bis(triethylammonium) salt (Alexa Fluor 488 hydroxylamine) (flow cytometry) were purchased from Invitrogen, Karlsruhe, Germany. Candesartan was provided by AstraZeneca, Wedel, Germany.

### **5.2.2.2. Cell culture**

LLC-PK1, an epithelial porcine kidney cell line with proximal tubule properties, was obtained from ATCC (Rockville, USA) and grown in DMEM medium (1.0 g/l glucose) supplemented with 10 % fetal calf serum, 1 % glutamine, 25 mM HEPES buffer and antibiotics.

The cells were split routinely twice a week to ensure exponential growth and were cultured for no more than 10 passages after thawing them from stock.

### **5.2.2.3. Isolated perfused mouse kidneys**

Male C57BL/6 mice (20 - 26 g body wt, Charles River) with free access to commercial pellet chow and tap water were used as kidney donors. The animals were anesthetized with an intraperitoneal injection of 5-ethyl-5-(1-methylbutyl)-2 thiobarbituric acid (100 mg/kg; Trapanal, Byk Gulden) and ketamine HCl (80 mg/kg; Curamed, Germany) and placed on a heating table. The abdominal cavity was opened by a midline incision, and the aorta was clamped distal to the right renal artery so that the perfusion of the right kidney was not disturbed during the subsequent insertion of the perfusion cannula into the abdominal aorta distal to the clamp. The mesenteric artery was ligated, and a metal perfusion cannula (0.8 mm OD) was inserted into the abdominal aorta. After removal of the aortic clamp, the cannula was advanced to the origin of the right renal artery and fixed in this position.

The aorta was ligated proximal to the right renal artery, and perfusion was started *in situ* with an initial flow rate of 1 ml/min. With the use of this technique, a significant ischemic period of the right kidney was avoided. Finally, the right kidney was excised, placed in a thermostated moistening chamber, and perfused at constant pressure (100 mmHg). Perfusion pressure was surveyed within the perfusion cannula (Isotec pressure transducer, Hugo Sachs Elektronik), and the pressure signal was used for feedback control of a peristaltic pump (model SCP 704, Hugo Sachs Elektronik). Finally, the renal vein was cannulated (1.5 - mm-OD polypropylene catheter). The venous effluent was drained outside the moistening chamber. The basic perfusion medium, supplied from a thermostated (37 °C) 200 ml reservoir, consisted of a modified Krebs-Henseleit solution containing all physiological amino acids at 0.2 - 2.0 mM, 8.7 mM glucose, 0.3 mM pyruvate, 2.0 mM L-lactate, 1.0 mM  $\alpha$ -ketoglutarate, 1.0 mM L-malate, and 6.0 mM urea. The perfusate was supplemented with 6 g/100 ml bovine serum albumin, 1 mU/100 ml vasopressin 8-lysine, and freshly washed human red blood cells (10 % hematocrit). Ampicillin (3 mg/100 ml) and flucloxacillin (3 mg/100 ml) were added to inhibit possible bacterial growth in the medium. To improve the functional preservation of the preparation, the perfusate was continuously dialyzed against a 10-fold volume of the same composition but without erythrocytes and albumin. For oxygenation of the perfusion medium, the dialysate was gassed with 94 % O<sub>2</sub> - 6 % CO<sub>2</sub>. Perfusate flow was calculated by collection and gravimetric determination of the venous effluent. Perfusion pressure was continuously monitored by a potentiometric recorder. After constant perfusion pressure was established, perfusate flow rates usually stabilized within 10 min. The stock solutions were added to the perfusate for 1 h with a latency of 10 min. After perfusion, the isolated mouse kidney was minced to small pieces in 3 ml buffer (RPMI 1640, 15 % DMSO, 1,8 % (w/v) NaCl) and sifted through a cell strainer with a mesh pore size of 100  $\mu$ m (Becton Dickinson, Heidelberg, Germany).

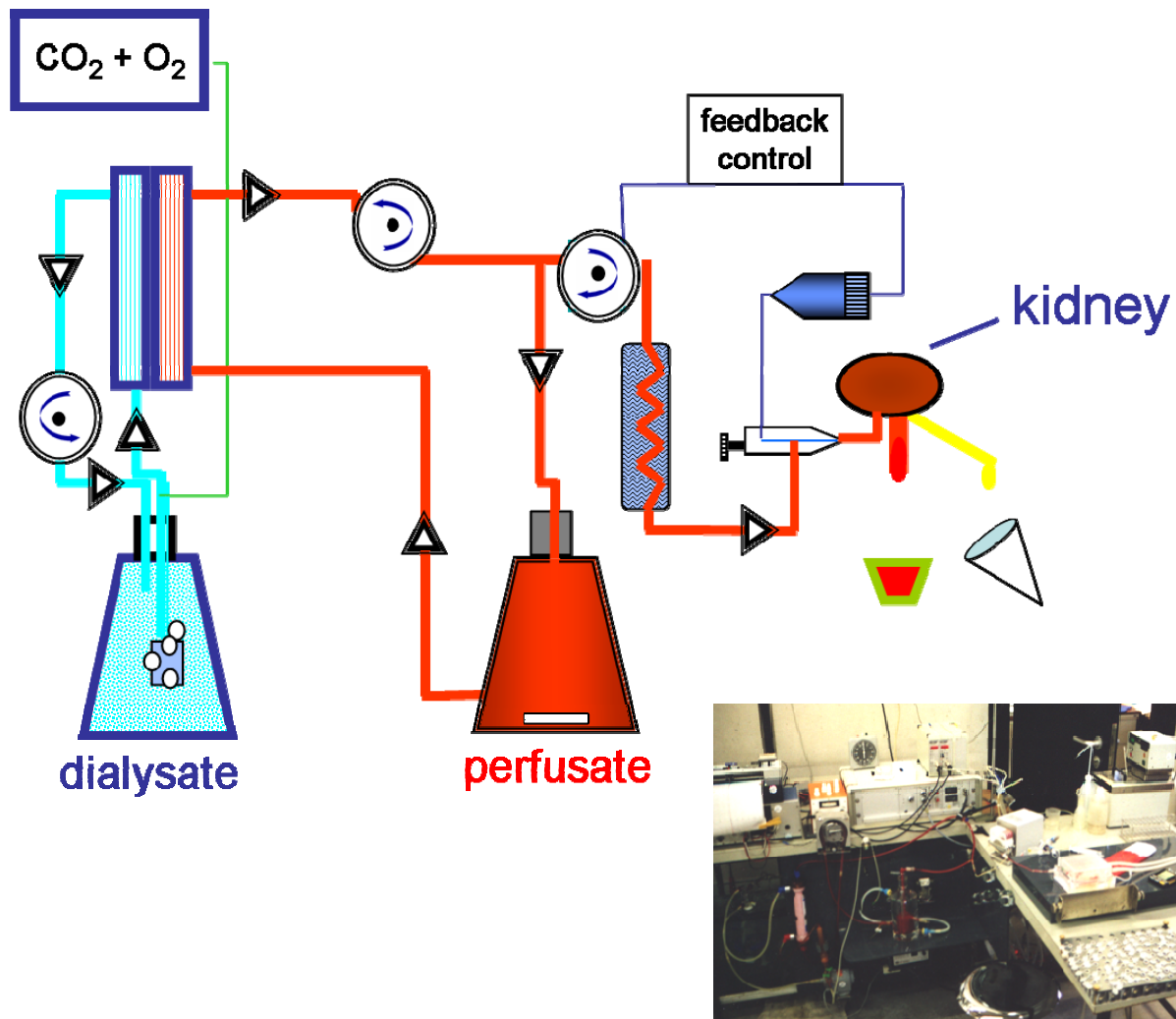


**Figure 35:** Scheme of the experimental set-up for the perfusion of isolated kidneys.  
 © PD Dr. Frank Schweda MD, Institute for Physiology, University of Regensburg

#### 5.2.2.4. Comet Assay

$3.5 \cdot 10^5$  LLC-PK1 cells seeded the day before in small culture flasks were treated for 4 h with test substances in 5 ml medium. Afterwards the cells were washed two times with PBS and supplied with 5 ml of fresh medium. After a recovery period of 0, 15, 30, 60, 120 min and 24 h, cells were harvested. Cell suspensions of extracted primary kidney cells or harvested LLC-PK1 cells were utilized for comet assay which was carried out as described by Schupp et al. [128], using a fluorescence microscope at a 200-fold magnification and computer aided image analysis (Komet 5, Kinetic Imaging Ltd., UK). After DNA staining with propidium iodide (20  $\mu\text{g/ml}$ ), 25 cells from each of two slides were measured, % tail DNA being the evaluation parameter. The alkaline comet assay detects single strand breaks, double strand breaks and alkali labile sites. The DNA fragments move during electrophoresis due to their negative

charge out of the nucleus in direction of the anode. Smaller fragments can move faster through the agarose in which the nuclei are embedded, resulting in characteristic comet-like structures.

#### **5.2.2.5. RNA isolation and semi quantitative reverse transcriptase PCR**

RNA isolation from mouse kidneys perfused with test substances for 1 h and PCR was performed. Primers were designed using the freeware Primer 3 (<http://frodo.wi.mit.edu/>). Sequences, annealing temperatures and PCR conditions were:

heme oxygenase (HO-1) (NM\_010442, 54 °C, 40 cycles, 664 bp):

For: 5'-GACATGGCCTTCTGGTATGG-3'; Rev: 5'-CCTCTGGCGAAGAACTCTG-3';

glutathione peroxidase (GPX) (NM\_008160, 54 °C, 40 cycles, 412 bp):

For: 5'-GTCCACCGTGTATGCCTTCT-3'; Rev: 5'-GATGTACTTGGGGTCGGTCA-3';

β-actin (NM\_007393, 54 °C, 40 cycles, 461 bp):

For: 5'-TAC AGCTTCACCACCACAGC-3'; Rev: 5'-GTGGACAGTGAGGCCAAGAT-3'

Electrophoresis was conducted using a 1.5 % agarose gel stained with ethidium bromide. Density of the DNA band was measured using the Gel Doc (BioRad, Hercules, CA, USA). Results are shown compared to the housekeeping gene β-actin.

#### **5.2.2.6. Determination of formamidopyrimidine DNA glycosylase (FPG) sensitive sites**

FPG-sensitive sites were determined by comet assay including an incubation step with formamidopyrimidine glycosylase (FPG), an enzyme which cleaves DNA at sites of oxidized purines and thereby detects 8-oxodG [89]. After treatment with test substances, embedding the cells in agarose and lysis of the cell membranes, the slides were washed 3 times for 5 min in cold buffer (40 mM HEPES-KOH, 100 mM KCl, 0.5 mM Na<sub>2</sub>EDTA and 0.2 mg/ml BSA) to remove the lysis solution. The FPG-sensitive sites were detected by incubation of the nuclei embedded in agarose with 0.005 µg/ml FPG protein (kindly donated by Professor Bernd Epe, Institute for Pharmacy, University of Mainz, Germany) for 60 min at 37 °C. Afterwards, the comet assay was carried out as described above. In this case, ethidium bromide (20 µg/ml) was used for DNA staining. The net level of FPG-sensitive sites was obtained as the

difference in score between samples incubated with FPG protein and samples incubated with buffer.

#### **5.2.2.7. Detection of phosphorylated $\gamma$ -H2AX sites**

10<sup>6</sup> LLC-PK1 cells seeded the day before in medium culture flasks were treated with test substances for 4 h, washed twice with PBS and supplied with fresh medium. After 0, 15, 30, 60, 120 min and 24 h cells were harvested, washed with cold PBS, and fixated for 1 h on ice with ice cold ethanol (70 %). Afterwards, cells were washed twice with cold PBS and permeabilized with 0.5 % Triton X in PBS for 10 min at room temperature. After washing, unspecific antibody binding sites were blocked for 30 min with 5 % fetal calf serum (FCS) in PBS. Thereafter, cells were centrifuged and incubated with primary antibody over night at 4 °C. The next day, cells were washed twice with FCS/PBS and incubated with secondary antibody for 45 min in the dark. After two times washing with FCS/PBS, 740  $\mu$ l PBS, 50  $\mu$ l saponin (1 % in PBS) and 10  $\mu$ l propidium iodide (PI) were added to each sample. Phosphorylated  $\gamma$ -H2AX foci were detected by flow cytometry (FACS LSR I, Becton-Dickinson, Mountain View, CA) after 10 minutes PI staining. Geometrical means were assessed using the “histogram statistics” function of Cell Quest Pro 4.0.

For immunofluorescence staining of phosphorylated  $\gamma$ -H2AX foci, cells were treated with test substances for 4 h, harvested, brought onto glass slides by cytopspin centrifugation and fixed in ice cold methanol for at least 2 h. The coverslips were again washed twice with PBS and incubated for 1 h at 37 °C with anti- $\gamma$ -H2AX antibody, then non-bound antibody was removed by extensive washing with PBS containing 0.2 % Tween (PBST). The coverslips were then incubated for 30 min at 37 °C in the dark with fluorescein isothiocyanate-conjugated secondary antibody. After thorough rinsing with PBST, nuclei were counterstained with Hoechst 33258.

Hereupon, the slides were rinsed two times with PBS and were mounted with Antifade Gold (Invitrogen, Karlsruhe, Germany). Images were visualized and captured using an Axioskop 2 (Zeiss, Germany) with a 100-fold oil immersion lens.

#### **5.2.2.8. Detection of abasic sites**

10<sup>6</sup> cells were treated with test substances for 4 h and harvested. Subsequently, the cells were fixed in ice cold ethanol (100 %) for 10 min at 4 °C. Afterwards, the cells were washed once with cold PBS and incubated for 120 min with 1 ml staining solution (5 µM Alexa Fluor 488 C<sub>5</sub>-aminooxyacetamide, bis(triethylammonium) salt (Alexa Fluor 488 hydroxylamine), 3 % acetic acid, 2 % dimethylformamide, 0.25 M MgCl<sub>2</sub> in PBS) per sample. Abasic sites were detected by flow cytometry. The medians of the resulting histograms were evaluated using the freeware WinMDI 2.9 (<http://facs.scripps.edu/software.html>).

For microscopic detection of abasic sites, 10<sup>6</sup> cells were treated with test substances for 4 h, harvested and brought to slides by cytopspin centrifugation. After fixation in ice cold methanol for at least 2 h, the cells were stained with 10 µl staining solution for 2 h. Hereupon, the slides were washed extensively with PBS and mounted with Antifade Gold. Images were visualized and captured using an Axioskop 2 (Zeiss, Germany) with a 40-fold magnification. For better comparison these pictures were magnified 2.5 times in Figure 41 B.

#### **5.2.2.9. Micronucleus frequency test**

10<sup>6</sup> cells were incubated for 2 h with the tested compound, afterwards 2 µg/ml cytochalasin B was added for 24 h to obtain binucleated cells (BN). After the incubation, the cells were brought onto glass slides by cytopspin centrifugation and fixed with methanol (-20 °C, 1 h). For staining, the slides were incubated with acridine orange (62.5 µg/ml in Sørensen buffer, pH 6.8) for 5 min, washed twice with Sørensen buffer for 5 min, and mounted for microscopy. The frequency of micronuclei was obtained after scoring 1000 BN cells on each of two slides. The averages of three independent experiments are shown.

#### **5.2.2.10. Statistics**

If not mentioned otherwise, data from at least 3 independent experiments ± standard deviation are depicted. Statistical significance among multiple groups was tested with Kruskal-Wallis over all groups and Mann-Whitney test was used to determine

significance between two groups. Results were considered significant if the  $p$  value was  $\leq 0.05$ .



### 5.2.3. Results

#### 5.2.3.1. Isolated perfused mouse kidney

Angiotensin II-induced DNA damage in isolated perfused mouse kidneys was measured with the comet assay (Figure 36 A). Compared to perfused control kidneys, a dose-dependent, significant increase in DNA damage after one hour of perfusion with 1, 10 and 50 nM angiotensin II was observed. Since the kidneys were perfused at a constant pressure of 100 mmHg, the vasoconstrictor angiotensin II dose-dependently reduced the perfusate flow (ml/g kidney).

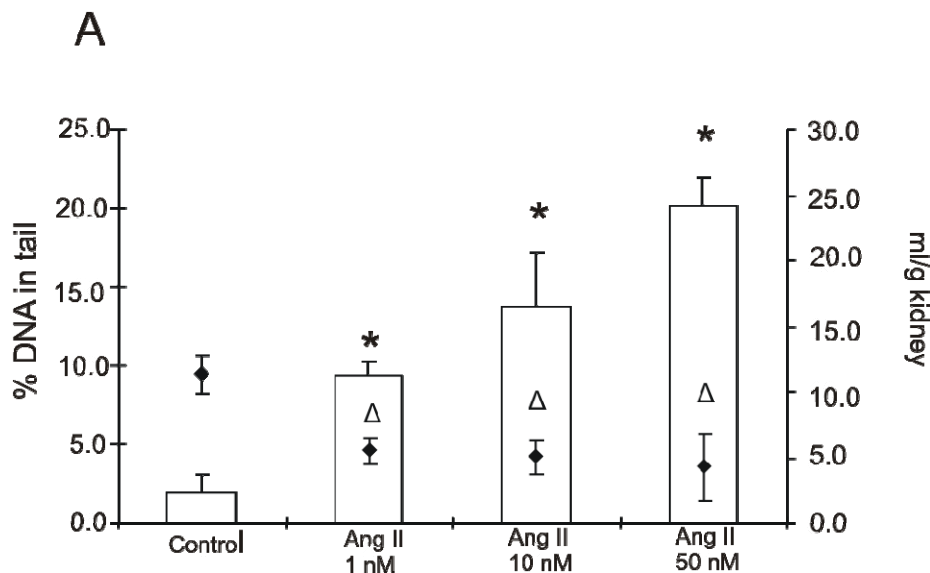


**Figure 36 A:** DNA damage in primary mouse kidney cells as measured by the comet assay (bars) and perfusate flow measured gravimetrically (dots) after 1 h treatment with perfusate buffer (control), various concentrations of angiotensin II (Ang II). \*  $p \leq 0.05$  vs. control, <sup>Δ</sup>  $p \leq 0.05$  vs. angiotensin II treatment (DNA damage); <sup>Δ</sup>  $p \leq 0.05$  vs. control, <sup>■</sup>  $p \leq 0.05$  vs. angiotensin II treatment (perfusate flow).

To exclude that the DNA damage was caused by mechanical stress or hypoxia due to the angiotensin II-induced vasoconstriction, the thromboxane mimetic U 46619 was infused in the same concentration as angiotensin II. Although application of U 46619 resulted in an even stronger vasoconstriction than angiotensin II it did not induce significant DNA damage (Figure 36 B).

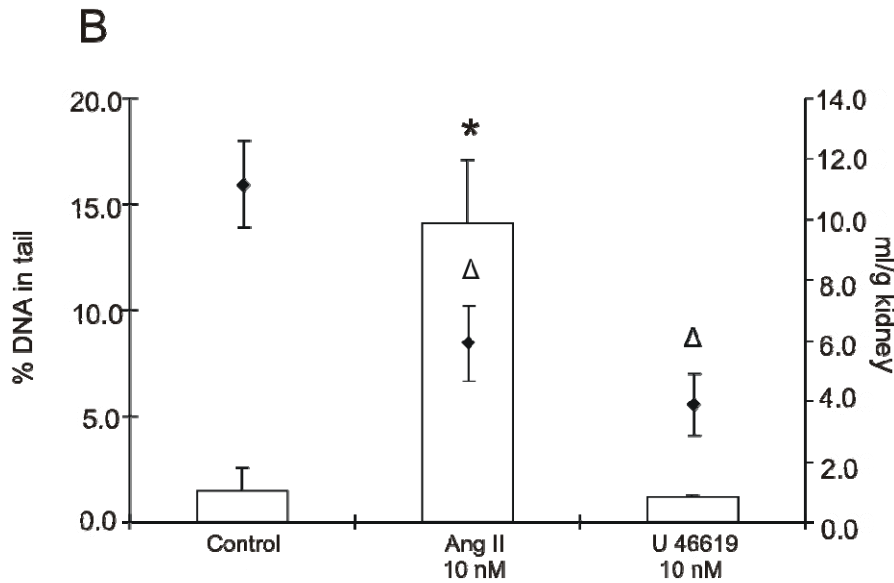


**Figure 36 B:** DNA damage in primary mouse kidney cells as measured by the comet assay (bars) and perfusate flow measured gravimetrically (dots) after 1 h treatment with perfusate buffer (control), 10 nM angiotensin II (Ang II) or 10 nM of the thromboxane mimetic U 46619. \*  $p \leq 0.05$  vs. control, <sup>Δ</sup>  $p \leq 0.05$  vs. angiotensin II treatment (DNA damage); ■  $p \leq 0.05$  vs. angiotensin II treatment (perfusate flow).

Previously conducted *in vitro* experiments in a rat kidney cell line (NRK) also did not reveal a significant induction of DNA strand breaks as measured by comet assay (Figure 37) after treatment with 100, 200 and 400 nM U 46619, concentrations which were much higher than the one infused in the isolated mouse kidney.

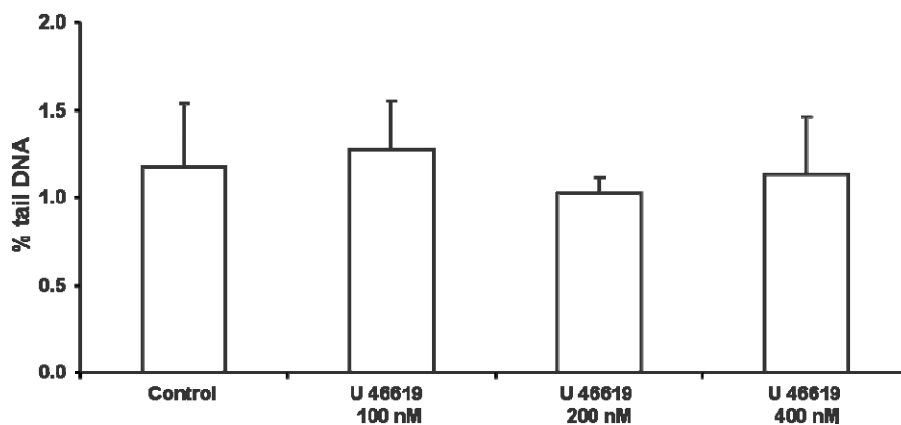


**Figure 37:** DNA damage in NRK cells as measured by the comet assay, after 2 hours treatment with three concentrations of the thromboxane mimetic U 46619 or hydrogen peroxide (H<sub>2</sub>O<sub>2</sub>) as positive control. Control: no treatment.

In order to examine whether the angiotensin II type 1 receptor (AT<sub>1</sub>R) is involved in the formation of angiotensin II-induced DNA strand breaks in *ex vivo* perfused mouse kidneys, the AT<sub>1</sub>R antagonist candesartan was applied. In fact, while 5  $\mu$ M

candesartan alone had no effect on DNA damage and perfusate flow, it completely prevented angiotensin II-induced DNA damage and vasoconstriction (Figure 36 C).

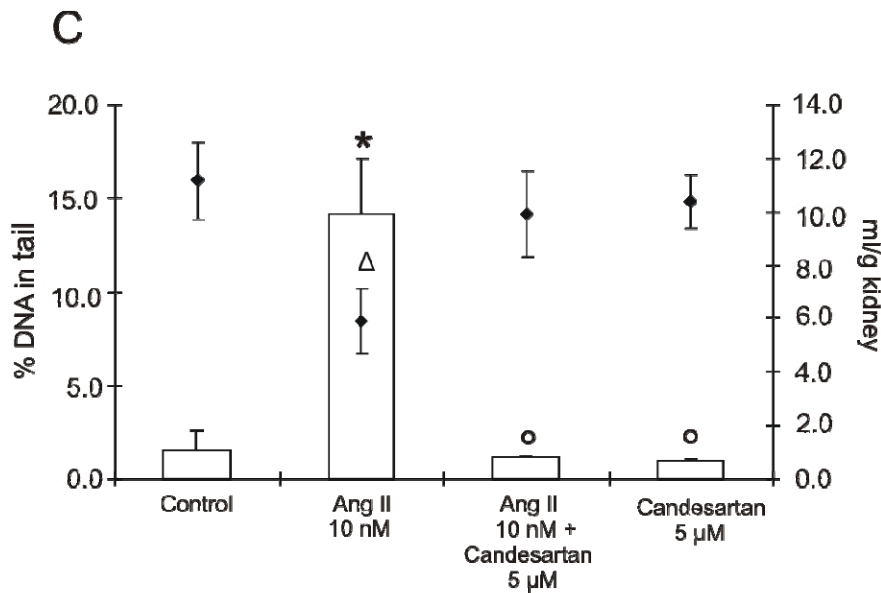


**Figure 36 C:** DNA damage in primary mouse kidney cells as measured by the comet assay (bars) and perfusate flow measured gravimetrically (dots) after 1 h treatment with perfusate buffer (control), and 10 nM angiotensin II (Ang II) with and without co-incubation with 5 µM candesartan. \*  $p \leq 0.05$  vs. control, °  $p \leq 0.05$  vs. angiotensin II treatment (DNA damage);  $\Delta$   $p \leq 0.05$  vs. control, ■  $p \leq 0.05$  vs. angiotensin II treatment (perfusate flow).

Next RNA was isolated from primary cells derived from the same perfused kidneys and as markers for the involvement of oxidative stress in the formation of DNA damage, the gene expression of glutathione peroxidase (GPX) and heme oxygenase (HO-1) was assessed (Figure 38). Compared to the untreated control, GPX expression was suppressed by angiotensin II while HO-1 expression was induced. Candesartan reduced GPX suppression and HO-1 induction without completely normalizing them. Treatment with candesartan alone had no impact on GPX gene expression but resulted in a suppression of HO-1 expression.

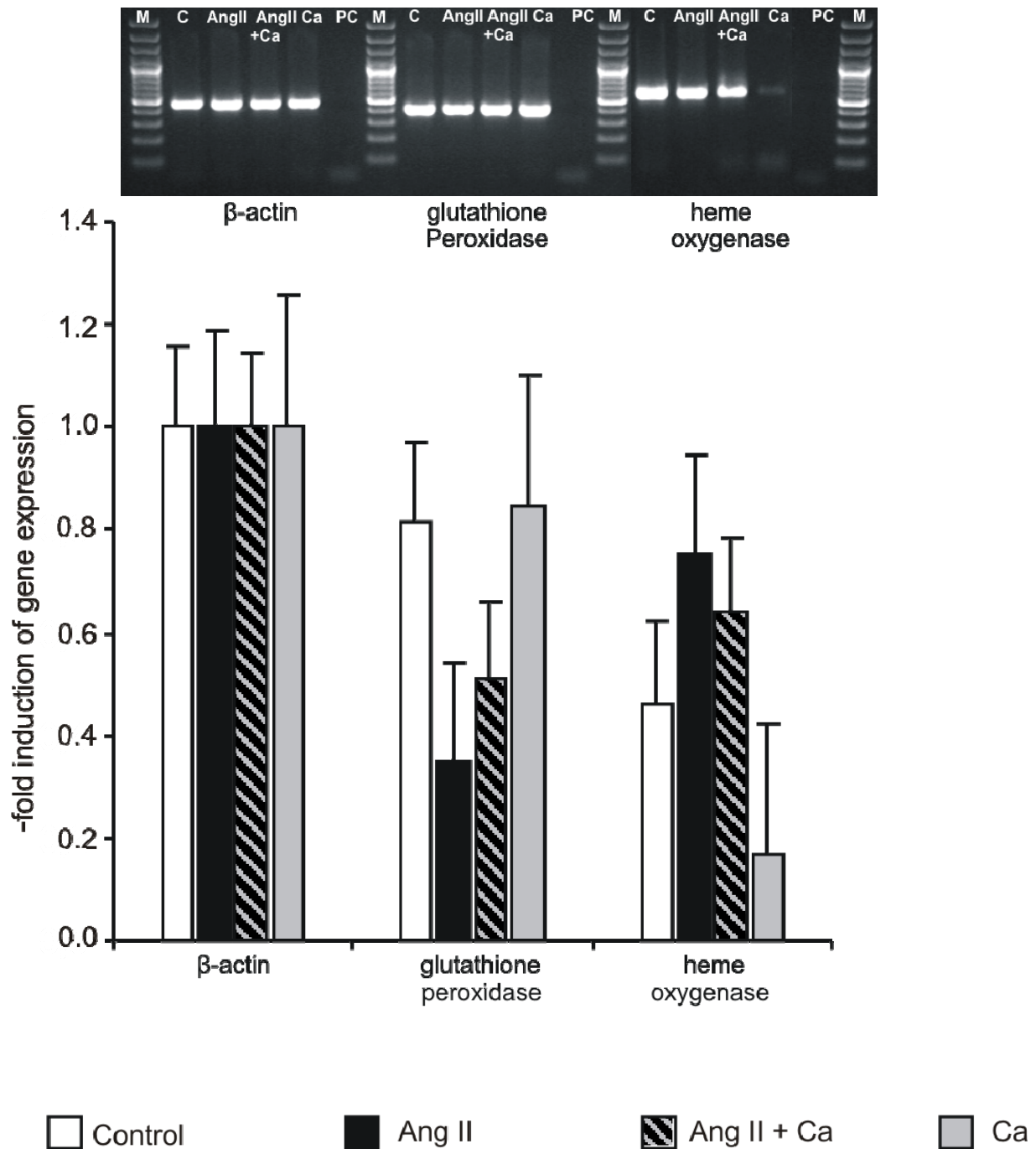


**Figure 38:** Glutathione peroxidase (GPX) and heme oxygenase (HO-1) expression in primary mouse kidney cells after 1 h perfusion with 10 nM angiotensin II (Ang II), or 5  $\mu$ M candesartan (Ca) alone and angiotensin II (Ang II) in combination with candesartan. Quantification of band densities derived from three independent experiments (with standard error) normalized to the housekeeping gene  $\beta$ -actin are shown. M = Marker; C = Control, Ang II = 10 nM angiotensin II, Ang II + Ca = 10 nM angiotensin II + 5  $\mu$ M candesartan, Ca = 5  $\mu$ M candesartan, PC = primer control.

### 5.2.3.2. Cell culture experiments

To characterize in more detail the angiotensin II-induced DNA damage, further experiments were conducted in LLC-PK1 cells, a porcine kidney cell line with proximal tubule properties.

Time response experiments with 200 nM angiotensin II, a concentration which was chosen after previous *in vitro* experiments [47], showed that in LLC PK1 cells, significant DNA strand break formation starts after 15 minutes and increases continuously up to 240 min (Figure 39).

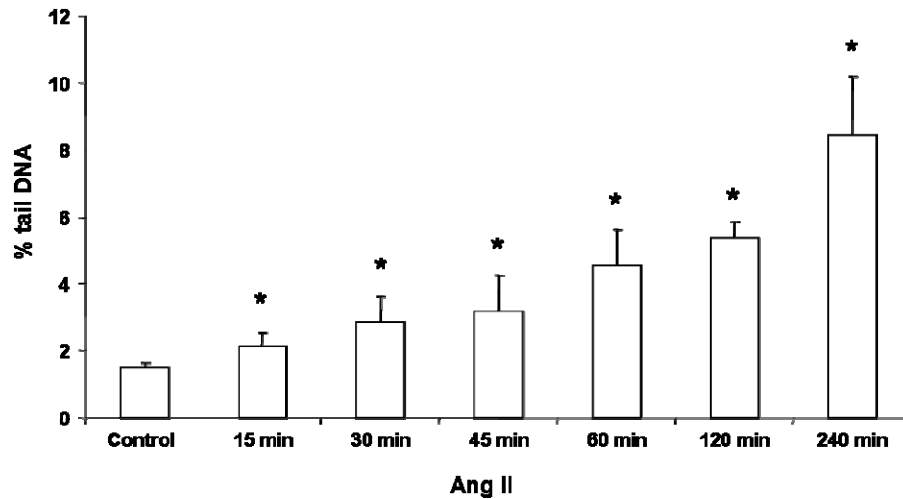


**Figure 39:** DNA damage in LLC-PK1 cells as measured by the comet assay treatment with PBS (control), 200 nM angiotensin II (Ang II) after the indicated timepoints. \*  $p \leq 0.05$  vs. control.

Furthermore, the occurrence of double strand breaks induced by angiotensin II was investigated. Immunofluorescence staining showed that treatment with 200 nM angiotensin II resulted in an increased frequency of  $\gamma$ -H2AX (Figure 41 A). The amount of foci varied extremely between the individual cells. Some cells resembled those treated with the positive control genisteine while others had as few foci as the negative control. Simultaneous treatment with angiotensin II and 5  $\mu$ M candesartan resulted in an inhibition of  $\gamma$ -H2AX foci formation. Additional flow cytometric quantification of  $\gamma$ -H2AX revealed a significant increase in fluorescence after treatment with angiotensin II (Figure 40 A). Again, co-treatment with angiotensin II and candesartan restored control levels.

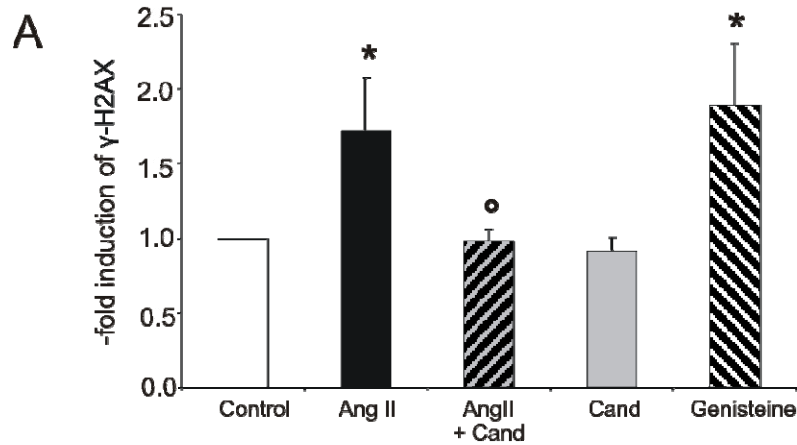


**Figure 40 A:** Flow cytometric quantification of  $\gamma$ -H2AX in LLC-PK1 cells after 4 h treatment with 200 nM angiotensin II (Ang II) with and without co-incubation with 5  $\mu$ M candesartan (Cand) or 100  $\mu$ M genisteine (positive control). Depicted is the geometrical mean of the resulting histograms normalized to control. \*  $p \leq 0.05$  vs. control, °  $p \leq 0.05$  vs. angiotensin II treatment.

DNA strand breaks detected by the comet assay may partially or completely be transient. To test if this is the case with angiotensin II-induced DNA damage, DNA repair after treatment with angiotensin II was measured in a time course experiment by comet assay over a time period of 24 h. Already after a recovery period of 15 minutes, the cells were able to repair approximately half of the induced DNA strand breaks and after 24 h, almost no strand breaks were detectable any more in the comet assay (Figure 40 B). Quantification of double strand breaks at the same time points by flow cytometry in contrast showed an increase of  $\gamma$ -H2AX in the course of the recovery period, suggesting the persistence of double strand breaks.

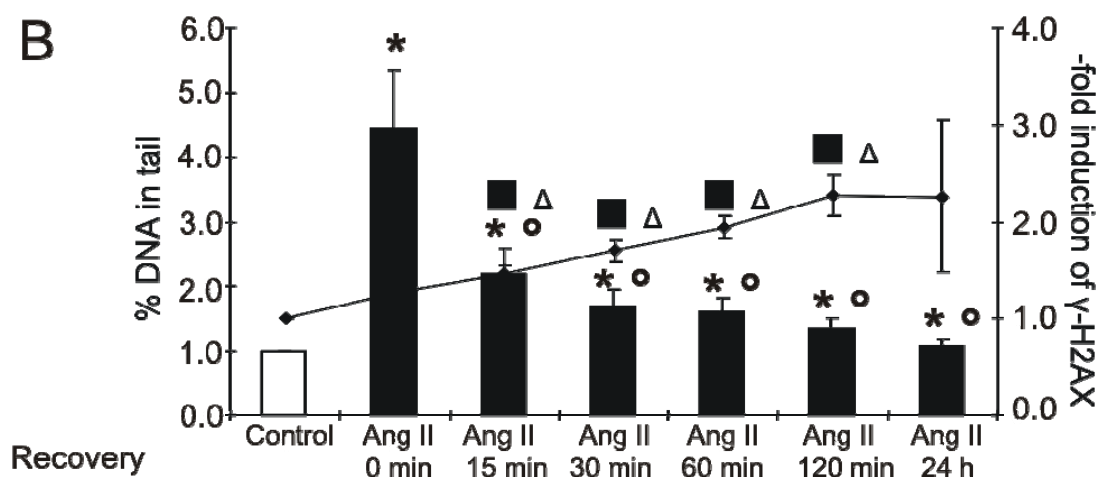


**Figure 40 B:** DNA damage in LLC-PK1 cells as measured by the comet assay (bars) and flow cytometric quantification of induction of  $\gamma$ -H2AX fluorescence (dots) after 4 h treatment with PBS (control), 200 nM angiotensin II (Ang II) and subsequent recovery periods of 0 to 24 h normalized to control. \*  $p \leq 0.05$  vs. control, °  $p \leq 0.05$  vs. angiotensin II treatment (DNA damage); Δ  $p \leq 0.05$  vs. control, ■  $p \leq 0.05$  vs. angiotensin II treatment ( $\gamma$ -H2AX fluorescence).

Beside single and double strand breaks, oxidative stress leads to the formation of DNA adducts like 8-hydroxydeoxyguanosine (8-oxodG) and abasic sites. The oxidized guanine 8-oxodG and formamidopyrimidines are the main adducts recognized by formamidopyrimidine DNA glycosylase (FPG), which incises the DNA at the site of the adduct, thereby generating additional strand breaks. The extent of these added strand breaks can be detected in the FPG-modified comet assay.

In Figure 40 C, which shows the amount of DNA damage quantified after incubation with FPG minus the DNA damage without incubation with FPG, it can be seen that treatment with angiotensin II significantly increased the occurrence of FPG-sensitive sites. Co-incubation with candesartan prevented the formation of these oxidative adducts.

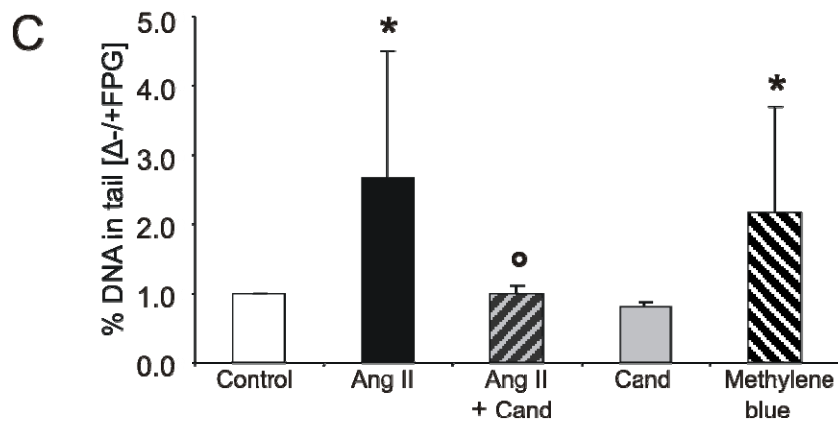


**Figure 40 C:** DNA damage as measured by the FPG-modified comet assay in LLC-PK1 cells after 4 h treatment with 200 nM angiotensin II (Ang II) with and without co-incubation with 5  $\mu$ M candesartan (Cand) or 0.05  $\mu$ g/ml methylene blue (positive control), the latter with an incubation time of only 10 min. Depicted is the difference in the percentage of DNA in tail between nuclei treated with FPG enzyme and nuclei not treated with FPG enzyme, normalized to control. \*  $p \leq 0.05$  vs. control, °  $p \leq 0.05$  vs. angiotensin II treatment.

Finally, abasic sites were detected by immunofluorescence staining and by flow cytometry. For this, the abasic sites were tagged with a fluorescent aldehyde-reactive probe. As can be seen in Figure 41 B, the nuclei of angiotensin II-treated cells are much brighter than those of the control or of candesartan-treated cells. Flow cytometric quantification revealed these differences in fluorescence-labeled abasic sites to be significant, while the co-treatment with candesartan yielded levels comparable to the untreated control (Figure 40 D).

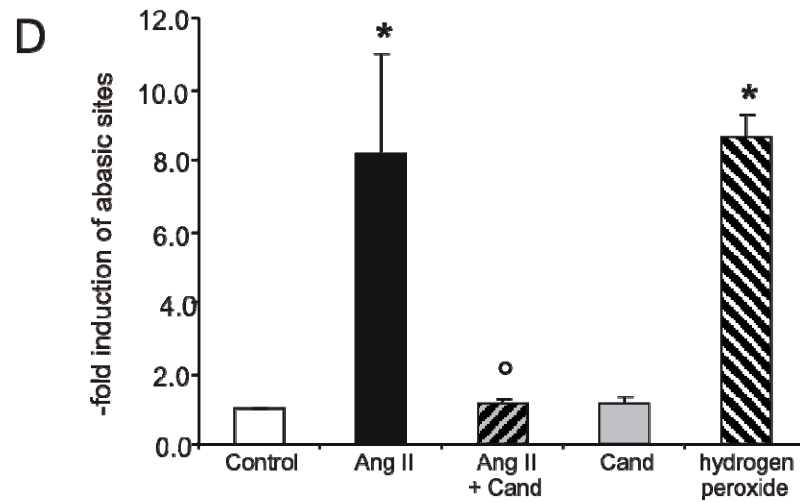


**Figure 40 D:** Induction of abasic sites in LLC-PK1 cells measured by flow cytometry after treatment with 200 nM angiotensin II (Ang II) with and without co-incubation with 5  $\mu$ M candesartan (Cand) or 750  $\mu$ M hydrogen peroxide (positive control), normalized to control. \*  $p \leq 0.05$  vs. control, °  $p \leq 0.05$  vs. angiotensin II treatment.



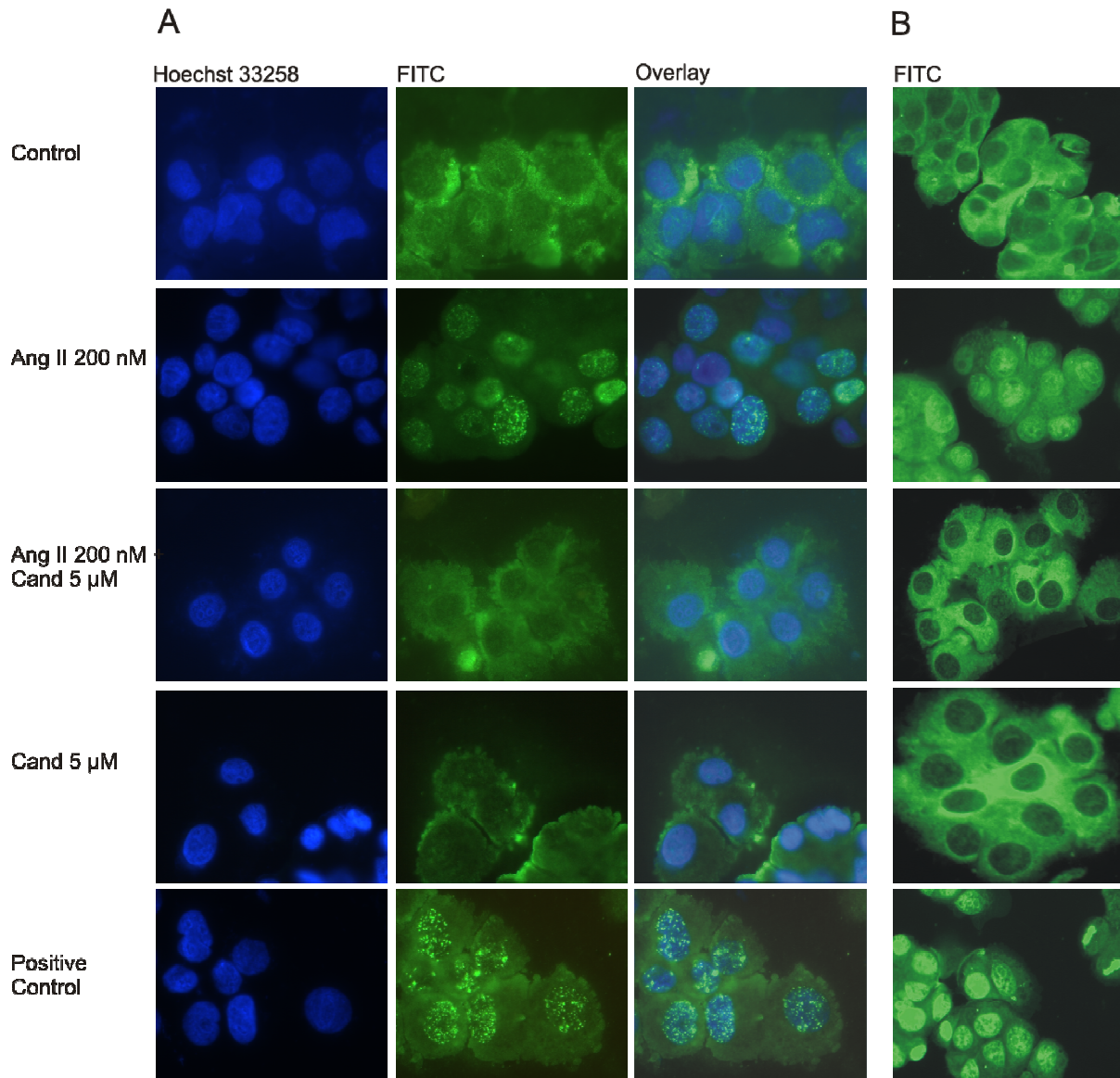


**Figure 41 A:** Incidence of  $\gamma$ -H2AX foci in LLC-PK1 cells after 4 h treatment with 200 nM angiotensin II (Ang II), 5  $\mu$ M candesartan (Cand), 200 nM angiotensin II together with 5  $\mu$ M candesartan, or 100  $\mu$ M genisteine (positive control). Representative images of the localization of  $\gamma$ -H2AX foci (green fluorescence), the Hoechst 33258 stained nuclei (blue fluorescence) and the overlay of both DNA stains are shown, captured at a 100-fold magnification. **Figure 41 B:** Incidence of abasic sites in LLC-PK1 cells after 4 h treatment with 200 nM angiotensin II (Ang II), 5  $\mu$ M candesartan (Cand), 200 nM angiotensin II together with 5  $\mu$ M candesartan or 750  $\mu$ M hydrogen peroxide (positive control). Representative images of the localization of the green fluorescing abasic sites are shown, captured at a 40-fold magnification and enlarged 2.5 times afterwards for better comparison with Figure 41 A.

#### 5.2.4. Discussion

In the isolated perfused kidney, angiotensin II caused dose-dependently DNA strand breaks and vasoconstriction. Since control kidneys, perfused for one hour without any pharmacological intervention, showed the same DNA damage values as unperfused kidneys subjected to the comet assay immediately after sacrifice of the mice (data not shown), it appears very unlikely that the perfusion *per se* has a major effect on the integrity of the DNA. Also cytotoxic effects of 1 to 50 nM angiotensin II are highly improbable, since not even a 4 hour incubation of cells *in vitro* with 800 nM angiotensin II caused a significant decrease in cell vitality. Furthermore, apoptotic effects of 1 to 50 nM angiotensin II in the perfused kidney can be ruled out, because the concentration of 200 nM angiotensin II, which is normally used *in vitro*, started to cause some apoptosis only after 4 hours of incubation.

Angiotensin II is a potent vasoconstrictor that significantly reduced kidney perfusion in our study. Since ischemia is known to cause tubular epithelial necrosis and apoptosis [172] and both processes would generate DNA damage detectable in the comet assay, it is critical for our conclusion that the observed effects of angiotensin II are not related to its vasoconstrictor effects. The thromboxane mimetic U 46619 generated a marked vasoconstriction, hereby drastically reducing kidney perfusion, but it did not induce DNA damage. This could also be shown in *in vitro* experiments conducted in a rat kidney cell line. Here, even concentrations from 100 nM to 400 nM U 46619 were not able to induce DNA strand breaks as measured in the comet assay after an incubation time of 2 h. These observations reinforce our hypothesis that the AT<sub>1</sub>R-mediated DNA damage in the isolated perfused kidneys indeed is independent of the hemodynamic effects of angiotensin II.

Moreover, angiotensin II regulated gene expression of enzymes associated with the defense against oxidative stress. On the one hand, angiotensin II induced an up-regulation of heme oxygenase expression that was attenuated by candesartan as previously reported elsewhere [151]. On the other hand, glutathione peroxidase was down-regulated and this down-regulation was also at least partially prevented by AT<sub>1</sub>R blockade. The down-regulation of glutathione peroxidase expression is in line with our own previous findings gained in promyelocytic cells stressed with the NAD(P)H oxidase activator phorbol 12-myristate 13-acetate (PMA) [170], and was already observed by other groups as a reaction to severe oxidative stress [173]. Co-

treatment with candesartan prevented the massive down-regulation of glutathione peroxidase observed after angiotensin II treatment, again proving the involvement of AT<sub>1</sub>R activation.

No other genotoxicity test could be executed with the terminally differentiated kidney cells, and DNA damage observed in the comet assay could theoretically be completely repaired. Therefore we conducted further experiments in the porcine kidney cell line LLC-PK1, to be able to evaluate the relevance of the DNA damage induced by angiotensin II *ex vivo*. First, it could be shown that not only in the isolated perfused kidney but also in the LLC-PK1 kidney cell line, significant DNA damage is measurable starting from 15 minutes incubation time thus enabling us to compare the *ex vivo* settings to those in cell culture.

The histone H2AX has been shown to be rapidly phosphorylated after induction of double strand breaks and is thought to promote repair protein recruitment [174].  $\gamma$ -H2AX can be visualized with the help of phospho-specific antibodies [175]. Flow cytometric measurements and immunofluorescence staining of  $\gamma$ -H2AX indicated that angiotensin II induced double strand breaks in a significant number, which even increased over 24 h, as shown in LLC-PK1 cells. Correlation of these data with the also conducted repair comet assay revealed that overall, the number of lesions decreased while that of double strand breaks increased. In an earlier study we have shown that, besides DNA damage detectable by comet assay, a 24 hour-incubation with angiotensin II also causes micronuclei [47]. Micronuclei, a subset of chromosomal aberrations, are chromatin-containing structures in the cytoplasm, surrounded by a separate membrane, which are formed for example after double strand breaks which lead to chromosome fragments lagging behind at the anaphase during nuclear division [90]. Our observation now implies that the micronuclei observed after angiotensin-treatment may result from the persisting double strand breaks which were not repaired.

The alkaline comet assay detects a variety of lesions: single and double strand breaks, incomplete excision repair sites, apurinic or apyrimidinic sites, which are alkali labile and therefore appear as breaks under the alkaline conditions of the assay [94]. To detect base oxidation the very sensitive FPG-modified comet assay was chosen. The significant increase in DNA damage achieved with this method supports the thesis that angiotensin II-induced damage is of oxidative nature. In addition, we

could show that abasic sites, which are also formed during oxidative DNA damage, increased after angiotensin II treatment.

In conclusion, this study shows that angiotensin II induces oxidative DNA damage not only in cell culture but also in the intact whole organ. Furthermore the main lesions assigned to an oxidative attack on DNA were quantified after angiotensin II-incubation: single and double strand breaks, oxidative adducts (8-oxodG), and abasic sites. On top we could show that double strand breaks persisted after other comet assay-detectable lesions were repaired long ago. The AT<sub>1</sub>R blocker candesartan was able to prevent all kinds of injury caused by angiotensin II, proving the damage to be mediated by this receptor.

## 6. Receptor Blockade – Mineralocorticoid Receptor

### 6.1. Aldosterone causes DNA strand breaks and micronuclei in renal cells

#### 6.1.1. Background

Aldosterone plays a major role in the maintenance of electrolyte and fluid balance and subsequent blood-pressure homeostasis. This regulation is achieved through binding of aldosterone to the intracellular mineralocorticoid receptor. The activated receptor is translocated into the nucleus, where it binds to hormone-responsive elements of target gene promoters and modulates their expression [67, 176, 177]. Beside these classical genomic actions, aldosterone also exerts rapid, non-genomic effects, which are either mediated by a not yet identified membrane receptor or by the mineralocorticoid receptor utilizing second messengers [178].

Epidemiological studies found a higher cancer mortality in hypertensive patients [141] and an increased risk to develop renal cancer, in particular after long-term diuretic therapy [50, 51]. We found angiotensin II, which is often elevated in hypertension, to be genotoxic in renal cells [47]. Although primary aldosteronism was originally thought to be an uncommon cause of hypertension, recent studies suggest that 10 - 15 % of hypertensive individuals fulfill the biochemical criteria for hyperaldosteronism [68]. Studies demonstrating the effectiveness of mineralocorticoid receptor antagonism in patients with resistant hypertension suggest an even higher prevalence of 20 % of hyperaldosteronism among this population [67, 68].

There are many publications reporting the interaction of angiotensin II and aldosterone in inducing cardiovascular injury, with angiotensin II stimulating mineralocorticoid receptor-dependent mechanisms [67, 179, 180]. Since we cannot at the present time rule out that the DNA damage induced by angiotensin II is solely mediated by the angiotensin II type 1 receptor (AT<sub>1</sub>R) without any participation of the mineralocorticoid receptor, the present study was undertaken to analyze potential genotoxic effects of aldosterone *in vitro* in the epithelial kidney cell lines HEK (human), LLC-PK1 (porcine) and NRK (rat). Furthermore, the omission of the adverse-effect profile by replacement of spironolactone, which is afflicted with endocrine side effects, with the more selective eplerenone has revived the interest in the therapeutic use of mineralocorticoid-receptor antagonists. Studies revealed an

effective intervention with regard to heart failure and other cardiovascular conditions. Yet, eplerenone is also not very well tolerated and may cause electrolyte disturbances, specifically hyperkalemia [69]. Attempts to design aldosterone antagonists which are non-steroidal and thus bind highly specific to the mineralocorticoid receptor have taken place and several substances are currently passing the preclinical phase. In addition, the potential prevention of these effects by steroidal and non-steroidal mineralocorticoid receptor antagonists was investigated.

## **6.1.2. Experimental**

### **6.1.2.1. Material**

If not mentioned otherwise, all chemicals were purchased from Sigma-Aldrich, Taufkirchen, Germany. Eplerenone, (S)-BR-4628 and (R)-BR-4628 were provided by Bayer Healthcare, Wuppertal.

### **6.1.2.2. Cell culture**

HEK 293, a human embryonic kidney cell line with proximal tubular properties, was obtained from ATCC (Rockville, USA). Cells were grown in DMEM medium (4.5 g/l glucose) supplemented with 10 % fetal calf serum, 1 % glutamine and antibiotics. For experiments,  $10^6$  cells were treated with test compounds in 5 ml culture medium. For experiments with reduced serum albumin, HEK cells were kept for the incubation time in medium with only 1.0 % fetal calf serum (FCS).

LLC-PK1 cells, an epithelial porcine kidney cell line with proximal tubule properties, were obtained from ATCC and grown as described by Schupp et al. [47]. For experiments,  $10^6$  cells were treated with test compounds in 5 ml culture medium. For experiments with reduced serum albumin, LLC-PK1 cells were kept for the incubation time in medium with only 0.5 % fetal calf serum (FCS).

NRK cells, an epithelial rat kidney cell line with proximal tubule properties were obtained from ECACC and grown in DMEM medium (4.5 g glucose/l), supplemented with 10 % FCS, 1 % glutamine, 1 % non-essential amino acids and antibiotics. For experiments,  $10^6$  cells were treated with test compounds in 5 ml culture medium. For experiments with reduced serum albumin, NRK cells were kept for the incubation time in medium with only 1.5 % fetal calf serum (FCS).

LLC-PK1 cells were routinely split twice a week, NRK and HEK cells three times a week to keep the exponential growth conditions and were cultured for no more than twenty passages after thawing them from stock.

### **6.1.2.3. Comet assay**

The comet assay was carried out as described earlier [47]. A fluorescence microscope at 200-fold magnification and a computer-aided image analysis system (Komet 5, Kinetic Imaging LTD, Liverpool, UK) were used for analysis. 50 cells in total (25 per slide) were analyzed and results were expressed as percentage of DNA in the tail region.

### **6.1.2.4. Micronucleus frequency test**

The micronucleus frequency test was carried out as described earlier [47]. Cells were incubated for 4 h with the tested compounds, then 3 µg/ml cytochalasin B was added for 24 h to obtain binucleated (BN) cells. The frequency of micronuclei was obtained after scoring 1000 BN cells on each of two slides.

### **6.1.2.5. Quantification of apoptotic cells**

During the analysis of the slides prepared for the micronucleus frequency test, also cells with nuclei which show characteristics of apoptotic nuclei (highly condensed chromatin) were counted and their number was referred to 1000 BN cells.

### **6.1.2.6. Proliferation index**

Furthermore, the slides prepared for the micronucleus frequency test were used to calculate the cytokinesis block proliferation index (CBPI) from 1000 cells of each sample.

$$\text{CBPI} = \frac{(\text{mononucleated cells} * 1) + (\text{binucleated cells} * 2) + (\text{polynucleated cells} * 3)}{\text{total cell number}}$$

### **6.1.2.7. Vitality assay**

The fluorescein-ethidium bromide vitality assay was carried out according to Yang et al. [181], with the following modifications: The staining solution contained 30 µg/ml FDA and 12 µg/ml EB. 35 µl cells were stained with 15 µl staining solution. 15 µl of this mixture was applied to the slide and the fractions of green and red cells in a total of 200 cells were counted at 200-fold magnification.



### **6.1.2.8. RT-PCR experiments**

The expression of mineralocorticoid receptor and glucocorticoid receptor mRNA was detected as described earlier [47]. The following primers with the respective GenBank accession number and predicted size were used for amplification (35-40 cycles):

mineralocorticoid receptor homo sapiens (M16801; 54 °C; 40 cycles; 623 bp)

For: 5'-ACTGGTTCCTCAGCTCTCCA-3', Rev: 5'-AGTCCAGCAGCTTGGTCAGT-3'

mineralocorticoid receptor pig (U88893; 54 °C; 35 cycles; 303 bp)

For: 5'-TGCACCAGTCTGCCATGTAT-3', Rev: 5'-ATTCCAACAAGTCGCTCACC-3'

mineralocorticoid receptor rat (M36074; 54 °C; 35 cycles; 679 bp)

For: 5'-CAGACCTTGGAGCGTTCTTC-3', Rev: 5'-TGTGTGACCTTGAGCCTCTG-3'

All primers were designed with the program Primer 3 [149].

### **6.1.2.9. Flow cytometric analysis of oxidative stress**

2',7'-Dichlorodihydrofluorescein diacetate (H<sub>2</sub>DCF-DA) was used to detect reactive oxygen species (ROS) production in cells. Cells were pre-incubated with 10 μM H<sub>2</sub>DCF-DA for 5 min at 37 °C and substances were added for additional 30 min. As a positive control 0.1 mM hydrogen peroxide was used. Cells were harvested, washed two times with PBS/1 % BSA, and analyzed (3\*10<sup>5</sup> cells/sample) by flow cytometry using a FACS LSR I (Becton-Dickinson, Mountain View, CA, USA) after incubation for 10 min on ice with 1 μg/ml propidium iodide.

### **6.1.2.10. Statistical analysis**

Data from at least 3 independent experiments are shown ± standard deviation. Statistical significance among individual groups was tested using the Mann-Whitney test. A *P* value of ≤ 0.05 was considered significant. For calculations SPSS 15.0 was used. Analysis of flow cytometry histograms was done with the free software WinMDI 2.9 (Scripps Research Institute Cytometry Software page at <http://facs.scripps.edu/software.html>).

### 6.1.3. Results

The presence of the expression of the mineralocorticoid receptor in HEK, LLC-PK1 and NRK cells was verified by RT-PCR (Figure 42).

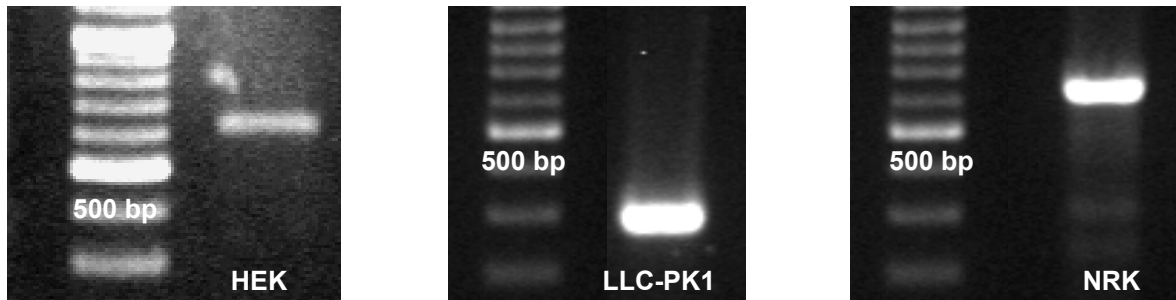


**Figure 42:** Fragments of mineralocorticoid receptors amplified by polymerase chain reaction and subjected to electrophoresis (80 V, 90 min) in a 1.5 % agarose gel.

To ensure the observation of genotoxic effects a possible cytotoxicity of aldosterone was eliminated by monitoring several end-points of cell vitality. Aldosterone in concentrations up to 10  $\mu\text{M}$  after 24 hours incubation did not decrease the number of viable cells and did not influence the cell number after 24 h incubation (Figures 43 A and B) in LLC-PK1 cells.

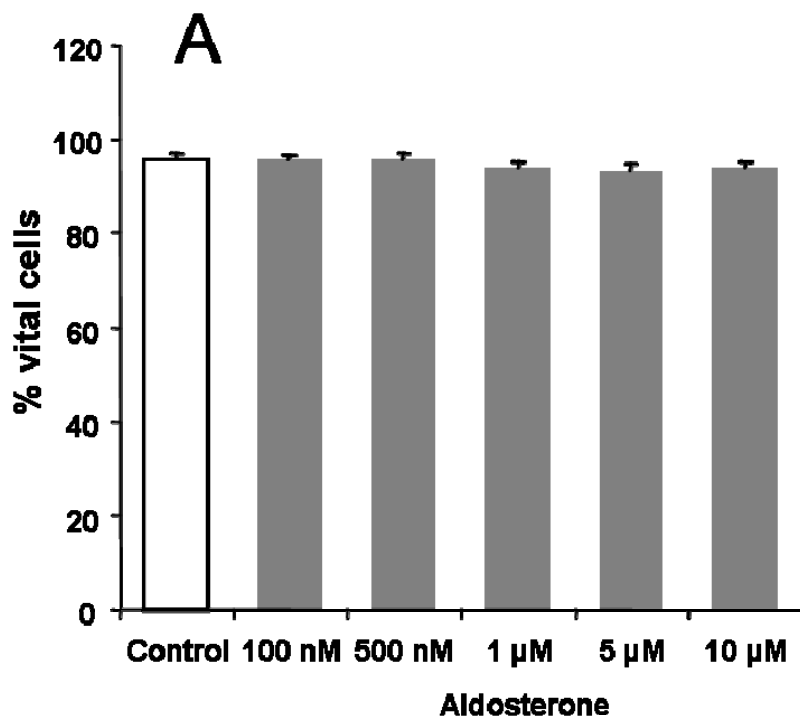


**Figure 43 A:** Quantification of the impact of aldosterone in the indicated concentrations on the vitality of LLC-PK1 cells after 24 hours incubation. Cells were stained with fluorescein diacetate, which stains vital cells green, and ethidium bromide, which stains dead or dying cells red. Shown is the percentage of vital cells.

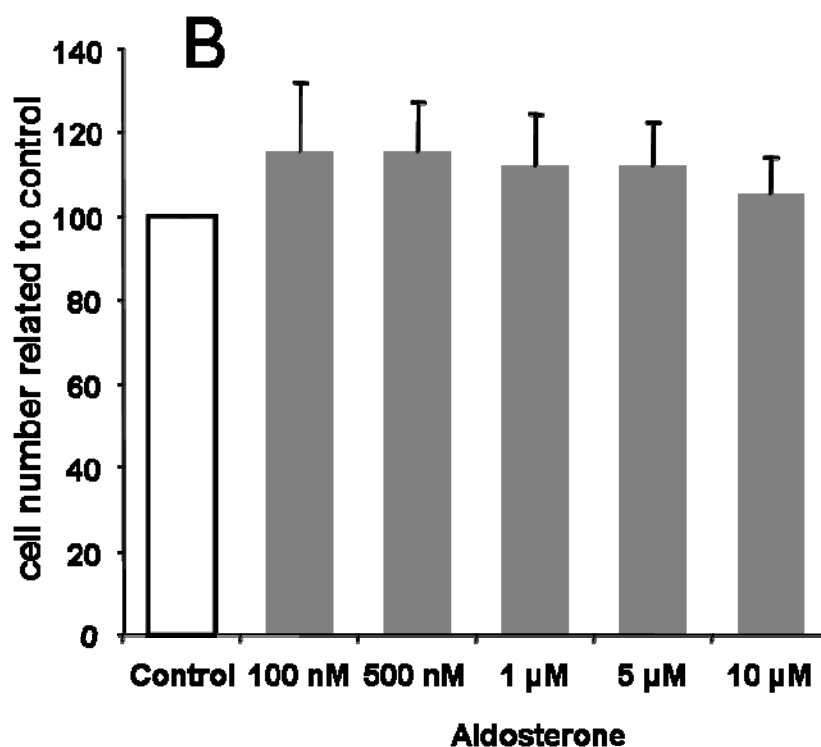


**Figure 43 B:** LLC-PK1 cell number after incubation with the indicated aldosterone concentrations for 24 hours in cell culture medium with 10 % FCS. The cell number of the control sample was set to 100, and the cell numbers of the other samples were related to the control.

Also the cytokinesis block proliferation index calculated after a 4 h exposure followed by 24 h recovery was not changed by up to 1 μM aldosterone and there was no increase of apoptotic cells except for the inter-experimental variations (Table 4).

**Table 4:** Effects of a 4 hour-incubation with aldosterone on proliferation and apoptosis of HEK, LLC-PK1 and NRK cells, \*  $p \leq 0.05$  vs. control.

	Treatment	HEK	LLC-PK1	NRK
Proliferation index	Control	1.989 ± 0.02	1.997 ± 0.007	2.001 ± 0.005
	0.1 μM Aldosterone	1.989 ± 0.00	1.998 ± 0.002	2.005 ± 0.008
	0.5 μM Aldosterone	1.996 ± 0.01	2.009 ± 0.008	2.002 ± 0.008
	1.0 μM Aldosterone	1.983 ± 0.01	2.011 ± 0.003*	1.994 ± 0.023
Number of apoptoses	Control	6.3 ± 2.47	8.33 ± 3.20	5.50 ± 1.76
	0.1 μM Aldosterone	2.5 ± 1.00	6.67 ± 4.97	10.17 ± 7.52
	0.5 μM Aldosterone	6.3 ± 3.33	7.00 ± 5.66	7.17 ± 5.12
	1.0 μM Aldosterone	5.2 ± 0.58	11.33 ± 3.27	7.00 ± 3.63

Aldosterone caused a dose-dependent DNA damage after a 4 hour incubation measured in the comet assay in HEK, LLC-PK1 and NRK cells. This test detects structural DNA damage, which may partially or completely be transient, and then leads to repair before mitosis or to cell death. Assuming a protein binding capacity of

aldosterone the comet assay was conducted with cells treated in medium with reduced FCS (HEK 1.0 %, LLC-PK1 0.5 %; NRK 1.5 %). In these experiments, the DNA damage was significant from aldosterone concentrations of 100 nM (Figure 44).

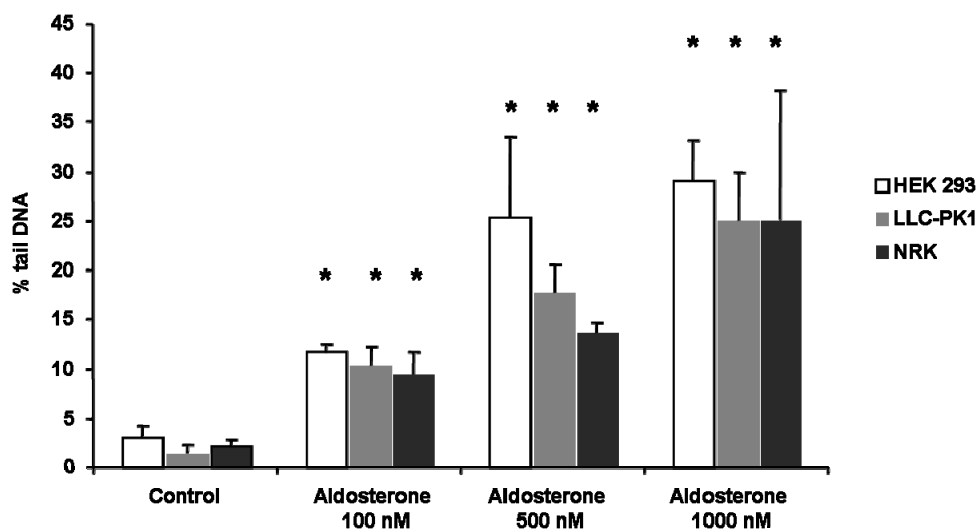


**Figure 44:** DNA damage induced by the indicated aldosterone concentrations quantified with the comet assay in HEK, LLC-PK1 and NRK cells incubated 4 hours in cell culture medium with 1 % FCS (HEK), 0.5 % FCS (LLC-PK1) and 1.5 % FCS (NRK). \*  $p \leq 0.05$  vs. control.

As a second endpoint of genotoxicity the micronucleus frequency test was chosen. Micronuclei are a subspecies of chromosomal aberrations, which are inherited to the first generation of daughter cells after mitosis. They are chromatin-containing structures in the cytosol, surrounded by a membrane without any link to the nucleus. Micronuclei are formed by exclusion of whole chromosomes or chromatin fragments during mitosis. They are counted in cells which have divided exactly once, enabling the comparison of DNA damage in cell populations with different division kinetics. To identify those cells, an inhibitor of actin polymerisation, cytochalasin B, is used, which prevents the separation of daughter cells but not of daughter nuclei, yielding binucleated (BN) cells. Treatment of HEK, LLC-PK1 and NRK cells with aldosterone concentrations from 100 nM led to the significant induction of micronuclei (Figure 45).

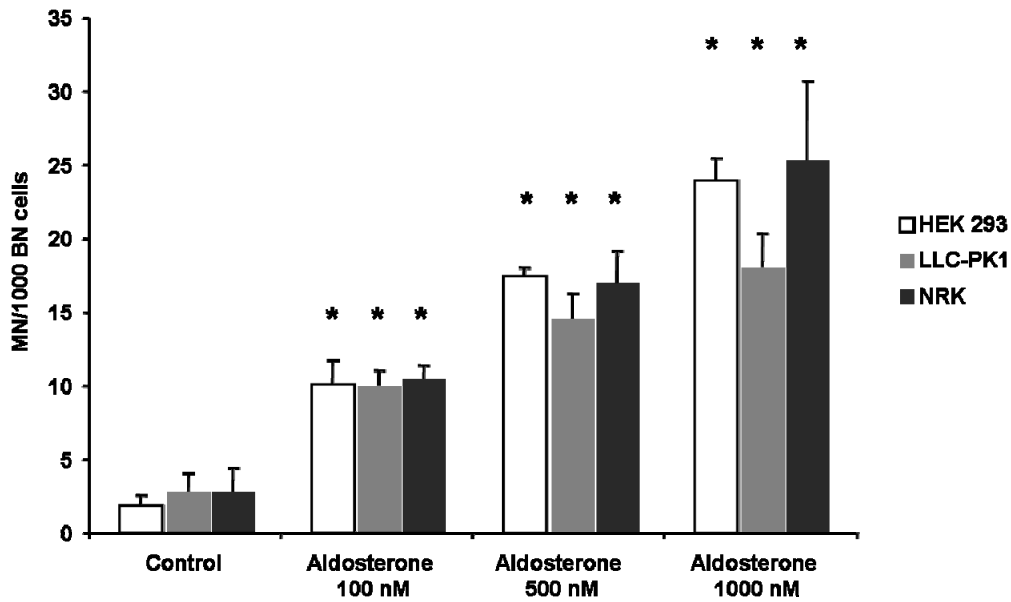


**Figure 45:** DNA damage induced by the indicated aldosterone concentrations quantified with the micronucleus test in HEK, LLC-PK1 and NRK cells incubated 4 hours in cell culture medium with 1.0 (HEK), 0.5 % (LLC-PK1) and 1.5 % (NRK) FCS, followed by 24 hours incubation in cell culture medium with 10 % FCS and 3 µg/ml cytochalasin B. Shown is the number of micronuclei per 1000 binucleated cells. MN = micronuclei, BN = binucleated cells, \* p ≤ 0.05 vs. control

For the following experiments, the lowest aldosterone concentration, which induced significant DNA damage in both genotoxicity assays, was chosen. As one possible underlying mechanism of the aldosterone-induced DNA damage, the formation of oxidative stress was analyzed. Indeed, 100 nM aldosterone caused a significant production of free radical species measured by flow cytometry in all kidney cell lines (Figure 46).

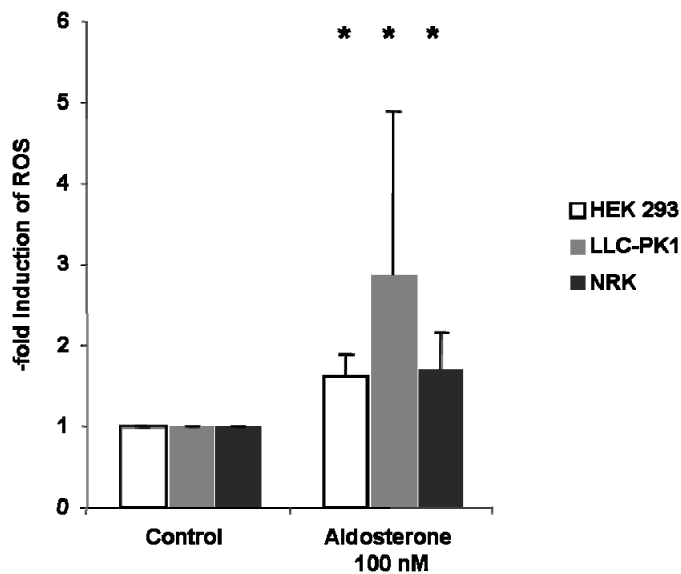


**Figure 46:** Quantification of the release of reactive oxygen species (ROS) induced by the indicated aldosterone concentration in HEK, LLC-PK1 and NRK cells after 30 min incubation in cell culture medium containing 1.0 % (HEK), 0.5 % (LLC-PK1) and 1.5 % (NRK) FCS, measured by flow cytometry, normalized to the untreated control. \* p ≤ 0.05 vs. control

In the following, two mineralocorticoid-receptor antagonists were analyzed with regard to their ability to inhibit the release of reactive oxygen species (ROS) and the subsequent formation of DNA strand breaks and micronuclei. With eplerenone, a substance was chosen, which does not possess any more the endocrine side effects of spironolactone. The second substance, BR-4628, was tested as (S)- and as (R)- isomer. As all antagonists are prone to bind to proteins, for all further experiments, cell culture medium with reduced fetal calf serum was used (1.0 % for HEK cells, 0.5 % for LLC-PK1 cells and 1.5 % for NRK cells).

Assessment of the inhibition of ROS release revealed that eplerenone and (S)-BR-4628 were both able to prevent the formation of oxidative stress, yet (S)-BR-4628 was more potent as it was effective in concentrations from 0.1  $\mu\text{M}$  on, whereas eplerenone only showed effects from 0.5  $\mu\text{M}$  on (Figures 47 A and B). The (R)- isomer of BR-4628, which shows no activity when bound to the mineralocorticoid receptor, was not able to prevent the formation of oxidative stress induced by aldosterone (Figure 47 C).

A

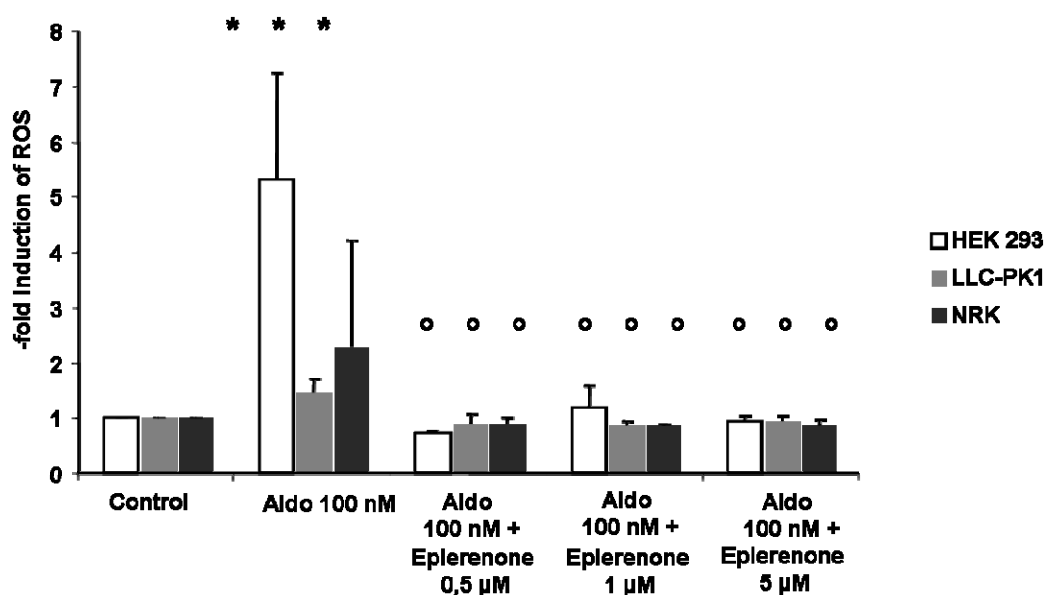


**Figure 47 A:** Quantification of the release of reactive oxygen species (ROS) induced by the indicated aldosterone (Aldo) concentration with and without co-incubation with eplerenone in the indicated concentrations in HEK, LLC-PK1 and NRK cells after 30 min incubation in cell culture medium containing 1.0 % (HEK), 0.5 % (LLC-PK1) and 1.5 % (NRK) FCS, measured by flow cytometry. \*  $p \leq 0.05$  vs. control, °  $p \leq 0.05$  vs. aldosterone treatment

B

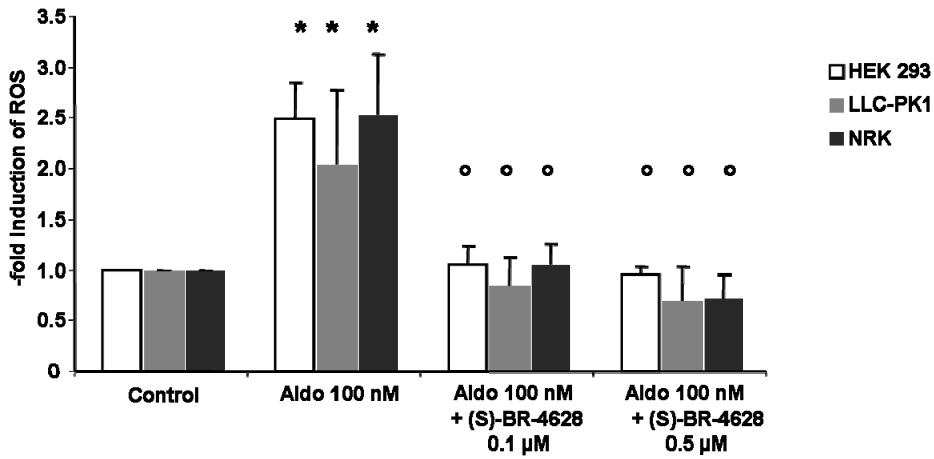


**Figure 47 B:** Quantification of the release of reactive oxygen species (ROS) induced by the indicated aldosterone (Aldo) concentration with and without co-incubation with (S)-BR-4628 in the indicated concentrations in HEK, LLC-PK1 and NRK cells after 30 min incubation in cell culture medium containing 1.0 % (HEK), 0.5 % (LLC-PK1) and 1.5 % (NRK) FCS, measured by flow cytometry. \*  $p \leq 0.05$  vs. control, °  $p \leq 0.05$  vs. aldosterone treatment

C

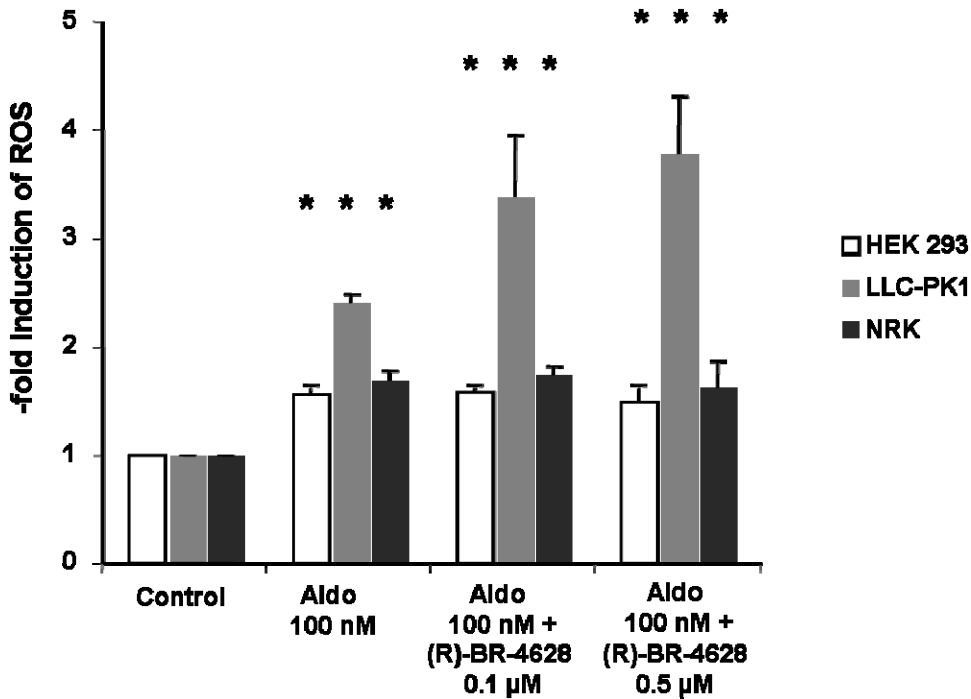


**Figure 47 C:** Quantification of the release of reactive oxygen species (ROS) induced by the indicated aldosterone (Aldo) concentration with and without co-incubation with (R)-BR-4628 in the indicated concentrations in HEK, LLC-PK1 and NRK cells after 30 min incubation in cell culture medium containing 1.0 % (HEK), 0.5 % (LLC-PK1) and 1.5 % (NRK) FCS, measured by flow cytometry. \*  $p \leq 0.05$  vs. control, °  $p \leq 0.05$  vs. aldosterone treatment

Further experiments investigating the potency of the mineralocorticoid receptor antagonists to inhibit not only the release of reactive oxygen species, but also the genomic damage most probably resulting from the oxidative stress, revealed that eplerenone and (S)-BR-4628 were both able to inhibit formation of DNA strand breaks (Figures 48 A and B) and micronuclei (Figures 49 A and B), whereas (R)-BR-4628 showed no such effects (Figures 50 A and B).

A

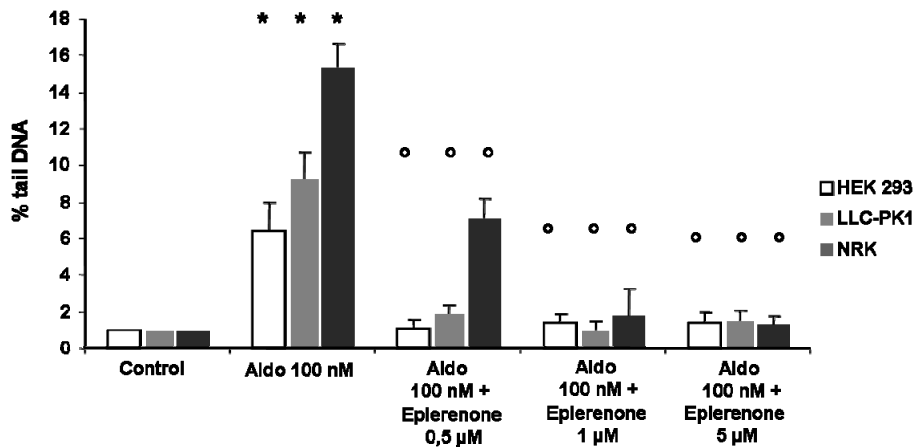


**Figure 48 A:** DNA damage induced by 100 nM aldosterone (Aldo) quantified with the comet assay in HEK, LLC-PK1 and NRK cells incubated 4 hours in cell culture medium containing 1.0 % (HEK), 0.5 % (LLC-PK1) and 1.5 % (NRK) FCS with and without co-incubation with eplerenone, shown is the induction of DNA damage related to the control. \*  $p \leq 0.05$  vs. control, °  $p \leq 0.05$  vs. aldosterone treatment.

B

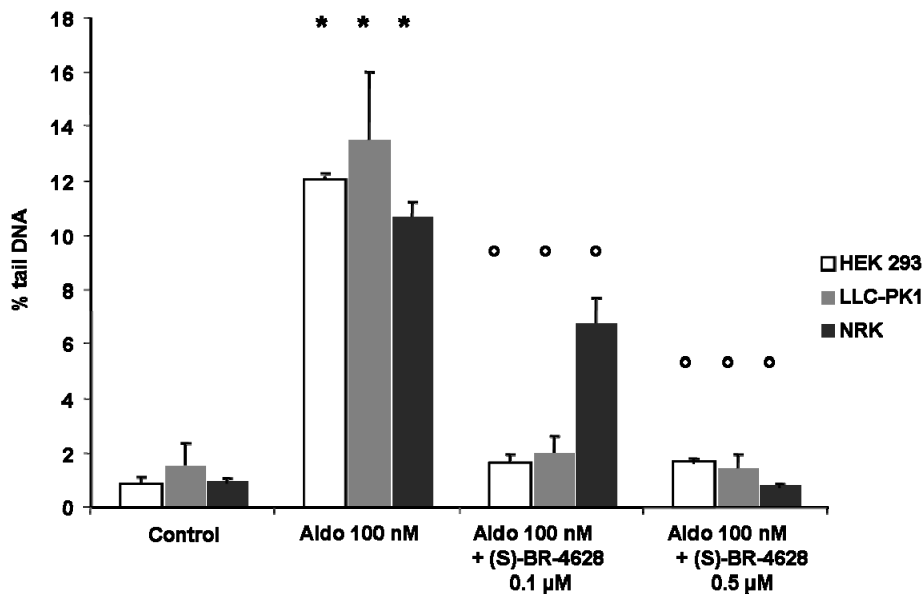


**Figure 48 B:** DNA damage induced by 100 nM aldosterone (Aldo) quantified with the comet assay in HEK, LLC-PK1 and NRK cells incubated 4 hours in cell culture medium containing 1.0 % (HEK), 0.5 % (LLC-PK1) and 1.5 % (NRK) FCS with and without co-incubation with (S)-BR-4628. \*  $p \leq 0.05$  vs. control, °  $p \leq 0.05$  vs. aldosterone treatment.



A

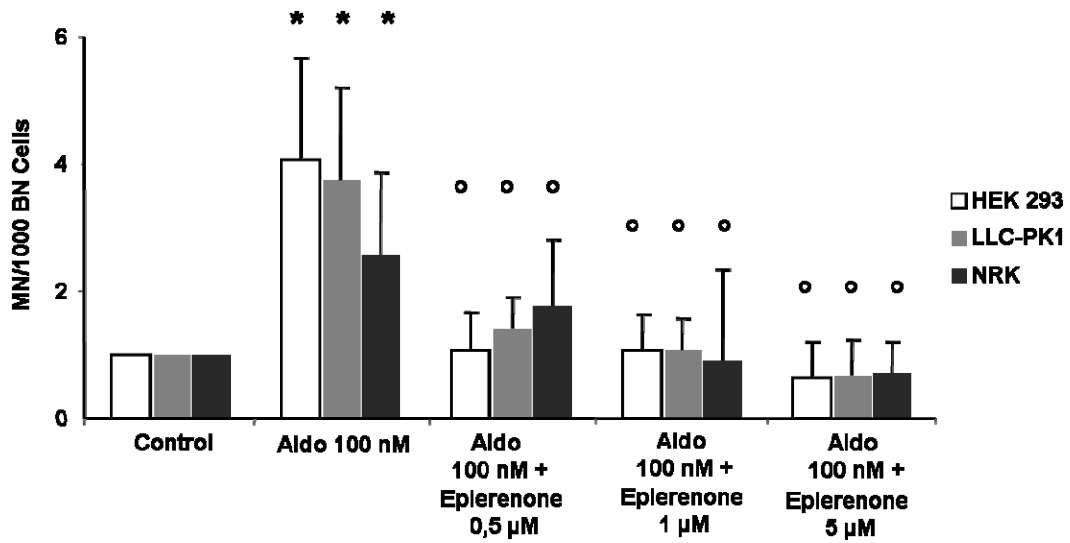


**Figure 49 A:** DNA damage induced by 100 nM aldosterone (Aldo) quantified with the micronucleus test in HEK, LLC-PK1 and NRK cells incubated 4 hours in cell culture medium containing 1.0 % (HEK), 0.5 % (LLC-PK1) and 1.5 % (NRK) FCS with and without co-incubation with eplerenone. Shown is the induction of DNA damage related to the control and subsequent doubling time of 24 h in cell culture medium containing 10 % FCS and 3 μg/ml cytochalasin B. \* p ≤ 0.05 vs. control, ° p ≤ 0.05 vs. aldosterone treatment.

B

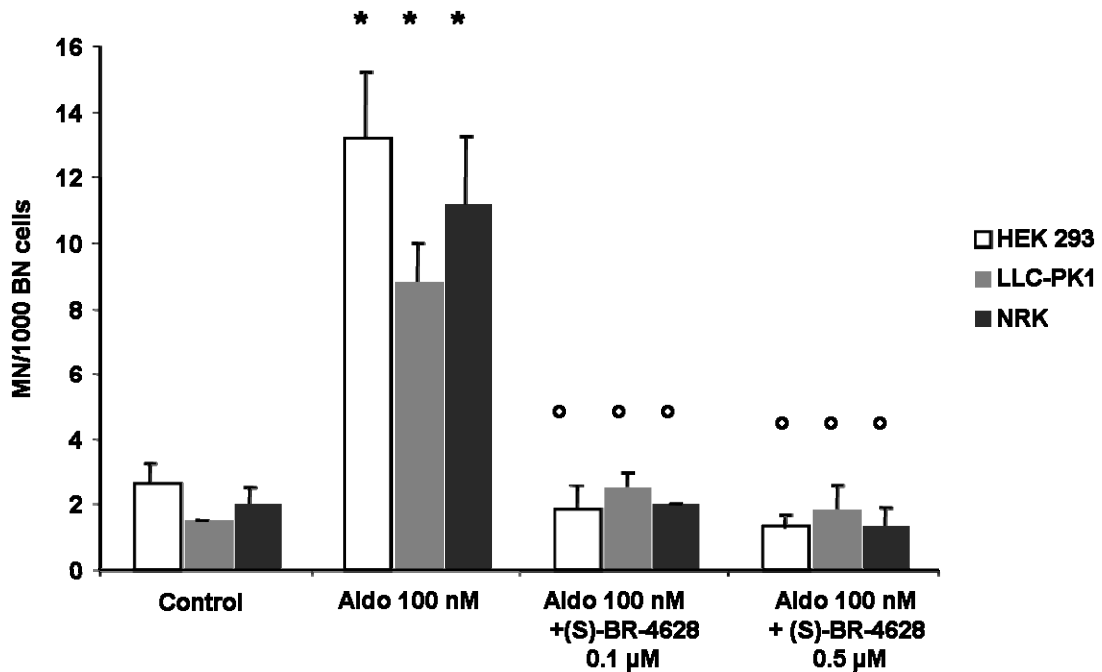
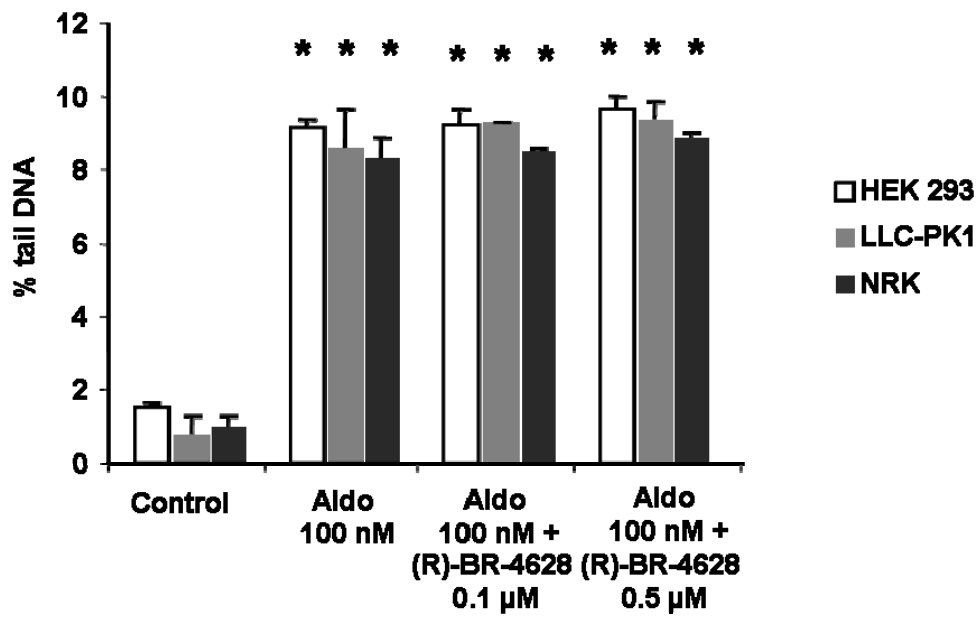


**Figure 49 B:** DNA damage induced by 100 nM aldosterone (Aldo) quantified with the micronucleus test in HEK, LLC-PK1 and NRK cells incubated 4 hours in cell culture medium containing 1.0 % (HEK), 0.5 % (LLC-PK1) and 1.5 % (NRK) FCS with and without co-incubation with (S)-BR-4628 and subsequent doubling time of 24 h in cell culture medium containing 10 % FCS and 3 μg/ml cytochalasin B. \* p ≤ 0.05 vs. control, ° p ≤ 0.05 vs. aldosterone treatment.

A



B

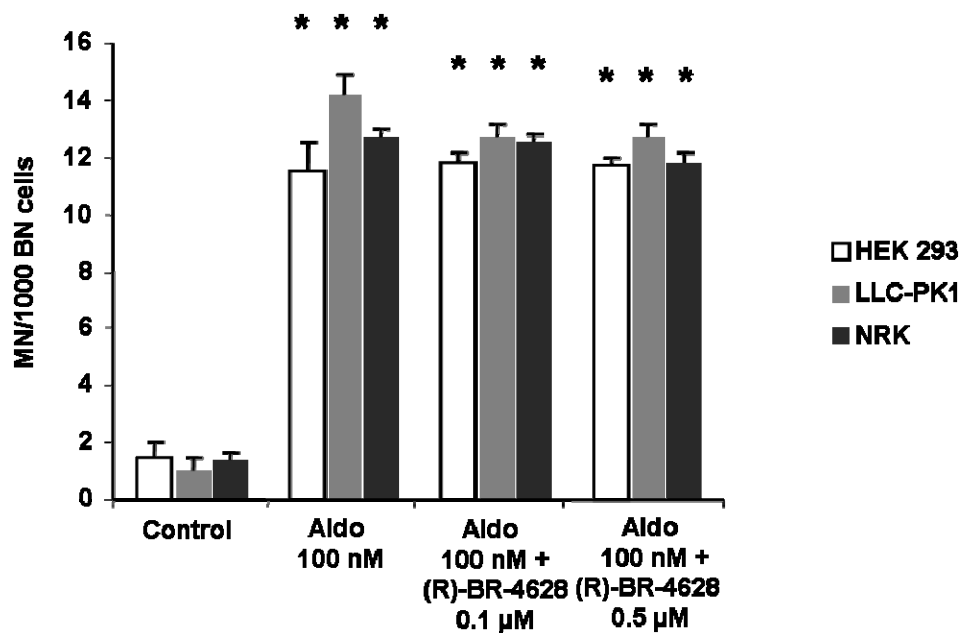


**Figure 50:** DNA damage induced by 100 nM aldosterone (Aldo) quantified with the comet assay in HEK, LLC-PK1 and NRK cells incubated 4 hours in cell culture medium with and without co-incubation with (R)-BR-4628 in cell culture medium containing 1.0 % (HEK), 0.5 % (LLC-PK1) and 1.5 % (NRK) FCS (A). DNA damage induced by 100 nM aldosterone (Aldo) quantified with the micronucleus test in HEK, LLC-PK1 and NRK cells incubated 4 hours in cell culture medium containing 1.0 % (HEK), 0.5 % (LLC-PK1) and 1.5 % (NRK) FCS with and without co-incubation with (R)-BR-4628 and subsequent doubling time of 24 h in cell culture medium containing 10 % FCS and 3 µg/ml cytochalasin B. (B) \*  $p \leq 0.05$  vs. control, °  $p \leq 0.05$  vs. aldosterone treatment.

#### 6.1.4. Discussion

In HEK human kidney cells, LLC-PK1 pig kidney cells as well as in NRK rat kidney cells, a DNA damaging potential of aldosterone could be observed. Aldosterone was capable of inducing DNA damage detectable in the comet assay, which consists of single and double strand breaks, alkali labile sites, DNA-DNA and DNA-protein crosslinks [182]. Depending on the class of DNA damage, these lesions can theoretically be repaired [183], with the perpetual risk of mutation by repair errors. Aldosterone also induced unreparable, inheritable DNA damage detected in the micronucleus frequency test. The two basic mechanisms leading to the formation of micronuclei are chromosome breakage and disturbance of the chromosome segregation machinery, leading to mutated daughter cells [117, 183].

DNA damage observed in the comet assay started from 10 nM in the cells incubated with reduced FCS. Normal plasma aldosterone levels in humans range from 20 to 420 pM (7 - 150 pg/ml plasma), while individuals with primary aldosteronism reach aldosterone concentrations of 900 pM in plasma, whereby 100 - 500 times higher concentrations can be reached in the adrenal veins [184-186]. The concentration at which first significant DNA damage is measured therefore is only approximately ten times higher than in individuals with primary aldosteronism and 25 - 500 times higher than in the general population.

In contrast to Patni et al. [187], who observed a significant induction of apoptosis at the aldosterone concentration of 100 nM, we did not find an increase of apoptotic cells, neither among HEK nor LLC-PK1 nor NRK cells. This might be due to the fact that we incubated the cells only for 4 hours, while the authors see first significant effects after 12 hours.

Aldosterone is known to induce oxidative stress through several mechanisms: up-regulation of the expression of NAD(P)H oxidase subunits, promotion of the “uncoupling” of nitric oxide synthase (NOS), inhibition of NADP<sup>+</sup> reduction by decrease of the activity of glucose-6-phosphate dehydrogenase [67]. We also could measure the formation of oxidative stress induced by aldosterone, already after 30 minutes. One function of free radicals is to act as second messengers in signal transduction and gene regulation in many conditions as well as in apoptosis [188].

Another possible effect of reactive oxygen species is the induction of the formation of DNA strand breaks and micronuclei, which in turn might be able to cause cancer [189]. Therefore, the possibility that oxidative stress is the mechanism underlying the

formation of the genomic damage was analyzed in the course of this study by addition of inhibitors of the mineralocorticoid receptor. With eplerenone, a well known steroidal substance without endocrine side effects, proved to be able to prevent the formation of ROS and subsequently the formation of DNA strand breaks and chromosomal aberrations manifesting themselves as micronuclei. Furthermore, the new non-steroidal inhibitor (S)-BR-4628 was also able to inhibit the release of ROS and in consequence the development of genomic damage as measured by comet assay and micronucleus frequency test. However, the also examined (R)-isomer of BR-4628, which shows no activity when bound to the mineralocorticoid receptor, has no such potential. It is therefore conceivable that the effects of the two aldosterone inhibitors tested are indeed mediated via the mineralocorticoid receptor.

This is, to the best of our knowledge, the first report of a genotoxic effect of aldosterone, the identification of possible underlying mechanisms and their prevention by mineralocorticoid receptor antagonists. Further investigations will have to be performed to elucidate the mechanisms which underlie these cellular processes.

## **6.2. Aldosterone induces oxidative stress and genomic damage *in vivo***

### **6.2.1. Background**

Aldosterone is produced in the adrenal zona glomerulosa upon stimulation by angiotensin II, potassium or the adrenocorticotrophic hormone (ACTH). Classically, it regulates sodium excretion and thereby blood pressure homeostasis through mineralocorticoid receptor-dependent genomic effects in the distal nephron of the kidney [190]. Furthermore it is, together with angiotensin II, the major effector of the renin-angiotensin-aldosterone system (RAAS). In addition to its classical effects on gene expression, aldosterone can exert non-genomic effects which occur within minutes via activation of protein kinase C (PKC) and mitogen-activated protein kinase [191]. It is hypothesized that these non-genomic effects of aldosterone could be independent from the mineralocorticoid receptor, yet experiments where the spironolactone-metabolites canrenoate and eplerenone were able to block non-genomic effects contradict this hypothesis [192].

Activation of the RAAS is associated with increased morbidity and mortality among patients with hypertension and congestive heart failure (CHF). These effects have been ascribed to the hypertrophic, proliferative, pro-inflammatory, prothrombotic and profibrotic effects of angiotensin II. Nowadays, there is an increasing body of evidence that aldosterone or mineralocorticoid receptor activation contribute to many of these effects and that there is an interaction of angiotensin II and aldosterone in inducing inflammation, fibrosis and proliferation [67].

*In vivo*, chronic aldosterone infusion at doses which can be observed in CHF causes myocardial fibrosis in the setting of high salt intake [193]. This fibrosis is characterized by antecedent inflammation which can be blocked together with the fibrosis by mineralocorticoid receptor antagonism [194]. Mineralocorticoid receptor activation during high salt intake can cause  $\text{Ca}^{2+}$  loading [195] which in turn causes oxidative stress and subsequent end-organ damage [67].

As hypertension caused by hyperaldosteronism is in most cases therapy resistant, there were several clinical trials examining the effect of combined mineralocorticoid receptor antagonism and ACE inhibition. During the RALES study, CHF patients who were already treated with an ACE inhibitor, diuretics and digoxin received additionally

spironolactone. This treatment regime reduced mortality by 30 % [196]. In the EPHEBUS study, eplerenone together with ACE inhibitors, angiotensin II type 1 receptor (AT<sub>1</sub>R) antagonists,  $\beta$ -blockers, digoxin and diuretics reduced all-cause and cardiovascular mortality in patients with left ventricular dysfunction [197].

These results indicate that hyperaldosteronism which was thought until now to be an uncommon cause of hypertension, has a high prevalence in hypertensive patients. As these patients have an elevated risk to develop kidney cancer [50, 51] and a higher risk to die from cancer overall [141], this study was undertaken to investigate DOCA/salt-induced hyperaldosteronism with regard to its DNA-damaging capacity. Furthermore, a steroidal and a non-steroidal mineralocorticoid receptor antagonist in comparison to an ACE inhibitor were tested for their potential to inhibit oxidative DNA damage.

## 6.2.2. Experimental

### 6.2.2.1. Material

If not mentioned otherwise, all chemicals were purchased from Sigma Aldrich, Taufkirchen, Germany. Spironolactone, enalapril and BR-4628 were provided by Bayer HealthCare AG, Wuppertal, Germany

### 6.2.2.2. Treatment of DOCA rats

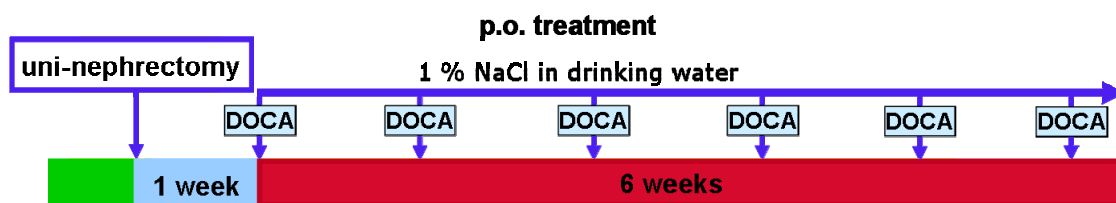
Male Sprague-Dawley rats were acclimated to their surroundings for one week before initiating the experiment. The 35 animals (5 per group), approximately 8 weeks old (250 to 300 g body weight), were anesthetized with 1.5 - 2 % isofluran in 66 % N<sub>2</sub>O and 33 % O<sub>2</sub> and uni-nephrectomized. Sham-control animals were anesthetized and operated but not nephrectomized.

After 7 days, desoxycorticosterone acetate (DOCA) (30 mg/kg BW in sesame oil), was applied once a week subcutaneously. Additionally, the animals received 1 % NaCl in their drinking water which was together with standard rat chow available *ad libitum*.

The test substances spironolactone (50 mg/kg BW), enalapril (10 mg/kg BW) and BR-4628 (10 mg/kg BW), all solved in 10 % ethanol, solutol 40 %, water 50 %, were applied by gavage daily for 6 weeks. The placebo treated animals only received the solvent. Positive control animals were treated like the placebo group for 5 weeks and 5 days and received 48 h before the end of the experiment cisplatin i. p. (2.5 mg/kg BW).

All animals were sacrificed after six weeks of treatment by overdosing them with CO<sub>2</sub>. As treatment of the test animals was executed by Bayer Healthcare AG, Wuppertal, all animal procedures were approved by the Animal Ethics Committee of Nordrhein-Westfalen.

## Induction of arterial hypertension, myocardial fibrosis and diastolic heart failure by DOCA/salt



Groups (n=5 animals/group):

- sham
- placebo
- spironolactone 50 mg/kg/d
- BR-4628 10 mg/kg/d
- enalapril 10 mg/kg/d
- placebo + cisplatin 2.5 mg/kg, single i.p.-application 48 h before the end of the experiment (n=5)

Figure 51: Treatment scheme

### 6.2.2.3. Extraction of primary kidney cells

Freshly obtained rat kidneys were minced on ice to small pieces. These pieces were suspended in 3 ml buffer consisting either of RPMI 1640, 15 % DMSO, 1.8 % (w/v) NaCl if destined for comet assay and flow cytometric measurement of oxidative stress, or Hanks Balanced Salt Solution (HBSS), 10 % DMSO and 20 mM Na<sub>2</sub>EDTA if destined for the micronucleus frequency test. The extracted isolated primary rat kidney cells were sifted through a cell strainer with a mesh pore size of 100 µm (Becton Dickinson, Heidelberg, Germany), centrifuged for 5 minutes at 1000 rpm and 4 °C and were finally resuspended in 1 ml of the respective buffer.

### 6.2.2.4. Comet Assay

RPMI-based cell suspensions of extracted primary kidney cells were utilized for comet assay which was carried out as described by Schupp et al. [128], using a fluorescence microscope at a 200-fold magnification and computer aided image analysis (Komet 5, Kinetic Imaging Ltd., UK). After DNA staining with propidium iodide (20 µg/ml), 50 cells from one slide were measured, % tail DNA being the evaluation parameter. The alkaline comet assay detects single strand breaks, double strand breaks and alkali labile sites. The DNA fragments move during electrophoresis due to their negative charge out of the nucleus in direction of the anode. Smaller



fragments can move faster through the agarose in which the nuclei are embedded, resulting in characteristic comet-like structures.

#### **6.2.2.5. Micronucleus frequency test**

HBSS-based cell suspensions were utilized for the micronucleus frequency test. Approximately  $4 \times 10^4$  cells were applied onto glass slides by cytopspin centrifugation and fixed in methanol ( $-20\text{ }^{\circ}\text{C}$ ) for at least two hours. Before counting, cells were stained for 3 minutes with acridine orange ( $62.5\text{ }\mu\text{l/ml}$  in Sørensen buffer, pH 6.8), washed twice with Sørensen buffer and mounted for microscopy. From each of two slides, 1000 cells were evaluated with regard to micronucleus frequency. Evaluation criteria were according to Fenech [118].

#### **6.2.2.6. Flow cytometric analysis of oxidative stress**

Approximately  $10^6$  primary rat kidney cells were treated for 10 minutes with  $10\text{ }\mu\text{M}$  2',7'-dichlorodihydrofluorescein diacetate ( $\text{H}_2\text{DCF-DA}$ ) in DMEM medium ( $1\text{ g/l}$  glucose) supplemented with 10 % fetal calf serum, 1 % glutamine, 25 mM HEPES buffer and antibiotics at  $37\text{ }^{\circ}\text{C}$ . Subsequently, cells were washed two times with cold PBS/1 % BSA, counterstained with propidium iodide ( $1\text{ }\mu\text{g/ml}$ ) to exclude dead cells and  $3 \times 10^4$  cells per sample were analyzed by using a FACS LSR I (Becton-Dickinson, Mountain View, CA). Medians of the histograms were assessed using the free software WinMDI 2.9 (Scripps Research Institute Cytometry Software, <http://facs.scripps.edu/software.html>).

#### **6.2.2.7. Statistics**

If not mentioned otherwise, data from at least 5 independent measurements  $\pm$  standard deviation are depicted. Statistical significance among multiple groups was tested with Kruskal-Wallis test over all groups and Mann-Whitney test was used to determine significance between two groups. Results were considered significant if the  $p$  value was  $\leq 0.05$ .

## 6.2.3. Results

### 6.2.3.1. Oxidative stress

Aldosterone-induced oxidative stress in male Sprague-Dawley rats was measured by flow cytometry (Figures 52 A and B). Compared to the operated but not treated Sham-group, DOCA-Placebo-treatment induced significant release of reactive oxygen species (ROS). Additional treatment with the steroidal mineralocorticoid receptor antagonist spironolactone (50 mg/kg BW), the non-steroidal mineralocorticoid receptor antagonist BR-4628 (10 mg/kg BW) and the angiotensin-converting-enzyme (ACE) inhibitor enalapril (10 mg/kg BW) resulted in a significant decrease of oxidative stress-induced fluorescence. BR-4628 proved to be the most potent substance since it reduced the release of ROS significantly not only compared to DOCA-Placebo-treatment but also to Sham-treatment. Additional treatment with cisplatin (2.5 mg/kg BW, i. p.) for 48 h resulted in an increase of ROS formation which was significant compared to the Sham-group but not to the DOCA-Placebo-treatment.

A

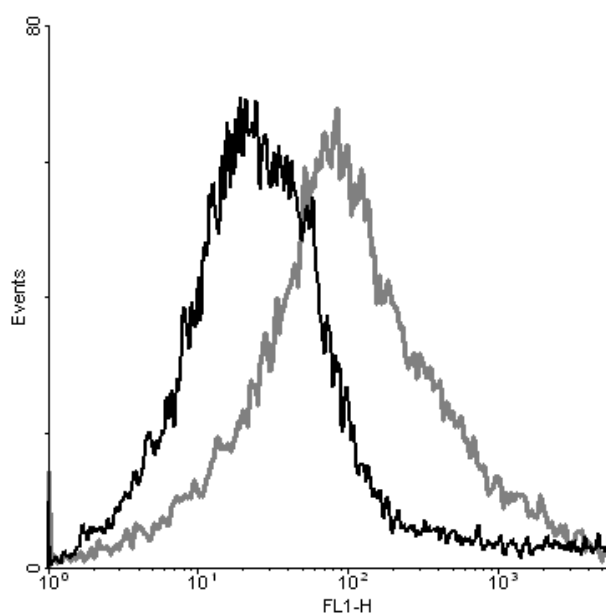


**Figure 52 A:** Flow cytometric analysis of DOCA/salt-induced reactive oxygen species (ROS) production in male Sprague Dawley rats. Shown is a representative frequency histogram of the green fluorescence of H<sub>2</sub>DCF-positive cells of Sham-operated animals (black line) and animals treated for 6 weeks with DOCA/salt and placebo (grey line).

B

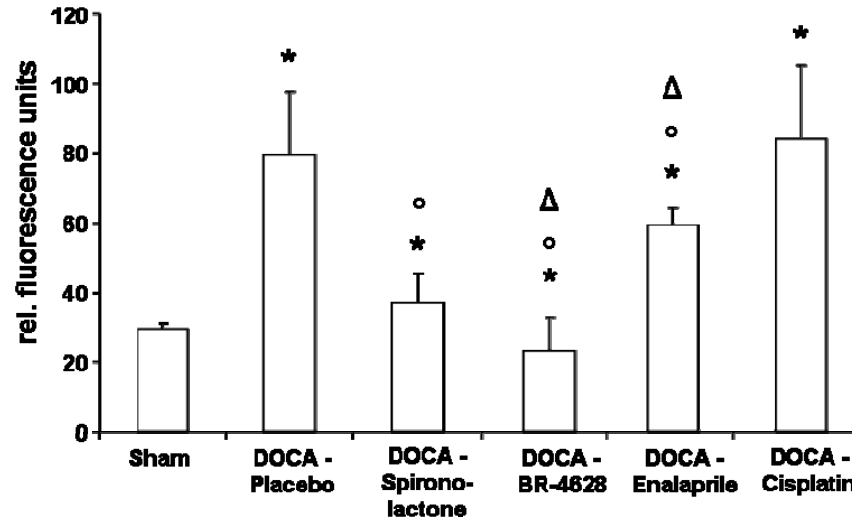


**Figure 52 B:** Quantification of the release of reactive oxygen species (ROS) after 6 weeks DOCA-treatment in male Sprague Dawley rats with and without co-treatment with spironolactone, BR-4628, enalapril and cisplatin, measured by flow cytometry. \*  $p \leq 0.05$  vs. Sham, °  $p \leq 0.05$  vs. DOCA-Placebo, Δ  $p \leq 0.05$  vs. DOCA-Spironolactone.

### 6.2.3.2. DNA damage

Measurements of the amount of DNA strand breaks (Figure 53 A) subsequent to DOCA-treatment assessed by the comet assay showed that DOCA induced significant formation of DNA single and double strand breaks and alkali labile sites compared to the untreated Sham-animals (Figure 53 B). After simultaneous treatment with spironolactone, BR-4628 and the ACE inhibitor enalapril, a significant decrease in the incidence of DNA strand breaks could be observed. Co-treatment with cisplatin resulted in a significant induction of DNA damage compared to Sham-animals, yet the induction was not higher than with DOCA alone.

A

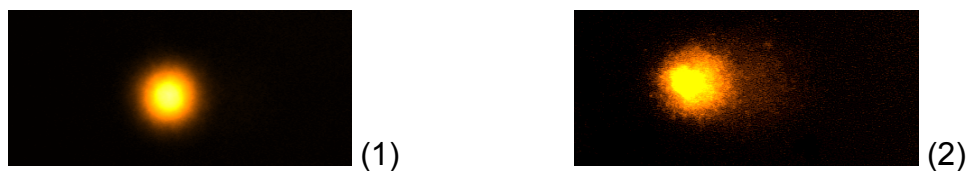


**Figure 53 A:** DNA damage in male Sprague Dawley rats as measured by the comet assay after 6 weeks DOCA-treatment. Exemplarily depicted are nuclei of a Sham-treated animal (1) and of a DOCA-Placebo-treated animal (2).

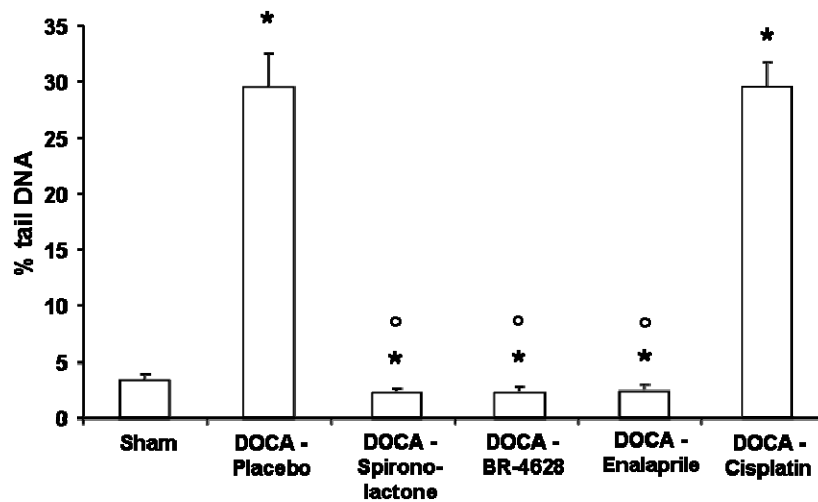


**Figure 53 B:** DNA damage in male Sprague Dawley rats as measured by the comet assay after 6 weeks DOCA-treatment with and without co-treatment with spironolactone, BR-4628, enalapril and cisplatin. \*  $p \leq 0.05$  vs. Sham, °  $p \leq 0.05$  vs. DOCA-Placebo.

### 6.2.3.3. Micronuclei, Mitoses and Apoptoses

Furthermore, the incidence of chromosomal aberrations, manifesting themselves as micronuclei (Figure 54 A, white arrow), was evaluated. DOCA-Placebo-treatment induced a significant increase in the number of micronuclei compared to the Sham-animals. Co-treatment with the mineralocorticoid receptor antagonists spironolactone and BR-4628 as well as the ACE inhibitor enalapril reduced micronuclei frequency almost to control levels whereas co-treatment with cisplatin resulted in an additional significant increase compared to DOCA-Placebo-treated animals (Figure 54 B).

A

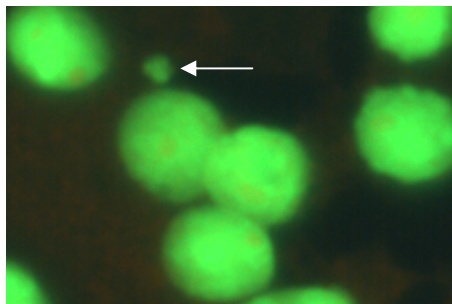


**Figure 54 A:** Micronucleus in male Sprague Dawley rats as measured by micronucleus frequency test after 6 weeks DOCA-Placebo treatment.

B

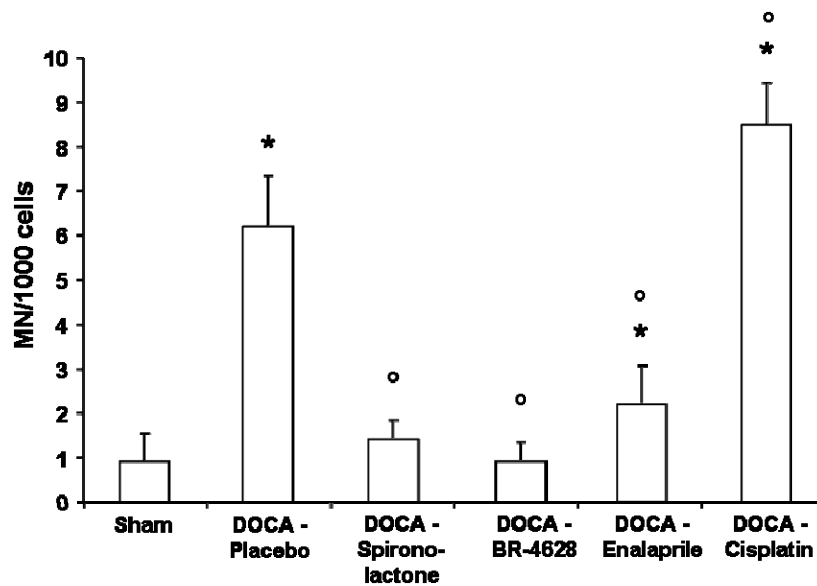


**Figure 54 B:** Micronuclei frequency in male Sprague Dawley rats as measured by the micronucleus frequency test after 6 weeks DOCA-treatment with and without co-treatment with spironolactone, BR-4628, enalapril and cisplatin. \*  $p \leq 0.05$  vs. Sham, °  $p \leq 0.05$  vs. DOCA-Placebo.

The same slides were evaluated with regard to the number of mitoses (Figure 55 A) and apoptoses (Figure 56 A) per 1000 cells. Neither DOCA-treatment nor DOCA-co-treatment with spironolactone, BR-4628, enalapril or cisplatin had any significant effect on the number of mitoses (Figure 55 B).

A

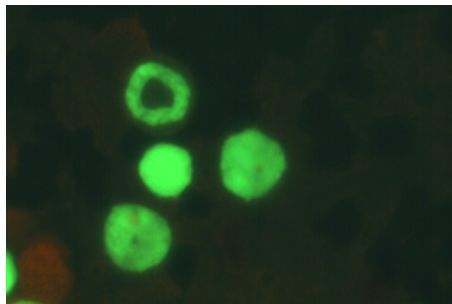


**Figure 55 A:** Mitosis in male Sprague Dawley rats after 6 weeks DOCA-Placebo treatment.

B

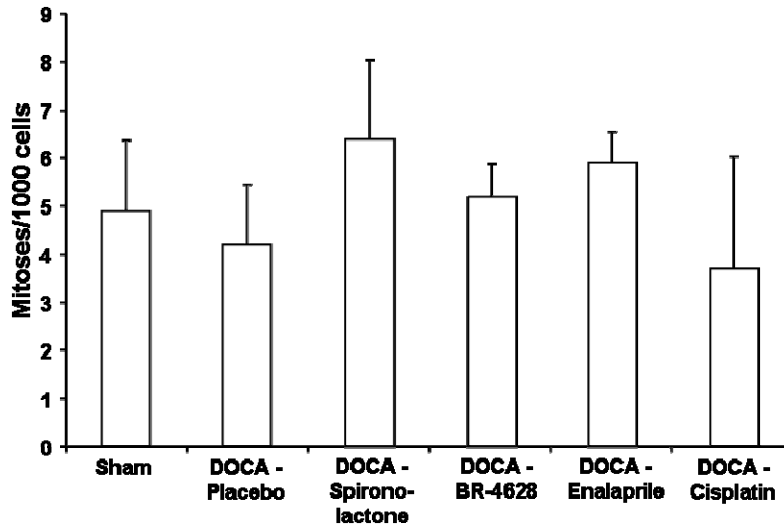


**Figure 55 B:** Mitosis frequency in male Sprague Dawley rats after 6 weeks DOCA-treatment with and without co-treatment with spironolactone, BR-4628, enalapril and cisplatin. \*  $p \leq 0.05$  vs. Sham.

The number of apoptoses was just altered significantly by DOCA-Cisplatin-treatment compared to the Sham-group. Treatment with DOCA alone also increased the frequency of apoptoses, yet not significantly. After simultaneous treatment with DOCA and spironolactone, BR-4628 or enalapril, a decrease in the number of apoptoses compared to DOCA-Placebo-treatment could be observed, yet no significance could be reached (Figure 56 B).

A

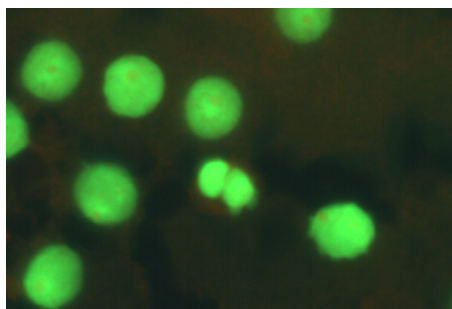


**Figure 56 A:** Apoptosis in male Sprague Dawley rats after 6 weeks DOCA-Placebo treatment.

B

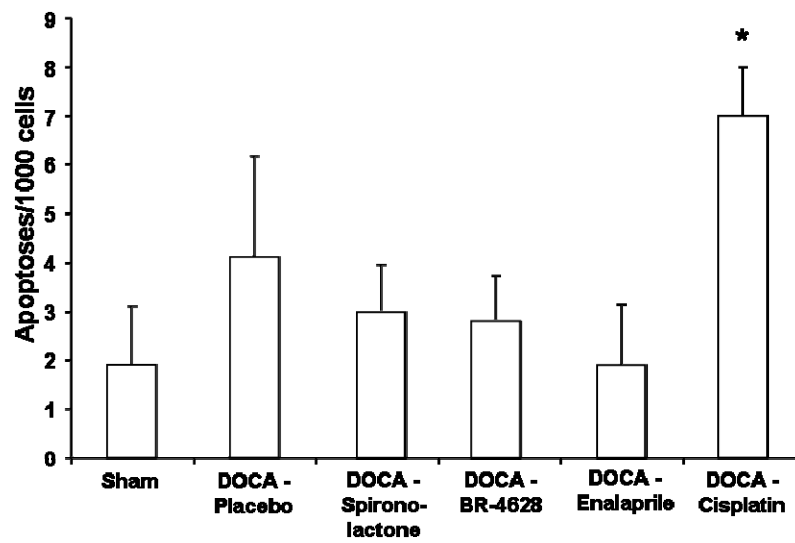


**Figure 56 B:** Apoptosis frequency in male Sprague Dawley rats after 6 weeks DOCA-treatment with and without co-treatment with spironolactone, BR-4628, enalapril and cisplatin. \*  $p \leq 0.05$  vs. Sham.

#### 6.2.4. Discussion

By aid of the DOCA/salt model, hypertension was induced in male Sprague-Dawley rats. It was already shown that aldosterone-induced end organ injuries were associated with increased expression of subunits of NAD(P)H oxidase and increased levels of reactive oxygen species (ROS) [198]. Consistent with these findings, significantly increased levels of ROS could be measured in DOCA-Placebo-treated animals.

ROS can not only play a physiological role as second messengers in signal transduction, gene expression and apoptosis, but can also trigger the formation of genomic damage, which in turn can cause cancer. Therefore, the incidence of DNA single and double strand breaks, alkali labile sites and crosslinks as assessed by comet assay [182, 183] and micronuclei as assessed by micronucleus frequency test following DOCA/salt-treatment were investigated.

For the, to the best of our knowledge, first time, DNA damage in whole end-organs caused by the hormone aldosterone, could be observed *in vivo*, as treatment with DOCA/salt resulted in a significant increase of DNA damage and micronuclei.

Both lesions are associated with the risk of formation of mutated daughter cells [117, 183]. In contrast to Patni et al. [187], who showed an elevated incidence of apoptotic cells following chronic treatment with aldosterone in a human kidney cell line, a significant increase in apoptotic cells could only be observed in the group of animals treated with the nephrotoxin cisplatin compared to the Sham-group. The DOCA-Placebo group exhibited a slight increase in the number of apoptoses, yet no significance could be reached.

It was already shown that enalapril was able to prevent renal damage in hypertensive rats [199]. In our experiments, simultaneous application of DOCA/salt and the ACE-inhibitor enalapril also yielded an inhibition of oxidative stress and genomic damage in the kidney, however, levels of sham-operated animals could not be reached.

Treatment of animals with spironolactone, a steroidal mineralocorticoid receptor antagonist, or BR-4628, a non-steroidal mineralocorticoid receptor antagonist, in combination with DOCA/salt resulted in a complete prevention of the formation of ROS. This is in line with already published findings where treatment with the steroidal mineralocorticoid receptor antagonist eplerenone prevented the elevation of ROS



levels and thereby ameliorated end-organ injuries [198] and own previous findings where eplerenone and (S)-BR-4628 were able to inhibit oxidative stress and genomic damage *in vitro* [48]. Furthermore, it could be shown for the first time that both mineralocorticoid receptor antagonists prevented not only oxidative stress but also the subsequent formation of DNA strand breaks and micronuclei *in vivo*.

With this study, previous findings concerning a genotoxic effect of aldosterone [48] *in vitro* could be confirmed in the DOCA/salt model. Co-treatment with enalapril and steroidal as well as non-steroidal mineralocorticoid receptor antagonists resulted in a prevention of DOCA-induced oxidative stress and subsequent oxidative DNA damage. However, the mineralocorticoid receptor antagonists, especially the non-steroidal substance, emerged to be the more effective drugs. In addition, the hypothesis could be substantiated that oxidative stress is the mechanism underlying the aldosterone-induced formation of genomic damage and that this process is mediated via the mineralocorticoid receptor. Clinical studies will have to be performed to further investigate the capacity of the mineralocorticoid receptor antagonists to exert beneficial effects with regard to blood pressure reduction and cancer prevention in hypertensive patients.

## 7. Activation of Defense Mechanisms

### ***7.1. Rosuvastatin protects against oxidative stress and DNA damage in vitro via up-regulation of glutathione synthesis***

#### **7.1.1. Background**

Statins, inhibitors of 3-hydroxy-3-methylglutaryl-coenzyme A (HMG-CoA) reductase, are widely used cholesterol-lowering drugs [200]. They inhibit the synthesis of mevalonic acid, which is a precursor of isoprenoid compounds, including cholesterol [76]. Clinical trials have shown that statins decrease cardiovascular morbidity and mortality in patients with and without coronary heart disease [77]. The effects of statins have been mainly ascribed to the inhibition of cholesterol biosynthesis and subsequent up-regulation of hepatic LDL receptor numbers, but not all therapeutic benefits can be explained solely by this property [81]. Pleiotropic non-lipid-dependent effects include improvement of endothelial function, reduced inflammation, stabilization of atherosclerotic plaques and inhibition of the thrombogenic response [82].

One of the pleiotropic mechanisms receiving much attention is the antioxidant effect of statins. Mechanisms for this may be the inhibition of oxidant formation by affecting NAD(P)H oxidase, blocking of the effects of reactive oxygen species (ROS) by up-regulation of antioxidant enzymes, or an increase in nitric oxide (NO) bioavailability which neutralizes radicals [84]. ROS, including free radicals such as  $\cdot\text{HO}$  and  $\cdot\text{O}_2^-$ , and molecules such as hydrogen peroxide, are involved and contribute to the development of atherosclerosis [201]. Important sources of ROS are NAD(P)H oxidases from endothelial cells, smooth muscle cells, fibroblasts and infiltrated monocytes/macrophages [202]. Also primed polymorphonuclear cells, which are involved in clinical states associated with high risk for developing cardiovascular disease and atherosclerosis, are a possible source for superoxide radicals and exert direct damage to endothelial cells [201, 203]. It is postulated that the priming of these cells initiates endothelial cell injury [203]. For this reason, leukocytes are of great value as a test model in the evaluation of oxidative stress and its modulation. *In vitro*, the HL-60 promyelocytic leukemia cell line has shown itself to be very reliable for investigation of proliferation, differentiation and cellular oncogene expression, as well as for the analysis of NAD(P)H oxidase activation [204, 205].

There is growing evidence that DNA is one of the most important targets of oxidative attack. If repair mechanisms fail to eliminate oxidative DNA damage, deleterious consequences for the cells may occur, including age-related dysfunctions and later development of malignancies [87]. Recently, elevated levels of oxidative DNA damage have also been found in all cell types of human atherosclerotic plaques of the carotid artery [88].

With regard to the potential role of DNA damage as a contributor to both cancer development and cardiovascular disease, investigations of the modulatory action of HMG-CoA reductase inhibitors are of special interest. Therefore we analyzed the effect of rosuvastatin on oxidative DNA damage and oxidative stress in HL-60 cells.

## **7.1.2. Experimental**

### **7.1.2.1. Material**

If not otherwise mentioned, chemicals were purchased from Sigma-Aldrich, Taufkirchen, Germany. Rosuvastatin was provided by AstraZeneca, London, UK. HL-60 cells were kindly donated by Prof. Schinzel, Vasopharm, Würzburg, Germany. Mevalonolactone was converted to sodium mevalonic acid as described by Wagner et al [206].

### **7.1.2.2. Cell culture**

HL-60 cells, a human promyelocytic cell line, were grown at 37 °C in a humidified atmosphere of 5 % CO<sub>2</sub> in RPMI medium supplemented with 10 % fetal calf serum, 1 % glutamine and antibiotics. Cells were routinely split three times a week. 1\*10<sup>6</sup> cells in cell culture flasks were treated with test compounds for the indicated time for the comet assay experiments and 1\*10<sup>6</sup> cells in 24 well plates for other experiments. Rosuvastatin was added simultaneously with other substances, if not mentioned otherwise.

### **7.1.2.3. Single cell gel electrophoresis**

Single cell gel electrophoresis (comet assay) was performed according to Singh et al. [94] with slight modifications as described by Stopper et al. [207]. Cells are embedded in agarose and exposed to an electrical field. From cells with damaged DNA (single- or double-strand breaks, alkali labile sites), more DNA can migrate than from cells with intact nuclear DNA. A comet-like structure is formed because smaller fragments and relaxed loops move faster than larger fragments and intact DNA. DNA was stained by adding 20 µl of propidium iodide (20 µg/ml). Cells were analyzed using a fluorescence microscope at a 500-fold magnification and computer-assisted image analysis. Images of 50 cells (25 from each of two slides) were evaluated using the software program Komet 5 (Kinetic Imaging Ltd., UK). The parameter measured was percentage of DNA in tail.

#### **7.1.2.4. Total glutathione determination**

DL-Buthionine-sulfoximine (500  $\mu\text{M}$ ) was added for 24 hours to achieve partial glutathione-depletion and thus enhance cellular sensitivity. Test substances were then added for 3 hours. After incubation, cells were washed twice with PBS and resuspended in 400  $\mu\text{l}$  1 % sulfosalicylic acid. After 15 min incubation on ice, cells were centrifuged (5000 g). 20  $\mu\text{l}$  of the supernatant was mixed with 260  $\mu\text{l}$  phosphate buffer [100 mM], 20  $\mu\text{l}$  dithiobis-2-nitrobenzoic acid [2.5 mM] and 300  $\mu\text{l}$  glutathione reductase solution (1.3 units glutathione reductase/ml, 50 mM phosphate buffer, 0.5 mM EDTA, 0.3 mM NADPH). The kinetics were determined at 410 nm using a U-2000 Spectrophotometer (Hitachi, Tokyo, Japan).

#### **7.1.2.5. Flow cytometric analysis of oxidative stress**

2',7'-Dichlorodihydrofluorescein diacetate ( $\text{H}_2\text{DCF-DA}$ ) was used to detect ROS production in cells [101]. HL-60 cells were preincubated with 10  $\mu\text{M}$   $\text{H}_2\text{DCF-DA}$  for 5 min at 37 °C, then test substances were added. Cells were harvested, washed two times with PBS/1 % BSA, and  $3 \cdot 10^5$  cells/sample analyzed by flow cytometry using a FACS LSR I (Becton-Dickinson, Mountain View, CA, USA) after incubation for 10 min on ice with 1  $\mu\text{g/ml}$  propidium iodide, as described by Schupp et al. [47].

#### **7.1.2.6. Determination of superoxide dismutase (SOD) activity**

$10^6$  cells were treated with test substances. Next, cells were harvested and washed with PBS. 500  $\mu\text{l}$  M-PER (Perbio Science, Bonn, Germany) was added for cell lysis. Cells were resuspended and put on a shaker for 10 minutes. Afterwards, cells were centrifuged (3000 rpm) and immediately put on ice. Per cuvette, 100  $\mu\text{l}$  diethylenamine pentaacetate [1.3 mM], 7,7  $\mu\text{l}$  catalase [1 U/ml], 100  $\mu\text{l}$  nitroblue tetrazolium [70  $\mu\text{M}$ ], 100  $\mu\text{l}$  xanthine [0.2 mM], 100  $\mu\text{l}$  bathocuproine disulfonate [0.05 mM], 392.3  $\mu\text{l}$  bovine serum albumin [0.13 mg/ml], 100  $\mu\text{l}$  sample and 100  $\mu\text{l}$  xanthine oxidase [0.05 U/ml] were added. Samples were measured for 5 minutes at 560 nm. SOD activity was calculated using the NADPH extinction coefficient of 6.22  $\text{mM}^{-1} \text{cm}^{-1}$  and expressed per mg of cellular protein [208].

### **7.1.2.7. Assay of cellular catalase (CAT)**

$10^6$  cells were treated and afterwards homogenized in M-PER. After 10 minutes shaking and centrifugation (3000 rpm), 50  $\mu$ l of sample were added to a quartz cuvette together with 650  $\mu$ l of potassium phosphate buffer [50 mM]. The reaction was started by adding 300  $\mu$ l of  $H_2O_2$  [30 mM]. The decomposition of  $H_2O_2$  was monitored at 240 nm, 25 °C for 2 min. Catalase activity was calculated as micromoles of  $H_2O_2$  consumed per min per milligram of cellular protein [208].

### **7.1.2.8. Determination of glutathione peroxidase (GPX) activity**

$10^6$  cells were treated and afterwards homogenized in M-PER. After 10 minutes shaking and centrifugation (3000 rpm), the homogenate was kept on ice for subsequent measurement of GPX activity within 1 h. To an assay cuvette containing 600  $\mu$ l of potassium phosphate [50 mM] (pH 7.0) and EDTA [1 mM], 100  $\mu$ l of sample, 100  $\mu$ l GSH [10 mM], 100  $\mu$ l glutathione reductase [2.4 U/ml] and 100  $\mu$ l NADPH [1.5 mM] were added ([-]-sample). The cuvette was incubated at 37 °C for 5 min and measured afterwards at 340 nm and 37 °C for 5 min. A second cuvette ([+]-sample) per sample was prepared, containing the same components as the [-]-sample except that 500  $\mu$ l buffer and 100  $\mu$ l of *tert*-butylhydroperoxide [12 mM] instead of 600  $\mu$ l buffer were added. The rate of NADPH consumption was monitored at 340 nm, 37 °C for 5 min and obtained by subtracting the consumption rate of the [-]-sample from the NADPH consumption rate of the [+]-sample. GPX activity was calculated using the extinction coefficient of  $6.22 \text{ mM}^{-1} \text{ cm}^{-1}$  and expressed per min per mg of cellular protein [208].

### **7.1.2.9. Determination of $\gamma$ -glutamylcysteine synthetase activity ( $\gamma$ -GCS)**

Cellular  $\gamma$ -glutamylcysteine synthetase ( $\gamma$ -GCS) activity was measured with L- $\alpha$ -aminobutyrate as analog of L-cysteine. This assay was performed by coupling formation of L- $\gamma$ -glutamyl-L- $\alpha$ -aminobutyrate and adenosine diphosphate (ADP) to pyruvate kinase, lactate dehydrogenase (LDH) and ultimately NADH oxidation and the consequent decrease in absorbance at 340 nm.  $10^6$  cells were treated, harvested and homogenized in M-PER, put on a shaker and centrifuged afterwards at 3000 g for 5 min at 4 °C. The resulting supernatant was collected and kept on ice for subsequent measurement of  $\gamma$ -GCS activity within 1 h. The reaction mixture (to be freshly prepared) contained 100  $\mu$ l Tris-HCl [0.1 M] (pH 8.0), 100  $\mu$ l KCl [150 mM],

100  $\mu$ l ATP [5 mM], 100  $\mu$ l phosphoenolpyruvate [2 mM], 100  $\mu$ l L-glutamate [10 mM], 100  $\mu$ l  $MgCl_2$  [20 mM], 100  $\mu$ l EDTA [2 mM], 100  $\mu$ l NADH [0.2 mM], pyruvate kinase [5 units/ml] and LDH [14 units/ml]. To the cuvettes 100  $\mu$ l of sample were added. The cuvettes were incubated at 37 °C for 5 min. After this pre-incubation, 100  $\mu$ l of deionized water and 100  $\mu$ l L- $\alpha$ -aminobutyrate [100 mM] (pre-warmed at 37 °C) were added and the changes in absorbance at 340 nm were monitored for 5 min at 37 °C.  $\gamma$ -GCS activity was calculated using the extinction coefficient of 6.22  $mM^{-1} cm^{-1}$  and expressed per mg of cellular protein [209].

#### **7.1.2.10. RNA isolation and semiquantitative PCR**

Total RNA was isolated from treated cells with the RNeasy mini kit (Qiagen, Hilden, Germany) and 2.5  $\mu$ g of RNA was used for cDNA synthesis using RevertAid™ First Strand cDNA Synthesis Kit (Fermentas GmbH, St. Leon-Rot, Germany). cDNA was amplified by polymerase chain reaction (PCR) using REDTaq™ ReadyMix™ PCR Reaction Mix (Sigma-Aldrich, Taufkirchen, Germany) for 35-40 cycles using the primers depicted further down. Primer sequences for the subunits p22, p47 and p67 of the phagocytic NAD(P)H oxidase were taken from Rupin et al. [210], and for gp91 from Rao et al. [211], while all others were designed with Primer 3 [149]. The following primers with the respective GenBank accession number and predicted size were used for amplification:

$\beta$ -actin homo sapiens (NM\_001101; 54 °C, 35/40 cycles, 591 bp)

For: 5'-TCCCTGGAGAAGAGCTACGA-3', Rev: 5'-GTCACCTTCACCGTTCCAGT-3'

catalase (CAT) homo sapiens (NM\_001752; 54 °C, 35 cycles, 472 bp)

For: 5'-ACATGGTCTGGGACTTCTGG-3', Rev: 5'-CTTGGGTCTGAAGGCTATCTG-3'

$\gamma$ -glutamylcysteine synthetase ( $\gamma$ -GCS) homo sapiens (NM\_001498; 54 °C, 35 cycles, 507 bp):

For: 5'-TTAGGCTGTCCTGGGTTTAC-3', Rev: 5'-CTTCAATGGCTCCAGTCCTC-3'

glycerine aldehyde dehydrogenase (GAPDH) homo sapiens (NM\_002046; 60 °C, 35 cycles, 788 bp):

For: 5'-GGTCGGAGTCAACGGATTTGGTCG-3', Rev: 5'-CCTCCGACGCCTGCT-TCACCAC-3'

gp91phox homo sapiens (NM\_000397; 52 °C, 35 cycles, 429 bp):

For: 5'-ATCCATGGAGCTGAACGAATTG-3', Rev: 5'-CTCTGTCCAGTCCCCAAC-GATG-3'

glutathione peroxidase (GPX) homo sapiens (NM\_000581; 52 °C, 40 cycles, 538 bp):

For: 5'-CCAGTCGGTGTATGCCTT-CT-3', Rev: 5'-GATGTCAGGCTCGATGTCAA-3'

glutathione reductase (GR) homo sapiens (NM\_00637; 52 °C, 40 cycles, 453):

For: 5'-GATCCCAAGCCCACAATAGA-3', Rev: 5'-CAGGCAGTCAACATCTGGAA-3'

glutathione synthetase (GSS) homo sapiens (NM\_000178; 52 °C, 40 cycles, 494 bp):

For: 5'-CAGCGTGCCATAGAGAATGA-3', Rev: 5'-TTCAGGGCCTGTACCATTTC-3'

heme oxygenase (HO-1) homo sapiens (NM\_002133; 52 °C, 35 cycles, 534 bp):

For: 5'-AACTTTCAGAAGGGCGAGGT-3', Rev: 5'-CAGCTGAATGTTGAGCAGGA-3'

p22phox homo sapiens (NM\_000101; 54 °C, 35 cycles, 317 bp):

For: 5'-GTTTGTGTGCCTGCTGGAGT-3', Rev: 5'-TGGGCGGCTGCTTGATGGT-3'

p40phox homo sapiens (NM\_000631; 54 °C, 35 cycles, 528 bp):

For: 5'-GCCAAAGTCTACGTGGGTGT-3', Rev: 5'-TAGGGGAGTGCTGCTGAGAT-3'

p47phox homo sapiens (NM\_000265; 52 °C, 35 cycles, 236 bp):

For: 5'-ACCTTCATCCGTCACATCG-3', Rev: 5'-TCAAACCACTTGGGAGCTG-3'

p67phox homo sapiens (NM\_000433; 54 °C, 35 cycles, 427 bp):

For: 5'-ATGCCTTCAGTGCCGTCCAG-3', Rev: 5'-TGCTTCCAGACACACTCCA-TCG-3'

superoxide dismutase 1 (SOD 1) homo sapiens (NM\_000454; 52 °C, 35 cycles, 355 bp):

For: 5'-GAAGGTGTGGGGAAGCATTA-3', Rev: 5'-ACCACAAGCCAAACGACTTC-3'

thioredoxin reductase (THI) homo sapiens (NM\_006440; 52 °C, 35 cycles, 418 bp):

For: 5'-ACTGGAGGAAGATGGCAGAA-3', Rev: 5'-ATGGAGGACATTTGCTGGTC-3'

PCR products were resolved on a 1.5 % agarose gel, stained with ethidium bromide. Results were related to the housekeeping genes GAPDH (HO-1) or  $\beta$ -actin (all other mRNAs) and subsequently normalized to the control. For quantification of the mRNA, the density of the bands was measured using Gel Doc 2000 with the software Multi-Analyst Version 1.0.2 (Bio-Rad, Hercules, CA, USA).

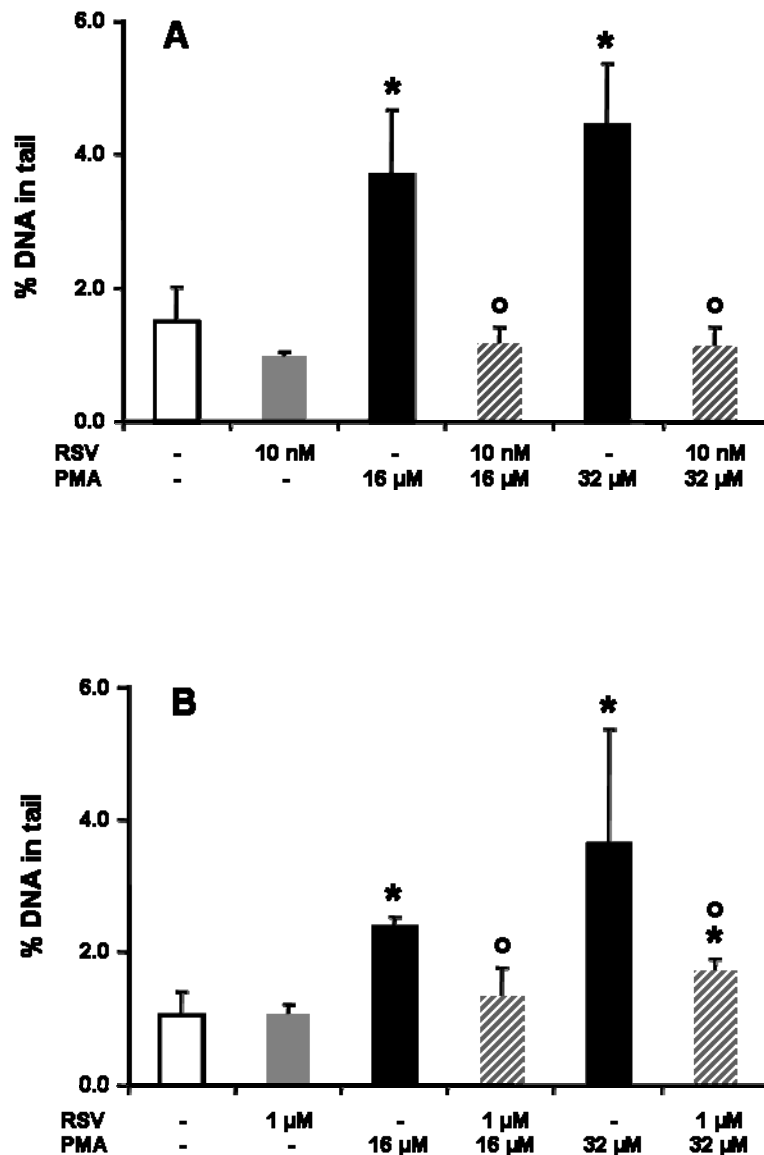


**7.1.2.11. Statistics**

Data from at least 3 independent experiments are shown  $\pm$  standard deviation (SD). Statistical significance among multiple groups was tested with the non-parametric Kruskal-Wallis test. Individual groups were tested using the Mann-Whitney test. A *P* value of  $\leq 0.05$  was considered significant. SPSS 15.0 was used for calculations and the free software WinMDI 2.8 (Scripps Research Institute Cytometry Software page at <http://facs.scripps.edu/software.html>) was used for analysing the flow cytometry histograms.

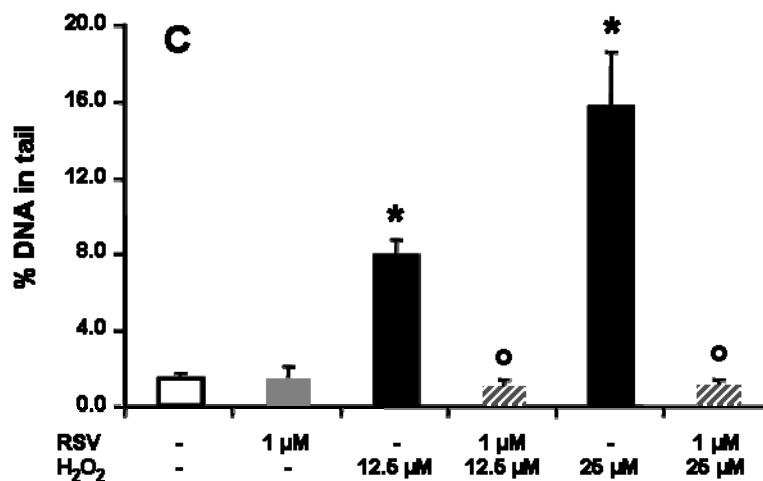
### 7.1.3. Results

PMA, which stimulates protein kinase C (PKC) and subsequently activates NAD(P)H oxidase, led to a significant increase of DNA damage in HL-60 cells measured by single cell gel electrophoresis (comet assay). PMA-induced structural DNA damage was significantly decreased by rosuvastatin even at the low dose of 10 nM (Figure 57 A) as well as at the higher dose of 1  $\mu$ M (Figure 57 B).



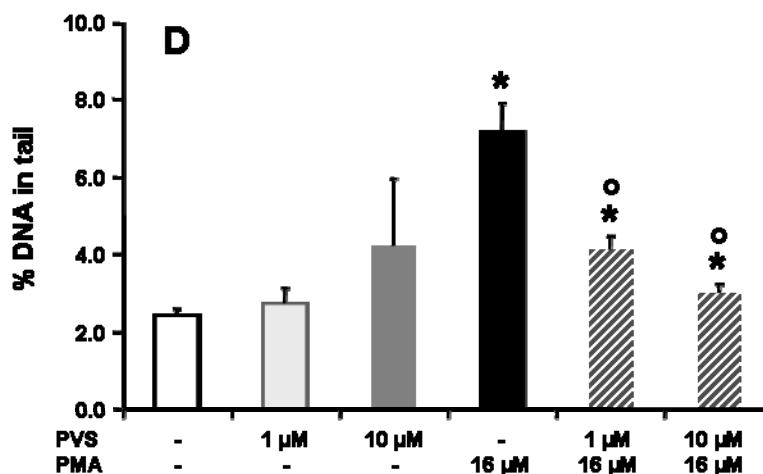
**Figure 57:** DNA damage in HL-60 cells quantified after single cell gel electrophoresis (comet assay) following 3 hours treatment with 16  $\mu$ M PMA with and without co-incubation with 10 nM (A) or 1  $\mu$ M (B) rosuvastatin (RSV). \*  $p \leq 0.05$  vs. control, °  $p \leq 0.05$  vs. PMA treatment.

NAD(P)H oxidase-independent oxidative DNA damage was provoked dose-dependently by hydrogen peroxide ( $\text{H}_2\text{O}_2$ ) in HL-60 cells (Figure 57 C). This  $\text{H}_2\text{O}_2$ -generated DNA damage was likewise reduced significantly by 10 nM (data not shown) and 1  $\mu\text{M}$  rosuvastatin (Figure 57 C).



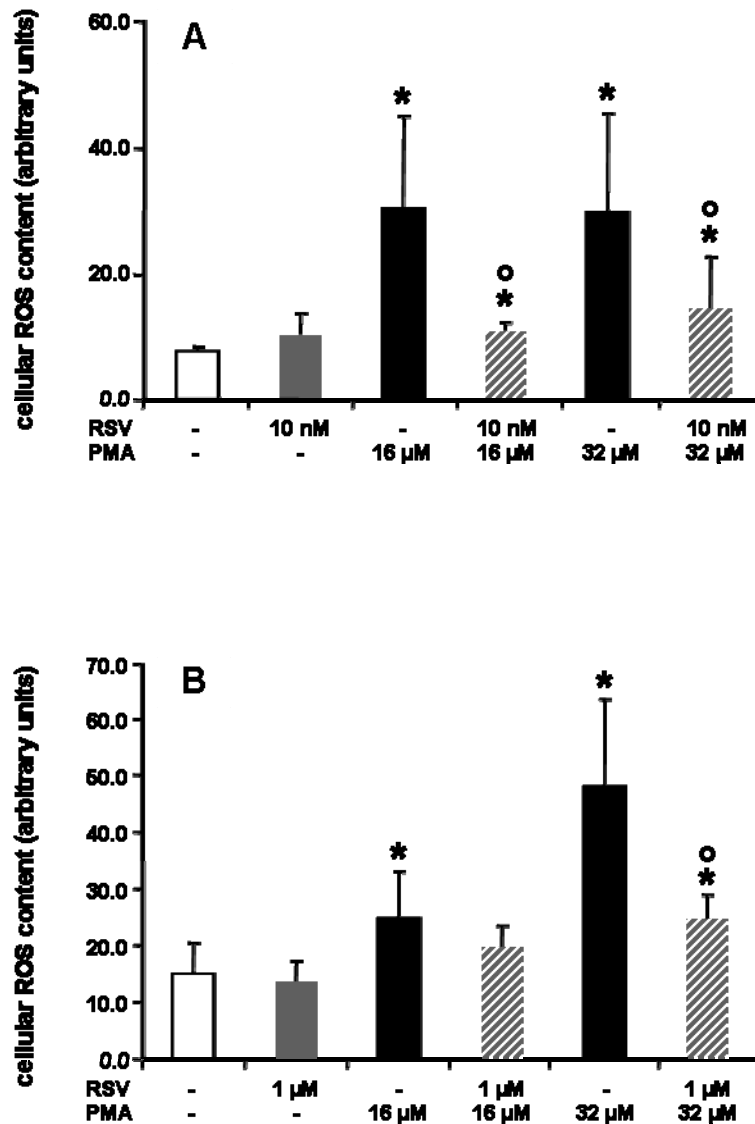
**Figure 57 C:** DNA damage in HL-60 cells after 30 min treatment with 25  $\mu\text{M}$   $\text{H}_2\text{O}_2$  with and without co-incubation with 1  $\mu\text{M}$  rosuvastatin (RSV). \*  $p \leq 0.05$  vs. control, °  $p \leq 0.05$  vs. PMA treatment.

Pravastatin, representing the older generation of statins, also did decrease PMA-induced DNA damage, but could not reduce the damage to control level, even in a concentration of 10  $\mu\text{M}$  (Figure 57 D).



**Figure 57 D:** DNA damage in HL-60 cells after 3 hours treatment with 16  $\mu\text{M}$  PMA with and without co-incubation with 1  $\mu\text{M}$  or 10  $\mu\text{M}$  pravastatin (PVS). Control: no treatment. \*  $p \leq 0.05$  vs. control, °  $p \leq 0.05$  vs. PMA treatment.

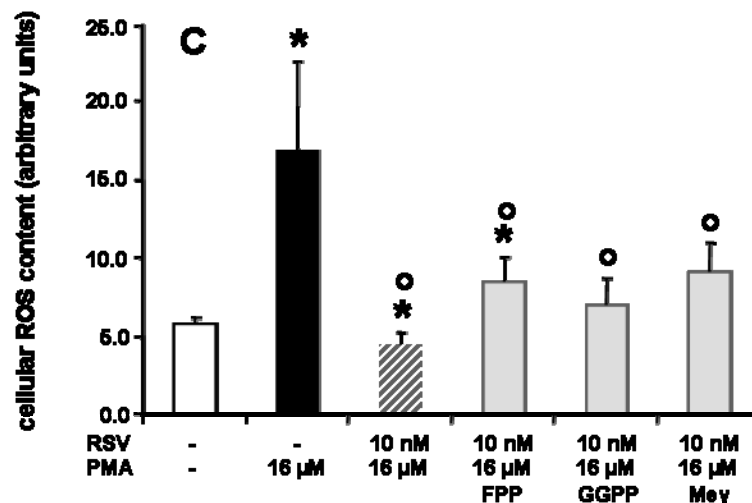
The DNA damage in this study was caused by reactive oxygen species (ROS). To measure the PMA- and H<sub>2</sub>O<sub>2</sub>-generated oxidative stress, flow cytometric analysis using H<sub>2</sub>DCF-DA was carried out. PMA caused a significant increase of ROS compared to control (Figures 58 A and B).



**Figure 58 A:** Flow cytometric analysis of ROS levels in HL-60 cells. HL-60 loaded with H<sub>2</sub>DCF-DA and propidium iodide were analyzed as described in the Experimental section. ROS content is shown as arbitrary units. Oxidative stress in cells incubated for 3 hours with 10 nM rosuvastatin (RSV) or 16 μM PMA separately or in combination. **Figure 58 B:** Oxidative stress in cells incubated for 3 hours with 1 μM RSV or 16 μM PMA separately or in combination. Control: no treatment. \*  $p \leq 0.05$  vs. control; °  $p \leq 0.05$  vs. PMA or H<sub>2</sub>O<sub>2</sub> treatment; +  $p \leq 0.05$  vs. simultaneous treatment with PMA and RSV.

Rosuvastatin in a concentration of 10 nM and 1  $\mu$ M reduced the production of ROS induced by PMA. The reduction of oxidative stress was significant, but not complete. Further experiments were conducted with a PMA concentration of only 16  $\mu$ M, since 32  $\mu$ M significantly induced cytotoxicity (not shown).

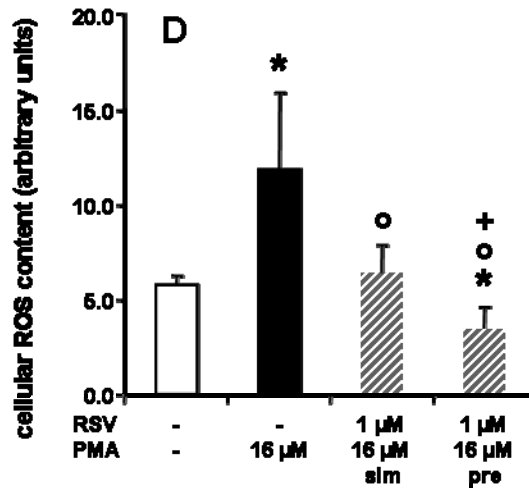
The inhibition of HMG-CoA reductase results in a reduction of the synthesis of its direct product, mevalonate and subsequent cholesterol pathway products. These include the isoprenoid compounds farnesyl pyrophosphate (FPP) and geranylgeranyl pyrophosphate (GGPP), which are important in the post-translational modification of signal transduction proteins like Ras, Rho or Rac [82]. If the effects observed here were produced by an HMG-CoA reductase-dependent mechanism, they should be reversed by the addition of the afore mentioned intermediates. For the analysis of this reversion, the lower concentration of 10 nM rosuvastatin was chosen, to achieve the highest possible impact of the intermediates. In combination with PMA and rosuvastatin, all three intermediates increased the oxidative stress only marginally (Figure 58 C).



**Figure 58 C:** Flow cytometric analysis of ROS levels in HL-60 cells. HL-60 loaded with H<sub>2</sub>DCF-DA and propidium iodide were analyzed as described in the Experimental section. ROS content is shown as arbitrary units. Oxidative stress in cells incubated for 3 hours with 1  $\mu$ M rosuvastatin (RSV) or 16  $\mu$ M PMA separately or in combination, and in combination with the cholesterol biosynthesis pathway intermediates farnesyl pyrophosphate (FPP), geranylgeranyl pyrophosphate (GGPP) and mevalonate (activated as described in the Experimental section). Control: no treatment. \*  $p \leq 0.05$  vs. control; <sup>°</sup>  $p \leq 0.05$  vs. PMA or H<sub>2</sub>O<sub>2</sub> treatment; <sup>†</sup>  $p \leq 0.05$  vs. simultaneous treatment with PMA and RSV.

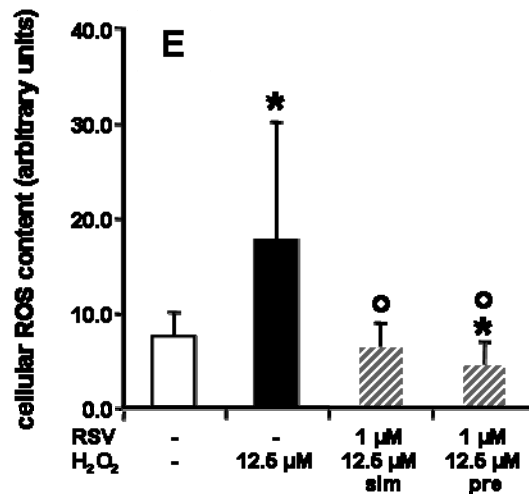
To analyze whether rosuvastatin exerts a direct antioxidative effect or whether its presence is not required, experiments were performed in which rosuvastatin was washed from the cells cultures after a 30-minutes incubation time. As can be seen in

Figure 58 D the protective effect of rosuvastatin countering PMA-induced oxidative stress is even higher when cells were pre-incubated.



**Figure 58 D:** Flow cytometric analysis of ROS levels in HL-60 cells. HL-60 loaded with H<sub>2</sub>DCF-DA and propidium iodide were analyzed as described in the Experimental section. ROS content is shown as arbitrary units. Oxidative stress in cells incubated for 3 hours alone with 16  $\mu$ M PMA, 3 hours simultaneously with 16  $\mu$ M PMA and 1  $\mu$ M rosuvastatin (RSV) (sim) or pre-incubated for 30 minutes with 1  $\mu$ M RSV, followed by removal of RSV and 3 hours incubation with 16  $\mu$ M PMA (pre). Control: no treatment. \*  $p \leq 0.05$  vs. control; °  $p \leq 0.05$  vs. PMA or H<sub>2</sub>O<sub>2</sub> treatment; +  $p \leq 0.05$  vs. simultaneous treatment with PMA and RSV.

Almost the same result was obtained with H<sub>2</sub>O<sub>2</sub> acting as the ROS-generating substance (Figure 58 E).



**Figure 58 E:** Oxidative stress in cells incubated for 30 minutes with 12.5  $\mu$ M H<sub>2</sub>O<sub>2</sub>, 30 minutes simultaneously with 12.5  $\mu$ M H<sub>2</sub>O<sub>2</sub> and 1  $\mu$ M rosuvastatin (RSV) (sim) or pre-incubated for 30 minutes with 1  $\mu$ M RSV, followed by removal of RSV and 30 minutes incubation with 12.5  $\mu$ M H<sub>2</sub>O<sub>2</sub> (pre). Control: no treatment. \*  $p \leq 0.05$  vs. control; °  $p \leq 0.05$  vs. PMA or H<sub>2</sub>O<sub>2</sub> treatment; +  $p \leq 0.05$  vs. simultaneous treatment with PMA and RSV.

Again, cells pre-incubated with rosuvastatin were better protected against oxidative stress, showing significantly less ROS than control cells. These results indicate that the protecting mechanism is involved in the expression or regulation of the activity of proteins. Three possible targets were analyzed: the down-regulation of NAD(P)H oxidase, the up-regulation of antioxidant defense enzymes and the expression of enzymes of glutathione metabolism.

Statins are known to down-regulate the expression of subunits of NAD(P)H oxidase, thereby reducing oxidative stress [212]. We analyzed the effect of rosuvastatin on the expression of the mRNA of the five subunits of NAD(P)H oxidase by reverse transcription polymerase chain reaction, and did find a significant decrease of p67 mRNA by rosuvastatin alone (Figure 59 A).

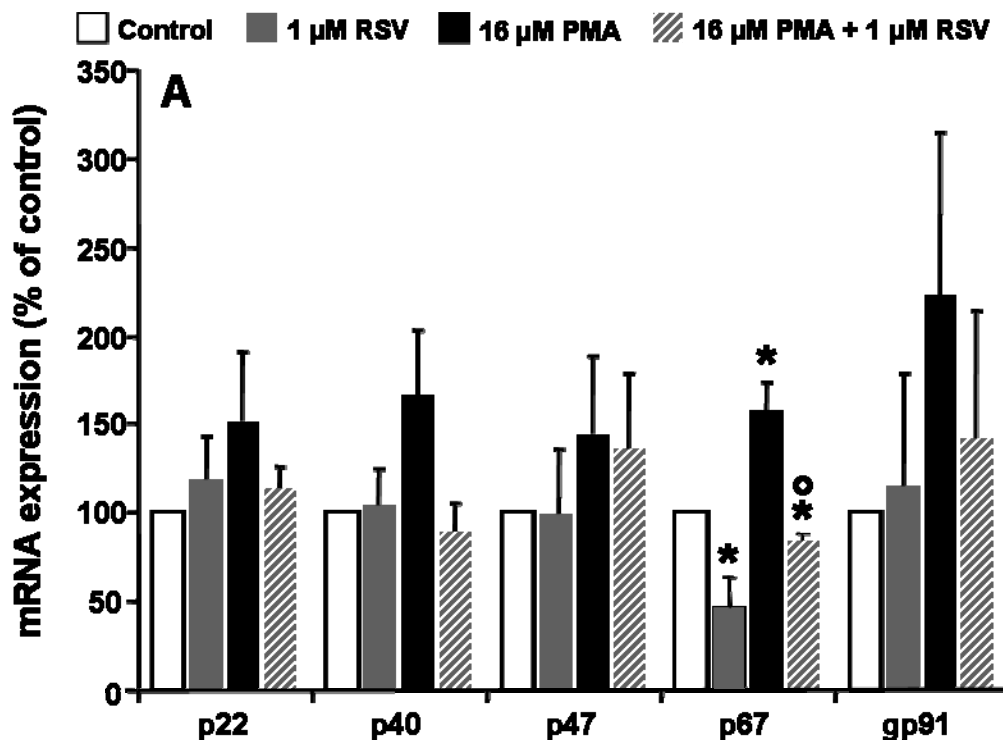


**Figure 59 A:** Effect of rosuvastatin and PMA on the expression of mRNAs of the five subunits of NAD(P)H oxidase p22, p40, p47, p67 and gp91. \*  $p \leq 0.05$  vs. control; °  $p \leq 0.05$  vs. PMA treatment.

Rosuvastatin's effect on the expression of antioxidant defense enzymes known to be affected by statins in other cells was also studied. Catalase and Cu/Zn-superoxide dismutase (SOD) mRNAs showed a tendency to be higher in cells treated with 1  $\mu$ M rosuvastatin alone or in combination with 16  $\mu$ M PMA (Figure 59 B), but this increase was only statistically significant for SOD.

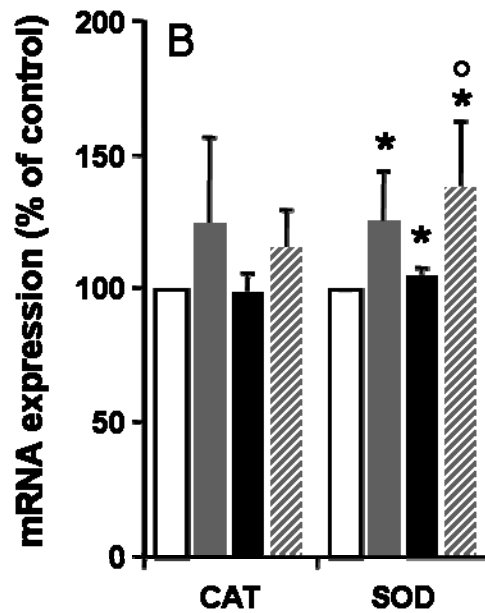


**Figure 59 B:** Effect of rosuvastatin and PMA on the expression of mRNAs and activity of different enzymes. HL-60 cells were treated for 3 hours with 1 μM rosuvastatin (RSV) or 16 μM PMA separately or in combination. Effect of rosuvastatin and PMA on the expression of mRNAs of catalase (CAT) and superoxide dismutase (SOD). \*  $p \leq 0.05$  vs. control; °  $p \leq 0.05$  vs. PMA treatment.

Additionally enzyme activities of catalase and SOD were tested and were increased as well in cells treated with rosuvastatin alone, but without reaching statistical significance (Figures 59 C and D).

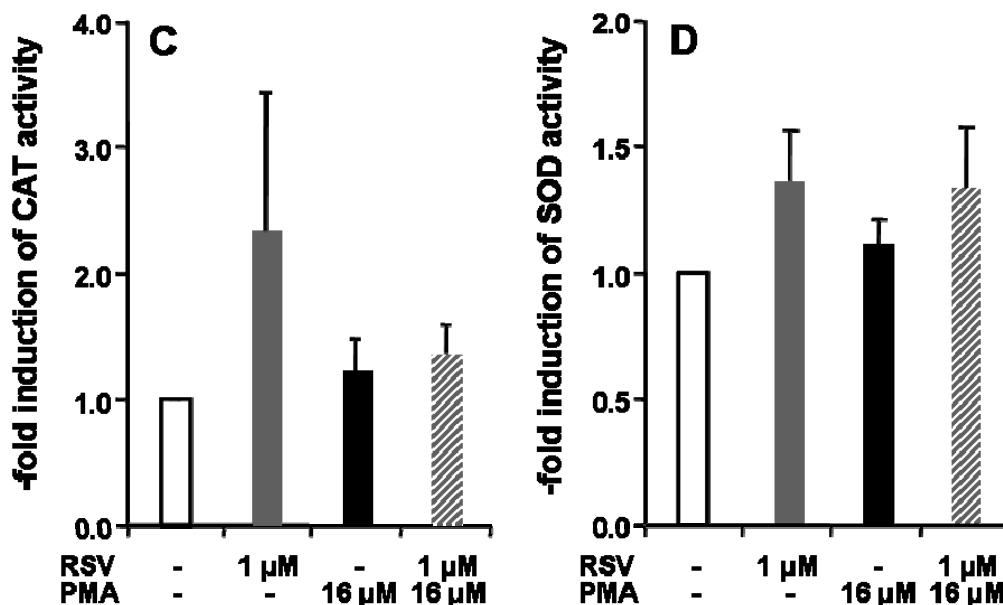


**Figure 59 C:** Effect of rosuvastatin (RSV) and PMA on the activity of CAT. **Figure 59 D:** Effect of rosuvastatin (RSV) and PMA on the activity of SOD. \*  $p \leq 0.05$  vs. control; °  $p \leq 0.05$  vs. PMA treatment.



Effects of statins on NAD(P)H oxidase mostly show a strong dependence on the inhibition of HMG-CoA reductase. Since in this study this dependence was not pronounced, one of the few published antioxidant mechanisms of statins which is independent of HMG-CoA reductase was investigated: the up-regulation of mRNA of the antioxidant defense protein heme oxygenase 1 (HO-1) [213]. In our experiments, rosuvastatin alone did not increase the amount of HO-1 mRNA (Figure 59 E). The HO-1 expression was highly increased by PMA alone and in combination with rosuvastatin (Figure 59 E).

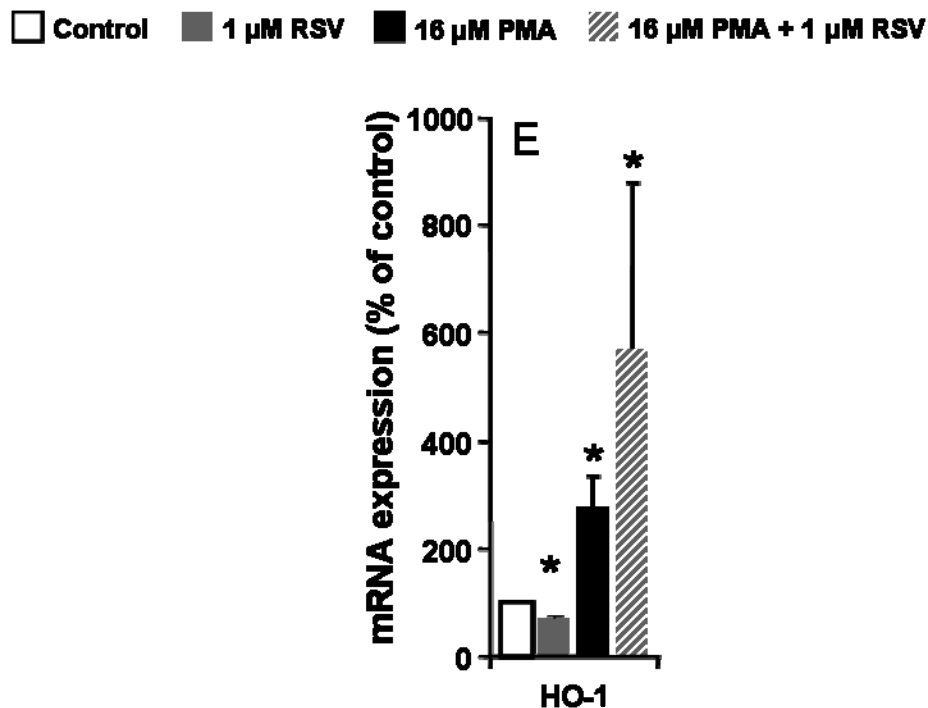


**Figure 59 E:** Effect of rosuvastatin (RSV) and PMA on the expression of mRNA of heme oxygenase (HO-1). \*  $p \leq 0.05$  vs. control; °  $p \leq 0.05$  vs. PMA treatment.

There exist consistent reports of animal and clinical studies demonstrating an up-regulation of glutathione peroxidase activity [84, 214], so we studied the effect of rosuvastatin on total glutathione levels. Rosuvastatin significantly increased the total glutathione content of glutathione-depleted HL-60 cells (Figure 60 A). PMA alone had no effect on the glutathione content compared to control. The co-incubation of cells with rosuvastatin and PMA led to a significantly higher amount of glutathione.

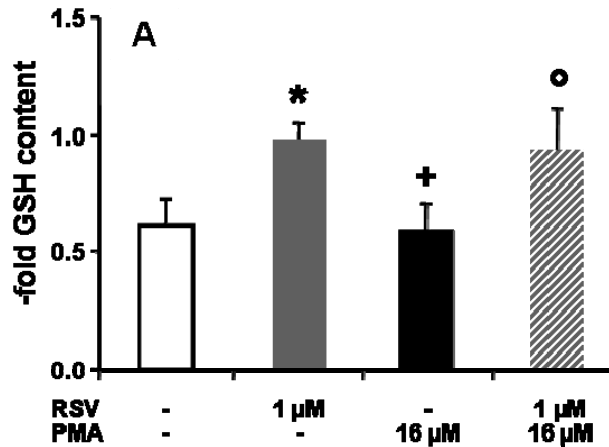


**Figure 60 A:** Effect of rosuvastatin and PMA on the glutathione system. HL-60 cells were treated for three hours with 16 µM PMA with and without co-incubation with 1 µM rosuvastatin (RSV) or with 1 µM RSV alone. Total glutathione (GSH) content of cells depleted of their GSH before PMA and rosuvastatin treatment. Results were normalized to the GSH content of undepleted control cells. \*  $p \leq 0.05$  vs. control, °  $p \leq 0.05$  vs. PMA treatment.

To analyze how rosuvastatin might lead to an increase of total glutathione, the expression of genes of the glutathione metabolism was assessed. Rosuvastatin alone significantly increased the mRNA amount of glutathione synthetase (GSS), glutathione peroxidase (GPX) and glutathione reductase (GR). PMA alone caused a reduction of the expression of GSS, GPX and GR. Rosuvastatin led to a lower reduction of the expression of all three mRNAs, but without reaching significance (Figure 60 B).

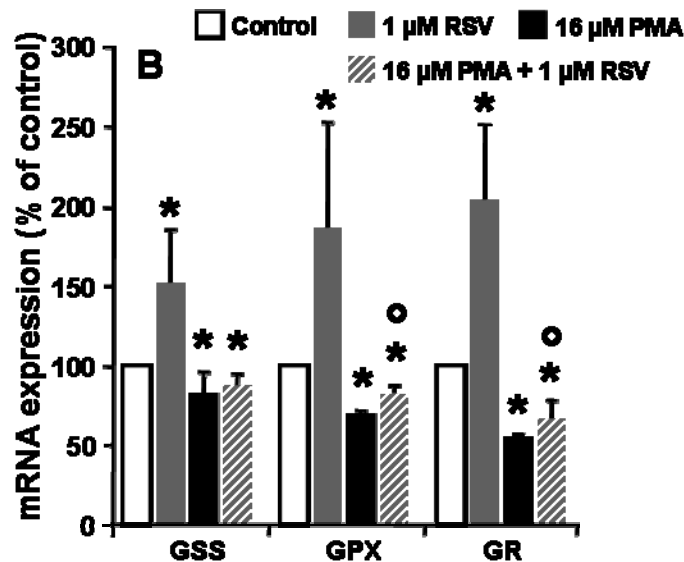


**Figure 60 B:** Effect of rosuvastatin (RSV) and PMA on the glutathione system. HL-60 cells were treated for three hours with 16 µM PMA with and without co-incubation with 1 µM rosuvastatin (RSV) or with 1 µM RSV alone. Effect of PMA and RSV on the expression of mRNAs of enzymes of the glutathione metabolism (GSS = glutathione synthetase, GPX = glutathione peroxidase, GR = glutathione reductase) in relation to the control. \*  $p \leq 0.05$  vs. control, °  $p \leq 0.05$  vs. PMA treatment.

In contrast to the mRNA expression, the activity of GPX was significantly higher in all treated cells compared to control (Figure 60 C). The highest activity was measured in cells only treated with rosuvastatin.

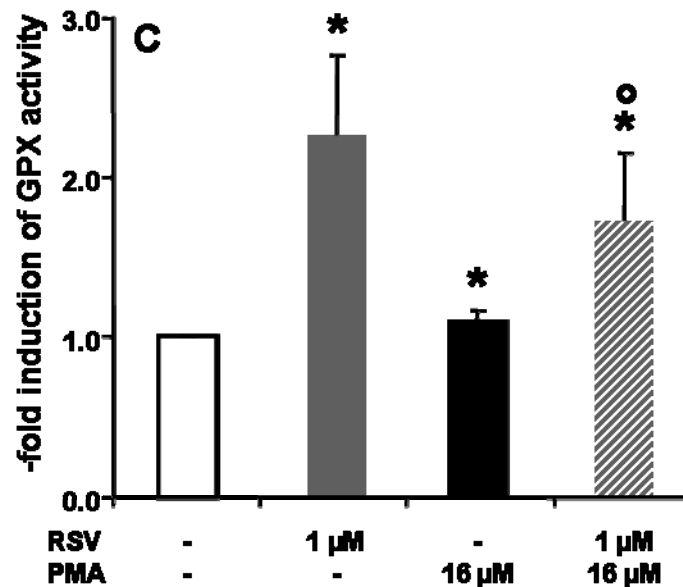


**Figure 60 C:** Effect of rosuvastatin and PMA on the glutathione system. HL-60 cells were treated for three hours with 16 µM PMA with and without co-incubation with 1 µM rosuvastatin (RSV) or with 1 µM RSV alone. Effect of PMA and RSV on the GPX activity, related to the control. \*  $p \leq 0.05$  vs. control, °  $p \leq 0.05$  vs. PMA treatment.

Rosuvastatin alone had the highest effect on the expression of the rate-limiting enzyme of the glutathione synthesis,  $\gamma$ -glutamylcysteine synthetase ( $\gamma$ -GCS), (Figure 60 D).

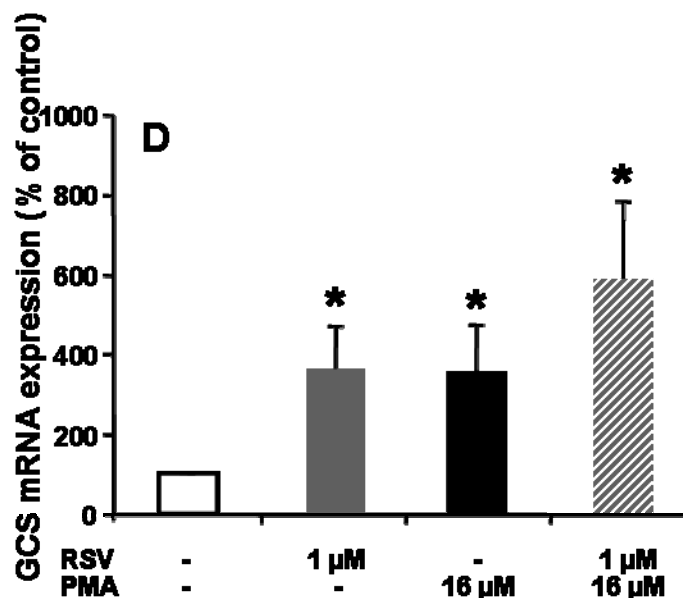


**Figure 60 D:** Effect of rosuvastatin and PMA on the glutathione system. HL-60 cells were treated for three hours with 16 µM PMA with and without co-incubation with 1 µM rosuvastatin (RSV) or with 1 µM RSV alone. Effect of PMA and RSV on the expression of mRNA of  $\gamma$ -glutamylcysteine synthetase ( $\gamma$ -GCS) in relation to the control. \*  $p \leq 0.05$  vs. control, °  $p \leq 0.05$  vs. PMA treatment.

PMA alone also caused a significant increase in  $\gamma$ -GCS mRNA, which was further increased by the addition of rosuvastatin. The induction of gene expression partially translated in a higher  $\gamma$ -GCS activity in those cells treated with rosuvastatin, while cells treated with PMA alone showed a reduced enzyme activity (Figure 60 E).

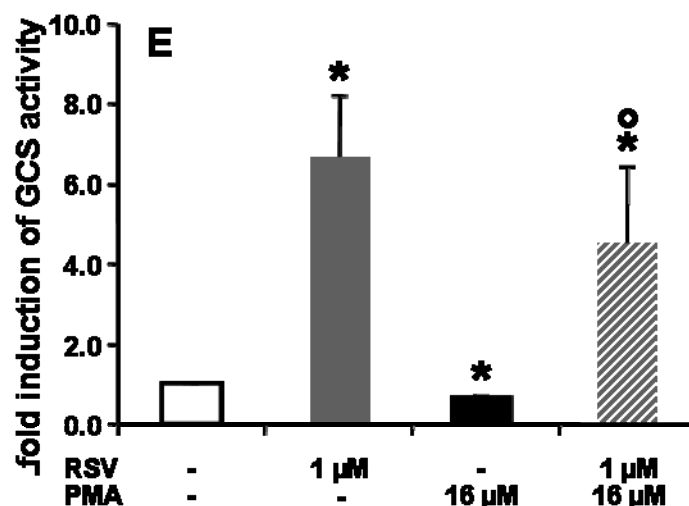


**Figure 60 E:** Effect of rosuvastatin and PMA on the glutathione system. HL-60 cells were treated for three hours with 16  $\mu$ M PMA with and without co-incubation with 1  $\mu$ M rosuvastatin (RSV) or with 1  $\mu$ M RSV alone. Effect of PMA and RSV on the  $\gamma$ -GCS activity, related to the control. \*  $p \leq 0.05$  vs. control, <sup>°</sup>  $p \leq 0.05$  vs. PMA treatment.

Since several of the tested enzymes showed an increase of expression or activity, rosuvastatin's participation in the DNA protective effect of the most prominently up-regulated enzyme  $\gamma$ -GCS was studied by the use of a specific inhibitor of  $\gamma$ -GCS. DL-Buthionine-sulfoximine (BSO), which was already used here to deplete the cells of glutathione to increase their sensitivity to oxidative stress, was now kept on the cells during the 3 hour incubation with PMA and rosuvastatin. This extended inhibition of glutathione synthesis led to a very low amount of glutathione in  $\gamma$ -GCS-inhibited cells compared to the BSO-depleted control (Figure 61 A).

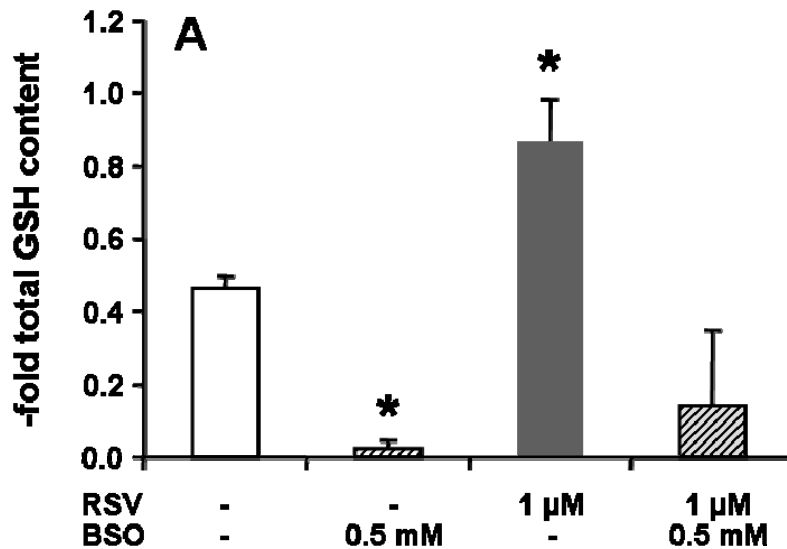


**Figure 61 A:** Effect of the  $\gamma$ -GCS inhibitor DL-buthionine sulfoximine (BSO) on the protective effect of rosuvastatin. Total glutathione (GSH) content of cells depleted of their GSH before treatment with 1  $\mu$ M rosuvastatin (RSV) and 0.5 mM BSO alone or in combination. Results were normalized to the GSH content of undepleted control cells. \*  $p \leq 0.05$  vs. control,  $^{\circ} p \leq 0.05$  vs. PMA treatment;  $^+ p \leq 0.05$  vs. simultaneous treatment with PMA and RSV.

Cells treated with rosuvastatin during the  $\gamma$ -GCS-inhibition retained more glutathione. The effect of  $\gamma$ -GCS-inhibition on the DNA-protective effect of rosuvastatin was also studied. Cells treated simultaneously with PMA, rosuvastatin and BSO indeed had a significantly higher DNA damage than cells without  $\gamma$ -GCS-inhibition, emphasizing the role of the  $\gamma$ -GCS-up-regulation for the damage protection (Figure 61 B).

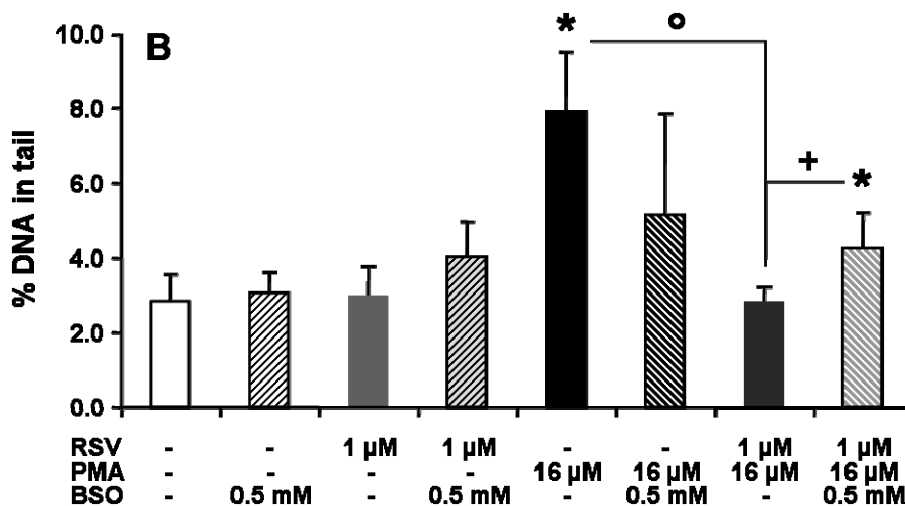


**Figure 61 B:** Effect of the  $\gamma$ -GCS inhibitor DL-buthionine sulfoximine (BSO) on the protective effect of rosuvastatin. DNA damage in HL-60 cells quantified after single cell gel electrophoresis (comet assay) following 3 hours treatment with 16  $\mu$ M PMA with and without co-incubation with 1  $\mu$ M rosuvastatin (RSV) with and without co-incubation with 0.5 mM BSO. \*  $p \leq 0.05$  vs. control,  $^{\circ} p \leq 0.05$  vs. PMA treatment;  $^+ p \leq 0.05$  vs. simultaneous treatment with PMA and RSV.

#### 7.1.4. Discussion

It is generally accepted that mechanisms beyond the improvement of the lipid profile contribute to the beneficial actions of statins [82]. Pleiotropic, cholesterol-independent effects of statins include antiinflammatory and antioxidant properties [215, 216]. Reactive oxygen species (ROS) contribute to vascular inflammation or endothelial cell injury [217], and may play a major role as endogenous initiators and promoters of DNA damage [218]. Oxidative DNA damage has been documented as playing a role in carcinogenesis [11] and several carcinogens have been shown to induce DNA oxidation in their target organs [219]. Antioxidants may represent an important defense against such agents, and various antioxidants have been studied as anticarcinogens [220]. In this study rosuvastatin was tested for its capacity to prevent oxidative stress-induced DNA damage in the human promyelocytic cell line HL-60.

To monitor DNA damage single cell gel electrophoresis (comet assay) was used. The comet assay measures DNA strand breaks, alkali labile sites, and relaxed chromatin in individual cells [221]. Phorbol 12-myristate 13-acetate (PMA), an inductor of NAD(P)H oxidase via protein kinase C (PKC), was used to induce measurable DNA damage in the comet assay, which it did dose-dependently. It did not induce apoptosis in HL-60 cells and up to 16  $\mu\text{M}$  it showed no significant cytotoxicity.

Rosuvastatin reduced the damage caused by PMA shown in the comet assay to control levels. Additionally, DNA damage caused by hydrogen peroxide was decreased. This potential to reduce oxidative DNA damage seems to be a class effect of statins, since pravastatin too did ameliorate PMA-induced damage. Using a flow cytometric method, both the production of ROS by exposure of HL-60 cells to PMA and its reduction by co-incubation with rosuvastatin could be shown. A pre-incubation with rosuvastatin revealed a persisting effect of rosuvastatin even after excessive washing-out of the drug. This indicates that the mechanism by which rosuvastatin protects the cells against oxidative stress and subsequent DNA damage affects gene expression or protein activity.

A destructive enzyme complex, whose expression is known to be affected by statins, is NAD(P)H oxidase. There are studies in which the expression of subunits of NAD(P)H oxidase was changed by incubation with statins. *In vitro* mRNA levels of p22 and protein levels of p47 were reduced [212, 222]. Rosuvastatin alone and

together with PMA in this study did reduce the amount of mRNA of p67 below control levels, which could result in a lower production of radicals. It remains to be elucidated if rosuvastatin has an influence on the assembly of the NAD(P)H oxidase in HL-60 cells, as was reported for monocytes [223]. Anyway, the inhibition of NAD(P)H oxidase should not protect against H<sub>2</sub>O<sub>2</sub>-induced oxidative stress, which pre-incubation with rosuvastatin was able to do.

It was reported that the expression and/or activity of several antioxidant defense proteins, like catalase (CAT) [216], superoxide dismutase (SOD) [224] and heme oxygenase-1 (HO-1) [213, 225], are up-regulated by statins either in animals or in cultured cells. In HL-60 cells these mRNAs and activities were not (HO-1) or only slightly (catalase, superoxide dismutase) increased by rosuvastatin alone, and can therefore not account for the observed protective effect.

Animal experiments and clinical studies have shown a beneficial effect of statins either on the amount of glutathione or on the expression of glutathione peroxidase (GPX), the enzyme which catalyzes the detoxification of ROS [214, 226]. *In vitro* the impact of statins on glutathione metabolism has not, to our knowledge, been analyzed before. Rosuvastatin alone in our study significantly increased total glutathione in HL-60 cells compared to PMA treatment. It also enhanced the expression of  $\gamma$ -glutamylcysteine synthetase ( $\gamma$ -GCS), the rate-limiting enzyme of glutathione synthesis, glutathione synthetase, glutathione peroxidase and glutathione reductase. But only  $\gamma$ -GCS is also up-regulated when cells were treated with PMA and rosuvastatin together. This up-regulation of  $\gamma$ -GCS therefore could account for the higher amount of total glutathione in cells treated with rosuvastatin alone and with the combination of PMA and rosuvastatin. This conclusion is supported by the results of the experiments with the  $\gamma$ -GCS inhibitor BSO, where the protective effect of rosuvastatin is decreased. Further studies should include the analysis of the influence of 10 nM rosuvastatin on gene expression by quantitative real time PCR, since our semi-quantitative method was not sensitive enough to detect effects. Also the mechanism which permits rosuvastatin to change gene expression of  $\gamma$ -GCS needs clarification.

The addition of intermediates of the cholesterol synthesis pathway, namely mevalonate, FPP and GGPP, only marginally restored the oxidative stress caused by PMA after reduction by rosuvastatin. This fact is suggestive of an HMG-CoA reductase-independent effect of rosuvastatin in the prevention of oxidative stress-

induced DNA damage. Most studies of the pleiotropic effects of statins found HMG-CoA reductase-dependent actions, which could be reversed by the exogenous addition of mevalonate or isoprenoids [216, 227]. Until now, only a few reports describe mechanisms independent of HMG-CoA reductase [213, 228].

Oxidative stress is increasingly recognized as an important cause of cancer [229]. Several large trials involving patients with cardiovascular disease have analyzed the protective association between statins and the development of cancer. Although most studies showed no apparent effect on the overall risk of cancer [230, 231], one study observed a reduction of up to 28 % in the overall risk of cancer [232] and two recent retrospective case-control studies with almost 500.000 included subjects found reduced risks to develop lung and pancreatic cancer [233, 234]. The results obtained in our study may add to our understanding of why statins possibly protect against cancer. Since there are reports of different effects of statins in different tissues [225], it will be interesting to also analyze the parameters effected in our leukocyte model in endothelial and vascular smooth muscle cells. The ability of rosuvastatin to exert antioxidative effects *in vitro* even in very low concentrations might be of relevance in the early stages of malignant transformation *in vivo*.



## 8. Discussion

In the 1980s, it could be shown for the first time that exposure of mouse fibroblasts to reactive oxygen species (ROS) can lead to transformation [27]. ROS have manifold effects on cells which are either anti-pathologic, for example promotion of cell cycle stasis, senescence, apoptosis, necrosis or other types of cell death as well as inhibition of angiogenesis, or pro-pathologic, for example promotion of proliferation, invasiveness, angiogenesis, metastasis and suppression of apoptosis [235]. Whether good or bad effects of ROS predominate in the development of diseases, especially in cancer, was elucidated by raising ROS levels via decrease of antioxidant defenses. Experiments with animals lacking enzymes like superoxide dismutase (SOD) [236], catalase (CAT) [237] or glutathione peroxidase (GPX) [238] indicated that these genotypes have an increased risk to develop several types of cancer and other pathological conditions. So the data point to a predominance of bad ROS-effects with regard to subsequent disease- and especially cancer-development.

In the course of this study, the process of DNA-damage formation subsequent to increased levels of ROS and ROS-induced oxidative DNA damage was investigated by aid of exogenous or endogenous inductors of oxidative stress and its modulation by aid of unspecific substances like antioxidants and specific compounds like receptor blockers as well as enzyme inhibitors.

As model substances and unspecific inductors of oxidative stress, three substances were chosen, namely hydrogen peroxide, 4-nitroquinoline-1-oxide (NQO) and phorbol 12-myristate 13-acetate (PMA). Hydrogen peroxide, which is produced in a variety of intracellular reactions, is not reactive toward DNA as most of its effects are due to the production of hydroxyl ions via the Fenton reaction [239]. NQO is a potent synthetic mutagen and carcinogen which is widely known to cause unspecific oxidative stress by inducing the release of superoxide radicals or hydrogen peroxide [240]. PMA on the other hand induces ROS-release by activating protein kinase C (PKC) and subsequently NAD(P)H oxidase [170]. It could be shown that all three substances induced significantly oxidative stress in the settings chosen for the respective experiments. This unspecific release of ROS could be inhibited by substances which either possess direct antioxidative capacity like antioxidants e. g. benfotiamine [72] and  $\alpha$ -tocopherol [123] or by substances which are able to up-regulate endogenous antioxidant defense systems like for example rosuvastatin [170].

In addition to these model substances, endogenous compounds were investigated. Two hormones lately received much attention, namely angiotensin II and aldosterone, because they are elevated in hypertension due to an activation of the renin-angiotensin-aldosterone system (RAAS) [241]. This disease occurs either alone or is associated with other diseases like diabetes mellitus, atherosclerosis, end stage renal disease (ESRD) or lipid disorders and has therefore become endemic over the past decades.

In the experiments conducted with aldosterone and angiotensin II could be shown that the two endogenous substances, both main effectors of the renin-angiotensin-aldosterone system, are able to cause oxidative stress in renal cells. This is in line with findings of other groups who observed an angiotensin II-induced activation of NAD(P)H oxidase, the enzyme, which is responsible for the release of ROS [242]. Mineralocorticoid receptor activation by its ligand aldosterone has also been already demonstrated to result in increased tissue oxidative stress and vascular inflammation [243]. Administration of aldosterone to animals for 8 or more weeks produced hypertension, cardiac hypertrophy and extensive interstitial and perivascular fibrosis. In addition, studies in experimental animals over a range of time frames have demonstrated and characterized inflammation and oxidative stress responses in the vessel wall as important precursory steps to the development of tissue fibrosis [244]. Furthermore, it could be shown in this study for the first time that subsequent to oxidative stress, oxidative DNA damage, as measured by comet assay and by micronucleus frequency test, can be induced by angiotensin II *in vitro* and in the isolated perfused kidney and by aldosterone *in vitro* and *in vivo*. Moreover, by the aid of several modulators including direct antioxidants, receptor antagonists and enzyme inhibitors, which were able to inhibit oxidative stress as well as oxidative DNA damage, the formation of ROS could be linked to the genotoxic effects.

Angiotensin II exerts its effects via activation of the angiotensin II type 1 receptor (AT<sub>1</sub>R), as inhibition of the AT<sub>1</sub>R by a receptor blocker prevented formation of oxidative stress and genomic damage whereas inhibition of the angiotensin II receptor type II (AT<sub>2</sub>R) by a specific inhibitor could not prevent oxidative stress and genomic damage. This is in line with findings of Jung et al. who observed processes like formation of oxidative stress and inflammation to be mediated by AT<sub>1</sub>R *in vivo* [245]. Furthermore, angiotensin II-induced oxidative end-organ damage and vasoconstriction in the isolated perfused mouse kidney could be achieved by

infusing angiotensin II concentrations which can be found in hypertensive patients. The effect not being due to hypoxia or mechanical stress could be proven by infusion of the thromboxane mimetic U 46619 which generated a vasoconstriction but no DNA damage. It could also be observed that angiotensin significantly induced double strand breaks which are not transient and thus probably provoke the generation of micronuclei after the cell cycle following the double strand break. In addition, angiotensin II caused formation of the oxidative DNA-adduct 8-hydroxydeoxyguanosine (8-oxodG), a common marker for oxidative DNA damage [96] as could be demonstrated by aid of the formamidopyrimidine glycosylase (FPG)-modified comet assay.

Aldosterone-induced release of ROS could be shown to be mineralocorticoid receptor-mediated in the course of this study. This was achieved *in vitro* and in the DOCA/salt animal model. Several investigators have already demonstrated that mineralocorticoid receptor activation results in increased cellular oxidative stress in a variety of cell types, and that this might be a key mechanism whereby mineralocorticoid receptor signalling is translated into proinflammatory and profibrotic signals. As the primary source of superoxide in the vasculature again the non-phagocytic NAD(P)H oxidase was identified, although other sources of ROS including xanthine oxidase and uncoupled endothelial nitric oxide synthase are clearly important as well [246]. The intracellular responses following aldosterone administration that have already been correlated with superoxide production [247], resulted in our experiments in the formation of genomic damage and could be reduced upon mineralocorticoid receptor blockade by steroidal as well as non-steroidal mineralocorticoid receptor antagonists [248]. This indicates the involvement of the receptor in the signalling process.

In addition, this work focused on substances which were thought to be able to prevent the formation of oxidative stress by unspecific or specific working mechanisms and may also be able to prevent the subsequent formation of oxidative DNA damage thus making them highly relevant for a possible prevention of the development of human cancer.

In the group of the unspecific substances,  $\alpha$ -tocopherol and benfotiamine have to be mentioned.  $\alpha$ -Tocopherol, as anticipated and widely known, has direct antioxidative capacity [123], a capacity which could be confirmed in a cell-free system. Furthermore,  $\alpha$ -tocopherol prevented the angiotensin II-induced release of ROS in

various renal cell lines most probably due to an inhibition of the radical chain reaction. As could be shown in the comet assay and the micronucleus frequency test, formation of genomic damage could also be stopped thus providing the link between ROS release and DNA strand breaks as well as micronuclei.

In contrast to the long known antioxidant capacity of  $\alpha$ -tocopherol, it could be demonstrated for the first time in the course of these experiments that the lipophilic prodrug benfotiamine also possesses a direct antioxidant capacity in renal cells in contrast to its active form thiamine. Thus, a completely new mechanism for the beneficial effects exerted by benfotiamine could be provided. In addition, the so far discussed up-regulation of gene expression and activity of the enzyme transketolase could be confirmed [112].

Beside the unspecific antioxidants, highly specific receptor antagonists were investigated. Candesartan, a specific inhibitor of AT<sub>1</sub>R, was able to inhibit angiotensin II-induced oxidative stress *in vitro* and oxidative stress and vasoconstriction in the isolated perfused mouse kidney. In contrast to this, the selective AT<sub>2</sub>R-inhibitor PD 123319 was not able to prevent oxidative stress and genomic damage thus indicating that the effects of oxidative stress are mediated via AT<sub>1</sub>R and following activation of protein kinase C (PKC) and NAD(P)H oxidase. This has also been shown by Yu et al. in an *in vivo* model [249]. In addition, the AT<sub>1</sub>R blocker candesartan was not able to inhibit hydrogen peroxide-induced oxidative stress. This implies that candesartan does not possess any direct antioxidative capacity. Moreover, candesartan could be shown to prevent the formation of the non-transient, not repairable angiotensin II-induced DNA double strand breaks. Thus, the connection between ROS release and subsequent formation of DNA single and double strand breaks and the following generation of micronuclei could be established for the first time.

In the group of the aldosterone receptor antagonists, the steroidal compound eplerenone and the non-steroidal substance BR-4628 in its two stereo-isoforms were investigated. *In vitro*, prevention of oxidative stress and also of DNA strand breaks and micronuclei could be observed after incubation with eplerenone and (S)-BR-4628. Yet, (S)-BR-4628 proved to be the more potent compound as lower drug-concentrations were needed to yield significant effects. The involvement of the mineralocorticoid receptor in the signalling cascade from oxidative stress to oxidative DNA damage was confirmed by additional experiments with the stereoisomer (R)-BR-4628. This isomer, which has been shown to have no activity when binding to the

mineralocorticoid receptor, could not prevent release of ROS and genomic damage. In the DOCA/salt model, BR-4628 also proved to be the most potent substance with regard to inhibition of oxidative stress and following DNA damage, manifesting itself in DNA strand breaks and micronuclei. In comparison with the also tested steroidal substance spironolactone and the ACE inhibitor enalapril where levels measured in negative control animals could not be reached, treatment with BR-4628 resulted in a complete prevention of the formation of ROS. These results are consistent with the findings previously gained *in vitro*.

The last substance investigated was rosuvastatin, a HMG-CoA reductase inhibitor. Older studies have focused primarily on the ability of statins to lower circulating levels of low-density lipoprotein cholesterol. More recent research has shown that statins may exert beneficial effects via pleiotropic processes which are not directly related to lipid lowering. These include adjustments in cell-signalling pathways that play a role in atherogenesis and that affect the expression of inflammatory elements, curtail oxidative stress, and enhance endothelial function [250]. In this study, rosuvastatin was shown to be able to prevent phorbol 12-myristate 13-acetate (PMA)-induced oxidative stress and subsequent oxidative DNA damage even when limited to a pre-incubation in human leukemia cells (HL-60). These findings indicate an involvement of the modulation of gene expression or enzyme activity. In contrast to the findings of other groups, who saw a down-regulation of p22phox [222], we observed a rosuvastatin-dependent down-regulation of p67phox. Investigation of gene expression levels of other enzymes associated with oxidative stress revealed no (heme oxygenase 1, (HO-1)) or only marginal effects (superoxide dismutase (SOD) or catalase (CAT)) [13]. As the intracellular antioxidative glutathione (GSH) system has already been shown to be affected by statins *in vivo* [251], this system was investigated with regard to it being a possible underlying mechanism for the indirect antioxidative capacity of rosuvastatin. The experiments showed an increase of total intracellular glutathione most probably due to an also observable enhanced gene expression of the rate-limiting enzyme for GSH-synthesis  $\gamma$ -glutamylcysteine synthetase ( $\gamma$ -GCS). Moreover, the independence of these rosuvastatin-mediated effects from HMG-CoA-reductase could be proven by addition of intermediates of the cholesterol synthesis, which did not result in the restoration of PMA-induced release of ROS and oxidative DNA damage.

In summary, this work provides important results concerning the capability of endogenous substances, like the in hypertensive patients elevated hormones angiotensin II and aldosterone, to cause oxidative stress and genotoxicity due to the release of ROS. Furthermore, data could be generated which might be able to contribute to further elucidation of the mechanisms underlying the development of human cancer subsequent to the formation of oxidative stress and oxidative DNA damage. Additionally, several substances which can be considered as anti-cancer drugs because of their direct or indirect antioxidative properties were investigated. In the course of these experiments, new working mechanisms for well known and commonly used drugs with regard to possible cancer-prevention could be provided. Nevertheless, many aspects remain to be enlightened in this area of research.

## 9. Summary

Reactive oxygen species (ROS) and the subsequently occurring oxidative stress are increasingly thought to be associated with many pathological conditions such as neurodegenerative disorders, end stage renal disease (ESRD), diabetes mellitus, atherosclerosis, lipid disorders and cardiovascular disease, which often come along with hypertension. Normally, patients suffer from more than one of these diseases and have a high risk to develop cancer. Therefore, we hypothesized that the elevated cancer risk may originate from DNA strand breaks, DNA adducts and chromosomal aberrations occurring subsequently to increased levels of ROS.

In the course of this study, several endogenous compounds and model substances were used to mimic the conditions in patients suffering from hypertension. As endogenous compounds, angiotensin II and aldosterone were chosen, because both substances can be elevated in hypertensive patients due to an activation of the renin-angiotensin-aldosterone system (RAAS). As model substances, 4-nitroquinoline-1-oxide (NQO) and hydrogen peroxide were selected because of their ability to provoke unspecifically the release of reactive oxygen species and phorbol 12-myristate 13-acetate (PMA) was selected because of its specific activation of the NAD(P)H oxidase.

The first part of this work concerns itself with two vitamins, namely benfotiamine, which is a lipophilic prodrug of thiamine (vitamin B1), and  $\alpha$ -tocopherol, which is commonly known together with other tocopherols and tocotrienols as vitamin E. Benfotiamine as well as  $\alpha$ -tocopherol proved in the course of the experiments conducted in three kidney cell lines of human, porcine and rat origin to be able to prevent angiotensin II-induced formation of oxidative DNA strand breaks and micronuclei. This could be due to an also observable prior inhibition of the release of reactive oxygen species and is in contrast to results which were achieved using thiamine, the hydrophilic active form of benfotiamine. Furthermore, experiments in which cells were pre-incubated with benfotiamine followed by incubation with NQO showed that under these conditions, benfotiamine was not able to prevent the induction of oxidative stress. The hypothesis that benfotiamine has, like  $\alpha$ -tocopherol, direct antioxidative capacity was fortified by measurements in cell free systems. The effects described above are independent from the also observable increased activity and gene expression of the enzyme transketolase, for which diphosphorylated

thiamine acts as co-factor and which exhibits a reduced activity especially in diabetic patients because of thiamine malabsorption and enhanced urinary excretion. In brief, a new working mechanism for benfotiamine in addition to the ones already known could be provided.

In the second part of the study, angiotensin II was shown to be dose-dependently genotoxic. This effect is mediated via the angiotensin II type 1 receptor (AT<sub>1</sub>R) which, upon activation, triggers the generation of reactive oxygen species by NAD(P)H oxidase. Experiments with the angiotensin II type 2 receptor (AT<sub>2</sub>R) blocker PD 123319 revealed that this substance had no influence on the formation of genomic damage. This is in contrast to the AT<sub>1</sub>R antagonist candesartan, which was able to prevent the angiotensin II-induced release of ROS and the induction of DNA strand breaks and micronuclei and was equally potent as the antioxidants  $\alpha$ -tocopherol and N-acetyl-cysteine. This indicates that the AT<sub>2</sub>R is not at all involved in the angiotensin II-induced oxidative damage.

Further experiments were extended from *in vitro* settings to the isolated perfused kidney. Here it could be shown that angiotensin II in concentrations which can be found in hypertensive patients, caused vasoconstriction and DNA strand breaks. Co-perfusion of kidneys with angiotensin II and candesartan prevented vasoconstriction and formation of strand breaks. DNA strand break formation due to mechanical stress or hypoxia could be ruled out after additional experiments with the thromboxane mimetic U 46619. In addition, an up-regulation of heme oxygenase 1 (HO-1) and a down-regulation of glutathione peroxidase (GPX) were observable. Detailed investigation and characterization of the DNA damage *in vitro* revealed that angiotensin II induces single strand breaks, double strand breaks and 8-hydroxydeoxyguanosine (8-oxodG)-adducts as well as abasic sites. Repair-comet assay in combination with measurement of phosphorylated histone 2AX ( $\gamma$ -H2AX) showed a complete repair of single strand breaks over 24 hours, whereas the number of double strand breaks even increased over this period. In the formamidopyrimidine DNA glycosylase (FPG)-modified alkaline comet assay, the amount of 8-oxodG-adducts was assessed. The results indicated an increase in the occurrence of FPG-sensitive sites after angiotensin II-incubation whereas co-incubation with candesartan prevented the formation of these adducts.

Investigations of the effects of aldosterone-treatment in kidney cells showed an increase of oxidative stress, DNA strand breaks and micronuclei which could be



prevented by the steroidal mineralocorticoid receptor antagonist eplerenone. Additional experiments with the non-steroidal mineralocorticoid receptor antagonist (S)-BR-4628 revealed that this substance was also able to prevent oxidative stress and genomic damage and proved to be more potent than eplerenone. In contrast, the isomer (R)-BR-4628, which shows no activity at the mineralocorticoid receptor, had no beneficial effect with regard to the release of ROS and to the formation of genomic damage.

*In vivo*, hyperaldosteronism, also often observable in hypertensive patients, was imitated in rats by aid of the deoxycorticosteroneacetate (DOCA) salt model. After this treatment, levels of DNA strand breaks and chromosomal aberrations in the kidney could be observed which were almost as high as in positive control animals which were treated with the nephrotoxic agent cisplatin. Furthermore, an increase in the release of ROS could be measured. Treatment of these animals with the antihypertensive drugs spironolactone (steroidal mineralocorticoid receptor antagonist), BR-4628 (non-steroidal mineralocorticoid receptor antagonist) and the angiotensin converting enzyme (ACE) inhibitor enalapril revealed that all antagonists were effective with regard to the prevention of oxidative stress and formation of DNA strand breaks and micronuclei in primary kidney cells but that the non-steroidal mineralocorticoid receptor antagonist BR-4628 was the most potent drug.

Finally, rosuvastatin, an inhibitor of the enzyme 3-hydroxy-3-methylglutaryl coenzyme A (HMG-CoA)-reductase which activates intracellular antioxidative defense mechanisms, was investigated. In HL-60 cells, the specific inductor of NAD(P)H oxidase, phorbol 12-myristate 13-acetate (PMA), caused oxidative stress. Rosuvastatin was able to prevent the release of ROS and subsequent oxidative DNA damage when co-incubated with PMA. Furthermore, not only an inhibition of PMA-induced oxidative stress but also inhibition of the unspecific release of ROS induced by hydrogen peroxide was observable. Addition of farnesyl pyrophosphate (FPP), geranylgeranyl pyrophosphate (GGPP), and mevalonate, intermediates of the cholesterol pathway, caused only a marginal increase of oxidative stress in cells treated simultaneously with PMA and rosuvastatin, thus indicating the effect of rosuvastatin to be HMG-CoA-reductase-independent.

Further experiments showed that rosuvastatin was even more effective after pre-incubation of the cells with rosuvastatin, excessive washing and subsequent

treatment with PMA or hydrogen peroxide. As rosuvastatin itself possesses no antioxidant capacity, other mechanisms had to be involved. Investigation of the gene expression of subunits of NAD(P)H oxidase revealed a down-regulation of p67phox - a cytosolic subunit of the enzyme generating the reactive oxygen species - following rosuvastatin-treatment. Slight increases in gene expression and enzyme activity could also be observed for superoxide dismutase (SOD) and catalase (CAT), which detoxify excess ROS intracellularly, in cells treated with rosuvastatin alone or in combination with PMA. Additionally, gene expression of heme oxygenase (HO-1) was increased significantly. Furthermore, it could be shown that rosuvastatin treatment alone or in combination with PMA increased total glutathione levels probably due to an induction of the gene expression and enzyme activity of  $\gamma$ -glutamylcysteine synthetase ( $\gamma$ -GCS), the pivotal enzyme of the glutathione system. Taken together, the results obtained in this study could add to a better understanding of the pathways from the release of reactive oxygen species to oxidative DNA damage and finally to the development of cancer. Furthermore, several drugs with entirely different working mechanisms were identified, which may have the capacity to exert beneficial effects with regard to the prevention of oxidative stress, the subsequent genomic damage and ultimately with regard to the prevention of human cancer.

## 10. Zusammenfassung

Immer häufiger werden reaktive Sauerstoffspezies (ROS) und der daraus resultierende oxidative Stress mit Krankheitsbildern wie neurodegenerativen Störungen, terminaler Niereninsuffizienz, Diabetes mellitus, Atherosklerose, Fettstoffwechselstörungen und kardiovaskulären Erkrankungen in Verbindung gebracht. Dies alles sind Erkrankungen, die in vielen Fällen mit Bluthochdruck einhergehen. Die Patienten leiden auch häufig nicht nur an einer dieser Krankheiten, sondern sind multimorbid und haben ein hohes Risiko, an Krebs zu erkranken. Aus diesem Grund stellten wir die Hypothese auf, dass das erhöhte Krebsrisiko in diesen Patienten von DNA-Strangbrüchen, DNA-Addukten und chromosomalen Aberrationen herrühren könnte, die als Folge von erhöhten ROS-Spiegeln entstehen. Im Zuge dieser Studie wurden sowohl endogene Substanzen als auch Modellsubstanzen eingesetzt, um die pathologischen Verhältnisse in Patienten, die an Bluthochdruck leiden, zu imitieren. Als endogene Substanzen wurden Angiotensin II und Aldosteron ausgewählt, da beide in an Bluthochdruck leidenden Patienten aufgrund einer Aktivierung des Renin-Angiotensin-Aldosteron-Systems erhöhte Konzentrationen aufweisen können. Als Modellsubstanzen wurden 4-Nitrochinolin-1-oxid (NQO) und Wasserstoffperoxid gewählt, da sie in der Lage sind, unspezifisch die Freisetzung von ROS auszulösen, Phorbol-12-myristat-13-acetat wurde wegen seiner Fähigkeit gewählt, spezifisch die NAD(P)H-Oxidase zu aktivieren.

Der erste Teil dieser Arbeit beschäftigt sich mit zwei Vitaminen, nämlich Benfotiamin, dem lipophilen Prodrug von Thiamin (Vitamin B1), und  $\alpha$ -Tocopherol, das zusammen mit anderen Tocopherolen und Tocotrienolen unter dem Namen Vitamin E bekannt ist. Sowohl Benfotiamin als auch  $\alpha$ -Tocopherol zeigten im Laufe der in drei Nierenzelllinien aus dem Menschen, der Ratte und dem Schwein durchgeführten Experimente, dass sie in der Lage sind, durch Angiotensin II verursachte DNA-Strangbrüche und chromosomale Aberrationen zu verhindern. Dies ist möglicherweise auf eine ebenfalls beobachtbare vorausgegangene Inhibition der Freisetzung reaktiver Sauerstoffspezies zurückzuführen und steht im Gegensatz zu Ergebnissen, die mit Thiamin, der hydrophilen, aktiven Form erzielt wurden. Des Weiteren zeigten Experimente, in denen Zellen mit Benfotiamin vorinkubiert wurden und sich daran die NQO-Behandlung anschloss, dass Benfotiamin unter diesen Versuchsbedingungen nicht in der Lage war, die Induktion von oxidativem Stress zu

verhindern. Die daraus resultierende Hypothese, dass Benfotiamin – wie  $\alpha$ -Tocopherol – direkte antioxidative Kapazität hat, wurde durch Messungen in zellfreien Systemen untermauert. Die bereits beschriebenen Effekte sind unabhängig von der ebenfalls beobachtbaren erhöhten Aktivität und verstärkten Gen-Expression des Enzyms Transketolase, das diphosphoryliertes Thiamin als Co-Faktor benötigt und das besonders in Diabetikern eine reduzierte Aktivität aufgrund von Thiamin-Malabsorption und verstärkter Ausscheidung im Harn aufweist. Zusammenfassend konnte ein neuer Wirkmechanismus für Benfotiamin vorgestellt werden.

Im zweiten Teil dieser Studie konnte nachgewiesen werden, dass Angiotensin II eine dosisabhängige Genotoxizität verursacht. Dieser Effekt wird durch den Angiotensin II-Rezeptor Typ 1 vermittelt, der nach Aktivierung die Bildung und Ausschüttung reaktiver Sauerstoffspezies durch die NAD(P)H-Oxidase auslöst. Weitere Experimente mit PD 123319, einem Inhibitor des Angiotensin II-Rezeptors Typ 2, zeigten, dass diese Substanz keinen Einfluss auf die Entstehung von Genomschäden hatte. Dies steht in Gegensatz zu Ergebnissen, die mit dem Angiotensin II-Rezeptor Typ 1-Inhibitor Candesartan erzielt wurden. Diese Substanz war in der Lage, die Angiotensin II-vermittelte Freisetzung reaktiver Sauerstoffspezies und die Induktion von DNA-Strangbrüchen und Mikrokernen zu verhindern, und war hierbei ebenso potent wie die Antioxidantien  $\alpha$ -Tocopherol und N-Acetylcystein. All diese Ergebnisse weisen darauf hin, dass der Angiotensin II-Rezeptor Typ 2 in keiner Weise am Angiotensin II-induzierten oxidativen DNA-Schaden beteiligt ist.

Im weiteren Verlauf der Studie wurden die *in vitro* Experimente auf das Modell der isolierten perfundierten Mäuseniere ausgeweitet. Hier konnte gezeigt werden, dass Angiotensin II in Konzentrationen, die in hypertensiven Patienten erreicht werden können, Vasokonstriktion und DNA-Strangbrüche verursacht. Co-Perfusion der Nieren mit Angiotensin II und Candesartan verhinderte hingegen die Vasokonstriktion und die Bildung von DNA-Strangbrüchen. Weitere Versuche mit dem Thromboxan-Mimetikum U 46619 zeigten, dass diese Substanz eine stärkere Vasokonstriktion als Angiotensin II verursachte, jedoch keine DNA Strangbrüche. Daher konnte die Verursachung von Strangbrüchen durch mechanischen Stress oder Hypoxie ausgeschlossen werden. Zusätzlich konnte eine Hochregulation der Häm-Oxygenase (HO-1) und eine Herunterregulation der Glutathionperoxidase (GPX) beobachtet werden.

Eine detaillierte Untersuchung und Charakterisierung der *ex vivo* beobachteten DNA-Schäden *in vitro* ließ erkennen, dass Angiotensin II Einzelstrangbrüche, Doppelstrangbrüche, die Bildung des DNA-Addukts 8-OxodG und abasische Stellen induziert. Ein Reparatur-Comet Assay, parallel durchgeführt mit der Messung des phosphorylierten Histons 2AX ( $\gamma$ -H2AX) über 24 h, zeigte eine vollständige Reparatur der Einzelstrangbrüche, wohingegen die Zahl der Doppelstrangbrüche in diesem Zeitraum sogar zunahm.

Im Formamidopyrimidin-DNA-Glycosylase (FPG)- modifizierten alkalischen Comet Assay wurde der Anteil der 8-OxodG-Addukte ermittelt. Die Ergebnisse wiesen auf einen Anstieg FPG-sensitiver Stellen nach Angiotensin II-Inkubation hin, wohingegen Co-Inkubation mit Candesartan die Bildung dieser Addukte verhinderte.

Untersuchungen der Effekte, die eine Aldosteron-Behandlung auf Nierenzellen hat, zeigten einen Anstieg des oxidativen Stress, der DNA Strangbrüche und der Mikrokerne. Diese Effekte konnten durch den steroidalen Mineralocorticoid Rezeptor-Antagonisten Eplerenon verhindert werden. Weitere Experimente mit dem nicht-steroidal Mineralocorticoid Rezeptor-Antagonisten (S)-BR-4628 zeigten, dass auch diese Substanz oxidativen Stress und DNA Schäden verhindern konnte und dabei potenter war als Eplerenon. Im Gegensatz hierzu hatte das (R)-Isomer, das keine Aktivität am Mineralocorticoid Rezeptor zeigt, keinen präventiven Effekt auf die Freisetzung von ROS oder die Entstehung von DNA-Schäden.

*In vivo* wurde der Hyperaldosteronismus, der in einem Teil der hypertensiven Patienten beobachtet werden kann, mit Hilfe des Deoxycorticosteronacetat- (DOCA) Salzmodells nachgeahmt. Unter dieser Behandlung konnten Level an DNA-Strangbrüchen und chromosomalen Aberrationen beobachtet werden, die ähnlich hoch waren wie die der mit dem Nephrotoxin Cisplatin behandelten Tiere. Des Weiteren konnten in den DOCA-Tieren erhöhte Level an oxidativem Stress gemessen werden. Wurden die Versuchstiere zusätzlich zur DOCA-Behandlung mit den Antihypertensiva Spironolacton (steroidaler Mineralocorticoid Rezeptor-Antagonist), BR-4628 (nicht-steroidaler Mineralocorticoid Rezeptor-Antagonist) und dem ACE-Inhibitor Enalapril behandelt, konnte gezeigt werden, dass alle Antagonisten wirksam waren im Hinblick auf die Prävention der Bildung von oxidativem Stress und von Genomschäden in primären Nierenzellen und dass der nicht-steroidale Mineralocorticoid Rezeptor-Antagonist BR-4628 potenter war als der

steroidale Mineralocorticoid Rezeptor-Antagonist Spironolacton und der ACE-Inhibitor Enalapril.

Zuletzt wurde mit Rosuvastatin, einem HMG-CoA-Reduktase-Inhibitor, eine Substanz untersucht, die die antioxidative Abwehr der Zellen aktivieren kann. In der humanen Leukämie-Zelllinie HL-60 verursachte der spezifische Induktor der NAD(P)H-Oxidase Phorbol-12-myristat-13-acetat (PMA) oxidativen Stress. Rosuvastatin war in der Lage, die Freisetzung von ROS und daraus resultierende DNA-Strangbrüche bei Co-Inkubation mit PMA zu verhindern. Außerdem konnte gezeigt werden, dass Rosuvastatin nicht nur PMA-induzierten oxidativen Stress, sondern auch die unspezifische Wasserstoffperoxid-induzierte Freisetzung von ROS verhinderte. Zugabe von Farnesylpyrophosphat (FPP), Geranylgeranylpyrophosphat (GGPP) und Mevalonat, Intermediaten der Cholesterolsynthese, bewirkte einen nur marginalen Anstieg des oxidativen Stresses in Zellen, die gleichzeitig noch mit PMA und Rosuvastatin behandelt wurden. Dies deutet darauf hin, dass der beobachtete Effekt unabhängig von der Wirkung auf die HMG-CoA-Reduktase ist. In weiteren Experimenten konnte gezeigt werden, dass Rosuvastatin sogar potenter war, wenn Zellen vorinkubiert, dann sorgfältig gewaschen wurden und erst anschließend die Behandlung mit PMA oder Wasserstoffperoxid durchgeführt wurde. Da Rosuvastatin selbst keine antioxidative Kapazität besitzt, mussten jedoch noch andere Mechanismen involviert sein. Die Untersuchung der Genexpression von Untereinheiten der NAD(P)H Oxidase, des Enzyms, das die ROS bildet, ergab, dass p67phox, eine zytosolische Untereinheit, nach Rosuvastatin-Behandlung herabreguliert wurde. Des Weiteren konnten erhöhte Aktivitäten und vermehrte Genexpression der Superoxiddismutase (SOD) und der Catalase (CAT) in Zellen, die mit Rosuvastatin alleine oder in Kombination mit PMA behandelt wurden, beobachtet werden. Beide Enzyme sind dafür zuständig, intrazelluläre ROS-Überschüsse zu vernichten. Auch die Genexpression der Häm-Oxygenase (HO-1) wurde signifikant erhöht. Behandlung mit Rosuvastatin allein oder zusammen mit PMA konnte außerdem die Glutathion-Spiegel erhöhen. Dies ist vermutlich auf die Induktion der Genexpression und der Enzymaktivität der  $\gamma$ -Glutamylcystein-Synthetase ( $\gamma$ -GCS), des Schrittmacherenzym des Glutathionsystems, zurückzuführen.

Zusammengefaßt könnten die im Laufe dieser Studie gewonnenen Ergebnisse zu einem besseren Verständnis der Vorgänge, angefangen mit der Freisetzung der ROS über die Entstehung oxidativer DNA-Schäden bis hin zur Bildung von Krebs,

beitragen. Des Weiteren konnten mehrere Arzneistoffe mit völlig unterschiedlichen Angriffspunkten identifiziert werden, die die Fähigkeit besitzen, förderliche Effekte im Hinblick auf die Prävention von oxidativem Stress, Genomschäden und in letzter Konsequenz möglicherweise auch auf die Prävention von Krebs auszuüben.

## 11. References

1. Touyz, R.M., *Molecular and cellular mechanisms in vascular injury in hypertension: role of angiotensin II*. *Curr Opin Nephrol Hypertens*, 2005. **14**(2): p. 125-31.
2. Halliwell, B., *Oxidative stress and cancer: have we moved forward?* *Biochem J*, 2007. **401**(1): p. 1-11.
3. Halazonetis, T.D., V.G. Gorgoulis, and J. Bartek, *An oncogene-induced DNA damage model for cancer development*. *Science*, 2008. **319**(5868): p. 1352-5.
4. Tain, Y.L. and C. Baylis, *Dissecting the causes of oxidative stress in an in vivo model of hypertension*. *Hypertension*, 2006. **48**(5): p. 828-9.
5. Droge, W., *Free radicals in the physiological control of cell function*. *Physiol Rev*, 2002. **82**(1): p. 47-95.
6. Vignais, P.V., *The superoxide-generating NADPH oxidase: structural aspects and activation mechanism*. *Cell Mol Life Sci*, 2002. **59**(9): p. 1428-59.
7. Rahman, K., *Studies on free radicals, antioxidants, and co-factors*. *Clin Interv Aging*, 2007. **2**(2): p. 219-36.
8. Valko, M., et al., *Free radicals, metals and antioxidants in oxidative stress-induced cancer*. *Chem Biol Interact*, 2006. **160**(1): p. 1-40.
9. Frei, B., et al., *Gas phase oxidants of cigarette smoke induce lipid peroxidation and changes in lipoprotein properties in human blood plasma. Protective effects of ascorbic acid*. *Biochem J*, 1991. **277 ( Pt 1)**: p. 133-8.
10. Kolachana, P., et al., *Benzene and its phenolic metabolites produce oxidative DNA damage in HL60 cells in vitro and in the bone marrow in vivo*. *Cancer Res*, 1993. **53**(5): p. 1023-6.
11. Halliwell, B. and J.M. Gutteridge, *Role of free radicals and catalytic metal ions in human disease: an overview*. *Methods Enzymol*, 1990. **186**: p. 1-85.
12. Sussman, M.S. and G.B. Bulkley, *Oxygen-derived free radicals in reperfusion injury*. *Methods Enzymol*, 1990. **186**: p. 711-23.
13. Cerutti, P., et al., *The role of the cellular antioxidant defense in oxidant carcinogenesis*. *Environ Health Perspect*, 1994. **102 Suppl 10**: p. 123-9.
14. Ames, B.N., M.K. Shigenaga, and L.S. Gold, *DNA lesions, inducible DNA repair, and cell division: three key factors in mutagenesis and carcinogenesis*. *Environ Health Perspect*, 1993. **101 Suppl 5**: p. 35-44.



15. Yu, B.P., *Cellular defenses against damage from reactive oxygen species*. *Physiol Rev*, 1994. **74**(1): p. 139-62.
16. Johnson, F. and C. Giulivi, *Superoxide dismutases and their impact upon human health*. *Mol Aspects Med*, 2005. **26**(4-5): p. 340-52.
17. Remacle, J., et al., *Importance of various antioxidant enzymes for cell stability. Confrontation between theoretical and experimental data*. *Biochem J*, 1992. **286 ( Pt 1)**: p. 41-6.
18. Cerutti, P.A. and B.F. Trump, *Inflammation and oxidative stress in carcinogenesis*. *Cancer Cells*, 1991. **3**(1): p. 1-7.
19. Menkes, M.S., et al., *Serum beta-carotene, vitamins A and E, selenium, and the risk of lung cancer*. *N Engl J Med*, 1986. **315**(20): p. 1250-4.
20. Albanes, D., et al., *Alpha-Tocopherol and beta-carotene supplements and lung cancer incidence in the alpha-tocopherol, beta-carotene cancer prevention study: effects of base-line characteristics and study compliance*. *J Natl Cancer Inst*, 1996. **88**(21): p. 1560-70.
21. Greenberg, E.R., et al., *A clinical trial of beta carotene to prevent basal-cell and squamous-cell cancers of the skin. The Skin Cancer Prevention Study Group*. *N Engl J Med*, 1990. **323**(12): p. 789-95.
22. Greenberg, E.R., et al., *A clinical trial of antioxidant vitamins to prevent colorectal adenoma. Polyp Prevention Study Group*. *N Engl J Med*, 1994. **331**(3): p. 141-7.
23. Jacob, R.A., et al., *Immunocompetence and oxidant defense during ascorbate depletion of healthy men*. *Am J Clin Nutr*, 1991. **54**(6 Suppl): p. 1302S-1309S.
24. Blot, W.J., et al., *Nutrition intervention trials in Linxian, China: supplementation with specific vitamin/mineral combinations, cancer incidence, and disease-specific mortality in the general population*. *J Natl Cancer Inst*, 1993. **85**(18): p. 1483-92.
25. Ames, B.N., et al., *Uric acid provides an antioxidant defense in humans against oxidant- and radical-caused aging and cancer: a hypothesis*. *Proc Natl Acad Sci U S A*, 1981. **78**(11): p. 6858-62.
26. Zimmerman, R. and P. Cerutti, *Active oxygen acts as a promoter of transformation in mouse embryo C3H/10T1/2/C18 fibroblasts*. *Proc Natl Acad Sci U S A*, 1984. **81**(7): p. 2085-7.

27. Weitzman, S.A., et al., *Phagocytes as carcinogens: malignant transformation produced by human neutrophils*. Science, 1985. **227**(4691): p. 1231-3.
28. Cerutti, P.A., *Oxy-radicals and cancer*. Lancet, 1994. **344**(8926): p. 862-3.
29. Burdon, R.H., V. Gill, and C. Rice-Evans, *Oxidative stress and tumour cell proliferation*. Free Radic Res Commun, 1990. **11**(1-3): p. 65-76.
30. Clayson, D.B., R. Mehta, and F. Iverson, *International Commission for Protection Against Environmental Mutagens and Carcinogens. Oxidative DNA damage--the effects of certain genotoxic and operationally non-genotoxic carcinogens*. Mutat Res, 1994. **317**(1): p. 25-42.
31. Ames, B.N., *Endogenous oxidative DNA damage, aging, and cancer*. Free Radic Res Commun, 1989. **7**(3-6): p. 121-8.
32. Weitzman, S.A., et al., *Free radical adducts induce alterations in DNA cytosine methylation*. Proc Natl Acad Sci U S A, 1994. **91**(4): p. 1261-4.
33. Halliwell, B. and O.I. Aruoma, *DNA damage by oxygen-derived species. Its mechanism and measurement in mammalian systems*. FEBS Lett, 1991. **281**(1-2): p. 9-19.
34. Floyd, R.A., et al., *Hydroxyl free radical adduct of deoxyguanosine: sensitive detection and mechanisms of formation*. Free Radic Res Commun, 1986. **1**(3): p. 163-72.
35. Grollman, A.P. and M. Moriya, *Mutagenesis by 8-oxoguanine: an enemy within*. Trends Genet, 1993. **9**(7): p. 246-9.
36. Demple, B. and L. Harrison, *Repair of oxidative damage to DNA: enzymology and biology*. Annu Rev Biochem, 1994. **63**: p. 915-48.
37. O'Driscoll, M. and P.A. Jeggo, *The role of double-strand break repair - insights from human genetics*. Nat Rev Genet, 2006. **7**(1): p. 45-54.
38. Subba Rao, K., *Mechanisms of disease: DNA repair defects and neurological disease*. Nat Clin Pract Neurol, 2007. **3**(3): p. 162-72.
39. Thoms, K.M., C. Kuschal, and S. Emmert, *Lessons learned from DNA repair defective syndromes*. Exp Dermatol, 2007. **16**(6): p. 532-44.
40. Satoh, M.S., et al., *DNA excision-repair defect of xeroderma pigmentosum prevents removal of a class of oxygen free radical-induced base lesions*. Proc Natl Acad Sci U S A, 1993. **90**(13): p. 6335-9.
41. Hakem, R., *DNA-damage repair; the good, the bad, and the ugly*. Embo J, 2008. **27**(4): p. 589-605.

42. Robbins, J.H., et al., *Xeroderma pigmentosum. An inherited diseases with sun sensitivity, multiple cutaneous neoplasms, and abnormal DNA repair.* Ann Intern Med, 1974. **80**(2): p. 221-48.
43. Jiricny, J., *The multifaceted mismatch-repair system.* Nat Rev Mol Cell Biol, 2006. **7**(5): p. 335-46.
44. Vasen, H.F., et al., *Guidelines for the clinical management of Lynch syndrome (hereditary non-polyposis cancer).* J Med Genet, 2007. **44**(6): p. 353-62.
45. Wilson, D.M., 3rd and V.A. Bohr, *The mechanics of base excision repair, and its relationship to aging and disease.* DNA Repair (Amst), 2007. **6**(4): p. 544-59.
46. Kanaar, R., C. Wyman, and R. Rothstein, *Quality control of DNA break metabolism: in the 'end', it's a good thing.* Embo J, 2008. **27**(4): p. 581-8.
47. Schupp, N., et al., *Angiotensin II-induced genomic damage in renal cells can be prevented by angiotensin II type 1 receptor blockage or radical scavenging.* Am J Physiol Renal Physiol, 2007. **292**(5): p. F1427-34.
48. Schmid, U., *Protection against oxidative DNA damage by antioxidants, hormone-receptor blockers and HMG-CoA-reductase inhibitors,* in *Toxicology.* 2008, University of Würzburg: Würzburg. p. 180.
49. Kearney, P.M., et al., *Global burden of hypertension: analysis of worldwide data.* Lancet, 2005. **365**(9455): p. 217-23.
50. Moore, L.E., R.T. Wilson, and S.L. Campelman, *Lifestyle factors, exposures, genetic susceptibility, and renal cell cancer risk: a review.* Cancer Invest, 2005. **23**(3): p. 240-55.
51. Friis, S., et al., *Angiotensin-converting enzyme inhibitors and the risk of cancer: a population-based cohort study in Denmark.* Cancer, 2001. **92**(9): p. 2462-70.
52. Ferrario, C.M., *Role of angiotensin II in cardiovascular disease therapeutic implications of more than a century of research.* J Renin Angiotensin Aldosterone Syst, 2006. **7**(1): p. 3-14.
53. Carey, R.M. and H.M. Siragy, *Newly recognized components of the renin-angiotensin system: potential roles in cardiovascular and renal regulation.* Endocr Rev, 2003. **24**(3): p. 261-71.

54. Dielis, A.W., et al., *The prothrombotic paradox of hypertension: role of the renin-angiotensin and kallikrein-kinin systems*. Hypertension, 2005. **46**(6): p. 1236-42.
55. Smith, G.R. and S. Missailidis, *Cancer, inflammation and the AT1 and AT2 receptors*. J Inflamm (Lond), 2004. **1**(1): p. 3.
56. Trapp, T., et al., *Heterodimerization between mineralocorticoid and glucocorticoid receptor: a new principle of glucocorticoid action in the CNS*. Neuron, 1994. **13**(6): p. 1457-62.
57. Funder, J.W., et al., *Mineralocorticoid action: target tissue specificity is enzyme, not receptor, mediated*. Science, 1988. **242**(4878): p. 583-5.
58. Lombes, M., et al., *Immunohistochemical and biochemical evidence for a cardiovascular mineralocorticoid receptor*. Circ Res, 1992. **71**(3): p. 503-10.
59. Funder, J.W., *Mineralocorticoid receptors: distribution and activation*. Heart Fail Rev, 2005. **10**(1): p. 15-22.
60. Weir, M.R., *Providing end-organ protection with renin-angiotensin system inhibition: the evidence so far*. J Clin Hypertens (Greenwich), 2006. **8**(2): p. 99-105; quiz 106-7.
61. Chobanian, A.V., et al., *Seventh report of the Joint National Committee on Prevention, Detection, Evaluation, and Treatment of High Blood Pressure*. Hypertension, 2003. **42**(6): p. 1206-52.
62. Mutschler, E., *Arzneimittelwirkungen*. 2001  
Stuttgart: Wissenschaftliche Verlagsgesellschaft.
63. Liu, Y.H., et al., *Effects of angiotensin-converting enzyme inhibitors and angiotensin II type 1 receptor antagonists in rats with heart failure. Role of kinins and angiotensin II type 2 receptors*. J Clin Invest, 1997. **99**(8): p. 1926-35.
64. *Effects of enalapril on mortality in severe congestive heart failure. Results of the Cooperative North Scandinavian Enalapril Survival Study (CONSENSUS)*. The CONSENSUS Trial Study Group. N Engl J Med, 1987. **316**(23): p. 1429-35.
65. Barnett, A.H., et al., *Angiotensin-receptor blockade versus converting-enzyme inhibition in type 2 diabetes and nephropathy*. N Engl J Med, 2004. **351**(19): p. 1952-61.

66. MacFadyen, R.J., et al., *How often are angiotensin II and aldosterone concentrations raised during chronic ACE inhibitor treatment in cardiac failure?* Heart, 1999. **82**(1): p. 57-61.
67. Marney, A.M. and N.J. Brown, *Aldosterone and end-organ damage.* Clin Sci (Lond), 2007. **113**(6): p. 267-78.
68. Calhoun, D.A., *Aldosteronism and hypertension.* Clin J Am Soc Nephrol, 2006. **1**(5): p. 1039-45.
69. McManus, F., G.T. McInnes, and J.M. Connell, *Drug Insight: eplerenone, a mineralocorticoid-receptor antagonist.* Nat Clin Pract Endocrinol Metab, 2008. **4**(1): p. 44-52.
70. Schmid, U., *Aldosterone induces oxidative stress and genomic damage in vivo.* 2008.
71. Schmid, U., Stopper, H, Schupp, N., *Aldosterone causes DNA strand breaks and chromosomal aberrations in renal cells.* 2008.
72. Schmid, U., et al., *Benfotiamine exhibits direct antioxidative capacity and prevents induction of DNA damage in vitro.* Diabetes Metab Res Rev, 2008.
73. Schmid U, S.H., Heidland A, Schupp N., *Benfotiamine exhibits direct antioxidative capacity and prevents induction of DNA damage in vitro.* Diabetes Metabolism Research and Reviews, 2008.
74. Jin, L., et al., *Increased reactive oxygen species contributes to kidney injury in mineralocorticoid hypertensive rats.* J Physiol Pharmacol, 2006. **57**(3): p. 343-57.
75. Buoncristiani, U., et al., *Oxidative damage during hemodialysis using a vitamin-E-modified dialysis membrane: a preliminary characterization.* Nephron, 1997. **77**(1): p. 57-61.
76. Alberts, A.W., *Discovery, biochemistry and biology of lovastatin.* Am J Cardiol, 1988. **62**(15): p. 10J-15J.
77. Ganesh, S.K., C.M. Nass, and R.S. Blumenthal, *Anti-atherosclerotic effects of statins: lessons from prevention trials.* J Cardiovasc Risk, 2003. **10**(3): p. 155-9.
78. LaRosa, J.C., *Statins and risk of coronary heart disease.* Jama, 2000. **283**(22): p. 2935-6.
79. Vaughan, C.J., A.M. Gotto, Jr., and C.T. Basson, *The evolving role of statins in the management of atherosclerosis.* J Am Coll Cardiol, 2000. **35**(1): p. 1-10.

80. Massy, Z.A. and C. Guijarro, *Statins: effects beyond cholesterol lowering*. *Nephrol Dial Transplant*, 2001. **16**(9): p. 1738-41.
81. Wierzbicki, A.S., R. Poston, and A. Ferro, *The lipid and non-lipid effects of statins*. *Pharmacol Ther*, 2003. **99**(1): p. 95-112.
82. Liao, J.K. and U. Laufs, *Pleiotropic effects of statins*. *Annu Rev Pharmacol Toxicol*, 2005. **45**: p. 89-118.
83. van den Akker, J.M., et al., *Atorvastatin and simvastatin in patients on hemodialysis: effects on lipoproteins, C-reactive protein and in vivo oxidized LDL*. *J Nephrol*, 2003. **16**(2): p. 238-44.
84. Stoll, L.L., et al., *Antioxidant effects of statins*. *Drugs Today (Barc)*, 2004. **40**(12): p. 975-90.
85. Halliwell, B., *Why and how should we measure oxidative DNA damage in nutritional studies? How far have we come?* *Am J Clin Nutr*, 2000. **72**(5): p. 1082-7.
86. Wiseman, H. and B. Halliwell, *Damage to DNA by reactive oxygen and nitrogen species: role in inflammatory disease and progression to cancer*. *Biochem J*, 1996. **313 ( Pt 1)**: p. 17-29.
87. Marnett, L.J., *Oxyradicals and DNA damage*. *Carcinogenesis*, 2000. **21**(3): p. 361-70.
88. Martinet, W., et al., *Elevated levels of oxidative DNA damage and DNA repair enzymes in human atherosclerotic plaques*. *Circulation*, 2002. **106**(8): p. 927-32.
89. Collins, A.R., *The comet assay for DNA damage and repair: principles, applications, and limitations*. *Mol Biotechnol*, 2004. **26**(3): p. 249-61.
90. Fenech, M., *Cytokinesis-block micronucleus assay evolves into a "cytome" assay of chromosomal instability, mitotic dysfunction and cell death*. *Mutat Res*, 2006. **600**(1-2): p. 58-66.
91. Cook, P.R., I.A. Brazell, and E. Jost, *Characterization of nuclear structures containing superhelical DNA*. *J Cell Sci*, 1976. **22**(2): p. 303-24.
92. Ostling, O. and K.J. Johanson, *Microelectrophoretic study of radiation-induced DNA damages in individual mammalian cells*. *Biochem Biophys Res Commun*, 1984. **123**(1): p. 291-8.

93. Koppen, G. and K.J. Angelis, *Repair of X-ray induced DNA damage measured by the comet assay in roots of Vicia faba*. Environ Mol Mutagen, 1998. **32**(3): p. 281-5.
94. Singh, N., et al., *A simple technique for quantitation of low levels of DNA damage in individual cells*. Exp Cell Res., 1988. **175**(1): p. 184-191.
95. Collins, A.R., et al., *The comet assay: what can it really tell us?* Mutat Res, 1997. **375**(2): p. 183-93.
96. Collins, A.R., et al., *Oxidative damage to DNA: do we have a reliable biomarker?* Environ Health Perspect, 1996. **104 Suppl 3**: p. 465-9.
97. Savage, J.R., *Update on target theory as applied to chromosomal aberrations*. Environ Mol Mutagen, 1993. **22**(4): p. 198-207.
98. Evans, H.J., *Cytogenetics: overview*. Prog Clin Biol Res, 1990. **340B**: p. 301-23.
99. Carter, S.B., *Effects of cytochalasins on mammalian cells*. Nature, 1967. **213**(5073): p. 261-4.
100. Fenech, M., *The in vitro micronucleus technique*. Mutat Res, 2000. **455**(1-2): p. 81-95.
101. LeBel, C.P., H. Ischiropoulos, and S.C. Bondy, *Evaluation of the probe 2',7'-dichlorofluorescein as an indicator of reactive oxygen species formation and oxidative stress*. Chem Res Toxicol, 1992. **5**(2): p. 227-31.
102. Baynes, J.W., *Role of oxidative stress in development of complications in diabetes*. Diabetes, 1991. **40**(4): p. 405-12.
103. Aragno, M., et al., *Dehydroepiandrosterone prevents oxidative injury induced by transient ischemia/reperfusion in the brain of diabetic rats*. Diabetes, 2000. **49**(11): p. 1924-31.
104. Aragno, M., et al., *Up-regulation of advanced glycated products receptors in the brain of diabetic rats is prevented by antioxidant treatment*. Endocrinology, 2005. **146**(12): p. 5561-7.
105. Matthews, D.R., et al., *Homeostasis model assessment: insulin resistance and beta-cell function from fasting plasma glucose and insulin concentrations in man*. Diabetologia, 1985. **28**(7): p. 412-9.
106. Nishikawa, T., et al., *Normalizing mitochondrial superoxide production blocks three pathways of hyperglycaemic damage*. Nature, 2000. **404**(6779): p. 787-90.

107. Peyroux, J. and M. Sternberg, *Advanced glycation endproducts (AGEs): Pharmacological inhibition in diabetes*. *Pathol Biol (Paris)*, 2006. **54**(7): p. 405-19.
108. Head, K.A., *Peripheral neuropathy: pathogenic mechanisms and alternative therapies*. *Altern Med Rev*, 2006. **11**(4): p. 294-329.
109. Malecka, S.A., K. Poprawski, and B. Bilski, *[Prophylactic and therapeutic application of thiamine (vitamin B1)--a new point of view]*. *Wiad Lek*, 2006. **59**(5-6): p. 383-7.
110. Abbas, Z.G. and A.B. Swai, *Evaluation of the efficacy of thiamine and pyridoxine in the treatment of symptomatic diabetic peripheral neuropathy*. *East Afr Med J*, 1997. **74**(12): p. 803-8.
111. Karachalias, N., et al., *Accumulation of fructosyl-lysine and advanced glycation end products in the kidney, retina and peripheral nerve of streptozotocin-induced diabetic rats*. *Biochem Soc Trans*, 2003. **31**(Pt 6): p. 1423-5.
112. Hammes, H.P., et al., *Benfotiamine blocks three major pathways of hyperglycemic damage and prevents experimental diabetic retinopathy*. *Nat Med*, 2003. **9**(3): p. 294-9.
113. Loew, D., *Pharmacokinetics of thiamine derivatives especially of benfotiamine*. *Int J Clin Pharmacol Ther*, 1996. **34**(2): p. 47-50.
114. Arima, Y., et al., *4-Nitroquinoline 1-oxide forms 8-hydroxydeoxyguanosine in human fibroblasts through reactive oxygen species*. *Toxicol Sci*, 2006. **91**(2): p. 382-92.
115. Motojima, M., et al., *Uremic toxins of organic anions up-regulate PAI-1 expression by induction of NF-kappaB and free radical in proximal tubular cells*. *Kidney Int*, 2003. **63**(5): p. 1671-80.
116. Haber, E., *Angiotensin-converting enzyme and lipoprotein(a) as risk factors for myocardial infarction*. *Circulation*, 1995. **91**(6): p. 1888-90.
117. Decordier, I. and M. Kirsch-Volders, *The in vitro micronucleus test: from past to future*. *Mutat Res*, 2006. **607**(1): p. 2-4.
118. Fenech, M., *The cytokinesis-block micronucleus technique: a detailed description of the method and its application to genotoxicity studies in human populations*. *Mutat Res*, 1993. **285**(1): p. 35-44.



119. Bendich, A. and L.J. Machlin, *Safety of oral intake of vitamin E*. Am J Clin Nutr, 1988. **48**(3): p. 612-9.
120. Stocker, R., *Vitamin E*. Novartis Found Symp, 2007. **282**: p. 77-87; discussion 87-92, 212-8.
121. Traber, M.G., B. Frei, and J.S. Beckman, *Vitamin E revisited: do new data validate benefits for chronic disease prevention?* Curr Opin Lipidol, 2008. **19**(1): p. 30-8.
122. Munne-Bosch, S., *Alpha-tocopherol: a multifaceted molecule in plants*. Vitam Horm, 2007. **76**: p. 375-92.
123. Burton, G.W., et al., *Vitamin E as an antioxidant in vitro and in vivo*. Ciba Found Symp, 1983. **101**: p. 4-18.
124. Chow, C.K., *Vitamin E and blood*. World Rev Nutr Diet, 1985. **45**: p. 133-66.
125. Ceriello, A., *Controlling oxidative stress as a novel molecular approach to protecting the vascular wall in diabetes*. Curr Opin Lipidol, 2006. **17**(5): p. 510-8.
126. Ortiz, M.C., et al., *Antioxidants block angiotensin II-induced increases in blood pressure and endothelin*. Hypertension, 2001. **38**(3 Pt 2): p. 655-9.
127. Manrique, C., et al., *Methods in the evaluation of cardiovascular Renin Angiotensin aldosterone activation and oxidative stress*. Methods Mol Med, 2007. **139**: p. 163-80.
128. Schupp, N., et al., *Genotoxicity of Advanced Glycation End Products: Involvement of Oxidative Stress and of Angiotensin II Type 1 Receptors*. Ann N Y Acad Sci, 2005. **1043**: p. 685-95.
129. Schupp, N., et al., *Angiotensin II-induced genomic damage in renal cells can be prevented by angiotensin II type 1 receptor blockage or radical scavenging*. Am J Physiol Renal Physiol, 2007.
130. Benzie, I.F. and J.J. Strain, *Ferric reducing/antioxidant power assay: direct measure of total antioxidant activity of biological fluids and modified version for simultaneous measurement of total antioxidant power and ascorbic acid concentration*. Methods Enzymol, 1999. **299**: p. 15-27.
131. Pulido, R., L. Bravo, and F. Saura-Calixto, *Antioxidant activity of dietary polyphenols as determined by a modified ferric reducing/antioxidant power assay*. J Agric Food Chem, 2000. **48**(8): p. 3396-402.

132. Benzie, I.F. and J.J. Strain, *The ferric reducing ability of plasma (FRAP) as a measure of "antioxidant power": the FRAP assay*. *Anal Biochem*, 1996. **239**(1): p. 70-6.
133. Babaei-Jadidi, R., et al., *Prevention of incipient diabetic nephropathy by high-dose thiamine and benfotiamine*. *Diabetes*, 2003. **52**(8): p. 2110-20.
134. Berrone, E., et al., *Regulation of intracellular glucose and polyol pathway by thiamine and benfotiamine in vascular cells cultured in high glucose*. *J Biol Chem*, 2006. **281**(14): p. 9307-13.
135. Cameron, N.E., et al., *Inhibitors of advanced glycation end product formation and neurovascular dysfunction in experimental diabetes*. *Ann N Y Acad Sci*, 2005. **1043**: p. 784-92.
136. Haupt, E., H. Ledermann, and W. Kopcke, *Benfotiamine in the treatment of diabetic polyneuropathy--a three-week randomized, controlled pilot study (BEDIP study)*. *Int J Clin Pharmacol Ther*, 2005. **43**(2): p. 71-7.
137. Milman, U., et al., *Vitamin E supplementation reduces cardiovascular events in a subgroup of middle-aged individuals with both type 2 diabetes mellitus and the haptoglobin 2-2 genotype: a prospective double-blinded clinical trial*. *Arterioscler Thromb Vasc Biol*, 2008. **28**(2): p. 341-7.
138. Huang, H.Y., et al., *Multivitamin/Mineral supplements and prevention of chronic disease: executive summary*. *Am J Clin Nutr*, 2007. **85**(1): p. 265S-268S.
139. Brown, B.G. and J. Crowley, *Is there any hope for vitamin E?* *Jama*, 2005. **293**(11): p. 1387-90.
140. Mateuca, R., et al., *Chromosomal changes: induction, detection methods and applicability in human biomonitoring*. *Biochimie*, 2006. **88**(11): p. 1515-31.
141. Grossman, E., et al., *Is there an association between hypertension and cancer mortality?* *Am J Med*, 2002. **112**(6): p. 479-86.
142. Laragh, J.H., Lewis K. Dahl Memorial Lecture. *The renin system and four lines fo hypertension research. Nephron heterogeneity, the calcium connection, the prorenin vasodilator limb, and plasma renin and heart attack*. *Hypertension*, 1992. **20**(3): p. 267-79.
143. Karalliedde, J. and G. Viberti, *Evidence for renoprotection by blockade of the renin-angiotensin-aldosterone system in hypertension and diabetes*. *J Hum Hypertens*, 2006. **20**(4): p. 239-53.

144. MacKenzie, S.M., et al., *Local renin-angiotensin systems and their interactions with extra-adrenal corticosteroid production*. J Renin Angiotensin Aldosterone Syst, 2002. **3**(4): p. 214-21.
145. Kaschina, E. and T. Unger, *Angiotensin AT1/AT2 receptors: regulation, signalling and function*. Blood Press, 2003. **12**(2): p. 70-88.
146. Deshayes, F. and C. Nahmias, *Angiotensin receptors: a new role in cancer?* Trends Endocrinol Metab, 2005. **16**(7): p. 293-9.
147. Hannken, T., et al., *Angiotensin II-mediated expression of p27Kip1 and induction of cellular hypertrophy in renal tubular cells depend on the generation of oxygen radicals*. Kidney Int, 1998. **54**(6): p. 1923-33.
148. Imlay, J.A. and S. Linn, *DNA damage and oxygen radical toxicity*. Science, 1988. **240**: p. 1302-1309.
149. Rozen, S. and H. Skaletsky, *Primer3 on the WWW for general users and for biologist programmers*. Methods Mol Biol, 2000. **132**: p. 365-86.
150. Ullian, M.E., et al., *N-Acetylcysteine Decreases Angiotensin II Receptor Binding in Vascular Smooth Muscle Cells*. J Am Soc Nephrol, 2005. **16**(8): p. 2346-2353.
151. Quan, S., et al., *Expression of human heme oxygenase-1 in the thick ascending limb attenuates angiotensin II-mediated increase in oxidative injury*. Kidney Int, 2004. **65**(5): p. 1628-39.
152. Mazza, F., et al., *Heme Oxygenase-1 Gene Expression Attenuates Angiotensin II-Mediated DNA Damage in Endothelial Cells*. Experimental Biology and Medicine, 2003. **228**(5): p. 576-583.
153. Wassmann, S. and G. Nickenig, *Pathophysiological regulation of the AT1-receptor and implications for vascular disease*. J Hypertens Suppl, 2006. **24**(1): p. S15-21.
154. Griendling, K.K., et al., *Angiotensin II stimulates NADH and NADPH oxidase activity in cultured vascular smooth muscle cells*. Circ Res, 1994. **74**(6): p. 1141-8.
155. Burlinson, B., et al., *Fourth International Workgroup on Genotoxicity testing: Results of the in vivo Comet assay workgroup*. Mutat Res, 2006.
156. Li, Z., J. Yang, and H. Huang, *Oxidative stress induces H2AX phosphorylation in human spermatozoa*. FEBS Lett, 2006. **580**(26): p. 6161-8.

157. Griendling, K.K. and M. Ushio-Fukai, *Reactive oxygen species as mediators of angiotensin II signaling*. Regul Pept, 2000. **91**(1-3): p. 21-7.
158. Wang, C.T., L.G. Navar, and K.D. Mitchell, *Proximal tubular fluid angiotensin II levels in angiotensin II-induced hypertensive rats*. J Hypertens, 2003. **21**(2): p. 353-60.
159. Siragy, H.M., et al., *Renal interstitial fluid angiotensin. Modulation by anesthesia, epinephrine, sodium depletion, and renin inhibition*. Hypertension, 1995. **25**(5): p. 1021-4.
160. Chow, W.H., et al., *Obesity, hypertension, and the risk of kidney cancer in men*. N Engl J Med, 2000. **343**(18): p. 1305-11.
161. Lindberg, H., et al., *Angiotensin converting enzyme inhibitors for cancer treatment?* Acta Oncol, 2004. **43**(2): p. 142-52.
162. Uemura, H., et al., *Antiproliferative efficacy of angiotensin II receptor blockers in prostate cancer*. Curr Cancer Drug Targets, 2005. **5**(5): p. 307-23.
163. Uemura, H., et al., *Pilot study of angiotensin II receptor blocker in advanced hormone-refractory prostate cancer*. Int J Clin Oncol, 2005. **10**(6): p. 405-10.
164. Rahgozar, M., et al., *Angiotensin II facilitates autoregulation in the perfused mouse kidney: An optimized in vitro model for assessment of renal vascular and tubular function*. Nephrology (Carlton), 2004. **9**(5): p. 288-96.
165. Schweda, F., et al., *Preserved macula densa-dependent renin secretion in A1 adenosine receptor knockout mice*. Am J Physiol Renal Physiol, 2003. **284**(4): p. F770-7.
166. Burlinson, B., et al., *Fourth International Workgroup on Genotoxicity testing: results of the in vivo Comet assay workgroup*. Mutat Res, 2007. **627**(1): p. 31-5.
167. Hartmann, A., et al., *Use of the alkaline in vivo Comet assay for mechanistic genotoxicity investigations*. Mutagenesis, 2004. **19**(1): p. 51-9.
168. Aizawa, T., et al., *Balloon injury does not induce heme oxygenase-1 expression, but administration of hemin inhibits neointimal formation in balloon-injured rat carotid artery*. Biochem Biophys Res Commun, 1999. **261**(2): p. 302-7.
169. Ishizaka, N. and K.K. Griendling, *Heme oxygenase-1 is regulated by angiotensin II in rat vascular smooth muscle cells*. Hypertension, 1997. **29**(3): p. 790-5.

170. Schupp, N., et al., *Rosuvastatin protects against oxidative stress and DNA damage in vitro via upregulation of glutathione synthesis*. *Atherosclerosis*, 2007.
171. Cowell, I.G., et al., *gammaH2AX Foci Form Preferentially in Euchromatin after Ionising-Radiation*. *PLoS ONE*, 2007. **2**(10): p. e1057.
172. Gobe, G.C. and D.W. Johnson, *Distal tubular epithelial cells of the kidney: Potential support for proximal tubular cell survival after renal injury*. *Int J Biochem Cell Biol*, 2007. **39**(9): p. 1551-61.
173. Aigner, T., et al., *Large-scale gene expression profiling reveals major pathogenetic pathways of cartilage degeneration in osteoarthritis*. *Arthritis Rheum*, 2006. **54**(11): p. 3533-44.
174. Forand, A., B. Dutrillaux, and J. Bernardino-Sgherri, *Gamma-H2AX expression pattern in non-irradiated neonatal mouse germ cells and after low-dose gamma-radiation: relationships between chromatid breaks and DNA double-strand breaks*. *Biol Reprod*, 2004. **71**(2): p. 643-9.
175. Rothkamm, K., et al., *Pathways of DNA double-strand break repair during the mammalian cell cycle*. *Mol Cell Biol*, 2003. **23**(16): p. 5706-15.
176. Connell, J.M. and E. Davies, *The new biology of aldosterone*. *J Endocrinol*, 2005. **186**(1): p. 1-20.
177. Good, D.W., *Nongenomic actions of aldosterone on the renal tubule*. *Hypertension*, 2007. **49**(4): p. 728-39.
178. Boldyreff, B. and M. Wehling, *Rapid aldosterone actions: from the membrane to signaling cascades to gene transcription and physiological effects*. *J Steroid Biochem Mol Biol*, 2003. **85**(2-5): p. 375-81.
179. Jaffe, I.Z. and M.E. Mendelsohn, *Angiotensin II and aldosterone regulate gene transcription via functional mineralocorticoid receptors in human coronary artery smooth muscle cells*. *Circ Res*, 2005. **96**(6): p. 643-50.
180. Luther, J.M., et al., *Angiotensin II induces interleukin-6 in humans through a mineralocorticoid receptor-dependent mechanism*. *Hypertension*, 2006. **48**(6): p. 1050-7.
181. Yang, H., et al., *In situ assessment of cell viability*. *Cell Transplant*, 1998. **7**(5): p. 443-51.
182. Brendler-Schwaab, S., et al., *The in vivo comet assay: use and status in genotoxicity testing*. *Mutagenesis*, 2005. **20**(4): p. 245-54.

183. Maluf, S.W., *Monitoring DNA damage following radiation exposure using cytokinesis-block micronucleus method and alkaline single-cell gel electrophoresis*. Clin Chim Acta, 2004. **347**(1-2): p. 15-24.
184. Paterna, S., et al., *Normal sodium diet versus low sodium diet in compensated congestive heart failure: is sodium an old enemy or a new friend?* Clin Sci (Lond), 2007.
185. Young, W.F., *Primary aldosteronism: renaissance of a syndrome*. Clin Endocrinol (Oxf), 2007. **66**(5): p. 607-18.
186. Plamondon, I., et al., *Morning plasma aldosterone predicts the subtype of primary aldosteronism independent of sodium intake*. Clin Exp Hypertens, 2007. **29**(2): p. 127-34.
187. Patni, H., et al., *Aldosterone promotes proximal tubular cell apoptosis: role of oxidative stress*. Am J Physiol Renal Physiol, 2007. **293**(4): p. F1065-71.
188. Gloire, G., S. Legrand-Poels, and J. Piette, *NF-kappaB activation by reactive oxygen species: fifteen years later*. Biochem Pharmacol, 2006. **72**(11): p. 1493-505.
189. Murgia, E., et al., *Validation of micronuclei frequency in peripheral blood lymphocytes as early cancer risk biomarker in a nested case-control study*. Mutat Res, 2008. **639**(1-2): p. 27-34.
190. Fejes-Toth, G., D. Pearce, and A. Naray-Fejes-Toth, *Subcellular localization of mineralocorticoid receptors in living cells: effects of receptor agonists and antagonists*. Proc Natl Acad Sci U S A, 1998. **95**(6): p. 2973-8.
191. Chun, T.Y. and J.H. Pratt, *Nongenomic renal effects of aldosterone: dependency on NO and genomic actions*. Hypertension, 2006. **47**(4): p. 636-7.
192. Michea, L., et al., *Eplerenone blocks nongenomic effects of aldosterone on the Na<sup>+</sup>/H<sup>+</sup> exchanger, intracellular Ca<sup>2+</sup> levels, and vasoconstriction in mesenteric resistance vessels*. Endocrinology, 2005. **146**(3): p. 973-80.
193. Brilla, C.G. and K.T. Weber, *Mineralocorticoid excess, dietary sodium, and myocardial fibrosis*. J Lab Clin Med, 1992. **120**(6): p. 893-901.
194. Rocha, R., et al., *Aldosterone: a mediator of myocardial necrosis and renal arteriopathy*. Endocrinology, 2000. **141**(10): p. 3871-8.
195. Ahokas, R.A., et al., *Aldosteronism and a proinflammatory vascular phenotype: role of Mg<sup>2+</sup>, Ca<sup>2+</sup>, and H<sub>2</sub>O<sub>2</sub> in peripheral blood mononuclear cells*. Circulation, 2005. **111**(1): p. 51-7.

196. Pitt, B., et al., *The effect of spironolactone on morbidity and mortality in patients with severe heart failure. Randomized Aldactone Evaluation Study Investigators.* N Engl J Med, 1999. **341**(10): p. 709-17.
197. Pitt, B., et al., *Eplerenone, a selective aldosterone blocker, in patients with left ventricular dysfunction after myocardial infarction.* N Engl J Med, 2003. **348**(14): p. 1309-21.
198. Nishiyama, A., T. Kusaka, and H. Kitajima, *[Role of aldosterone in oxidative stress and renal injury].* Yakugaku Zasshi, 2007. **127**(9): p. 1331-7.
199. Kim, S., et al., *Role of angiotensin II in renal injury of deoxycorticosterone acetate-salt hypertensive rats.* Hypertension, 1994. **24**(2): p. 195-204.
200. Maron, D.J., S. Fazio, and M.F. Linton, *Current perspectives on statins.* Circulation, 2000. **101**(2): p. 207-13.
201. Mazor, R., et al., *Primed polymorphonuclear leukocytes constitute a possible link between inflammation and oxidative stress in hyperlipidemic patients.* Atherosclerosis, 2007.
202. Zalba, G., et al., *Phagocytic NADPH oxidase-dependent superoxide production stimulates matrix metalloproteinase-9: implications for human atherosclerosis.* Arterioscler Thromb Vasc Biol, 2007. **27**(3): p. 587-93.
203. Jacobi, J., et al., *Priming of polymorphonuclear leukocytes: a culprit in the initiation of endothelial cell injury.* Am J Physiol Heart Circ Physiol, 2006. **290**(5): p. H2051-8.
204. Collins, S.J., *The HL-60 promyelocytic leukemia cell line: proliferation, differentiation, and cellular oncogene expression.* Blood, 1987. **70**(5): p. 1233-44.
205. Muranaka, S., et al., *Mechanism and characteristics of stimuli-dependent ROS generation in undifferentiated HL-60 cells.* Antioxid Redox Signal, 2005. **7**(9-10): p. 1367-76.
206. Wagner, A.H., et al., *Improvement of nitric oxide-dependent vasodilatation by HMG-CoA reductase inhibitors through attenuation of endothelial superoxide anion formation.* Arterioscler Thromb Vasc Biol, 2000. **20**(1): p. 61-9.
207. Stopper, H., et al., *Comet-assay analysis identifies genomic damage in lymphocytes of uremic patients.* Am J Kidney Dis, 2001. **38**(2): p. 296-301.

208. Cao, Z. and Y. Li, *Chemical induction of cellular antioxidants affords marked protection against oxidative injury in vascular smooth muscle cells*. *Biochem Biophys Res Commun*, 2002. **292**(1): p. 50-7.
209. Cao, Z., et al., *Induction of cellular glutathione and glutathione S-transferase by 3H-1,2-dithiole-3-thione in rat aortic smooth muscle A10 cells: protection against acrolein-induced toxicity*. *Atherosclerosis*, 2003. **166**(2): p. 291-301.
210. Rupin, A., et al., *Role of NADPH oxidase-mediated superoxide production in the regulation of E-selectin expression by endothelial cells subjected to anoxia/reoxygenation*. *Cardiovasc Res*, 2004. **63**(2): p. 323-30.
211. Rao, P.V., et al., *Expression of nonphagocytic NADPH oxidase system in the ocular lens*. *Mol Vis*, 2004. **10**: p. 112-21.
212. Christ, M., et al., *Glucose increases endothelial-dependent superoxide formation in coronary arteries by NAD(P)H oxidase activation: attenuation by the 3-hydroxy-3-methylglutaryl coenzyme A reductase inhibitor atorvastatin*. *Diabetes*, 2002. **51**(8): p. 2648-52.
213. Grosser, N., et al., *Rosuvastatin upregulates the antioxidant defense protein heme oxygenase-1*. *Biochem Biophys Res Commun*, 2004. **325**(3): p. 871-6.
214. Molcanyiova, A., et al., *Beneficial effect of simvastatin treatment on LDL oxidation and antioxidant protection is more pronounced in combined hyperlipidemia than in hypercholesterolemia*. *Pharmacol Res*, 2006. **54**(3): p. 203-7.
215. Heeneman, S., et al., *Drug-induced immunomodulation to affect the development and progression of atherosclerosis: a new opportunity?* *Expert Rev Cardiovasc Ther*, 2007. **5**(2): p. 345-64.
216. Wassmann, S., et al., *Cellular antioxidant effects of atorvastatin in vitro and in vivo*. *Arterioscler Thromb Vasc Biol*, 2002. **22**(2): p. 300-5.
217. Haendeler, J., et al., *Antioxidant effects of statins via S-nitrosylation and activation of thioredoxin in endothelial cells: a novel vasculoprotective function of statins*. *Circulation*, 2004. **110**(7): p. 856-61.
218. Imaeda, A., et al., *Protective effects of fluvastatin against reactive oxygen species induced DNA damage and mutagenesis*. *Free Radic Res*, 2001. **34**(1): p. 33-44.



219. Nakae, D., et al., *Involvement of 8-hydroxyguanine formation in the initiation of rat liver carcinogenesis by low dose levels of N-nitrosodiethylamine*. *Cancer Res*, 1997. **57**(7): p. 1281-7.
220. Bjelakovic, G., et al., *Antioxidant supplements for prevention of gastrointestinal cancers: a systematic review and meta-analysis*. *Lancet*, 2004. **364**(9441): p. 1219-28.
221. Kassie, F., W. Parzefall, and S. Knasmuller, *Single cell gel electrophoresis assay: a new technique for human biomonitoring studies*. *Mutat Res*, 2000. **463**(1): p. 13-31.
222. Inoue, I., et al., *Lipophilic HMG-CoA reductase inhibitor has an anti-inflammatory effect: reduction of mRNA levels for interleukin-1beta, interleukin-6, cyclooxygenase-2, and p22phox by regulation of peroxisome proliferator-activated receptor alpha (PPARalpha) in primary endothelial cells*. *Life Sci*, 2000. **67**(8): p. 863-76.
223. Delbosc, S., et al., *Statins, 3-hydroxy-3-methylglutaryl coenzyme A reductase inhibitors, are able to reduce superoxide anion production by NADPH oxidase in THP-1-derived monocytes*. *J Cardiovasc Pharmacol*, 2002. **40**(4): p. 611-7.
224. Carneado, J., et al., *Simvastatin improves endothelial function in spontaneously hypertensive rats through a superoxide dismutase mediated antioxidant effect*. *J Hypertens*, 2002. **20**(3): p. 429-37.
225. Hsu, M., et al., *Tissue-specific effects of statins on the expression of heme oxygenase-1 in vivo*. *Biochem Biophys Res Commun*, 2006. **343**(3): p. 738-44.
226. Jahovic, N., et al., *Effects of statins on experimental colitis in normocholesterolemic rats*. *Scand J Gastroenterol*, 2006. **41**(8): p. 954-62.
227. Furman, C., et al., *Rosuvastatin reduces MMP-7 secretion by human monocyte-derived macrophages: potential relevance to atherosclerotic plaque stability*. *Atherosclerosis*, 2004. **174**(1): p. 93-8.
228. Wagner, A.H., et al., *3-hydroxy-3-methylglutaryl coenzyme A reductase-independent inhibition of CD40 expression by atorvastatin in human endothelial cells*. *Arterioscler Thromb Vasc Biol*, 2002. **22**(11): p. 1784-9.
229. Valko, M., et al., *Free radicals and antioxidants in normal physiological functions and human disease*. *Int J Biochem Cell Biol*, 2007. **39**(1): p. 44-84.
230. Bjerre, L.M. and J. LeLorier, *Do statins cause cancer? A meta-analysis of large randomized clinical trials*. *Am J Med*, 2001. **110**(9): p. 716-23.

231. Pfeffer, M.A., et al., *Safety and tolerability of pravastatin in long-term clinical trials: prospective Pravastatin Pooling (PPP) Project*. *Circulation*, 2002. **105**(20): p. 2341-6.
232. Graaf, M.R., et al., *The risk of cancer in users of statins*. *J Clin Oncol*, 2004. **22**(12): p. 2388-94.
233. Khurana, V., et al., *Statins Reduce the Risk of Lung Cancer in Humans: A Large Case-Control Study of US Veterans*. *Chest*, 2007. **131**(5): p. 1282-8.
234. Khurana, V., et al., *Statins reduce the risk of pancreatic cancer in humans: a case-control study of half a million veterans*. *Pancreas*, 2007. **34**(2): p. 260-5.
235. Akram, S., et al., *Reactive oxygen species-mediated regulation of the Na<sup>+</sup>-H<sup>+</sup> exchanger 1 gene expression connects intracellular redox status with cells' sensitivity to death triggers*. *Cell Death Differ*, 2006. **13**(4): p. 628-41.
236. Elchuri, S., et al., *CuZnSOD deficiency leads to persistent and widespread oxidative damage and hepatocarcinogenesis later in life*. *Oncogene*, 2005. **24**(3): p. 367-80.
237. Ishii, K., et al., *Prevention of mammary tumorigenesis in acatalasemic mice by vitamin E supplementation*. *Jpn J Cancer Res*, 1996. **87**(7): p. 680-4.
238. Chu, F.F., et al., *Bacteria-induced intestinal cancer in mice with disrupted Gpx1 and Gpx2 genes*. *Cancer Res*, 2004. **64**(3): p. 962-8.
239. Imlay, J.A., S.M. Chin, and S. Linn, *Toxic DNA damage by hydrogen peroxide through the Fenton reaction in vivo and in vitro*. *Science*, 1988. **240**(4852): p. 640-2.
240. Hozumi, M., *Production of hydrogen peroxide by 4 hydroxyaminoquinoline 1-oxide*. *Gann*, 1969. **60**(1): p. 83-90.
241. Kobori, H., et al., *The intrarenal renin-angiotensin system: from physiology to the pathobiology of hypertension and kidney disease*. *Pharmacol Rev*, 2007. **59**(3): p. 251-87.
242. Polizio, A.H., et al., *Angiotensin II Regulates Cardiac Hypertrophy via Oxidative Stress but Not Antioxidant Enzyme Activities in Experimental Renovascular Hypertension*. *Hypertens Res*, 2008. **31**(2): p. 325-34.
243. Young, M.J., et al., *Early inflammatory responses in experimental cardiac hypertrophy and fibrosis: effects of 11 beta-hydroxysteroid dehydrogenase inactivation*. *Endocrinology*, 2003. **144**(3): p. 1121-5.

- 
244. Young, M., et al., *Mineralocorticoids, hypertension, and cardiac fibrosis*. J Clin Invest, 1994. **93**(6): p. 2578-83.
  245. Jung, K.H., et al., *Blockade of AT1 receptor reduces apoptosis, inflammation, and oxidative stress in normotensive rats with intracerebral hemorrhage*. J Pharmacol Exp Ther, 2007. **322**(3): p. 1051-8.
  246. Paravicini, T.M. and R.M. Touyz, *Redox signaling in hypertension*. Cardiovasc Res, 2006. **71**(2): p. 247-58.
  247. Miyata, K., et al., *Aldosterone stimulates reactive oxygen species production through activation of NADPH oxidase in rat mesangial cells*. J Am Soc Nephrol, 2005. **16**(10): p. 2906-12.
  248. Stas, S., et al., *Mineralocorticoid receptor blockade attenuates chronic overexpression of the renin-angiotensin-aldosterone system stimulation of reduced nicotinamide adenine dinucleotide phosphate oxidase and cardiac remodeling*. Endocrinology, 2007. **148**(8): p. 3773-80.
  249. Yu, Y., et al., *Effects of an ARB on endothelial progenitor cell function and cardiovascular oxidation in hypertension*. Am J Hypertens, 2008. **21**(1): p. 72-7.
  250. Campese, V.M. and J. Park, *HMG-CoA reductase inhibitors and the kidney*. Kidney Int, 2007. **71**(12): p. 1215-22.
  251. Broncel, M., M. Koter-Michalak, and J. Chojnowska-Jeziarska, *[The effect of statins on lipids peroxidation and activities of antioxidants enzymes in patients with dyslipidemia]*. Przegl Lek, 2006. **63**(9): p. 738-42.

---

## 12. Acknowledgements

I would like to thank

- ◇ Professor Dr. Helga Stopper for the supervision of my PhD work and the scientific support
- ◇ Dr. Nicole Schupp for her continuous input and support
- ◇ Professor Dr. Thomas Roitsch for supervising my PhD work on behalf of the faculty of biology
- ◇ PD Dr. Frank Schweda (University of Regensburg) for the excellent cooperation in the “isolated perfused kidney” project
- ◇ Dr. Peter Kolkhof (Bayer Healthcare) and Dr. Stefan Schäfer (Bayer Healthcare) for the excellent cooperation in the aldosterone *in vitro* and *in vivo* projects
- ◇ Thomas Büdel, Jessica Böhm, Marlies Hamann, Michael Kessler, Elisabeth Rüb-Spiegel, Maria Scheurich, Betty Stein and Michaela Wolf for their excellent technical assistance and help
- ◇ last but not least my family for their patience and support

## Curriculum vitae

Ursula Schmid

\* October 17<sup>th</sup> 1980 in Rottweil, Germany

Leistenstr. 19a

97082 Würzburg

### Education

- |                   |   |
|-------------------|---|
| 01.2006 – present | Graduate study and Ph.D. thesis in toxicology at the Institute of Pharmacology and Toxicology, Department of Toxicology, University of Würzburg, Germany                        |
| 28.11.2005        | 3 <sup>rd</sup> state examination in Pharmacy and License to practice Pharmacy (Approbation)  |
| 05.2005 – 11.2005 | Internship at the Rathaus-Apotheke, Rathausstr.2, 78532 Tuttlingen, Germany (praktisches Jahr)  |
| 11.2004 – 04.2005 | Internship at the Institute of Pharmacology and Toxicology, Department of Toxicology, working group of Prof. Dr. H. Stopper, University of Würzburg, Germany (praktisches Jahr) |
| 11.1999 – 10.2004 | Undergraduate studies of pharmacy at the University of Würzburg, Germany<br>Degree: 2 <sup>nd</sup> state examination in Pharmacy   |
| 09.1997 – 06.1999 | Secondary school, Albertus-Magnus-Gymnasium, Rottweil, Germany<br>Degree: general qualification for university entrance (Abitur)  |
| 08.1990 – 07.1997 | Secondary school, Droste-Hülshoff-Gymnasium, Rottweil, Germany  |
| 02.1988 – 06.1990 | Primary school. Eichendorff-Schule, Rottweil, Germany   |
| 08.1986 – 02.1988 | Primary school, Schlossbergschule, Dotternhausen, Germany   |

## Publications

### 1. published

Schupp N, Schmid U, Rutkowski P, Lakner U, Kanase N, Heidland A, Stopper H.  
Angiotensin II-induced genomic damage in renal cells can be prevented by angiotensin II type 1 receptor blockage or radical scavenging.  
Am J Physiol Renal Physiol. 2007 May;292(5):F1427-34. Epub 2007 Jan 16

Schupp N, Schmid U, Heidland A, Stopper H.  
Rosuvastatin protects against oxidative stress and DNA damage in vitro via up-regulation of glutathione synthesis.  
Atherosclerosis. 2007 Dec 20; [Epub ahead of print]

Abraham SK, Schupp N, Schmid U, Stopper H.  
Antigenotoxic effects of the phytoestrogen pelargonidin chloride and the polyphenol chlorogenic acid.  
Mol Nutr Food Res. 2007 Jul;51(7):880-7

Schupp N, Schmid U, Heidland A, Stopper H.  
New approaches for the treatment of genomic damage in end-stage renal disease.  
J Ren Nutr. 2008 Jan;18(1):127-33

Schmid U, Stopper H, Heidland A, Schupp N.  
Benfotiamine exhibits direct antioxidative capacity and prevents induction of DNA damage in vitro.  
Diabetes Metab Res Rev. 2008 Apr 2; [Epub ahead of print]  
PMID: 18384109 [PubMed - as supplied by publisher]

Helga Stopper, Anna-Teresa Treutlein, Udo Bahner, Nicole Schupp, Ursula Schmid, Andreas Brink, Alessandra Perna, August Heidland  
Reduction of the genomic damage level in hemodialysis patients by folic acid and vitamin B12 supplementation  
Nephrology dialysis transplantation

### 2. submitted

Ursula Schmid, Helga Stopper, Frank Schweda, Nicole Schupp  
Angiotensin II induces DNA damage in the isolated perfused kidney  
Cancer research

Nicole Schupp, Eva Maria Dette, Ursula Schmid, Udo Bahner, Michaela Winkler, August Heidland, Helga Stopper  
Benfotiamine reduces genomic damage in peripheral lymphocytes of hemodialysis patients  
Naunyn-Schmiedebergs Archives of Pharmacology

Nicole Schupp, Nina Queisser, Ursula Schmid, August Heidland, Helga Stopper  
Aldosterone causes DNA strand breaks and chromosomal aberrations in renal cells  
Endocrinology

## Oral Presentations and Posters

Nina Queisser, Ursula Schmid, Helga Stopper and Nicole Schupp

Aldosteron causes oxidative DNA damage

49<sup>th</sup> Spring Meeting Deutsche Gesellschaft für Experimentelle und Klinische Pharmakologie und Toxikologie March 11<sup>th</sup> – 13<sup>th</sup> 2008, Mainz

Poster

Nicole Schupp, Ursula Schmid, Frank Schweda, Gholamrezal Fazel and Helga Stopper

Angiotensin II is not only genotoxic *in vitro* but also causes DNA strand breaks in the isolated perfused kidney

49<sup>th</sup> Spring Meeting Deutsche Gesellschaft für Experimentelle und Klinische Pharmakologie und Toxikologie March 11<sup>th</sup> – 13<sup>th</sup> 2008, Mainz

Poster

Nicole Schupp, Ursula Schmid, Frank Schweda, August Heidland and Helga Stopper

Angiotensin II is genotoxic *in vitro* and causes DNA strand breaks in the isolated perfused kidney

Gordon Research Conference - Angiotensin, 24<sup>th</sup> – 29<sup>th</sup> 2008, Ventura, CA

Poster

Ursula Schmid, Nicole Schupp, August Heidland, Helga Stopper

DNA-protective and antioxidative properties of benfotiamine *in vitro*

NDT, Volume 22, Supplement 6, 2007, vi222

XLII<sup>nd</sup> Congress of the European Renal Association – European Dialysis and Transplant Association, 2007 in Barcelona

Oral presentation

Ursula Schmid, Nicole Schupp, Lisanne Krens, August Heidland and Helga Stopper

AT<sub>1</sub> receptor-mediated genotoxicity of angiotensin II

Naunyn-Schmiedeberg's Archives of Pharmacology, Volume 375, Supplement 1 / März 2007

48<sup>th</sup> Spring Meeting Deutsche Gesellschaft für Experimentelle und Klinische Pharmakologie und Toxikologie March 13<sup>th</sup> – 15<sup>th</sup> 2007, Mainz

Poster

Nicole Schupp, Ursula Schmid, August Heidland and Helga Stopper

Rosuvastatin protects against oxidative stress and DNA damage by up-regulation of the cellular antioxidant defense

48<sup>th</sup> Spring Meeting Deutsche Gesellschaft für Experimentelle und Klinische Pharmakologie und Toxikologie Mainz, March 13<sup>th</sup> – 15<sup>th</sup> 2007, Mainz

Poster

Nicole Schupp, Ursula Schmid, August Heidland, Helga Stopper

Receptor-mediated DNA damage by the endogenous substances angiotensin II and aldosterone

Gordon Research Conference – Genetic Toxicology, July 29<sup>th</sup> - August 3<sup>rd</sup> 2007 Oxford

Poster

Nicole Schupp, Ursula Schmid, Peter Kolkhof, Nina Queisser, Stefan Schäfer, August Heidland and Helga Stopper

Aldosterone-induced genomic damage is reduced by mineralocorticoid receptor antagonists

31<sup>st</sup> Scientific congress Hypertonie 2007, November 22<sup>nd</sup> – 24<sup>th</sup>, Bochum  
Oral presentation

Nicole Schupp, Ursula Schmid, Frank Schweda, Gholamreza Fazeli, August Heidland and Helga Stopper

Angiotensin II causes DNA strand breaks in the isolated perfused kidney

31<sup>st</sup> Scientific congress Hypertonie 2007, November 22<sup>nd</sup> – 24<sup>th</sup>, Bochum  
Oral Presentation

Nicole Schupp, Ursula Schmid, Lianne Krens, August Heidland and Helga Stopper

AT<sub>1</sub> receptor-mediated genotoxicity of angiotensin

30. Scientific congress Hypertonie 2006, November 22<sup>nd</sup> – 24<sup>th</sup>, Munich  
Poster

Nicole Schupp, Ursula Schmid, Eva Arnold, August Heidland and Helga Stopper

Rosuvastatin protects against oxidative stress and DNA damage in vitro

30. Scientific congress Hypertonie 2006, November 22<sup>nd</sup> – 24<sup>th</sup>, Munich  
Poster

Nicole Schupp, Ursula Schmid, Eva Arnold, August Heidland and Helga Stopper

Rosuvastatin reduces oxidative stress and DNA damage in human promyelotic HL-60 cells

XIV. International Symposium on Atherosclerosis, June 18<sup>th</sup> – 22<sup>nd</sup> 2006, Rome  
Poster

Nicole Schupp, Ursula Schmid, Eva Arnold, August Heidland and Helga Stopper

Rosuvastatin reduces oxidative stress and DNA damage in human promyelotic HL-60 cells

47<sup>th</sup> Spring Meeting Deutsche Gesellschaft für Experimentelle und Klinische Pharmakologie und Toxikologie, March 4<sup>th</sup> – 15<sup>th</sup> 2006, Mainz  
Poster

Nicole Schupp, Ursula Lakner, Przemyslaw Rutkowski, Ursula Schmid, August Heidland and Helga Stopper

Genotoxicity of angiotensin II is receptor-mediated

22<sup>nd</sup> GUM-meeting, February 21<sup>st</sup> – 24<sup>th</sup> 2006, Darmstadt  
Poster

Nicole Schupp, Ursula Schmid, Eva Arnold, August Heidland and Helga Stopper

Reduction of oxidative stress and DNA damage by Rosuvastatin in human promyelotic HL-60 cells

29. Scientific congress Hypertonie 2005, November 23<sup>rd</sup> – 25<sup>th</sup>, Berlin  
Poster

Nicole Schupp, Ursula Schmid, Maria Scheurich, August Heidland and Helga Stopper

Oxidative stress-induced DNA damage in cultured cells: modulation by statins

46<sup>th</sup> Spring Meeting Deutsche Gesellschaft für Experimentelle und Klinische Pharmakologie und Toxikologie, March 15<sup>th</sup> – 17<sup>th</sup> 2005, Mainz  
Poster



---

Nicole Schupp, Ursula Schmid, Ursula Lakner, Michael Gekle, August Heidland  
and Helga Stopper

Genotoxicity of advanced glycation end products: protective effects of modulators of the  
renin-angiotensin system

XLI ERA-EDTA Congress, May 15<sup>th</sup> – 18<sup>th</sup> 2004, Lissabon

Poster

**Ehrenwörtliche Erklärung**

Hiermit erkläre ich, dass ich die Arbeit selbständig verfasst habe und keine anderen als die von mir angegebenen Quellen und Hilfsmittel benutzt habe.

Ferner erkläre ich, dass ich nicht anderweitig mit oder ohne Erfolg versucht habe, diese Dissertation in gleicher oder ähnlicher Form einzureichen.

Ich habe keine Doktorprüfung an einer anderen Hochschule abgelegt oder endgültig nicht bestanden.

Würzburg, den 28.04.2008

Ursula Schmid